

**CRANFIELD UNIVERSITY**

**Richard Oliver-Hall**

**Friction Characteristics of Skewed Roller Brakes**

**College of Aeronautics**

**EngD Thesis**

# **CRANFIELD UNIVERSITY**

**College of Aeronautics**

**Engineering Doctorate Thesis**

**Academic Years 1993-1998**

**RICHARD OLIVER-HALL**

**‘Friction Characteristics of Skewed Roller Brakes’**

**Academic Supervisor: Dr. R. Jones**  
**Industrial Supervisor: Mr. P. Strothers**  
**Management Supervisor: Dr. A. Harrison**

**October 1998**

This thesis is submitted in partial fulfilment of the requirements for the Degree of Doctor of Engineering

# SUMMARY

The project sponsors design and manufacture skewed roller brake devices for use in aircraft flight control actuation systems. Design tools have previously been developed to predict the torque characteristics of these devices. A fundamental deficiency of these tools is the use of empirical friction coefficient data gathered from a limited test sample. A need was identified to develop a friction coefficient model based on the operational parameters of the design, namely load, speed and lubricant viscosity. The development and validation of this model formed the basis of the technical research objective.

A cost benefit analysis indicated that the sponsors could reasonably expect to gain a significant technical competitive advantage over their competitors if the technical research objective could be achieved. This advantage should provide opportunities for premium pricing of the product and enhanced opportunities to enter new markets. Additionally, the sponsors could expect lead time reductions and cost savings of £69000 from the removal of the need to conduct prototype tests to assess the effective friction coefficient.

A friction coefficient model and skewed roller torque equation design tool have been successfully developed, satisfying the technical research objective. The friction coefficient model is defined in terms of lubrication number. The lubrication number parameter incorporates lubricant viscosity, roller speed, roller load and contact surface roughness terms, fully describing the operational parameters of a design. Experimental evidence has validated the model using two lubricants, a hydraulic fluid, Brayco 795 and a mineral oil, Catenex 79. The tests cover a lubrication number range from  $2 \times 10^{-5}$  to  $6 \times 10^{-2}$  with a mean Hertzian stress from 0.27 to 0.61 Gpa.

The success of this project has ensured that the sponsors will reap the cost and design lead time savings predicted in the cost benefit analysis and have the tools necessary to develop new markets and premium pricing business opportunities.

# ACKNOWLEDGEMENTS

The author would like to thank Dr. Robert Jones, the academic supervisor, for his advice, encouragement and support during the course of this project.

The contribution of Dr. Alan Harrison as the management supervisor is also acknowledged with thanks.

Thanks also go to Mr Jim Yost for his introduction to the Engineering Doctorate and his encouragement, advice and support at the key stages of the project.

The author particularly thanks and acknowledges James Parker, Undergraduate Trainee, for his enthusiasm, commitment and assistance in conducting experiments and compilation of the Figures and Tables in this thesis.

The support and commitment of Mr. Paul Strothers of Dowty Aerospace Wolverhampton is acknowledged and appreciated.

The author would also like to extend his gratitude to all academics at Cranfield and Leeds Universities and particularly employees at Dowty who have contributed knowledge and assistance during the course of this research.

Final thanks go to Adrienne for her patience and understanding through many absent weekends during the production of this thesis.

# CONTENTS

Summary	ii
Acknowledgements	iii
Contents	iv
List of Tables	ix
list of Figures	x
Notation	xiv
<b>1.0 BUSINESS CASE FOR THE RESEARCH</b>	
Chapter Summary	1-1
1.1 Background	1-2
1.2 Literature Review	1-9
1.2.1 Introduction	1-9
1.2.2 Friction and Lubrication Modes	1-10
1.2.3 Surface Roughness	1-11
1.2.4 film Thickness to Roughness Ratio	1-12
1.2.5 Friction Models	1-14
1.3 Project Motivation	1-21
1.4 Technical Research Objective	1-22
1.5 Commercial Objectives	1-22
1.6 Research Method	1-23
1.7 Cost Benefit Analysis of the Research	1-24
1.7.1 The Business Decision	1-24
1.7.2 The Market Place	1-24
1.7.3 The Competitors	1-28
1.7.4 Skewed Roller Devices, Alternatives and Advantages	1-30
1.7.4.1 Boeing Commercial Aircraft	1-30
1.7.4.2 Airbus Industrie	1-30
1.7.4.3 AVRO and British Aerospace	1-32

1.7.5	Skewed Roller Devices, Summary	1-32
1.7.6	New Business Process	1-32
1.7.7	Financial Analysis	1-34
1.7.8	Alternative Approaches	1-35
	1.7.8.1 Do Nothing	1-35
	1.7.8.2 Empirical Approach	1-35
	1.7.8.3 Develop Alternative Brake Technologies	1-36
1.7.9	Cost Benefit Analysis Summary	1-37
1.8	Project Management Topics	1-37
	1.8.1 Introduction	1-37
	1.8.2 Project Plan	1-38
	1.8.3 Project Budget	1-39
	1.8.4 Project Risk Assessment	1-39
	1.8.5 Project Management Summary	1-40
1.9	Business Case Summary	1-40
<b>2.0</b>	<b>SKEWED ROLLER BRAKE TESTING</b>	
	Chapter Summary	2-1
2.1	Introduction	2-2
2.2	Test Rig Description	2-3
2.3	Description of the Test Unit	2-5
2.4	Test Procedure	2-9
2.5	Inherent Test Unit Drag	2-10
	2.5.1 Brayco 795	2-10
	2.5.2 Catenex 79	2-13
2.6	Torque Characteristics	2-14
	2.6.1 Brayco 795	2-15
	2.6.2 Catenex 79	2-15
2.7	Stribeck Diagram	2-18
2.8	Film Thickness Considerations	2-25
2.9	Discussion of the Test Results	2-26
	2.9.1 Brayco 795	2-26

2.9.2	Catenex 79	2-29
2.9.3	Maximum and Minimum Friction Coefficient	2-30
2.9.4	Combining the Data Points	2-30
2.10	Results Conclusion and Business Case Implications	2-32
<b>3.</b>	<b>FRICITION COEFFICIENT MODELLING</b>	
	Chapter Summary	3-1
3.1	Introduction	3-2
3.2	Lubricant - Liquid or Solid State	3-3
3.3	Friction Mode Diagram	3-5
3.4	Friction Coefficient	3-7
	3.4.1 Mixed Lubrication Mode	3-7
	3.4.2 Boundary Lubrication Mode	3-7
	3.4.3 Elastohydrodynamic Regime	3-8
	3.4.4 Analytical Values	3-11
3.5	The Hess and Soom Model	3-12
3.6	Conclusions and Implications for the Business Case	3-13
<b>4.</b>	<b>DESIGN TOOL DEVELOPMENT</b>	
	Chapter Summary	4-1
4.1	Introduction	4-2
4.2	Comparison of Predicted and Measured Friction Coefficients	4-2
4.3	Friction Coefficient Model Development	4-5
4.4	Achievement of the Technical Research Objective	4-8
	4.4.1 Friction Coefficient Model	4-8
	4.4.2 Torque Characteristic	4-9
	4.4.3 Technical Research Objective	4-10
<b>5.</b>	<b>USE OF THE DESIGN TOOL AND LIMITATIONS</b>	
	Chapter Summary	5-1
5.1	Introduction	5-2
5.2	General Design Considerations	5-2

5.3	Design Equations	5-5
5.3.1	Torque Equation	5-5
5.3.2	Lubrication Number	5-7
5.3.3	Friction Coefficient	5-9
5.4	Limitations	5-9
5.4.1	Contact Stress	5-9
5.4.2	Semifluid Lubrication	5-11

## **6. TECHNICAL REVIEW AND RECOMMENDATIONS FOR FURTHER WORK**

	Chapter Summary	6-1
6.1	Introduction	6-2
6.2	Technical Discussion	6-2
6.3	Direction of Further Work	6-5
6.3.1	Hertzian Stress Levels	6-5
6.3.2	Choice of Lubricant	6-5
6.3.3	Environmental Temperature Variations	6-6
6.3.4	Roller Length	6-7
6.3.5	Design Case Study	6-8

## **7. REVIEW OF THE BUSINESS CASE AND OVERALL CONCLUSIONS**

	Chapter Summary	7-1
7.1	Introduction	7-2
7.2	The Business Case for the Research	7-3
7.2.1	Financial Justification	7-4
7.2.2	Technical Risk	7-4
7.2.3	The Marketing Tool	7-4
7.3	Technical Conclusions	7-5
7.4	Business Case Conclusions	7-6
7.5	Direction of Further Work	7-7
7.6	Overall Conclusions	7-8



## REFERENCES AND BIBLIOGRAPHY

R-1

## APPENDICES

A	The Engineering Doctorate Programme	A-1
B	Cost Benefit Analysis	B-1
C	Project Management Tools	
C1	Four Year Work Plan	C-1
C2	Project Budget	C-2
C3	Risk Assessment	C-3
D	Detailed Test Procedure	D-1
E	Skewed Roller Torque Characteristics	E-1
F	Lubrication Number Analysis and Film Thickness Calculations	F-1
G	Fluid Rheological Data	G-1
H	Derivation of Skewed Roller Torque	H-1

# LIST OF TABLES

Table 1.7-1	Major Competitors
Table 1.7-2	Skewed Roller Device Applications
Table 2.3-1	Component Materials
Table 2.3-2	Surface Finish Measurements
Table 2.4-1	Test Conditions Summary
Table D-1	Pre-loading Conditions
Table D-2	Test Measurement Times
Table D-3	The Suggested Test Sequence
Table F-1	Lubrication Analysis Results, Brayco 795, 15° Skew.
Table F-2	Lubrication Analysis Results, Brayco 795, 25° Skew.
Table F-3	Lubrication Analysis Results, Brayco 795, 35° Skew.
Table F-4	Lubrication Analysis Results, Brayco 795, 45° Skew.
Table F-5	Lubrication Analysis Results, Brayco 795, 55° Skew.
Table F-6	Lubrication Analysis Results, Catenex 79, 15° Skew.
Table F-7	Lubrication Analysis Results, Catenex 79, 25° Skew.
Table F-8	Lubrication Analysis Results, Catenex 79, 35° Skew.
Table F-9	Lubrication Analysis Results, Catenex 79, 45° Skew.
Table F-10	Lubrication Analysis Results, Catenex 79, 55° Skew.
Table F-11	Elastohydrodynamic Film Thickness Calculations, Brayco 795, 15° Skew.
Table F-12	Elastohydrodynamic Film Thickness Calculations, Brayco 795, 25° Skew.
Table F-13	Elastohydrodynamic Film Thickness Calculations, Brayco 795, 35° Skew.
Table F-14	Elastohydrodynamic Film Thickness Calculations, Brayco 795, 45° Skew.
Table F-15	Elastohydrodynamic Film Thickness Calculations, Brayco 795, 55° Skew.
Table F-16	Elastohydrodynamic Film Thickness Calculations, Catenex 79, 15° Skew.
Table F-17	Elastohydrodynamic Film Thickness Calculations, Catenex 79, 25° Skew.
Table F-18	Elastohydrodynamic Film Thickness Calculations, Catenex 79, 35° Skew.
Table F-19	Elastohydrodynamic Film Thickness Calculations, Catenex 79, 45° Skew.
Table F-20	Elastohydrodynamic Film Thickness Calculations, Catenex 79, 55° Skew.
Table G-1	Rheological Data.

# LIST OF FIGURES

- Figure 1.1-1 Arrangement of Skewed Roller Elements
- Figure 1.1-2 Typical Thrust Bearing Installation
- Figure 1.1-3 Skewed Roller Brake Device
- Figure 1.1-4 Typical Civil Aircraft Flight Control Surfaces
- Figure 1.1-5 Typical Geared Rotary Actuator Flap Transmission System
- Figure 1.1-6 Typical Ballscrew Actuator Actuation System
- Figure 1.2-1 The Stribeck Diagram for a Journal Bearing
- Figure 1.2-2 Lubrication Mode Transitions
- Figure 1.2-3 Flow Diagram to Determine Frictional Behaviour and Lubrication Mode
- Figure 1.7-1 DAW Turnover Analysis for 1998
- Figure 1.7-2 Mechanical Actuation Sales for 1998
- Figure 1.7-3 Projected Mechanical Actuation Sales for 2005
- Figure 2.2-1 Test Rig Installation
- Figure 2.3-1 Skewed Roller Test Unit
- Figure 2.3-2 Components Removed from the Skewed Roller Device
- Figure 2.3-3 A Skew Plate and Rollers
- Figure 2.3-4 Brake Plate Measurement Positions
- Figure 2.5-1 Inherent Drag in the Freewheel Direction, Brayco 795 Lubrication.
- Figure 2.5-2 Inherent Drag in the Braking Direction, Brayco 795 Lubrication.
- Figure 2.5-3 Inherent Drag in the Freewheel Direction, Catenex 79 Lubrication
- Figure 2.5-4 Inherent Drag in the Braking Direction, Catenex 79 Lubrication
- Figure 2.6-1 Torque Characteristics with Skew Angle, Axial Load and Speed, Brayco 795 Lubrication
- Figure 2.6-2 Torque Characteristics with Axial Load, Speed and Skew Angle, Brayco 795 Lubrication
- Figure 2.6-3 Torque Characteristics with Skew Angle, Axial Load and Speed, Catenex 79 Lubrication
- Figure 2.6-4 Torque Characteristics with Axial Load, Speed and Skew Angle, Catenex 79 Lubrication
- Figure 2.7-1 Friction Curves for Skewed Roller Brake, Brayco 795 Lubrication

- Figure 2.7-2 Friction Curves for Skewed Roller Brake, Brayco 795 Lubrication
- Figure 2.7-3 Friction Curves for Skewed Roller Brake, Catenex 79 Lubrication
- Figure 2.7-4 Friction Curves for Skewed Roller Brake, Catenex 79 Lubrication
- Figure 2.9-1 Friction Coefficient Values Grouped by Skew Angle, Brayco 795 Lubrication.
- Figure 2.9-2 Friction Characteristics Combining the Brayco and Catenex Test Results
- Figure 3.3-1 Mode Transition Diagram
- Figure 3.4-1 Illustrative Elastohydrodynamic Friction Mode Map
- Figure 3.4-2 Theoretical Friction Coefficient Value Boundaries
- Figure 4.2-1 Theoretical Friction Coefficient Model and Experimental Test Results
- Figure 4.3-1 Modified Friction Coefficient Model and Experimental Test Results
- Figure D-1 Sectional View of the Skewed Roller Test Unit.
- Figure E-1 Torque Characteristics with Skew Angle at 50 rpm with Brayco 795 Lubrication.
- Figure E-2 Torque Characteristics with Skew Angle at 75 rpm with Brayco 795 Lubrication.
- Figure E-3 Torque Characteristics with Skew Angle at 100 rpm with Brayco 795 Lubrication.
- Figure E-4 Torque Characteristics with Skew Angle at 250 rpm with Brayco 795 Lubrication.
- Figure E-5 Torque Characteristics with Skew Angle at 350 rpm with Brayco 795 Lubrication.
- Figure E-6 Torque Characteristics with Skew Angle at 450 rpm with Brayco 795 Lubrication.
- Figure E-7 Torque Characteristics with Skew Angle at 550 rpm with Brayco 795 Lubrication.
- Figure E-8 Torque Characteristics with Skew Angle at 650 rpm with Brayco 795 Lubrication.
- Figure E-9 Torque Characteristics with Axial Load at 50 rpm with Brayco 795 Lubrication.
- Figure E-10 Torque Characteristics with Axial Load at 75 rpm with Brayco 795 Lubrication.

- Figure E-11 Torque Characteristics with Axial Load at 100 rpm with Brayco 795 Lubrication.
- Figure E-12 Torque Characteristics with Axial Load at 250 rpm with Brayco 795 Lubrication.
- Figure E-13 Torque Characteristics with Axial Load at 350 rpm with Brayco 795 Lubrication.
- Figure E-14 Torque Characteristics with Axial Load at 450 rpm with Brayco 795 Lubrication.
- Figure E-15 Torque Characteristics with Axial Load at 550 rpm with Brayco 795 Lubrication.
- Figure E-16 Torque Characteristics with Axial Load at 650 rpm with Brayco 795 Lubrication.
- Figure E-17 Torque Characteristics with Skew Angle at 50 rpm with Catenex 79 Lubrication.
- Figure E-18 Torque Characteristics with Skew Angle at 75 rpm with Catenex 79 Lubrication.
- Figure E-19 Torque Characteristics with Skew Angle at 100 rpm with Catenex 79 Lubrication.
- Figure E-20 Torque Characteristics with Skew Angle at 250 rpm with Catenex 79 Lubrication.
- Figure E-21 Torque Characteristics with Skew Angle at 350 rpm with Catenex 79 Lubrication.
- Figure E-22 Torque Characteristics with Skew Angle at 450 rpm with Catenex 79 Lubrication.
- Figure E-23 Torque Characteristics with Skew Angle at 550 rpm with Catenex 79 Lubrication.
- Figure E-24 Torque Characteristics with Skew Angle at 650 rpm with Catenex 79 Lubrication.
- Figure E-25 Torque Characteristics with Axial Load at 50 rpm with Catenex 79 Lubrication.
- Figure E-26 Torque Characteristics with Axial Load at 75 rpm with Catenex 79 Lubrication.

- Figure E-27 Torque Characteristics with Axial Load at 100 rpm with Catenex 79 Lubrication.
- Figure E-28 Torque Characteristics with Axial Load at 250 rpm with Catenex 79 Lubrication.
- Figure E-29 Torque Characteristics with Axial Load at 350 rpm with Catenex 79 Lubrication.
- Figure E-30 Torque Characteristics with Axial Load at 450 rpm with Catenex 79 Lubrication.
- Figure E-31 Torque Characteristics with Axial Load at 550 rpm with Catenex 79 Lubrication.
- Figure E-32 Torque Characteristics with Axial Load at 650 rpm with Catenex 79 Lubrication.
- Figure F-1 Velocity Definitions.
- Figure F-2 Entrainment Velocity.
- Figure F-3 Surface Velocities and Entrainment Velocity.
- Figure G-1 Dynamic Viscosity with Temperature, Brayco 795 and HVI 650 (Catenex 79).
- Figure H-1 Skewed Roller Geometry.
- Figure H-2 Work Done During Rotation of the Roller.

# NOTATION

BAe	British Aerospace	
bl	Boundary Lubrication	
cla	Centre-line Average	
DAW	Dowty Aerospace Wolverhampton	
ehl	Elastohydrodynamic	
EngD	Engineering Doctorate	
GRA	Geared Rotary Actuator	
MBA	Master of Business Administration	
ml	Mixed Lubrication	
NPV	Net Present Value	
PCD	Pitch Circle Diameter	
PhD	Doctor of Philosophy	
WBS	Work Breakdown Structure	
THSA	Trimmable Horizontal Stabiliser Actuator	
$C_1, C_2$	Hess and Soom Coefficients	
$D$	Brake PCD	(m)
$E$	Youngs Modulus	(Pa)
$E'$	Equivalent Youngs Modulus	(Pa)
$F$	Axial load	(N)
$F'$	Load per Unit Length	(N/m)
$h$	Film Thickness	(m)
$K$	Thermal Conductivity	(W/mK)
$L$	Lubrication Number	
$L_{ehl/ml}$	Lubrication Number, elastohydrodynamic to mixed lubrication regime	
$L_{ml/bl}$	Lubrication Number mixed to boundary lubrication regime	
$l$	Roller length	(m)
$N$	Number of Skewed Roller Stages	
$\bar{p}$	Mean Hertzian Stress	(Pa)

$R$	Brake Pitch-circle Radius	(m)
$R_a$	Average Centre-line Surface Roughness	(m)
$R_e$	Equivalent Radius	(m)
$r$	Roller Radius	(m)
$T$	Torque	(Nm)
$T_m$	Maximum Traction Force	(N)
$\bar{u}$	Entrainment Velocity	(m/s)
$V$	Contact Velocity	(m/s)
$V_+$	Sum Velocity	(m/s)
$V_-$	Difference Velocity	(m/s)
$\alpha_0$	Pressure-viscosity index at ambient pressure	(m <sup>2</sup> /N)
$\bar{\alpha}$	Mean Pressure-viscosity Index	(m <sup>2</sup> /N)
$\beta$	Temperature-viscosity index	(K <sup>-1</sup> )
$\phi$	Skew Angle	(degrees)
$\eta$	Dynamic Viscosity	(kg/ms)
$\eta_0$	Dynamic viscosity at Ambient Pressure	(kg/ms)
$\Lambda$	Film Thickness to Roughness Ratio	
$\mu$	Coefficient of Friction	
$\mu_{bl}$	Coefficient of Friction in the Boundary Lubricated Regime	
$\mu_{ehl}$	Coefficient of Friction in the ehl Regime	
$\mu_{ml}$	Coefficient of Friction in the Mixed Lubrication Regime	
$\nu_0$	Kinematic Viscosity	(centistokes)
$\theta$	Temperature	(°C)
$\theta_I$	Temperature in the Contact Inlet Zone	(°C)
$\theta_{LS}$	Lubricant Glass Transition Temperature	(°C)
$\rho$	Stribeck Stress Term	(N/m <sup>2</sup> )
$\sigma$	RMS surface Roughness	(m)
$\tau_0$	Eyring Stress	(Pa)
$\tau_1$	Lubricant Limiting Shear Stress	(Pa)
$\Omega$	Roller Rotational Velocity about its Own Axis	(rads/sec)



$\omega$	Rotational Speed	(rads/sec)
$\omega_{shaft}$	Rotational Speed of the Skewed Roller Driving Shaft	(rpm)
$\zeta$	Non-dimensional Parameter	

# 1. THE BUSINESS CASE FOR THE RESEARCH

## Chapter Summary

This chapter introduces the background to the thesis and provides a reasoned analysis of the financial and non-financial benefits of conducting the research. Within the chapter is a review of available literature concerning the tribology of a rolling/sliding line contact. Identified are three friction models that can potentially be used to predict traction, based on the operational and geometrical parameters of the contact. The integration of these models with the existing design equation at Dowty Aerospace Wolverhampton, and hence the creation of an engineering design tool forms the essence of the technical objective of this research. A cost benefit analysis of the research and the project management aspects of the work are discussed in this chapter. The chapter is structured as follows:

- 1.1 Background
- 1.2 Literature Review
- 1.3 Project Motivation
- 1.4 Technical Research Objective
- 1.5 Commercial Objectives
- 1.6 Research Method
- 1.7 Cost Benefit Analysis of the Research
- 1.8 Project Management Topics
- 1.9 Business Case Summary

Fulfilment of the objectives of this research project should enable a competitive advantage to be exploited by the sponsor. This should, in turn, provide enhanced opportunities to open new markets and allow the skewed roller technical solutions offered by the sponsor to be premium priced. The achievement of the technical research objective will create a design tool that should remove the need for future design phase prototype tests, generating savings of £69000 and important time savings at crucial stages of new projects.

## 1.1 BACKGROUND

This project is essentially concerned with the development of an analytical tool to aid the design of 'skewed roller' brake devices.

A skewed roller device employs cylindrical roller elements, as found in a conventional roller element thrust bearing, but with the rollers arranged not in a radial direction, as in a thrust bearing, but at a 'skew' angle, Figure 1.1-1.

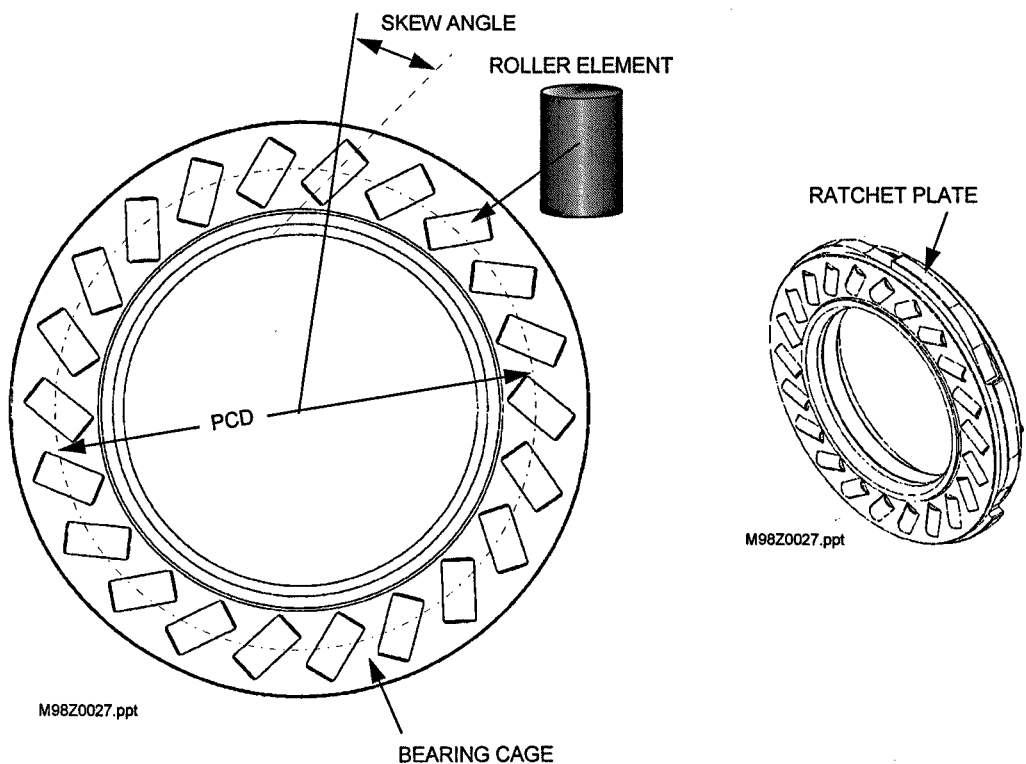


Figure 1.1-1. Arrangement of skewed roller elements.

A bearing cage incorporating skewed rollers can be incorporated in to a machine in exactly the same manner as a conventional thrust bearing, Figure 1.1-2.

Intuitively the rotation of a shaft supported on a skewed thrust bearing would require a higher driving torque than if the shaft was supported by a conventional

thrust bearing. This is apparent since rotation of the shaft requires the roller elements to rotate. In a conventional thrust bearing the roller element rolls perfectly at its mean radius, however at other points along its length there is necessarily an acceptably small amount of sliding action. Conversely, in a skewed roller device the roller motion is described both by rolling action and a significant amount of sliding action.

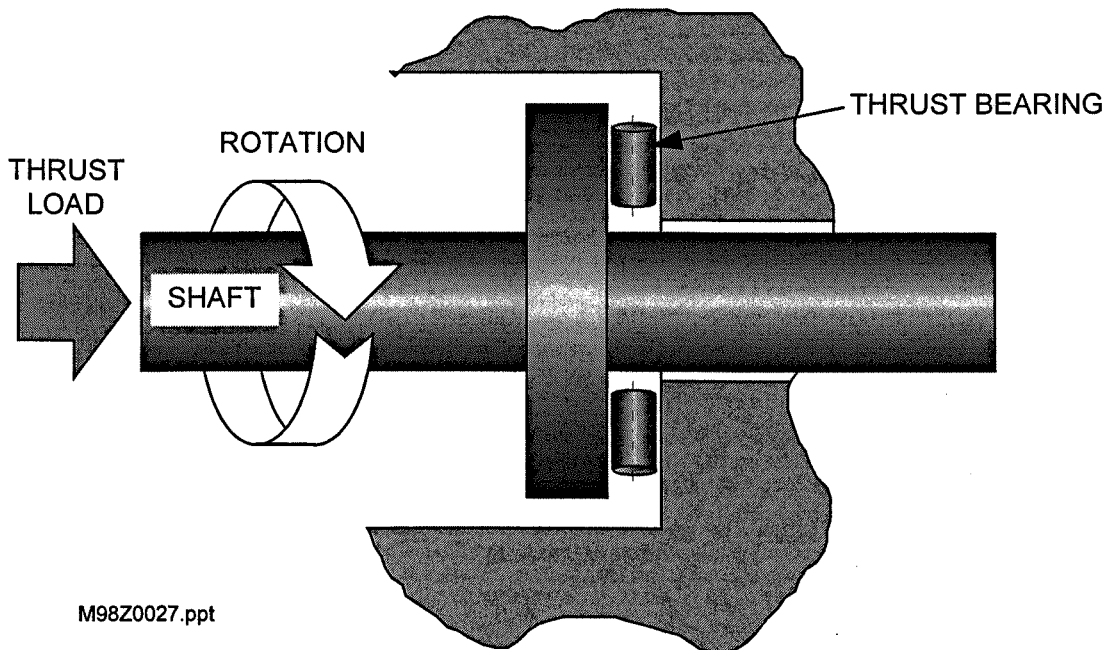


Figure 1.1-2. Typical Thrust Bearing Installation.

Generally, thrust bearing losses are required to be minimised and in some instances the roller length will be divided in to two parts to achieve this. However, if a torque opposing the shaft rotation is the design requirement, as in a brake device, the skewed rollers can be used to perform this function. Again intuitively the torque would be expected to be a function of the skew angle, pitch circle diameter, (PCD), of the rollers and thrust loading. Additionally, multiple stages of skewed rollers may be arranged so as to increase the braking torque capacity.

A skewed roller brake unit which is supplied by Dowty Aerospace Wolverhampton, (DAW), the sponsors of this research project, and used within the trailing edge flap actuation system of a large civil aircraft is shown in Figure 1.1-3. This device employs six stages of rollers and generates a nominal torque of 42.9 Nm.

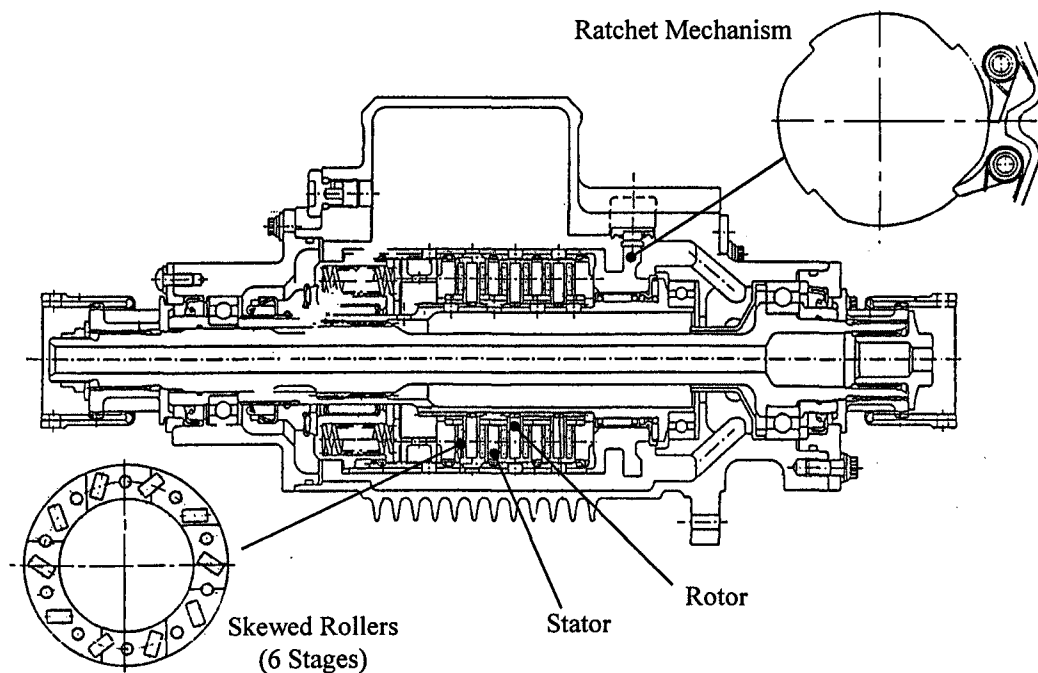


Figure 1.1-3. Skewed Roller Brake Device.

In this specific example, when the flap system is retracting the ratchet mechanism engages and locks the stators to the brake housing. Rotation of the central shaft and rotors necessitates relative motion between the rotors and stators. These are separated by the skewed roller elements and hence a brake torque is generated. The same generic principal of operation can be applied to other brake applications.

DAW are a manufacturer of aircraft flight control actuation systems. Figure 1.1-4 shows the typical aircraft flight control surfaces. Skewed roller devices find applications as brake units within leading edge slat and trailing edge flap actuation systems and in trimmable horizontal stabiliser actuators, (THSA).

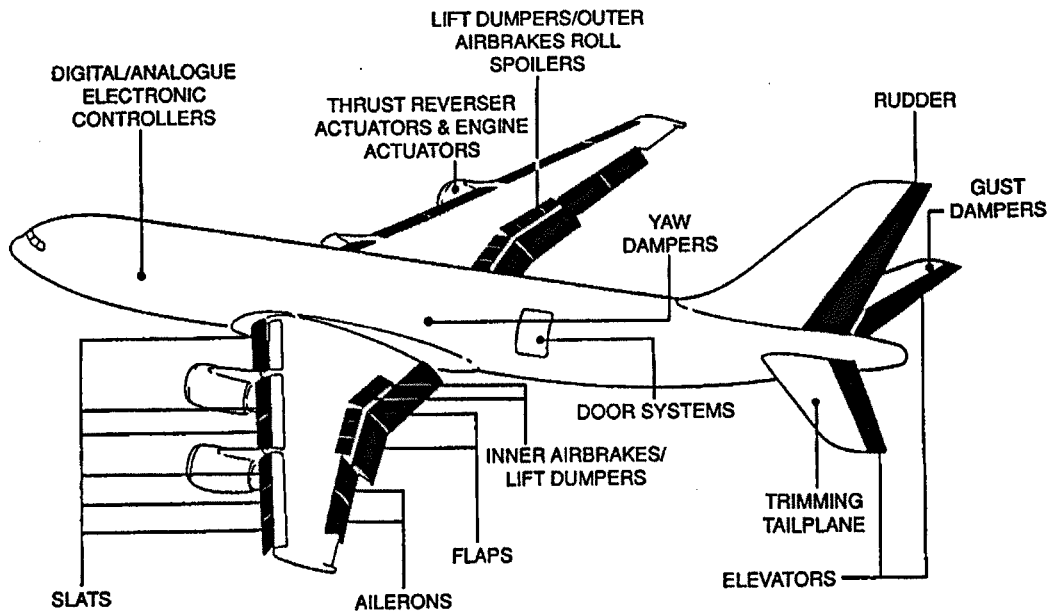


Figure 1.1-4. Typical Civil Aircraft Flight Control Surfaces.

Typical examples of flap and slat actuation systems are shown in Figures 1.1-5 and 1.1-6. Generally these systems comprise a central power drive unit incorporating hydraulic or electrical motors which drive through a gearbox arrangement to rotate some form of transmission shafting system. The transmission shafts transmit power to actuators mounted on the flap or slat panels. The actuators are generally high reduction ratio gearboxes known as Geared Rotary Actuators, (GRA's) as shown in Fig. 1.1-5, or ballscrew actuators, Figures 1.1-6.

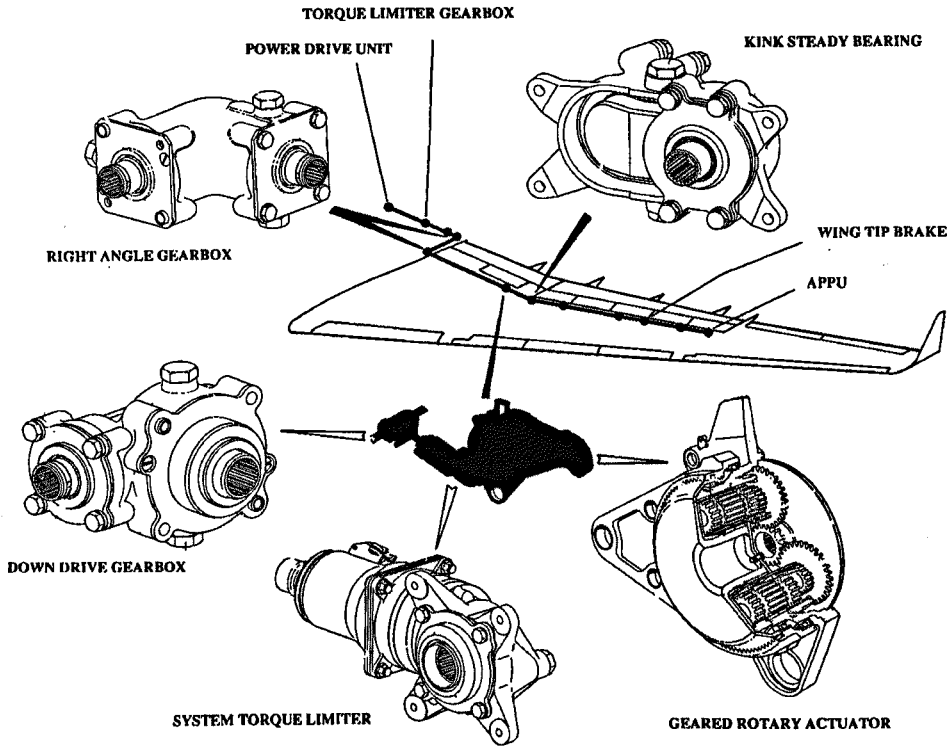


Figure 1.1-5. Typical Geared Rotary Actuator Flap Transmission System.

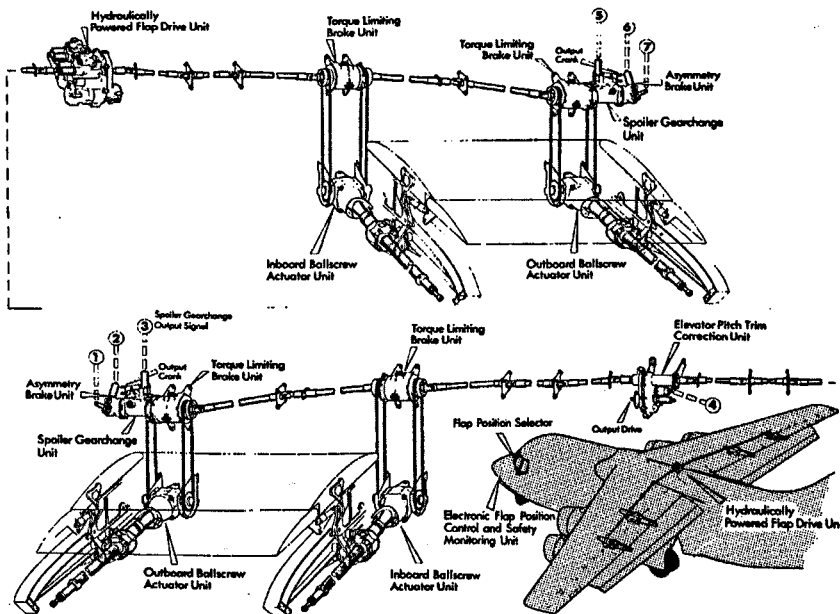


Figure 1.1-6. Typical Ballscrew Actuator Actuation System.

The second major function of the transmission shaft system is to provide a robust, effective and reliable method of synchronising the position of the slat or flap panels across the whole wing. Asymmetry failure modes of panels are defined in the certification rules as 'flight safety critical' hence the probability of an asymmetrical situation must not exceed  $10E-9$  per flight hour. Since the failure of a single component such as a shaft is more likely than this value, back-up braking systems are required to hold the panels in a fixed position following a failure and thus prevent an asymmetry.

During the normal operation of flap and slat systems the panels must be held at predetermined positions which are dictated by the flight phase of the aircraft, such as take-off, approach, landing and the cruise. During these periods the systems are stationary and the aerodynamic loads on the flap and slat panels are reacted by the brake devices within the actuation system.

Various brake devices are available and fall into two broad categories. Active brakes which require computer monitoring of the actuation system and electrical signalling and control of the brake, or passive mechanical brakes. Passive devices provide a braking torque as a function of their mechanical design. The skewed roller brake is such a passive device.

The architecture of individual actuation systems will determine the exact function of the brake device within the system. For example, the device shown in Figure 1.1-3 is a redundant brake which is only required to operate in the event that the primary brakes within the system have failed. This redundancy is required in order to meet the probability requirement of  $10E-9$  per flight hour for asymmetry and uncommanded movement of the panels. In the case of a trimmable horizontal stabiliser actuator a skewed roller brake could be the primary brake, possibly with a hydraulic pressure release clamp type brake as a back-up.



Aircraft actuation system components are required to perform in accordance with their design specification over the full life of the aircraft. This may be for 40 000 flights and 100 000 flight hours over a 25 year service life. A design requirement is often that the equipment should not require any scheduled maintenance through this time. Economics of flight demand that equipment is designed to be minimum weight consistent with meeting the specification. Consequently the designer must be able to accurately predict and maintain the performance of the equipment throughout the full life.

With respect to a skewed roller brake unit, the design engineer must be able to analyse the performance of the design based on the operational parameters of the equipment. Such parameters would include skew angle, PCD, roller dimensions, thrust loading and the frictional characteristic of the roller to race contact. At DAW, an equation has been developed which predicts the torque generated by a skewed roller brake, equation 1.1-1, Thomas and Harris (1993).

$$T = F \cdot \mu \cdot \left( \frac{D}{2} \cdot \sin \phi + \frac{2}{3} \cdot l \right) \cdot N \quad 1.1-1$$

where,  $T$  = torque generated,

$F$  = axial load on the rollers,

$\mu$  = friction coefficient,

$D$  = pitch circle diameter of the rollers,

$\phi$  = roller skew angle,

$l$  = roller length,

$N$  = number of roller stages.

Unfortunately,  $\mu$  in equation 1.1-1 is not the coefficient of friction between two steel components taken from standard reference texts such as Williams (1996) or Kempes Engineers Year Book (1996). The  $\mu$  value is an 'effective coefficient of friction' used to balance the equation and presently can only be determined by

test if an accurate value is required. Consequently, the current design practice at DAW is to use a  $\mu$  value range of 0.066 to 0.092 which has been established from test work conducted on the design shown in Figure 1.1-3. This is sufficient for initial design work, but a development test is also conducted using the actual parameters of the design to establish the actual  $\mu$  value.

The development test work requires a prototype to be manufactured and often a bespoke test rig to be constructed in order to complete the test. This approach is both time consuming and costly. The ideal situation would be that a design tool could be developed which accurately predicted the brake torque generated by a design, based on the known geometrical parameters of the components, and knowledge of the friction coefficient between the rollers and the race.

## **1.2 LITERATURE REVIEW**

### **1.2.1 INTRODUCTION**

A search of open literature has shown that there is no published data which deals directly with the application of skewed roller technology. The author is aware that these devices have been used by American actuation equipment manufacturers, and suspects that data which does exist is proprietary and hence has not been published.

A skewed roller device can be considered to be an inefficient thrust bearing and the tribology which governs traction in line contact bearings can be expected to also govern traction in a skewed roller brake device.

Rolling contact thrust bearings, are well covered by published works. Schroeder (1994) produced a paper defining background terminology and bearing concepts and Zhou and Hashimoto (1995) covered the 'running-in' characteristic of bearings. They found that all bearings exhibit changes in measured friction characteristics as changes to the metal surfaces occur through the initial loading cycles.

Others have considered the general design aspects of bearings from the perspective of wear characteristics, Glaesner et al (1994), and lubrication, Sayles and Webster (1985). The effect of contamination within lubricants for bearing and gear applications has also been researched, Sayles et al (1990).

## 1.2.2 FRICTION AND LUBRICATION MODES

With respect to friction, the classical Stribeck diagram, Williams (1996) is well documented. The Stribeck diagram, Figure 1.2-1, shows the four modes of lubrication found in contacts between surfaces. The diagram shows friction coefficient,  $\mu$ , as a function of lubricant viscosity  $\eta$ , a speed parameter  $\omega$ , and a stress term  $\rho$ . In the case of hydrostatic and hydrodynamic bearings, satisfactory operation of the bearing requires that the solid surfaces are completely separated by a fluid film. As loads increase, the maintenance of a fluid film requires the elastic deformation of the solid surfaces and the increase in viscosity due to pressure to be taken into account, in order to maintain complete separation of the surfaces. This is the classical elastohydrodynamic regime, (ehl).

As loads increase further, or speeds reduce, it is difficult to build up a sufficiently thick film to entirely separate the bearing surfaces. No engineering surface is perfectly flat but consists of a number of asperities and troughs. Some contact of the opposing surface asperities is inevitable and this condition describes the mixed regime. The frictional characteristics are determined by a combination of fluid film effects and surface contact effects.

Eventually the surfaces may only be protected by films with thicknesses on a molecular scale. The bulk properties of the lubricant are not important, the frictional behaviour being determined by the physical and chemical properties of the thin surface films. This state is known as boundary lubrication.

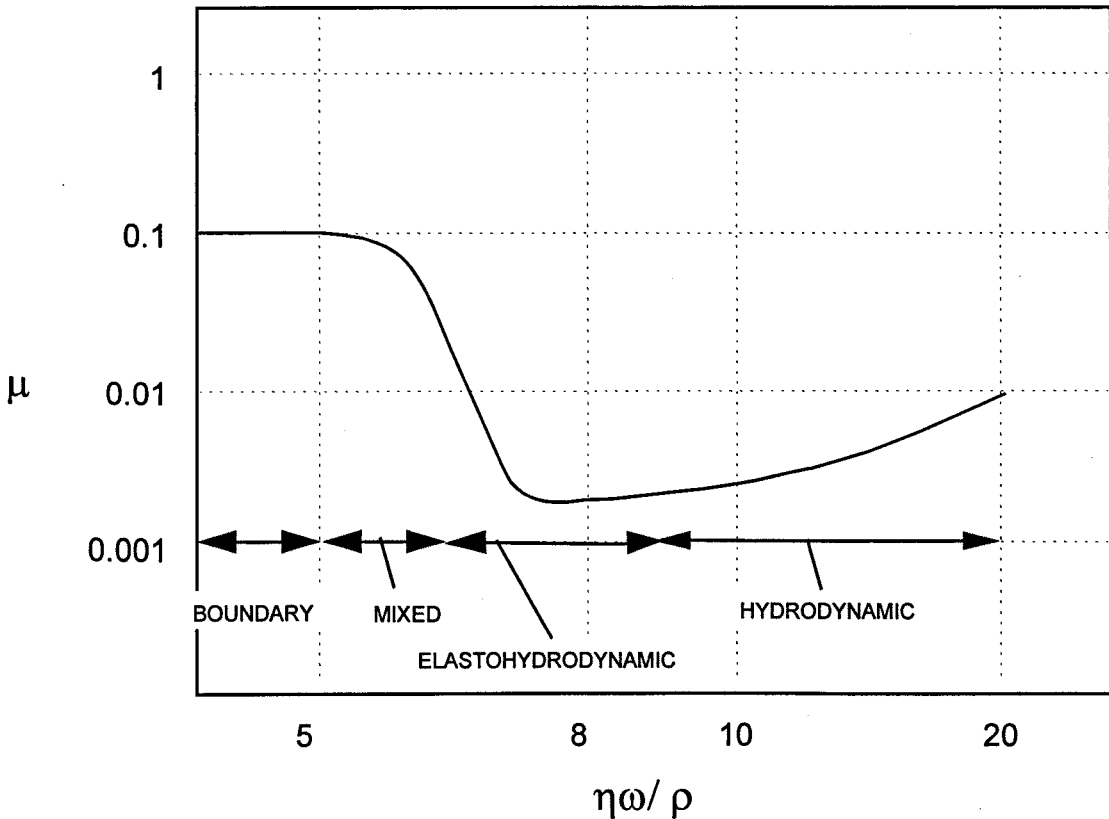


Figure 1.2-1. The Stribeck Diagram for a Journal Bearing. (Based on Williams, 1996).

### 1.2.3 SURFACE ROUGHNESS

The Stribeck diagram was initially developed for the case of a journal bearing, however, other researchers have applied the Stribeck diagram technique to the analysis of friction between steel rollers and a flat plate. This is essentially the geometry of a thrust bearing.

Lin et al (1993) and Horng et al (1994) studied the effect of surface irregularities on the tribological behaviour of steel rollers. The aim of this research was to analyse the lubrication and wear rates of the rollers. A range of surface finish conditions with asperity heights from  $0.2\mu\text{m}$  to  $1.2\mu\text{m}$  and various roughness orientations were considered. The surface roughness orientations were related to the direction of the machining marks relative to the rollers axis. The effect of an extreme pressure additive to the lubricant, was also considered. The papers concluded that both the asperity height and roughness orientation were important

in determining the friction coefficient and that the asperity height was particularly influential with respect to wear rate.

Experimental data had been previously gathered by Jeng (1990). This paper concluded that the orientation of the surface machining marks was more important in determining the friction coefficient than was the asperity height. The transverse orientation always produced the lowest friction, irrespective of asperity height. The lower the asperity height, for a given orientation of machining marks did, however, usually result in a lower coefficient of friction.

These papers confirmed that the Stribeck characteristic was reproducible for those conditions applicable to the experiments reported. They did not however make any attempt to predict the coefficient of friction in the various lubrication regimes.

#### 1.2.4 FILM THICKNESS TO ROUGHNESS RATIO

The transition from one lubrication regime to another has been linked to a dimensionless film thickness ratio, Mech 5270, defined as:

$$\Lambda = \frac{\text{effective film thickness}}{\text{surface roughness (RMS)}} = \frac{h}{\sigma} \quad 1.2-1$$

The effective film thickness for elastohydrodynamic films between smooth surfaces can be calculated from formulas presented in most tribology text books, Dowson and Higginson (1977) and Williams (1996) being examples. It is normal to express the minimum film thickness as a function of a load parameter,  $F'/E'R_e$ , a speed parameter,  $\bar{u}\eta_0/E'R_e$ , and a material parameter,  $\alpha_0E'$ . The semi-empirical power law formula for minimum film thickness, from Mech 5270, is then of the form

$$h_{\min} = 2.65 \cdot R_e \cdot (\alpha_0 E')^{0.54} \left( \frac{\bar{u} \eta_0}{E' R_e} \right)^{0.7} \left( \frac{F'}{E' R_e} \right)^{-0.13} \quad 1.2-2$$

where,  $R_e$  = equivalent radius,

$\alpha_0$  = pressure – viscosity index,

$E'$  = equivalent modulus,

$\bar{u}$  = entrainment velocity,

$\eta_0$  = viscosity at ambient pressure,

$F'$  = load per unit length.

The film thickness over the larger part of the contact is greater than this by about 30%, Williams (1996). These equations indicate a number of significant features of elastohydrodynamic contacts. The relative lack of dependence of film thickness on load, and the virtual independence on contact modulus. The dominant parameters are the entrainment velocity and the viscosity characteristics of the fluid, both in terms of viscosity at ambient pressure,  $\eta_0$  and the pressure-viscosity index  $\alpha$ .

Much research has been dedicated to refinement of the above analysis. Tichy (1995) proposed a model which considered the surfaces to be porous, and Houpert and Hamrock (1986) developed a numerical approach for the calculation of film thickness and pressures in ehl contacts. These and other researchers have attempted to model to higher orders of accuracy film thickness and pressure distributions, often developing complex numerical analyses in the process. The effects of surface irregularities in line contacts have also been modelled and the influence of surface roughness on film collapse within thin elastohydrodynamic films, Shieh and Hamrock, (1991). This paper illustrated that slide to roll ratios of up to two do not significantly influence the minimum film thickness values. However, at ratios above two it can be expected that film collapse will be more likely and a mixed or boundary contact would ensue. Shieh and Hamrock also acknowledge that the lubricant viscosity model chosen has a high influence on the results.

A variety of rheology models have also been applied to film thickness analysis. Jang and Tichy (1995) compared three different models, and Chang and Zhou (1995) compared Newtonian versus non-Newtonian models. In both cases the analysis was aimed at calculation of pressure distribution and film thickness.

Although much effort has been applied in the field of film thickness analysis, few research papers appear to have been published which deal directly with traction at the contact.

### 1.2.5 FRICTION MODELS

The prediction of lubrication regimes for line contacts with lubricants operating in the liquid state was investigated by Schipper et al (1989). They summarised the general assumption at that time that for  $\Lambda$  greater than 3, full film lubrication will occur and for  $\Lambda$  less than 3 mixed lubrication can be expected. They also draw on research by Bair and Winer (1982), who had identified three regimes of behaviour depending on the variation in  $\Lambda$ .

For  $\Lambda$  above approximately five, the film is sufficiently thick for the surface roughness effect to be negligible. The traction force will be a function of the bulk rheological properties of the lubricant at the operating load, speed and temperature.

When the film thickness and the surface roughness are of comparable magnitude,  $1.0 < \Lambda < 10$ , according to Bair and Winer, the traction will be determined by the bulk rheological properties of the fluid, but at the local asperity contact operating conditions.

At lower values of  $\Lambda$ ,  $< 1.0$ , asperity interaction becomes more severe. Bair and Winer referred to this regime as 'boundary lubrication'. Here Bair and Winer attributed the traction coefficient observed to the shear properties of the films adsorbed into the solid surfaces.

Schipper et al (1989) were doubtful that  $\Lambda$  as a characteristic number in the mixed regime is applicable. They argued that the calculation of film thickness is based on smooth surface theory which is not valid in the mixed regime, and that the actual surface roughness of the elastically deformed surfaces was not known. Irrespective of these reservations, the analysis and results presented in their paper are characterised by a lubrication number, ( $L$ ), which is itself a relationship between film thickness and centre-line-average (cla) surface roughness,  $R_a$ . The use of  $R_a$  is somewhat at odds with other researchers who tend more commonly to use the RMS surface roughness,  $\sigma$ .

The investigation used four different lubricants and defined the boundaries between mixed-elastohydrodynamic and boundary-mixed in quantitative terms, as shown on Figure 1.2-2.

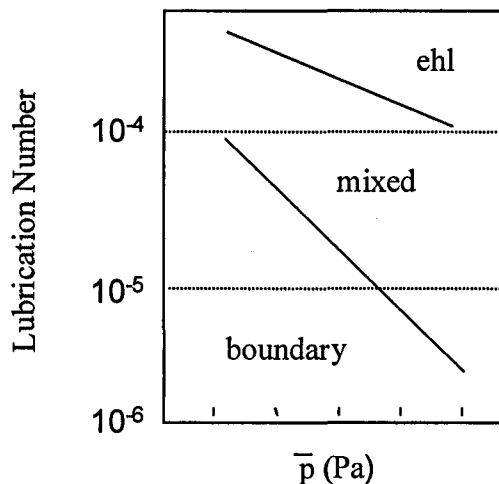


Figure 1.2-2. Lubrication Mode Transitions. [from Schipper et al (1989)]

Schipper and de Gee (1995) extended the work above by the same authors and studied the concept of the lubricant behaving in either a liquid or solid state. The behaviour of fluids in the liquid state and solid state is a concept previously researched. Evans and Johnson (1986a) detailed the rheological properties of three fluids commonly used in elastohydrodynamic contacts. Alsaad et al (1978)



had also conducted research on the transition between the liquid and solid state, the so called ‘glass transition’.

Schipper and de Gee (1995) restated their earlier work (1989) on lubrication mode prediction in the lubricant liquid state. Additionally, they presented experimental data and developed an analysis of the frictional behaviour of these contacts under conditions of full film lubrication taking into account the lubricant solid state behaviour. A flow diagram, Figure 1.2-3, provides a quantitative method of determining lubrication mode as well as frictional behaviour as a function of operating conditions.

Further more, for the liquid state equation 1.2-3 was claimed to predict the coefficient of friction in the mixed regime.

$$\mu_{ml} = \mu_{ehl} + \left[ \frac{\mu_{bl} - \mu_{ehl}}{\ln(2.5\bar{p}^{0.5} \cdot R_a^{0.5})} \right] \cdot (\ln L_{ehl/ml} - \ln L) \quad 1.2-3$$

where,

$\mu_{ml}$  = friction coefficient in the mixed regime

$\mu_{ehl}$  = friction coefficient in the ehl regime

$\mu_{bl}$  = friction coefficient in the boundary lubrication mode

$L$  = lubrication number

$\bar{p}$  = mean Hertzian stress

$R_a$  = surface roughness

Stating that  $\mu_{ehl}$  can be obtained from ‘well known and established ehl theory’, such as Evans and Johnson, (1986b). Coefficient of friction in the boundary regime,  $\mu_{bl}$  is quoted as a bi value coefficient of magnitude 0.09 or 0.13 as the contact moves form micro-ehl to boundary lubrication.

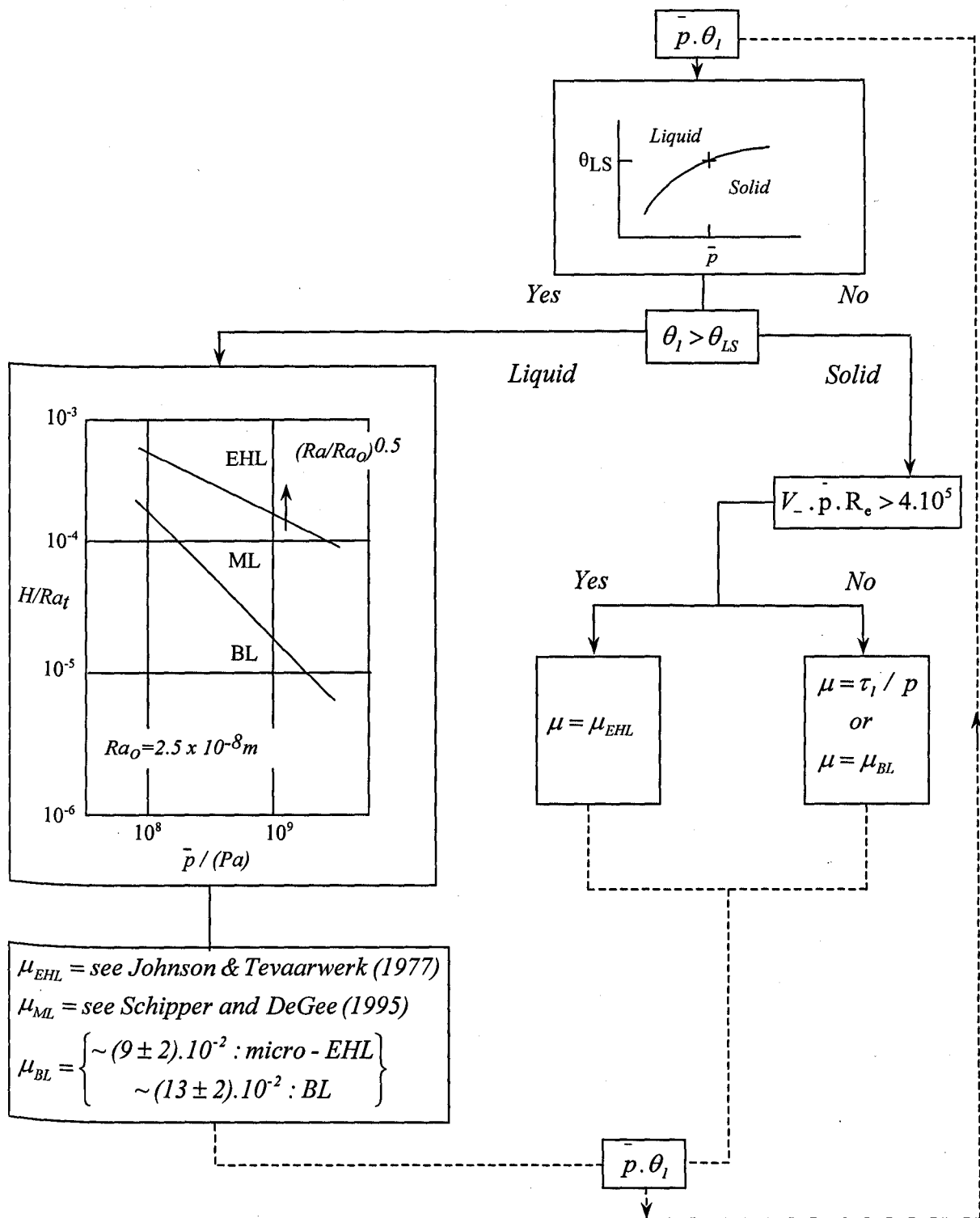


Figure 1.2-3. Flow Diagram to Determine Frictional Behaviour and Lubrication Mode. [Schipper and de Gee (1995)].

Schipper and de Gee (1995) concluded by identifying the following crucial unknowns in their analysis:

- actual temperature of the lubricant as it enters the contact zone and therefore the inlet viscosity. The actual temperature in the inlet is higher than the bulk temperature of the oil due to heat dissipation in the contact and shear heating in the inlet.
- the micro geometry of the surface and hence the  $R_a$  which determine the transitions are not known as a function of wear rate.  $R_a$  values as wear continues are not available analytically.

The contribution of this paper lies in the attempt to provide a quantitative assessment of the coefficient of friction in line concentrated contacts, from operational parameters of load, speed and temperature.

Evans and Johnson (1986b) researched the traction characteristics of full film ehl line contacts for the case of smooth surfaces. They concluded that the frictional characteristic was only a function of the rheological properties of the lubricant. These rheological properties in turn depend on the properties of the fluid and the imposed conditions of load, speed and temperature. For the three lubricants considered, Evans and Johnson created traction maps and associated equations for the prediction of traction coefficient. The co-ordinates for these maps were non-dimensional pressure and a parameter closely related to film thickness. Evans and Johnson maintain that from the known values of load, speed and temperature a point on the map can be identified. The maximum traction coefficient can then be calculated from the constitutive equations.

The maximum traction coefficient calculated by this method links to the analysis conducted by Schipper and de Gee (1995), equation 1.2-3, since this traction coefficient provides a value for  $\mu_{ehl}$ .

The maps produced by Evans and Johnson identified four regimes which differentiated the rheological properties of the fluid. These regimes were identified as Newtonian, Eyring, visco-elastic and elastic-plastic.

In the Newtonian regime where the shear stress is relatively low, the viscosity is a linear relationship of shear stress and shear strain rate. This is the definition of a Newtonian fluid. This condition, Evans and Johnson maintain, occurs at low pressure, high temperature and with thick films.

As the viscosity in the contact increases, with increasing pressure or reduced temperature the shear stress to shear strain rate is no longer a linear relationship. Evans and Johnson adopt the 'Eyring' model to describe the relationship of shear rate to shear stress. The Eyring model had been proposed earlier by Johnson and Tevaarwerk (1977).

Further increase in pressure moves the contact in to the area of the map where traction force is determined by visco-elastic effects in the fluid and also by elastic compliance of the surfaces. Beyond the visco-elastic boundary the contact enters the so called elastic-plastic region. In this region, at small strain rates the traction response is linear but at higher shear rates the fluid can sustain a limited shear stress. The traction force reaches a maximum at a value defined by this limiting shear stress which is a characteristic of the fluid.

The effect of surface roughness was investigated by Evans and Johnson (1987) and related to their earlier work on traction maps (1986b) and the research conducted by Bair and Winer (1982). They concluded that for  $\Lambda$  greater than five, the traction between rolling and sliding surfaces is negligibly influenced by surface roughness. The traction is predictable using the traction maps discussed above. For  $\Lambda$  in the range 0.5 to 6, it was proposed that the effect of asperity interaction was important but that the traction was still governed by the bulk rheological properties of the lubricant. Asperity interaction has the effect of increasing pressure in the local area of the asperity. This has the effect of moving

the operating point to the right in the maps proposed by Evans and Johnson. With very thin films so that  $\Lambda < 0.5$  conditions of asperity interaction and boundary lubrication prevail.

Friction models for line contacts operating under unsteady loading conditions were investigated by Hess and Soom (1990) and Polycarpou and Soom (1995). Hess and Soom published equation 1.2-4 for friction coefficient, this provided a good fit to the data generated in their laboratory.

$$\mu = \frac{\mu_{bl}}{1 + C_1 \left( \frac{\eta V}{\sqrt{FE}} \right)^2} + C_2 \cdot \frac{\eta V I}{F} \quad 1.2-4$$

where,  $\eta$  = lubricant viscosity,

$V$  = velocity in the contact,

$E$  = Youngs Modulus,

$C_1, C_2$  = constants.

It is claimed that the first term of the equation describes the coefficient of friction within the mixed lubrication regime, with the second term added to determine the friction coefficient in the hydrodynamic regime. The constants which provided a good data fit for Hess and Soom are:  $C_1 = 1.43 \times 10^{17}$ ,  $C_2 = 8.19 \times 10^2$  and  $\mu_{bl} = 0.145$ .

Polycarpou and Soom (1995) extended the research in to friction models applicable to conditions of unsteady sliding contacts operating in boundary and mixed lubrication regimes. The introduction to this paper states that *'theoretically based friction relationships are not available for contacts operating in the mixed or boundary lubrication regimes'*. The reference list within the paper cites the work discussed earlier in this chapter by Bair and Winer and Evans and Johnson. However, it does not acknowledge the work of

Schipper et al (1989). Conversely the work by Schipper et al does not cite previous work in the field by Polycarpou and Soom.

### 1.3 PROJECT MOTIVATION

The analysis methods available to DAW are not sufficiently advanced to allow a skewed roller brake design to be prepared and hardware manufactured which will meet the design specification, without the need for design phase prototype testing. The results of the prototype test are used in an iterative loop until the specification is met. The design phase applies to both the competitive bid situation prior to contract award and after contact award when the design is being developed in to detail component drawings. These prototype tests are required to minimise technical risk, which cannot be mitigated by the presently inadequate analysis techniques.

The preceding literature review has demonstrated that published data dealing directly with skewed roller devices does not exist. The literature which is available and which provides analytical methods of calculating traction coefficients illustrates that analytical models for traction are complex. Models do not exist which can be readily utilised in engineering design calculations.

The traction maps presented by Evans and Johnson (1986b and 1987) appear to be an accepted approach for the case of full film lubrication. However, for very thin films, such that the contact operates in the mixed or boundary lubrication regimes, the literature search did not uncover any widely accepted models. Models have been proposed by Schipper and de Gee (1995) and Polycarpou and Soom (1995). In both of these cases the models were based on experimental data and the models no doubt reasonably reflect the respective data sets.

The above models can be used in combination with equation 1.1-1 to predict the torque capacity of a skewed roller device. The accuracy of these predictions is not established or validated against experimental data.

The motivation for this project is to develop a design tool for use by design engineers within DAW and to establish the boundaries within which that tool may be used with confidence. This should obviate the need to conduct design phase prototype tests.

#### **1.4 TECHNICAL RESEARCH OBJECTIVE**

The specific objective of this project can be defined as:

*To develop an analytical design tool such that skewed roller brake performance can be predicted from operational and geometrical design parameters, without recourse to prototype testing during the design or proposal phase of the project.*

#### **1.5 COMMERCIAL OBJECTIVES**

The Engineering Doctorate programme, (EngD), differs from traditional technical PhD research. It requires research to be directed at a specific problem of relevance to the sponsoring organisation, in this instance Dowty Aerospace Wolverhampton. The EngD also fundamentally requires an inter-disciplinary approach such that the researcher has a significant appreciation of the commercial issues associated with the work, and develops core management skills and competencies. (Ref. Appendix A).

Consequently, this research had commercial objectives in addition to the technical objective defined above. The commercial objectives were:

- i) To prepare a business case for the research defining the commercial deliverables and justifying the resource allocation to the programme.
- ii) To develop a deeper technical understanding of the frictional characteristics of skewed roller devices so that DAW technical expertise

may be used as a marketing tool when competing for new business. This technical differentiation relative to competitors may enable premium pricing of the DAW solution, or open up new markets.

To enable the project to meet these objectives, project management tools and techniques must be employed to complete the project within the constraints of the allocated budget and timescale.

Additionally, it should be recognised that the author is in full time employment within DAW, and must maintain his position within a competitive management team. Hence, elements of the experimental work must be completed by undergraduate student trainees. These are on industrial placements as part of their sandwich courses. This approach is entirely consistent with the Engineering Doctorate objectives, Sanderson (undated).

## **1.6 RESEARCH METHOD**

To achieve the technical objective the project was broken down in to four stages.

Stage one recognised that an established design tool already existed at DAW and that the apparent deficiency with this tool was the accurate prediction of the coefficient of friction. Stage one therefore had the objective of completing a literature review which would identify analytical models which would allow traction coefficients to be predicted based on the operation parameters of the contact.

Stage two involved gathering test data. Within the limitations of the test equipment available at DAW, the largest range of contact pressure at the rollers, rotational speed and skew angle of the rollers would be tested. The baseline lubricant would be Brayco 795, as used in the DAW production unit. Comparative tests using Catenex 79 fluid would also be conducted since rheological data on this lubricant is widely available in the literature.



Stage three would compare the analytical friction coefficient model predictions to the measured test result data set. This process would possibly identify deficiencies in the design tool currently available other than the prediction of traction coefficients.

Stage four recognised the likely outcome from stage three and had the objective of developing the design tool to meet the overall objective of accurate analysis based on operational parameters. Additionally, the scope of applicability of the tool would need to be defined. Clearly, stage four represents the conclusion of the research with the delivery of a validated design tool.

The detail tasks required to follow this research method were identified and planned across the four years using project management tools as discussed in the section 1.8.

## **1.7 COST BENEFIT ANALYSIS OF THE RESEARCH**

### **1.7.1 THE BUSINESS DECISION**

Should DAW spend £38000 (Appendix B) on a project to develop a skewed roller design tool ?

### **1.7.2 THE MARKET PLACE**

DAW manufacture aircraft flight control actuation systems for military and civil aircraft. These actuation systems can be divided into two principal product technology groups:

- i) Hydraulic actuators, mainly for primary flight control surfaces. Included in this product technology are also hydraulic engine thrust reverser systems.

ii) Mechanical actuation systems and components mainly for flap and slat actuation systems. DAW has ambitions to also manufacture trimmable horizontal stabiliser actuators, since these comprise many of the fundamental elements found in a typical flap actuation system.

The distribution of the companies turnover for 1998 between the hydraulic and mechanical technologies is shown in Figure 1.7-1

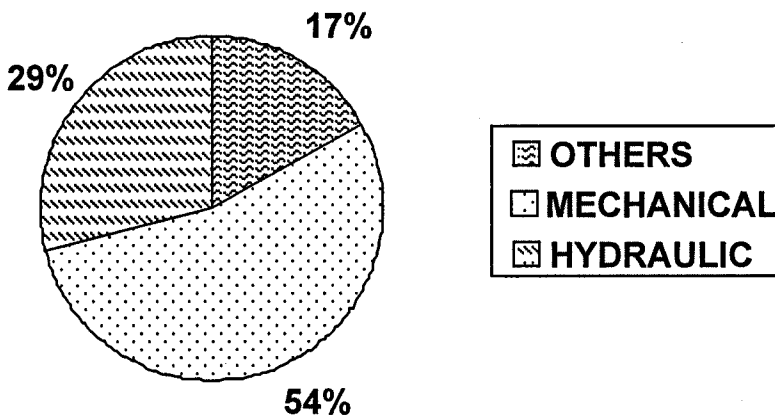


Figure 1.7-1. DAW Turnover Analysis for 1998. (DAW internal data)

Brake devices, where skewed roller technology finds applications are used within the mechanical actuation systems. Thrust reversers and hydraulic actuators will not be considered further in this thesis.

DAW sales of mechanical actuation equipment is shown in Figure 1.7-2 for 1998.

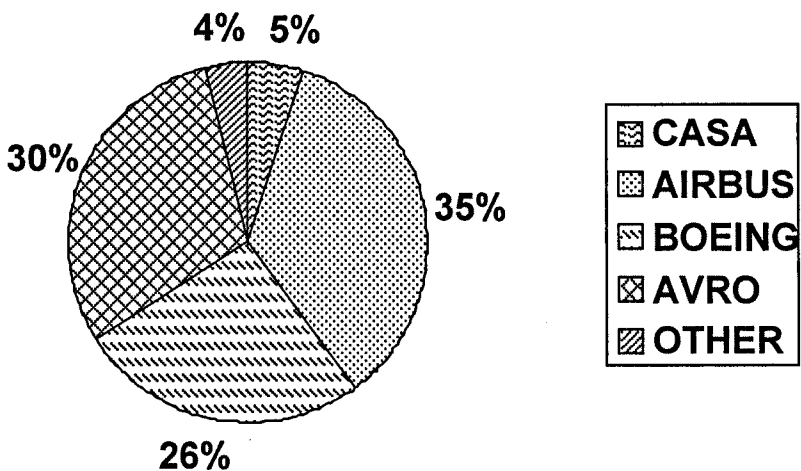


Figure 1.7-2. Mechanical Actuation Sales for 1998. (DAW internal data)

The above sales picture clearly changes over time. Recent new business success's on Boeing 767-400 and major modifications programmes to the Airbus A340-500/600 could also be included. Both programmes are in the design phase and hence have not entered production. Projecting this analysis forward to the year 2005, Figure 1.7-3 illustrates the dominance of Boeing and Airbus products within the business.

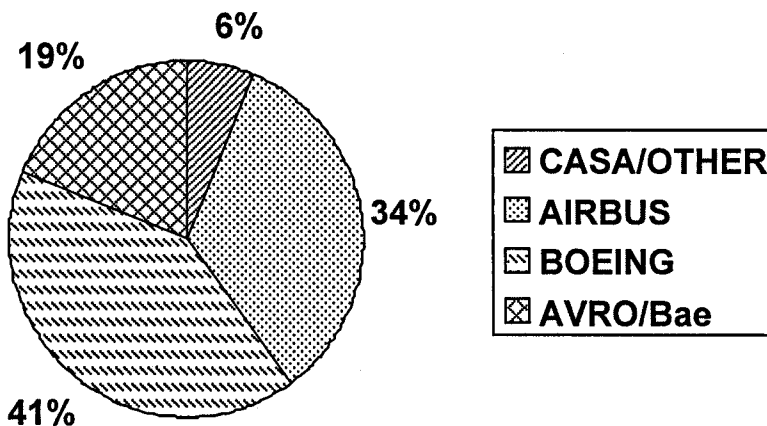


Figure 1.7-3 Projected Mechanical Actuation Sales for 2005. (DAW data)

DAW operate within a global market place. Many aircraft, manufactured by many different airframe manufacturers require the type of actuation systems designed and manufactured by DAW. Aerospace requirements for minimum weight products which meet a specific aircraft specification demand that systems are designed specifically for the aircraft concerned, off the shelf actuation systems are not generally appropriate. Consequently, the overall market is enormous, ranging from aircraft such as the Boeing 747 to small business jets in the civil sector, and an equally broad range in the military sector. DAW does not have the resources to compete in every new programme which is launched in the above market.

The DAW strategy is to segment this global market and to concentrate on a small number of customers, in either the civil or military sectors. With respect to civil aircraft this strategy means focusing on Boeing and Airbus, who jointly dominate the civil aircraft manufacturing market. The market for aircraft above 100 seats is dominated by Boeing and Airbus, with each taking 50% market share, Flight International (July 1998). Of the remaining manufacturers, DAW concentrate on Avro and in the wider context the parent company, British Aerospace. Military programmes are notoriously politically biased, but concentration on British Aerospace tends to cover this sector.

In summary, the market in which DAW operate could be summarised as:

*Mechanical actuation systems and components for flap, slat and trimmable horizontal stabiliser applications at Boeing Commercial Aircraft, Airbus and British Aerospace.*

Opportunities with other customers outside of the above definition are also pursued when it is perceived that DAW has a competitive advantage and the programme is considered to be robust.

### 1.7.3 THE COMPETITORS

Actuation systems and components in the above market are designed to meet a specification. When a new programme is launched by a manufacturer such as Airbus for example, the specification for particular equipment or systems is issued to potential suppliers. The suppliers are in a competitive situation and must propose a design solution meeting the specification at a fixed price. The aircraft manufacturer will then select one supplier who will be awarded the contract to design and manufacture the proposed solution.

The competitors differ depending on which customer is considered. The main competitors are defined in Table 1.7-1

A number of factors influence the selection of the supplier. Common criteria such as past delivery performance, quality and price are all crucial in securing new business. The engineering functions within organisations such as Boeing and Airbus also have an influential impact. Hence developing a good relationship with these engineering functions is important.

In practical terms this means that DAW must support and build relationships with four different engineering teams:

- i) Boeing Commercial Aircraft, high lift team.
- ii) Airbus high lift team, in practice this responsibility lies with Daimler Benz based in Bremen and Hamburg.
- iii) Avro International, based in Woodford, UK.

Customer	US Competitors	European Competitors	Asian Competitors	Comments
<b>Boeing Commercial Aircraft</b>	Sunstrand Moog Western Gear Curtis Wright	Liebherr	Shimadzu	Very strong. Established position with strong engineering capability.  As per Sunstrand.  In decline.  Appear to be in decline, due to engineering deficiencies.  No Boeing products hence high barriers to entry.  Strong in manufacturing, weaker in design. Tend to concentrate on make to print*.
<b>Airbus (Daimler Benz)</b>	Sunstrand Curtis Wright	Liebherr/Lucas team.		Weak. No position in flight controls at Airbus. Not European. High barriers to entry. As for Sunstrand.  Dominant position. Make complete flap and slat systems for A300/310/319/320/321. Complete slat system on A330/340 and share flap system with DAW on same aircraft.
<b>British Aerospace and Avro</b>		Liebherr/Lucas		As above for BAe Airbus.  RJ146 flap system DAW supply. Turboprop and business jets business sold to Raytheon. High Lucas content.

Table 1.7-1 Major Competitors. \* Make to print is manufacture by the supplier to the drawings of the customer.

iv) British Aerospace - Airbus, based in Filton, Bristol.

General methods by which these relationships can be developed include research into new technology and the sharing of data associated with such research, and successfully completing those new projects which are won.

## 1.7.4 SKEWED ROLLER DEVICES, ALTERNATIVES AND ADVANTAGES

### 1.7.4.1 Boeing Commercial Aircraft.

The asymmetry protection devices used by Boeing tend to be passive or self energising mechanical components.

Boeing have used skewed roller devices for many years in low integrity, non-flight control applications. Over recent years, certainly since 1993, skewed roller brakes have also been introduced into flight control systems. Table 1.7-2 defines the known flight control applications.

Aircraft	Application	Introduction into service date	Design Authority
Boeing 757	Flap Ballscrew Actuator	not known	Boeing
Boeing 777	Flap System No-Back Brake	1996	DAW
Boeing 737-600/700/800	Trimmable Horizontal Stabiliser Actuator	1997	Boeing

Table 1.7-2. Skew Roller Device Applications.

### 1.7.4.2 Airbus Industrie

Airbus engineering tend to take an alternative approach to asymmetry protection. Active hydraulic brakes are used. These are signalled by control computers which detect an asymmetrical situation and signal the brakes to lock the system. This architecture requires a high integrity, high iteration rate

computer in order to detect the fault and signal the brakes before the asymmetry exceeds acceptable thresholds.

Passive brakes in general do not feature in the flap and slat actuation system architecture described above.

THSA's at Airbus do incorporate passive friction plate brakes. These are an ideal candidate for skewed roller technology. A trade study performed by DAW (DAW, 1998) on a THSA application identified that an actuator designed using a skewed roller brake would be 5.5 kg (3.3%) lighter and require 68.2 litres per minute less hydraulic flow than the comparable friction plate design. In this example, the brake had to fit over the THSA output ballscrew shaft and hence the operating diameter of the brake was determined by the diameter of this shaft. Combining this diameter with the friction characteristics of conventional friction discs resulted in a brake torque considerably higher than required. This became the sizing case for the hydraulic driving motors. A skewed roller brake could be designed to more equally match the required brake torque by selection of the skew angle and hence allowed the hydraulic motors to be smaller.

Passive brakes using paper based, sintered bronze and more recently carbon and graphite materials have been employed for many years. The main disadvantage of these materials is susceptibility to wear and friction coefficient stability over the life of the unit. Brakes designed to use these materials, in flight control applications, usually incorporate wear detection devices and require maintenance to replace brake surfaces. The best materials, carbon and graphite, are more resistant to wear. However, they are also more costly than the materials used in skewed roller devices.

Definite advantages, in terms of wear resistance, cost and reduced complexity exist for skewed roller devices. The key issue to be overcome before they would be readily accepted at Airbus is technical risk.



#### **1.7.4.3 AVRO and British Aerospace.**

The AVRO RJ 146 aircraft uses active asymmetry brakes as per the architecture described above. Future AVRO philosophy is unclear at the present time.

Skewed rollers are being incorporated into the ballscrew actuators driving the Nimrod 2000 Maritime Patrol Aircraft flap panels. These actuators are being designed by DAW.

#### **1.7.5 SKEWED ROLLER DEVICES, SUMMARY**

The major market for these devices is at Boeing. They are compatible with the Boeing philosophy with respect to asymmetry protection and are an established technology with accepted low technical risk. Sundstrand and Lucas Aerospace are probably the major competitors within this market segment. Both companies capabilities in skewed roller technology is unknown.

At Airbus, the current flap and slat asymmetry protection philosophy does not require passive brake technology and hence skewed roller devices are not applicable. Applications do exist in THSA but the technology has not been used before at Airbus and hence would be considered a technical risk. A thorough understanding of the theoretical background of the devices would be part of a strategy to convince Airbus that this technical risk was low.

#### **1.7.6 NEW BUSINESS PROCESS**

Most new business competitions follow essentially the same process. The customer will write a specification for a system or component and issue it to potential suppliers. Those suppliers typically have six to eight weeks in which to prepare a proposal.

The competing proposals are assessed by the customer based on a wide range of factors, but certainly including technical acceptability of the solution and price. The conclusion to the assessment phase is usually a contractual negotiation leading to the signing of a contract.

The six to eight week proposal time is a short period of intense activity. From an engineering point of view the objective is to design a solution which as a minimum is technically acceptable and represents a minimum cost and weight solution. If possible some form of technical differentiation should be developed in the proposal. The aim is to promote the solution from the general category of 'technically acceptable' to 'wanted by the engineers'. It is often the case that if a solution is differentiated in this way from the competing proposals, it allows some element of premium pricing, generating a better return for the business.

Skewed roller technology provides a direct method of differentiating DAW from most of our competitors, particularly at Boeing. These devices can generate real advantages, particularly in terms of weight, flow consumption and wear over life. However, the need to design, construct and test a prototype unit within the six to eight week proposal phase is both expensive and challenging. An established design tool would achieve two objectives. Firstly, remove the need to perform such testing and secondly, allow DAW to be recognised as developing the technology whilst sharing the results with our customers. This process helps to cement the relationships between DAW and our customer engineering functions.

Post contract award, the normal product development process at DAW involves a design phase culminating in the production of detail drawings for the manufacture of the initial batch of test units. When these units are available a development test activity ensures that the equipment functions in accordance with the specification and the design intent. This development testing precedes the formal qualification tests, which demonstrate the equipment is fit for flight.

Equipment with a particular technical risk, which cannot be mitigated fully by analysis, will require extra prototype testing during the design phase to minimise the risk.

The removal of the need to conduct these design phase prototype tests is a key benefit both from a financial point of view and by allowing the engineering resource to concentrate on enhancing the benefits of the design, rather than designing and building prototype units. This could improve the probability of winning new business during a proposal phase, and reduce the time to market in the post contract phase.

### 1.7.7 FINANCIAL ANALYSIS

Net Present Value, (NPV), techniques have been applied in order to construct a financial model for the project. The details are defined in Appendix B.

The investment costs of £38000 relate to the cost of sponsorship on the EngD programme at Cranfield and the cost of undergraduate support of the research at DAW. The principal direct financial returns from the project, on achievement of the technical research objective, will be the removal of the need to conduct prototype testing in the future. It has been assumed that two prototype tests will not be required as a result of this research programme. These savings can be combined with the EPSERC grant and hence the total returns from the project were estimated to be £69000.

This direct financial benefit is important, but the most significant business benefit to DAW would be enhanced opportunities to win new contracts. The returns in this case would far exceed the £69000 associated with test reductions. However, leverage of the research to potentially win new business cannot be included in an NPV analysis.

The financial analysis shows that the project yields a healthy NPV of £10358 and hence on financial grounds meets the assessment criteria.

## 1.7.8 ALTERNATIVE APPROACHES

### 1.7.8.1 Do Nothing

In this case the current ranges of effective friction coefficient would continue to be adopted and each proposal would need to be backed by a development test or at least the commitment to conduct such a test early in the design phase.

This approach means that the build up of data is very slow, dictated by the proposal frequency which include a skewed roller. Hence, the DAW experience base remains low and our technical understanding of the device remains low. In this case it is unlikely that DAW will overcome the technical risk issues which will be raised by Airbus.

Similarly, DAW will not be seen as proactively developing the technology. This is important, particularly at Boeing where a willingness to share information and technology is integral with developing the engineering relationship.

The cost of running development tests during proposals is in excess of the costs of supporting the EngD research. The 'do nothing' option is untenable.

### 1.7.8.2 An Empirical Approach

The risk associated with the 'do nothing' option discussed above could be reduced by conducting a series of development tests as part of a smaller scale research programme than the EngD.

The results of the development tests could form an empirical database of information to be used in future designs. This approach would not move DAW any closer to the objective of developing a design tool. The selection of the test conditions would be very difficult. It is unlikely that the selected conditions would be a match for the conditions required on a future design. Consequently, without the theoretical background gain through the EngD approach, extrapolation of the results would be difficult.

Finally, the cost of this approach would be approximately the same as conducting the tests during a bid phase. Hence, no financial benefit accrues from this approach whilst it does not meet the technical objectives.

### **1.7.8.3 Develop Alternative Brake Technologies**

As an alternative to developing design capabilities with respect to skewed roller devices, resources could be spent developing alternative brake technologies.

The principal alternative is the conventional friction disc device. DAW have experience with these devices and understand the disadvantages of them, as discussed in section 1.7.4.2. Hence defining a research programme with the objectives of finding solutions to these disadvantages would be relatively simple.

Skewed roller devices have a recognised market at Boeing and a potential market at Airbus. The suspension of development of skewed roller technology will erode DAW's ability to win contracts at Boeing and will prevent penetration of the Airbus market.

Research and development of existing or novel brake technology is not an alternative to developing skewed roller technology but should be considered in addition to this work.

## 1.7.9 COST BENEFIT ANALYSIS SUMMARY

Boeing and Airbus are the two key DAW customers. The relationship between engineers at DAW and these customers has a significant impact on the ability to win new contracts. At Boeing this research will help to develop these relationships further through the sharing of information. At Airbus it will help to win the technical risk debate and open the Airbus market to DAW skewed roller technology.

The advantages of skewed roller technology compared to conventional passive brake technologies are clear in terms of resistance to wear, stability of torque produced and cost. This research programme should increase the design capability of DAW in skewed roller technology beyond both that of customers and competitors. This technical differentiation will provide the opportunity to premium price the DAW product.

The achievement of the technical research objective will provide a robust, validated design tool and enhance the design and analysis techniques available at DAW. This will remove the need in the future for design phase prototype tests, generating savings in both time and money. The financial case is made.

## 1.8 PROJECT MANAGEMENT TOPICS

### 1.8.1 INTRODUCTION

The successful completion of any project requires the project deliverable to be produced on time and within the defined project budget. Management tools and techniques are widely adopted within industry to ensure that projects are managed successfully. The tools applied to this project comprise a sub-set of the tool kit used at DAW.

Initially a large project is split in to smaller, more manageable work packages. These are defined within a documented Work Breakdown Structure, WBS. The project stages defined by the research methodology, plus the commercial objectives discussed above, together with the taught modules within the EngD are effectively the WBS for this project. These stages were broken down in to detail tasks and scheduled across the four year timeframe of the EngD to create the project plan.

The project budget was defined and agreed by the sponsors as part of agreement of the business plan. A thorough risk analysis was also conducted on the project to define those risks which would most likely occur and have the most impact on the project. These were then singled out for specific risk reduction actions.

## 1.8.2 PROJECT PLAN

A four year summary plan and a more detailed year by year plan was used to control the project work. The year by year plans were updated at the start of each year and progress was reviewed against the plan at regular intervals.

Appendix C1 presents the initial four year plan which was created at the beginning of the project. Also presented is a revised four year plan which more accurately reflects the actual order and timescale of the events as they occurred, together with a description of why events occurred as they did.

The four year plan was used to define the requirements for resource other than the author. This resource was required to complete the test work defined under stage two and any validation of a revised design tool under stage four.

### 1.8.3 PROJECT BUDGET

The project budget is presented in Appendix C2. The budget defines the explicit costs of the project to the sponsor. For the purposes of the budget, the overhead cost associated with the authors employment and that of the undergraduate trainee's who assisted with the work have not been included. The total budget was set at £8591, and was overspent by £427. This was primarily due to the unbudgeted travel costs to attend the specialist engineering courses at Leeds University.

### 1.8.4 PROJECT RISK ASSESSMENT

The risk assessment was conducted against the objective of developing the design tool as described in section 1.4. The approach used at DAW was adopted. This entails a quantitative judgement of the likelihood of the risk occurring and a quantitative judgement of the impact of that risk on the outcome of the project if the risk is realised.

Appendix C3 defines the 3×3 matrix used to rank the individual risks. Those risks which are both highly likely to occur and have a major project impact must have a risk mitigation action defined. Completion of this mitigation action must make the risk either less likely to occur, or have a lower impact if it does.

The author has used this particular method of risk analysis on a number of occasions and found it to be an essential management tool. For the generic project situation, the brainstorming session required to determine the risks involves all project team members. Definition of the mitigation actions and their subsequent completion provides an effective method of forcing, often unpleasant, measures to be taken.



#### 1.8.5 PROJECT MANAGEMENT SUMMARY

This project has been delivered on time and within budget. By definition, the project management of this project has been acceptable.

#### 1.9 BUSINESS CASE SUMMARY

Achievement of the technical research objective of this project will provide DAW with a validated skewed roller design tool. This will potentially provide a means to demonstrate, particularly at Airbus Industrie, that skewed roller technology is low risk, and to Boeing that DAW have developed a competitive advantage in the design of these devices.

Demonstration to Airbus of this design capability may enhance future opportunities to open this new market for skewed roller devices. Also, in established markets such as Boeing, the design tool may enable the DAW solution to be premium priced due to DAW's technical superiority relative to their competitors.

In addition to these new business opportunities, the cost benefit analysis clearly indicates a positive effect of the project over the next ten years. The primary benefits are in terms of design and proposal phase time and cost reductions through the elimination of design phase, prototype test requirements.

A number of friction models have been identified in the literature survey which provide starting points for the development of the required design tool. No published data is available specifically relating to skewed roller devices. The academic challenge of the project is sufficient.

## **2. SKEWED ROLLER BRAKE TESTING**

### **Chapter Summary**

This chapter discusses the experimental work conducted to investigate the frictional characteristics of skewed roller devices. Test equipment, analysis methods and experimental results are all discussed.

- 2.1 Introduction
- 2.2 Test Rig Description
- 2.3 Description of the Test Unit
- 2.4 Test Procedure
- 2.5 Inherent Test Unit Drag
- 2.6 Torque Characteristics
- 2.7 Stribeck Diagram
- 2.8 Film Thickness Considerations
- 2.9 Discussion of the Test Results
- 2.10 Results Conclusion and Business Case Implications

The essential conclusions drawn from the experimental work are that:

- i) It has been confirmed that the brake torque is an approximately sinusoidal function of skew angle and apparently linear function of axial load.
- ii) When plotted across a sufficiently wide range of lubrication number the classical 'Stribeck' diagram is produced.
- iii) The currently employed method at DAW of taking a 0.092 maximum and 0.066 minimum value for friction coefficient irrespective of operational conditions is inadequate.

## 2.1 INTRODUCTION

In order to support proposals which were submitted during 1992 and 1993, DAW conducted a number of ad-hoc tests on skewed roller devices. These were tests designed to assess the torque characteristic of the specific design being developed at that time. A structured series of experiments across a range of speeds, applied loads and skew angle conditions have not previously been conducted by DAW, although the company has had access to a limited dataset produced by another organisation, with their permission. Hence the envelope of operational parameters across which the DAW torque equation, Equation 1.1-1, is applicable has not been explored.

Consequently, the objectives of conducting tests to support this thesis were:

- a) Assess the torque characteristic of skewed roller devices across a range of speed, applied loads and skew angles.
- b) Assess the effect on the torque characteristic of different lubricants. The aerospace hydraulic fluid used in the DAW produced unit for Boeing is known as Brayco 795. Rheological data for this fluid is not generally available in published literature, and hence linking performance with published friction models was not easily achieved. As a comparator, the performance of the device when with a commercial lubricant, Shell Catenex 79, was to be established. Rheological data for Catenex 79 is widely available in published literature since this fluid has been widely used in lubrication analysis in the past, albeit under the alternative trade names of Vitrea 79 and HVI 650.

- c) To provide a data set for use in comparison with theoretically derived friction coefficient values and their applicability to the existing DAW formula for torque calculation.

An existing test rig at DAW was recommissioned in order to conduct the testing, and is described in the following section.

The test specimen was an adaptation of an existing DAW qualification test unit. This unit was adapted to house a double stage of skewed rollers. Roller cage test pieces were manufactured with skew angles from 15 to 55 degrees in 10 degree increments. The test unit is described in detail in section 2.3.

## 2.2 THE TEST RIG DESCRIPTION

The test rig was initially used in 1992 as an early development and production acceptance test rig. It was replaced by an automated rig for the testing of production units in 1993.

The rig is shown in Figure 2.2-1 and can be seen to comprise of:

- A Lebow Torque Cell.
- A proprietary 3 kW motor and drive.
- A holding fixture for the test unit.
- A cooling fan (not relevant to this thesis).

The torque cell allows the torque to be constantly monitored during testing through an output that can be connected directly to a plotter. The motor speed control was via a Radio Energie tachometer to a variable potentiometer allowing variations in speed to be made between up to a maximum of 650rpm. The speed

could be recorded, but the control system was very stable and hence did not warrant constant monitoring.

The test unit was mounted to a fixture that was bolted onto the bed of the test rig. The input coupling of the test unit was connected to the output side of the drive motor, through the torque cell. The motor speed and the torque cell signal were both displayed on the control cabinet front panel.

A computer was used to monitor the temperature of the unit throughout each test at one-second intervals. The thermocouple is a K-Type and is positioned in the base drain plug. Due to its positioning it is constantly submerged in the lubricant.

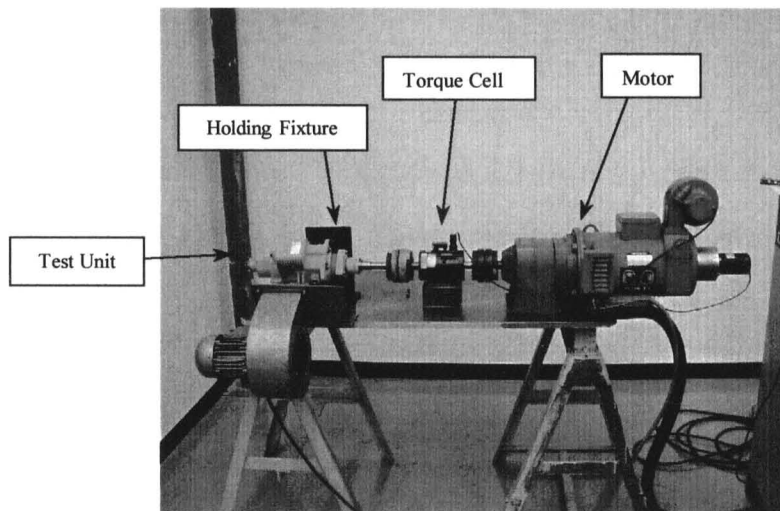


Figure 2.2-1 –Test Rig Installation

Detailed Information on the test rig, including component specifications and calibration certificates can be found in Appendix D.

### 2.3 DESCRIPTION OF THE TEST UNIT

The skewed roller test unit is shown in Figure 2.3-1. The central shaft is supported on roller bearings and locates the skewed roller brake components. These are contained within the brake housing which rotates with the central shaft in one direction and is held fixed to the casing by a ratchet in the opposite direction. Hence these are known as the 'freewheel' and 'braking' directions. A single plain brake disc is splined to the central shaft and is called the rotor. Two plain brake discs are splined to the brake housing, and are designated stators since they do not rotate in the braking direction. The rotor and stators are separated by the skewed rollers, housed in the pockets of the skew plates or cages.

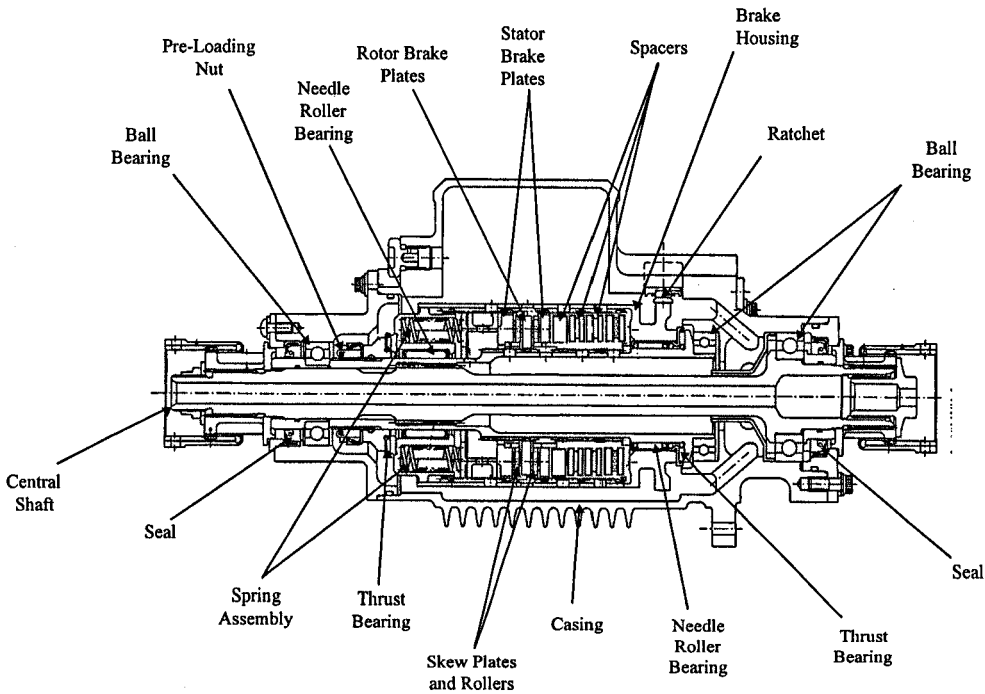


Figure 2.3-1 – Skewed Roller Test Unit

An exploded view of the test unit components are shown on Figures 2.3-2 and 2.3-3.

When rotating in the freewheel direction there is no relative motion between stators and rotors. However, in the braking direction the central shaft and rotor rotate, the stators remain fixed, and the skew rollers act as inefficient thrust bearings.

The axial load on the skewed rollers is applied by a number of helical springs, reacted by the pre-loading nut. The preload was determined using a separate test fixture which measures the installed spring load of the device. Seven evenly distributed springs were used when the unit was pre-loaded with 890N and fourteen springs were used for the 1780, 2670, 3560 and 4450N pre-load settings.

After the pre-load has been determined, the fully assembled brake housing was lowered into the casing. The top half of the casing was then located in place and the unit was filled with 1250ml of lubricant and positioned onto the test rig.



Figure 2.3-2 – Components Removed from the Skewed Roller Device.

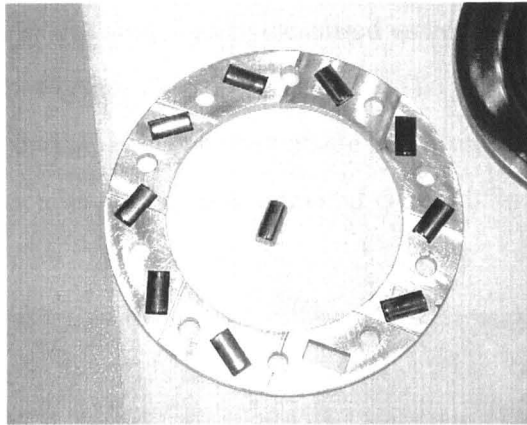


Figure 2.3-3 – A Skew Plate and Rollers

The material properties for the brake plates, rollers and skew plates are defined in table 2.3-1: -

Component	Material
Cage ( 35° Skew)	Aluminium Nickel AMS 4640
Cage ( 0/15/25/45/55° Skew)	Aluminium
Cylindrical Roller	Tool Steel M50 AMS 6491
Stator	Steel BSI S82
Rotor	Steel BSI S82

Table 2.3-1 – Component Materials

Prior to and at the end of testing the surface finish of the stator and a rotor was measured at four points as shown on Figure 2.3-4. The  $R_a$  values measured are defined in table 2.3-2 : -

		$R_a$ Value measured at point				
Comment	Type	1	2	3	4	Average
Prior to any testing	Stator (Plate A)	0.108 $\mu$ m	0.119 $\mu$ m	0.117 $\mu$ m	0.098 $\mu$ m	0.111 $\mu$ m
	Rotor (Plate B)	0.096 $\mu$ m	0.114 $\mu$ m	0.112 $\mu$ m	0.104 $\mu$ m	0.106 $\mu$ m
After all testing	Stator (Plate A)	0.103 $\mu$ m	0.098 $\mu$ m	0.091 $\mu$ m	0.097 $\mu$ m	0.097 $\mu$ m
	Rotor (Plate B)	0.088 $\mu$ m	0.112 $\mu$ m	0.114 $\mu$ m	0.110 $\mu$ m	0.106 $\mu$ m

Table 2.3-2 – Surface Finish Measurements



The surface roughness values were measured using a stylus type evaluation unit supplied by Mahr Perthner (Perthometer S5P). The measurements were taken across the mid section, between the outside and inside diameter of the brake plates with the evaluation length being 4.8mm and cut off 0.8mm.

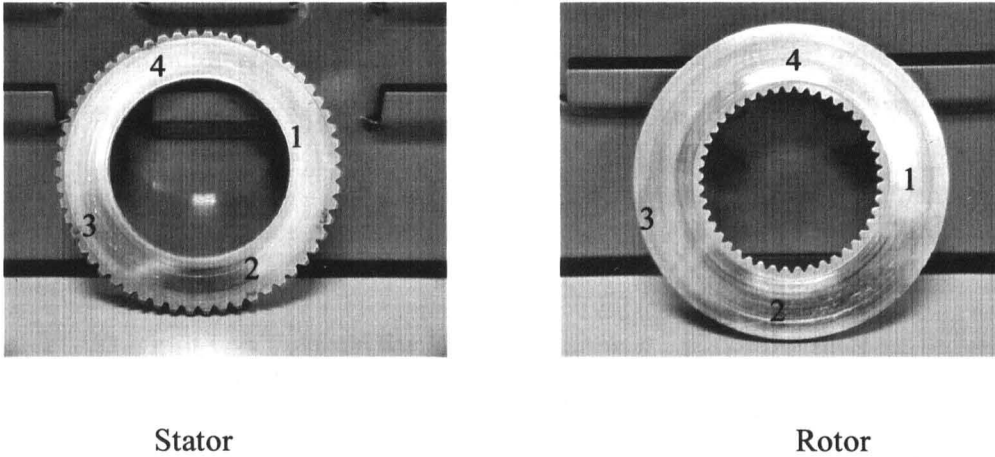


Figure 2.3-4 – Brake Plate Measurement Positions

The average surface roughness of each component appears to have improved slightly for the stator but not changed for the rotor. The variations in point surface roughness show a generally slight improvement in surface roughness for both stator and rotor.

The surface roughness value used in the subsequent lubrication analysis took the overall average to one decimal place of  $0.1\mu\text{m}$ .

## 2.4 TEST PROCEDURE

The test work was conducted in accordance with a written test procedure, which is included as Appendix D.

In summary, the general procedure followed was to assemble the unit with the roller cage containing pockets machined at the required skew angle. The spring preloading fixture was then used to establish the required axial force on the roller stack, and the lock nut within the unit fixed in position. The fully assembled unit was then fitted to the test rig and run-in for fifty revolutions at a constant speed of 250 rpm.

The unit was then run for 320 revolutions at each of the selected input shaft speeds defined in Table 2.4-1. This speed range was selected to cover as wide a speed range as possible within the power and gearbox constraints of the rig driving motor. During each test the driving torque and the bulk temperature of the lubricant was continuously recorded using a Microlink Data-acquisition unit. On completion of testing across the speed range, the test unit was partially disassembled and the axial force reset to the next test point. The tests were then repeated. Table 2.4-1 also defines the mean Hertzian contact stress values associated with each axial load setting.

On completion of the above tests, the test unit was dismantled then reassembled with the next skew angle and the procedure repeated.

<b>Skew Angle</b>	0 °	15°	25°	35°	45°	55°		
<b>Speed (rpm)</b>	50	75	100	250	350	450	550	650
<b>Axial load (N)</b>	890	1780	2670	3560	4450			
<b>Mean Hertzian Stress (N/mm<sup>2</sup>)</b>	274	388	475	549	613			

Table 2.4-1. Test Conditions Summary. Each skew angle was tested across the input shaft speed range, for each axial load value.

The zero degree tests were conducted in order to establish the inherent drag of the test unit in each direction of rotation as discussed in section 2.5.

## 2.5 INHERENT TEST UNIT DRAG

Figure 2.3-1 illustrates that the inherent drag in the freewheel direction includes three roller bearings, the two shaft seals and churning losses as the internal components of the unit rotate in the lubricant. The design of the device is such that when rotated in the opposite direction the brake is locked by a simple ratchet mechanism. Hence the input drive must overcome the brake torque of the unit. When roller cages with zero degree skew angles are fitted, the inherent drag in the 'braking' direction increases relative to the freewheel value due to the addition of four commercial thrust bearings and the zero degree skew angle bearing.

The relevance of this is that torque measurements from the rig torque transducer include inherent drags. To focus only on the torque produced by the skewed roller components the inherent drag of the device must be subtracted from the raw torque transducer measurements. The process described below was followed in order to assess these inherent drag values.

### 2.5.1 BRAYCO 795

The inherent drag characteristic in the freewheeling direction, when the brake pack produces no torque, is shown on Fig 2.5-1. It can be seen to increase with speed from approximately 0.2 Nm at low speed to 0.70 Nm at 650 rpm.

In the freewheeling direction the three major contributory factors to this drag are the shaft seals, three roller bearings and the churning losses as the internal components rotate in the lubricant. Based on DAW knowledge of seal friction values it is reasonable to use the working assumption that at low speed, 50 to

100 rpm, the drag is dominated by the seals and the bearing losses. The increase in drag with speed can be attributable to the increasing churning losses.

The seal and roller bearing loss, from Figure 2.5-1 has been taken as 0.2 Nm.

The inherent drag in the braking direction but with zero degree skewed rollers is shown on Figure 2.5-2. The data is somewhat scattered, especially at low speed, but the trend is clearly increasing drag with axial load. These drag values include the seal and roller bearing losses discussed above, plus the extra four thrust bearings and the two zero degree skew stages which are operating when the brake is working.

A straight line curve fit has been put through the data and used to calculate an adjustment as a function of axial load. This was subtracted from the raw input torque measurements. The magnitude of the adjustment was given by equation 2.5-1, where  $\bar{T}$  is the value of the straight line curve fit from Figure 2.5-2 for any given axial load.

$$adjustment = \left[ (\bar{T} - 0.2) \times \frac{4}{6} \right] + 0.2 \quad 2.5-1$$

In Equation 2.5-1, the 0.2 Nm relates to the seal and roller bearing drag. The  $\frac{4}{6}$  represents the proportion of drag associated with the four commercial thrust bearings, which is constant as skew angle varies. The remaining  $\frac{2}{6}$  is contributed by the zero degree skew angle bearings and clearly this term will vary with skew angle.

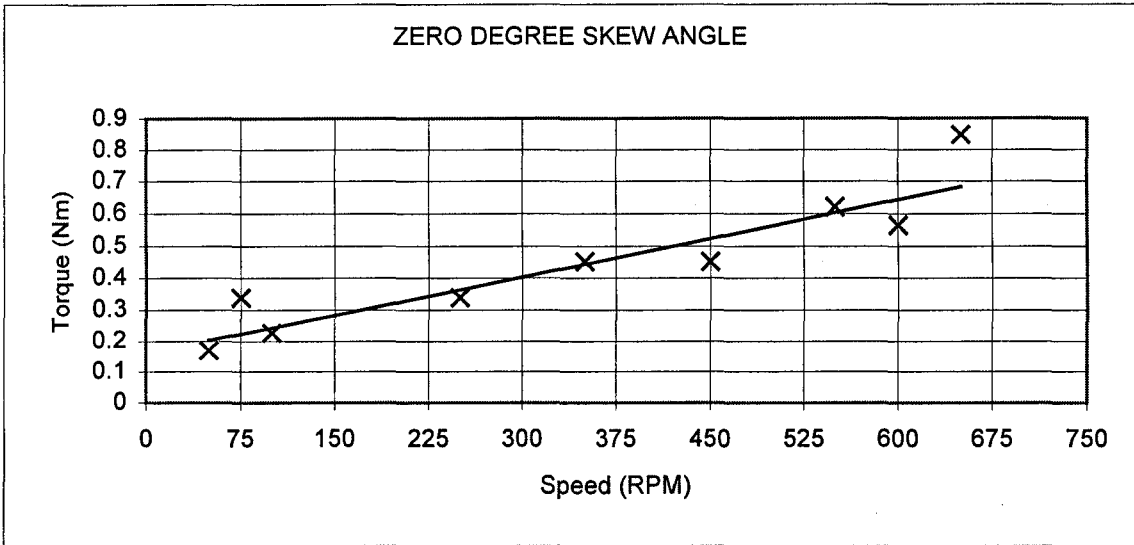


Figure 2.5-1. Inherent Drag in the Freewheel Direction, Brayco 795 Lubrication.

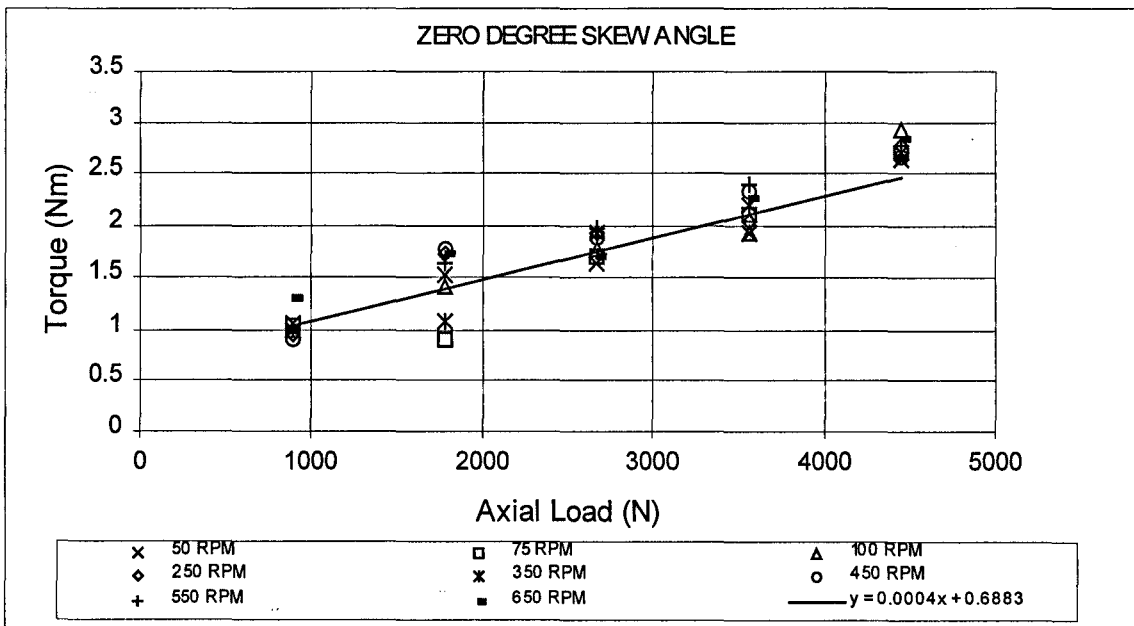


Figure 2.5-2. Inherent Drag in the Braking Direction, Brayco 795 Lubrication.

## 2.5.2 CATENEX 79

The Catenex 79 lubricant is an order of magnitude more viscous than Brayco 795. The consequence of this can be seen on Figures 2.5-3 and 2.5-4.

In the freewheel direction the inherent drag values are significantly higher than for Brayco. It is still however reasonable to assume that the seal friction is approximately the same as for Brayco, at 0.2 Nm and that the extra drag at low speed is caused by viscous churning losses.

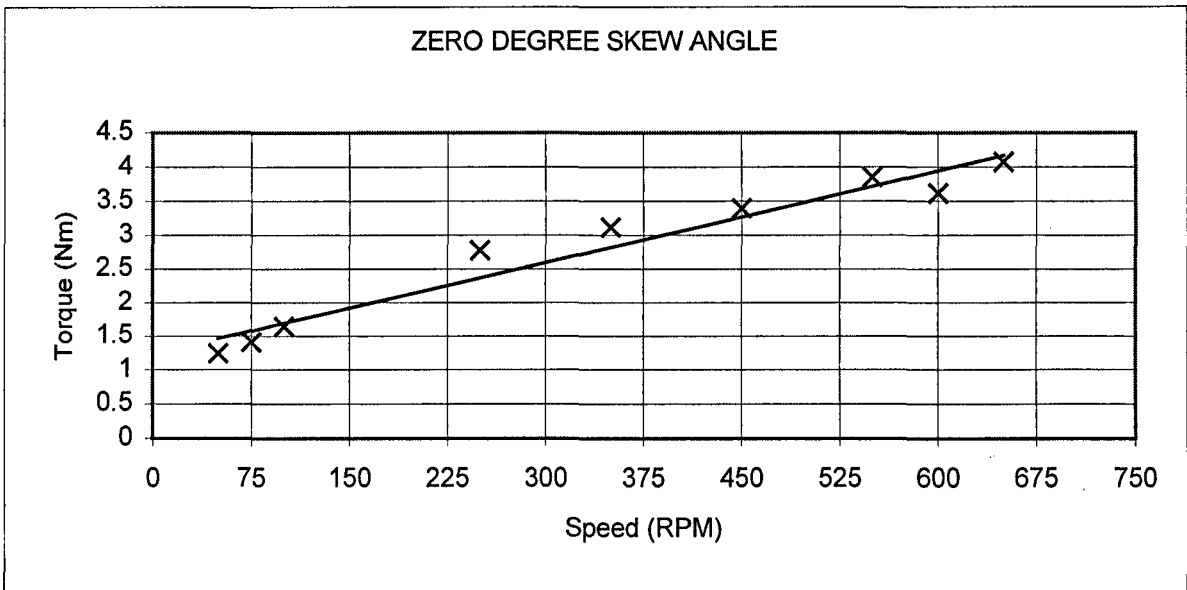


Figure 2.5-3. Inherent Drag in the Freewheel Direction, Catenex 79 Lubrication.

Figure 2.5-4 shows that the speed effects cannot be ignored. The drag values are clearly a function of speed, with a generally steady increase in drag as speed increases. The test speeds were selected at 50, 75 and 100 rpm and 250 through 650 rpm. The apparent grouping into two groups is due to the relatively large step between 100 and 250 rpm. In order to allow for the apparent difference in inherent drag as a function of speed, in addition to axial

load, two straight line curve fits have been used for the data, depending on the speed range. Based on the grouping of the data points this approach seems a reasonable method of adjusting the raw torque values measured by the torque transducer so as to derive the skewed roller frictional torque, without excessively over or under compensating at the extremes of the speed range.

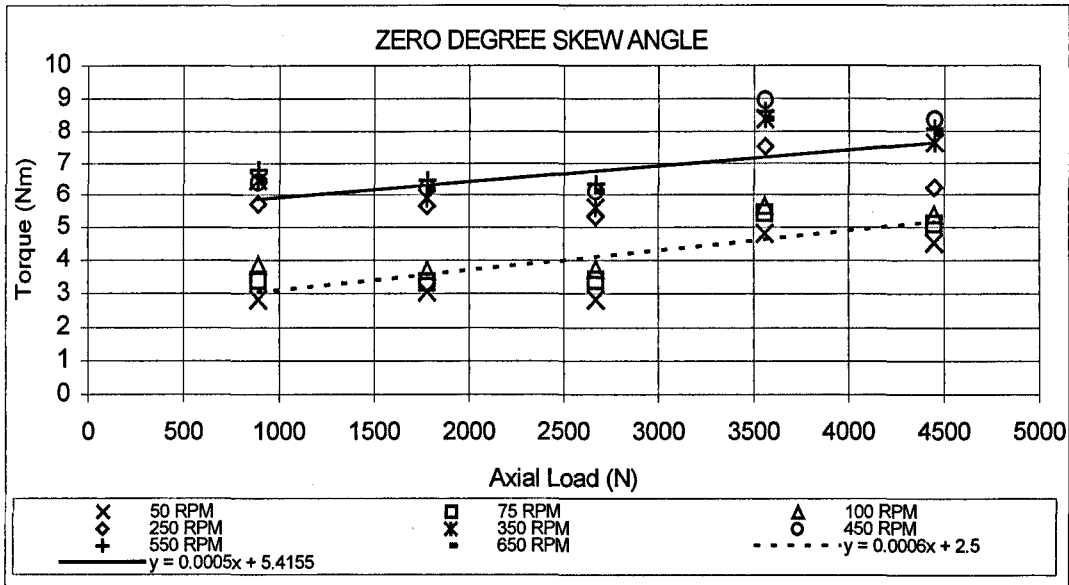


Figure 2.5-4. Inherent Drag in the Braking Direction, Catenex 79 Lubrication.

Using the curve fits shown on Figure 2.5-4, the adjustment was calculated using Equation 2.5-1 for the Catenex lubricant.

## 2.6 TORQUE CHARACTERISTICS

The torque characteristics of the test unit when lubricated by the two different fluids are presented in Appendix E.

Figure 2.6-1 to 2.6-4 summarise the results and illustrate the general trends. For clarity on the figures, only the extreme cases from the tested operational parameters have been plotted. It can be seen that the torque increase is non-linear with increasing skew angle; and appears linear with increasing load.

### 2.6.1 BRAYCO 795

Figures 2.6-1 and 2.6-2 illustrate the characteristic of the device when lubricated with Brayco 795. As speed increases for any load or skew angle, the torque generated reduces. At 55° skew angle and 4450N axial load the speed range from 50 rpm to 650 rpm results in a fall in the torque generated of 27%. This torque reduction at a skew angle of 25° is 20%. For 55° and 890N axial load the same speed range produces a 27% fall in generated torque. At 25° skew angle the comparative fall is 30%

Also shown on Figure 2.6-1 are the predicted torque's using Equation 1.1-1. The value of coefficient of friction selected are 0.066 and 0.092, the range currently used by DAW in design of skewed roller devices. It can be seen that the equation produces the correct form. At low axial loads the equation gives good accuracy. At higher loads, the lower friction coefficient limit of 0.066 overestimates the measured torque by approximately 2.5 Nm. At what would be considered 'normal' skew angles of 30-55°, this approximately equates to an error of 10 %.

### 2.6.2 CATENEX 79

The torque results for Catenex are somewhat more scattered than for Brayco. The reduction in torque generated with increasing speed is clear, and shows the same general characteristics on the Brayco results, but with somewhat higher percentage reduction in torque with speed. At 55° skew angle, 4450N axial load the torque falls by approximately 40% a speed increase from 50 to 650rpm. The comparable Brayco result was 27%.



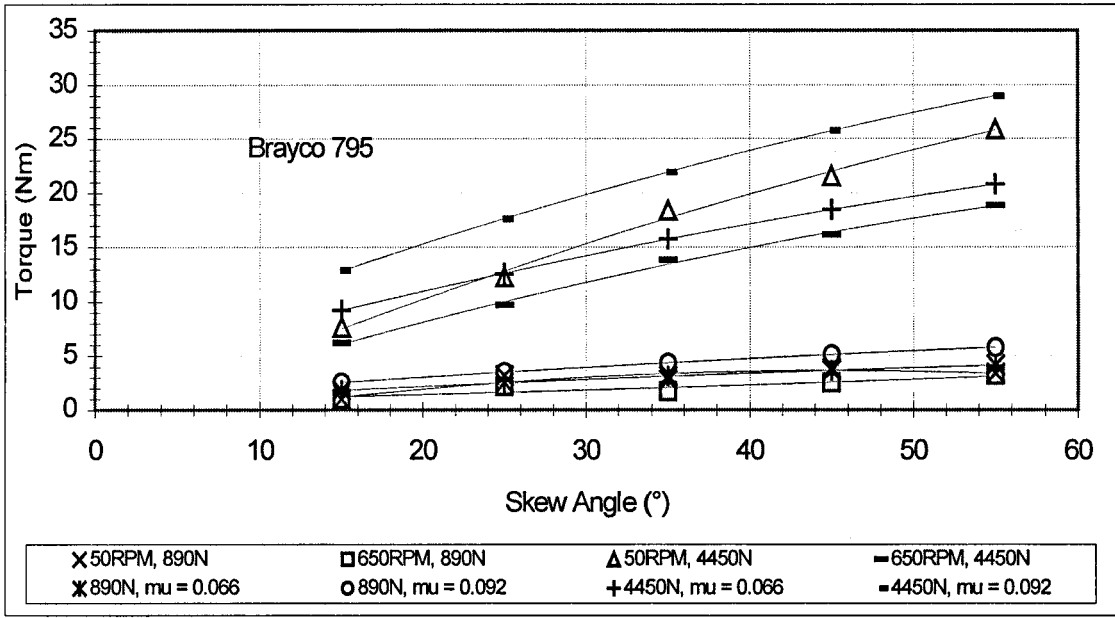


Figure 2.6-1. Torque Characteristic with Skew Angle, Axial Load and Speed, Brayco 795 Lubrication.

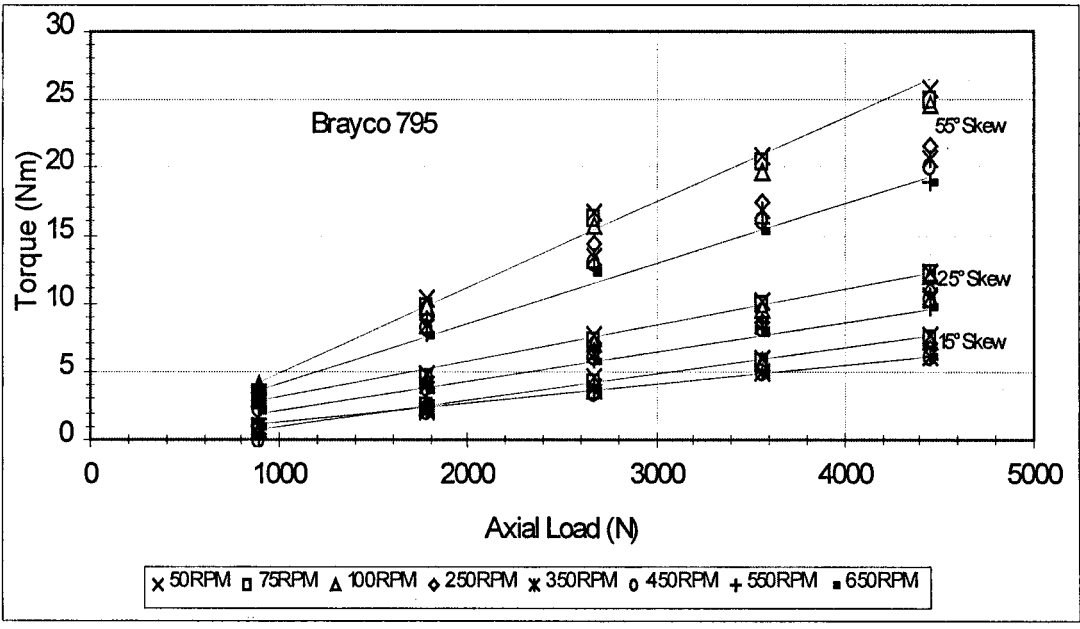


Figure 2.6-2. Torque Characteristic with Axial Load, Speed and Skew Angle, Brayco 795 Lubrication.

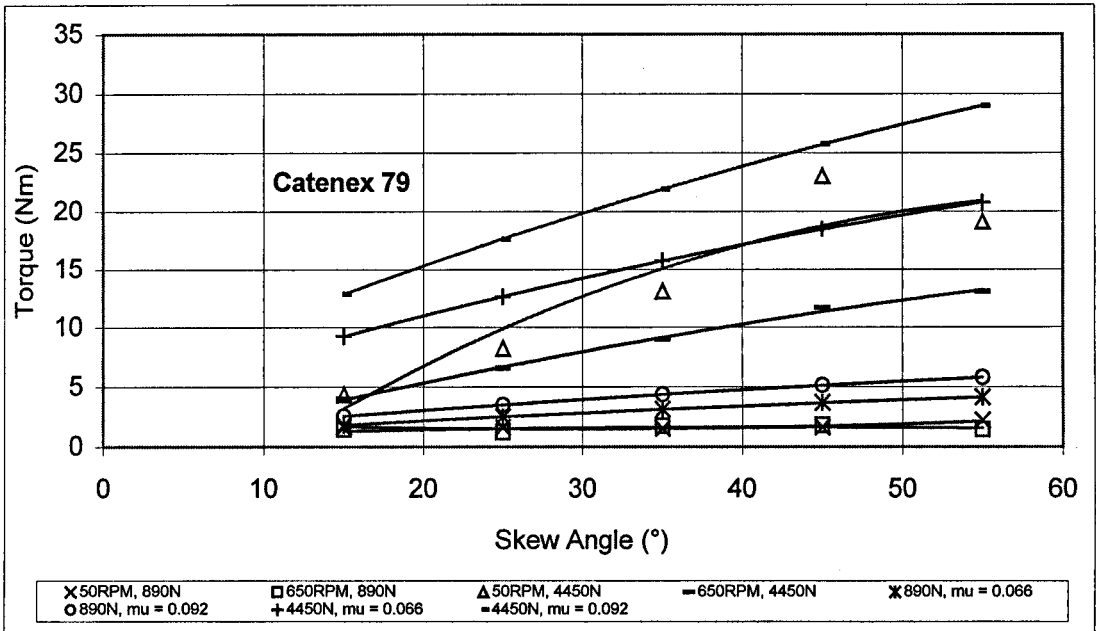


Figure 2.6-3. Torque Characteristic with Skew Angle, Axial Load and Speed, Catenex 79 Lubrication

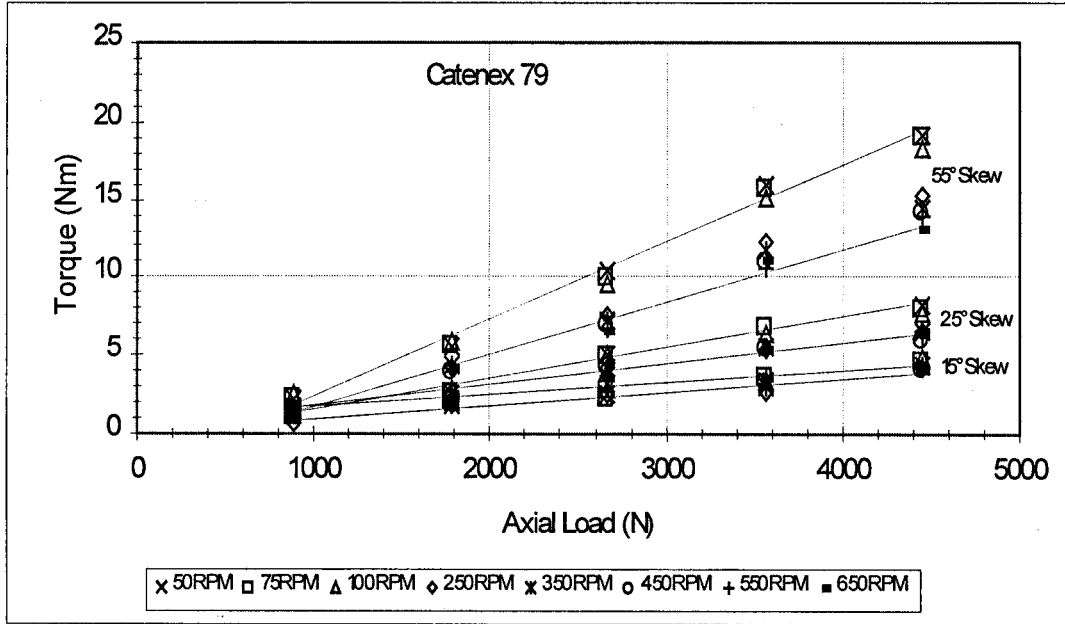


Figure 2.6-4. Torque Characteristic with Axial Load, Speed and Skew Angle, Catenex 79 Lubrication

The torque predictions using equation 1.1-1 however show significant discrepancies compared to the measured data. The measured data indicates that the effective friction coefficient when lubricated with Catenex is significantly lower than when lubricated with Brayco. It should be borne in mind here that the 0.066-0.092 values were derived from a Brayco lubricated, 35° Skew angle device. These results demonstrate that the characteristics of the lubricant have a significant effect on the torque produced by the device.

Figure 2.6-3 illustrates the torque characteristic with skew angle for the 4450N and 890 N axial load cases at 50 rpm and 650 rpm.

## 2.7 STRIBECK DIAGRAM

Presentation of friction data using the Stribeck diagram is common in tribology analysis. The Stribeck diagram, Williams (1996), can be used to show the different modes of lubrication in a contact. Theoretically, the friction coefficient should be a constant value in the boundary lubricated regime, with a value perhaps between 0.1 and 0.15. The coefficient falls through the mixed regime to a minimum value of approximately 0.03. The coefficient then increases at a low rate through the elastohydrodynamic regime and into the fully hydrodynamic region, the value being perhaps 0.03 to 0.04.

The abscissa is normally expressed as a term of the form  $\eta\omega/p$ , a function comprising fluid viscosity, speed and load related terms. Occasionally, Hess and Soom (1990), the abscissa is expressed in terms of the film thickness to roughness ratio,  $\Lambda$ . With boundary lubrication occurring at  $\Lambda$  values less than 1 and mixed lubrication between 1 and 5. Elastohydrodynamic lubrication occurs when  $\Lambda$  is in the range 5 to 10 and full hydrodynamic lubrication with  $\Lambda$  greater than 10. These are approximate values with the transition from between modes being progressive, rather than sharp edged.

Schipper and de Gee (1995) introduced a refinement with their 'lubrication number',  $\eta V_+ / \bar{p} R_a$ , which introduces the surface roughness,  $R_a$ , of the contact components in to the analysis.

Researchers such as those mentioned above, tend generally to be conducting laboratory experiments concerning lubrication at point or line contacts. Generally, a pin on disk or disk on plate type of test rig is used and friction measurements are taken under various conditions relevant to the researcher. A single point or line contact is used in these test machines, with measurements of normal load and traction force being made from load transducers. These measurements allow the coefficient of friction to be calculated directly, and when plotted across a sufficiently wide range of lubrication number the Stribeck type diagram is produced.

Presentation of the experimental torque data for the skewed roller tests conducted during this project required a choice of abscissa and a method of presenting friction coefficient to be developed.

The abscissa was selected as the lubrication number discussed above. This selection was made because it is relatively conventional with only the addition of the surface roughness term, and it relates directly to a friction coefficient model whose applicability to the analysis of skewed roller devices was to be tested.

The numerical values of the terms within the lubrication number parameter require some interpretation, particularly the sum velocity term. In this analysis of skewed rollers the sum velocity term has been related to entrainment velocity and factored according to the sine of the skew angle. Hence, as skew angle increases the entrainment velocity reduces somewhat for fixed input shaft speeds. The derivation and interpretation of the terms within the lubrication number are detailed in Appendix F. Fluid viscosity data is available

in the published literature for Catenex 79, formerly known as HVI 650 and Vitrea 79 and hence often referred to as such, but is not published for Brayco 795. The viscosity of the Brayco 795 fluid was measured at a commercial rheology test facility specifically to support this project. The results are presented in Appendix G, along with a summary of other rheological data for both fluids.

Three options were considered for the presentation of friction coefficient. A simple relationship between torque and the axial load applied to the rollers was considered but rejected since the skew angle is not represented in the formula. The existing DAW formula for the analysis of skewed roller devices can be used to calculate  $\mu$  directly from torque measurements. Alternatively a slightly modified version of the same equation, derived in Appendix H and shown below, can be used.

$$T = F \cdot \mu \cdot \left( \frac{D}{2} \cdot \sin\phi + \frac{l}{2} \right) \quad 2.7-1$$

The coefficient values calculated by these three methods are tabulated in Appendix F, as part of the lubrication number analysis. For summary Figures 2.7-1 to 2.7-4 illustrate the experimental test data for the two fluids when presented using the Stribeck diagram. The title ‘implied friction coefficient’ is used to indicate that the coefficient has been calculated using the respective formula and the measured torque values, adjusted for inherent drag as discussed in the previous section.

### Brayco 795 Lubrication

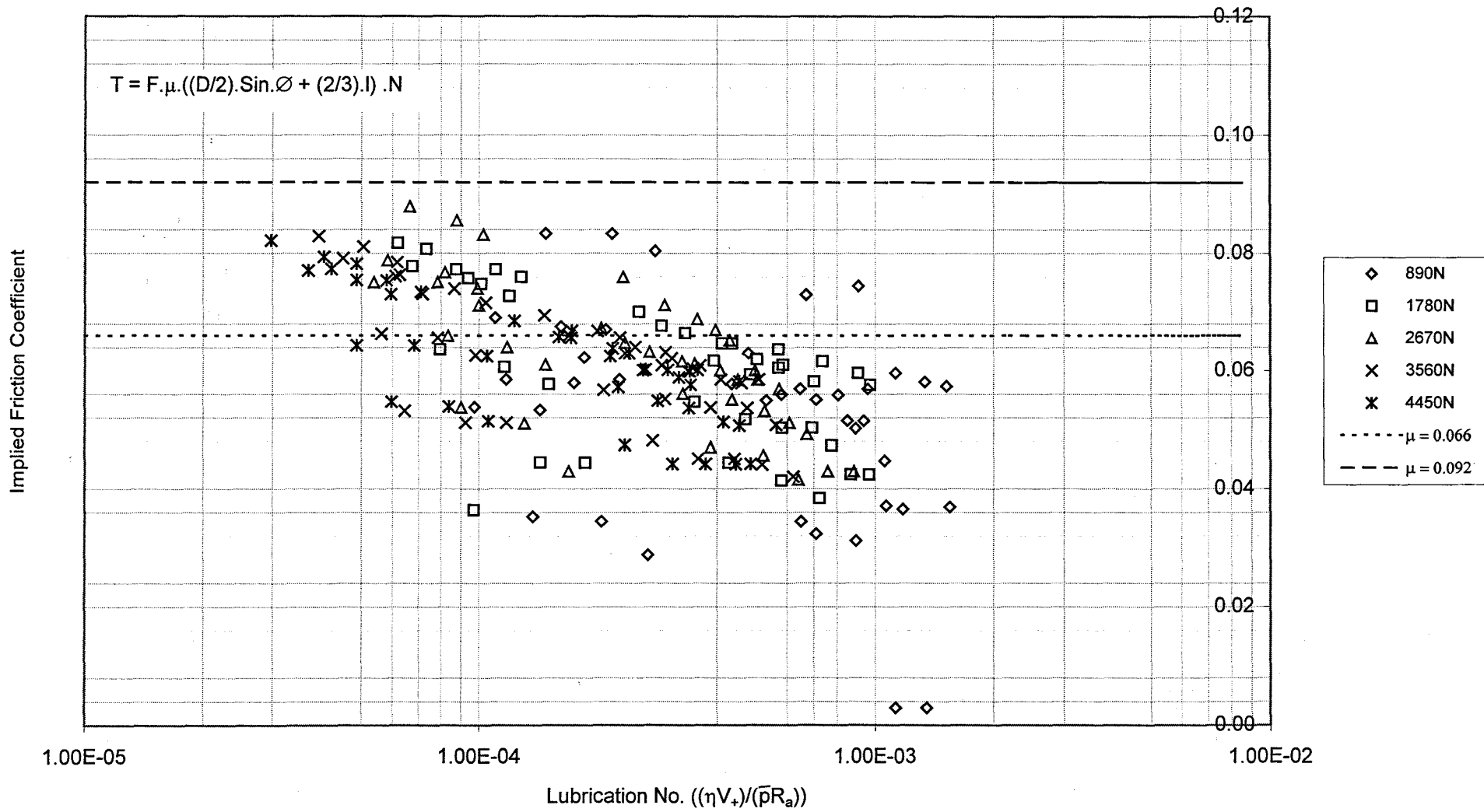


Figure 2.7-1 Friction Curves for Skewed Roller Brake, Brayco 795 Lubrication

Brayco 795 Lubrication

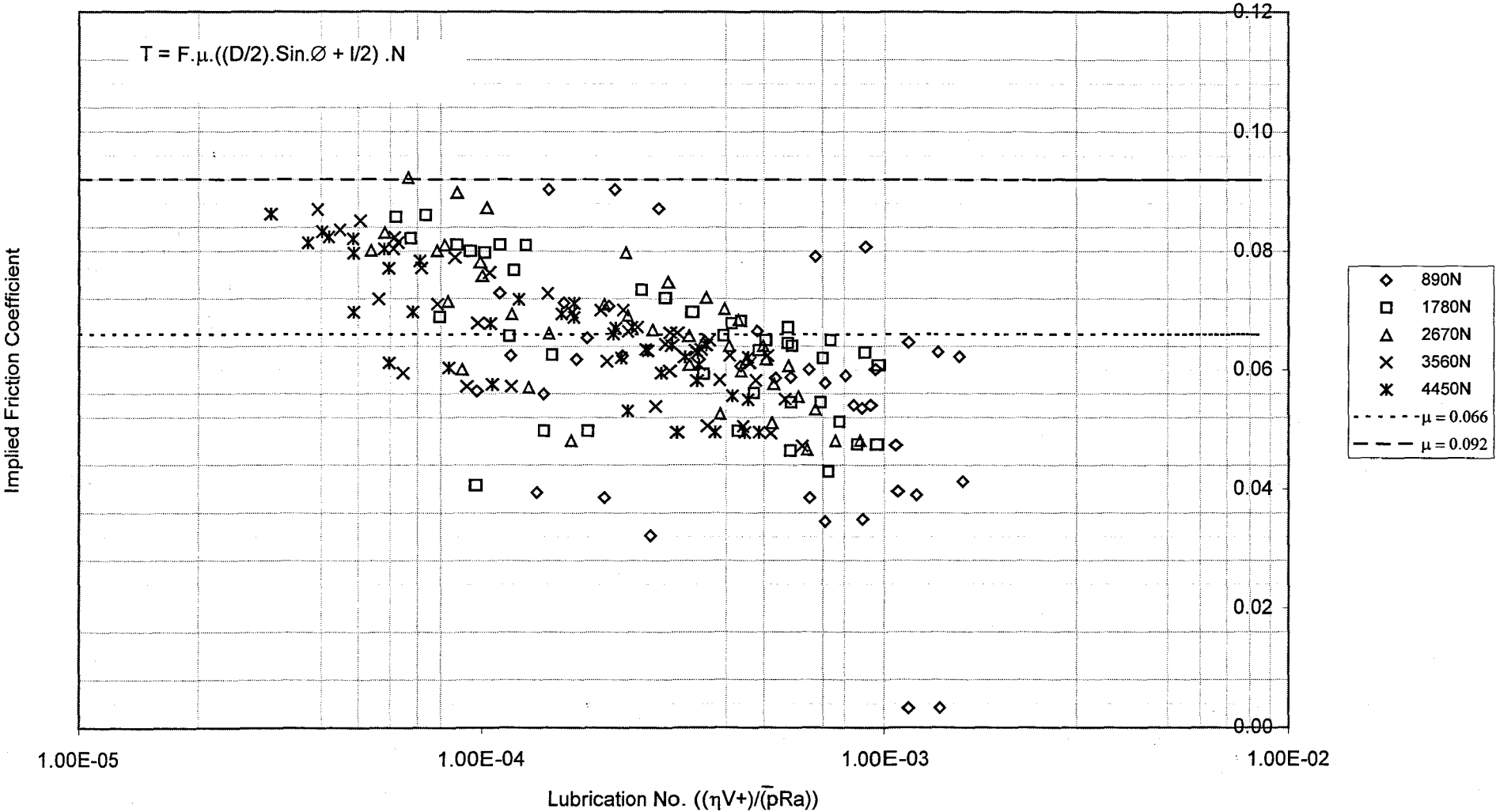


Figure 2.7-2 Friction Curves for Skewed Roller Brake, Brayco 795 Lubrication

Catenex 79 Lubrication

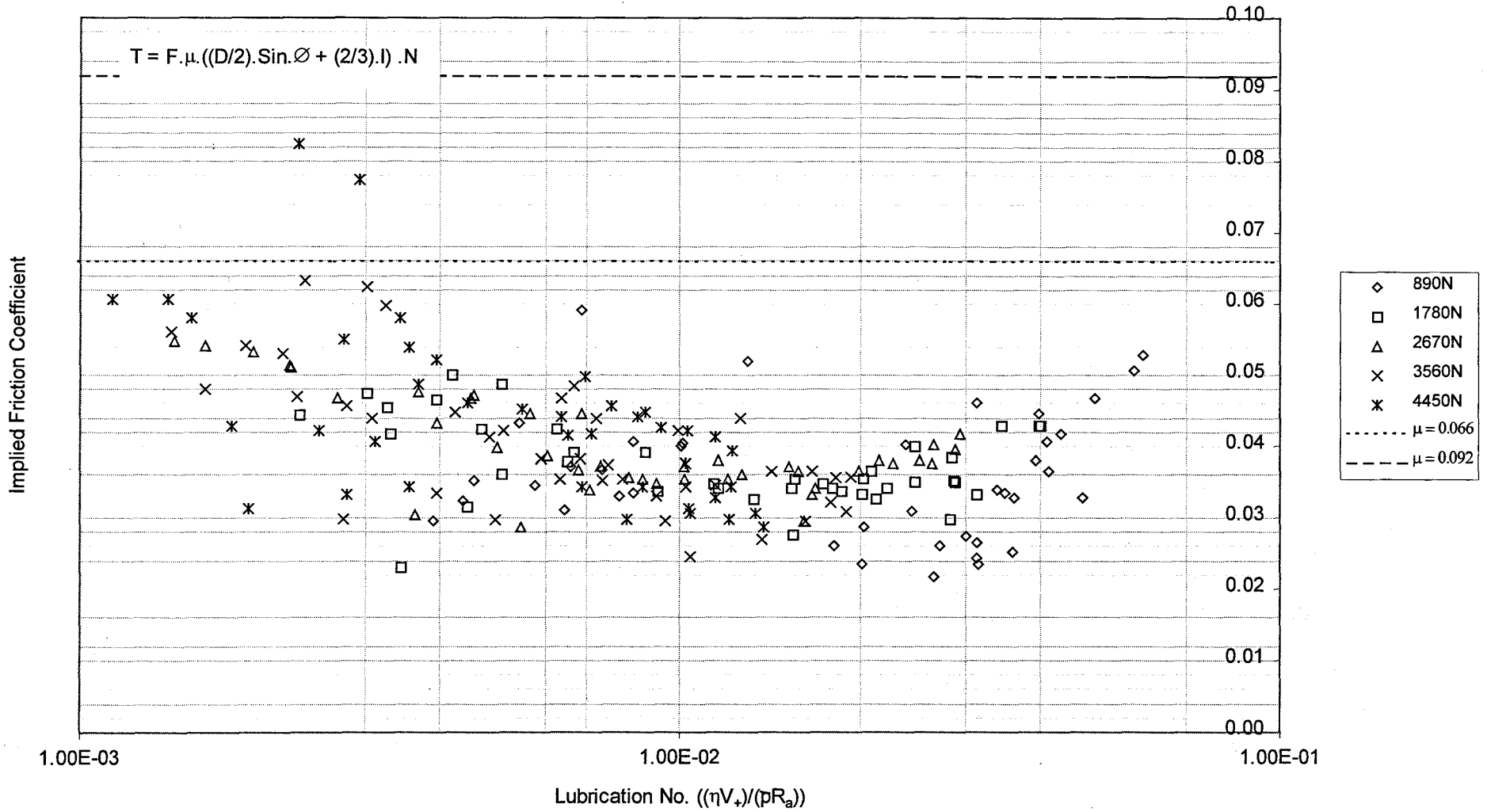


Figure 2.7-3 Friction Curves for Skewed Roller Brake, Catenex 79 Lubrication

2-23



### Catenex 79 Lubrication

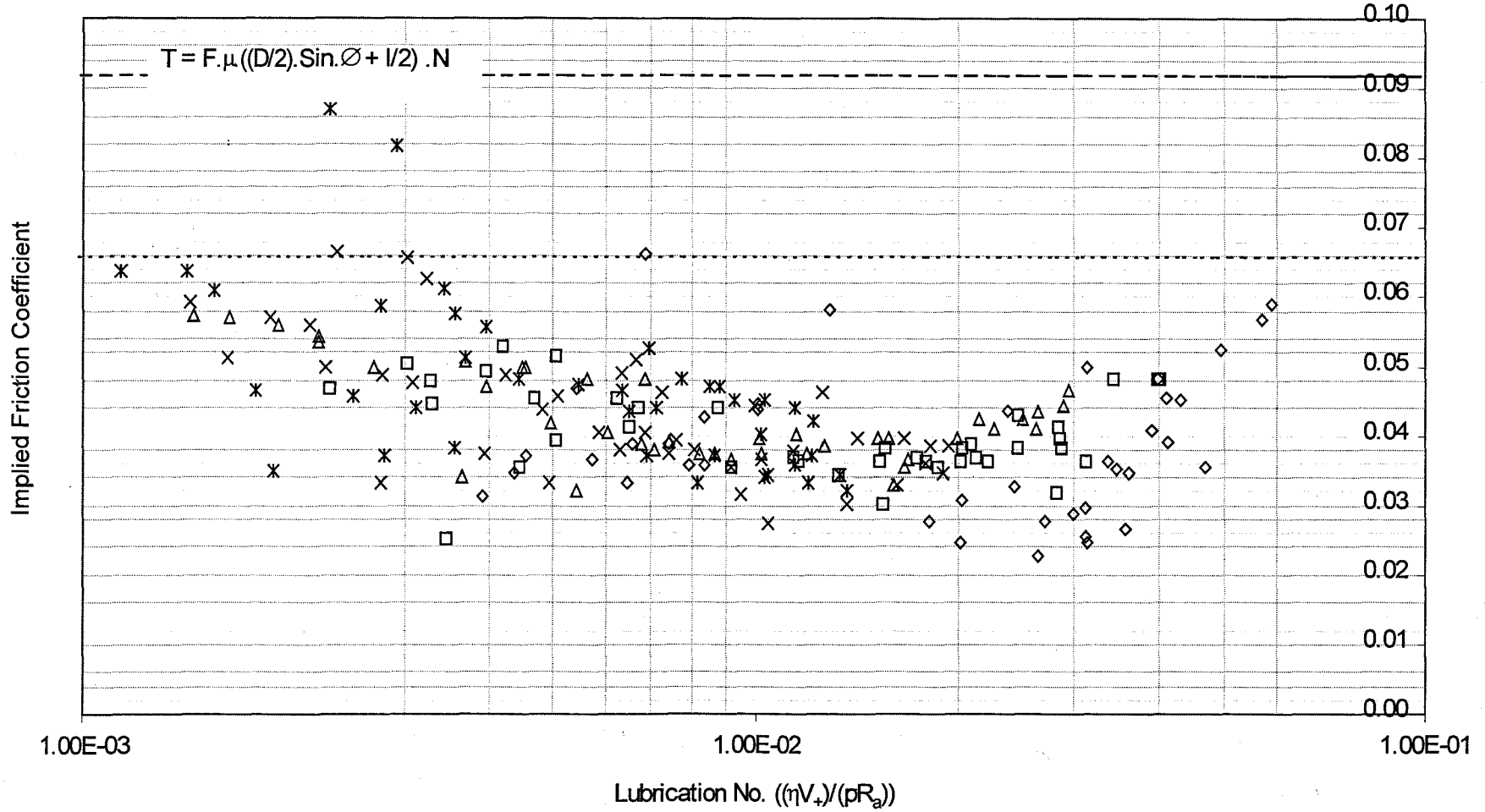


Figure 2.7-4 Friction Curves for Skewed Roller Brake, Catenex 79 Lubrication

2-24

The maximum and minimum friction coefficient values, 0.092 and 0.066, traditionally used by DAW have also been included in these Figures.

## 2.8 FILM THICKNESS CONSIDERATIONS

The methods for calculating elastohydrodynamic film thickness are well established and were mentioned in section 1.2.5. When used to consider the transition between lubrication modes it is often the non-dimensionalised film thickness to roughness ratio parameter,  $\Lambda$ , which is used. This parameter has been assessed for both Brayco and Catenex lubricants across the operating range of the testing. The results are presented in the Tables of Appendix F.

The findings were that for Brayco,  $\Lambda$  ranges from 0.1 to 1.1. This would suggest that all of the Brayco tests were conducted with the contact operating in the boundary lubricated regime. The author believes this in practice to be unlikely for reasons discussed in section 2.9.

For Catenex, the influence of the higher viscosity of the fluid results in significantly thicker films, with  $\Lambda$  ranging from 1.3 to 14.6. This would suggest that the Catenex lubricated contact does not operate in the boundary regime, but spans mixed, elastohydrodynamic and full hydrodynamic regimes. The exact mode depends on the particular conditions of load and speed. The results which appear to be in the hydrodynamic regime are the 890N axial load values at speeds over 350 rpm. The remaining results are fairly evenly divided between mixed and elastohydrodynamic regimes.

## 2.9 DISCUSSION OF THE TEST RESULTS

### 2.9.1 BRAYCO 795

Figures 2.7-1 and 2.7-2 show that the traditional Stribeck curve is not produced in its entirety. The film thickness calculations discussed in section 2.8 would suggest that the contact is boundary lubricated. Here we should see an approximately constant coefficient of friction value, in the range 0.1 to 0.15. In a boundary lubricated contact there is likely to be evidence of surface distress on the roller and reaction plates due to asperity contact. The evidence of the test work conducted to support this thesis and previously at DAW is contrary to these expectations. Surface distress and wear are not features of the skewed roller device and constant values of friction coefficient, in the range 0.1 to 0.15 are not produced.

The test results presented in Figures 2.7-1 and 2.7-2 clearly show a decreasing friction coefficient with increasing lubrication number. The evidence is suggestive of a mixed lubrication mode. Additionally, the friction coefficient values, ranging from approximately 0.04 up to 0.09 are consistent with published values, for example Schipper and de Gee (1995). The conclusion that can be drawn from this data is that the contact is operating in the mixed lubrication mode and not the boundary regime.

Comparison of Figures 2.7-1 and 2.7-2 shows that the modified equation, Equation 2.7-1, has no impact on the data collapse. The general level of the friction coefficient value is raised by approximately 0.01. The differences between the two equations do not appear significant.

The data collapse well, except for the 890N axial load results which are particularly scattered and do not show a particularly strong trend. Indeed, the two values with friction coefficients at approximately 0.003 appear to be rogues. If the 890N results are ignored, the remaining data show remarkably

little scatter and follow the trend of decreasing friction coefficient with increasing lubrication number.

The 890N results are arguably more sensitive to experimental error than the others in a number of areas. For example, the initial axial load setting, the effect of inherent drag adjustment on torque values and the fact that the raw torque values are of the order of 1% of the torque cell measuring range. Hence, considering these features it is perhaps not too surprising we see considerable scatter on these particular results.

Figure 2.9-1 illustrates the effect of skew angle on friction coefficient. This data shows that at higher skew angles, 35° and above, the results are very consistent. At the lower skew angles the data tends to segregate as a function of skew angle and imply lower friction coefficients. It should be remembered that those values which appear to buck this trend, the high 25° skew angle and the low 15° skew angle values are the 890N axial load points discussed above.

The experimental error in the measurement and calculation of the implied friction coefficient was estimated to be 1% of reading and is a function of the torque measurement accuracy. The potential error in calculating the lubrication number is dominated by the effect of temperature measurement on viscosity. Although the bulk temperature of the lubricant could be measured to an accuracy of 1°C, or 1%, two larger errors exist. Firstly, shear heating in the contact will ensure that a difference will exist between the bulk temperature and the temperature of the fluid in the contact inlet. According to Schipper and de Gee (1995) this is still an unsolved problem. Since the actual contact temperature could not be measured in the research, the average bulk temperature during each test was used as the reference temperature for calculating viscosity values. The error associated with calculating the average lubricant temperature and the consequential effect on viscosity and lubrication number could range from 3% to 13%.

Brayco 795 Lubrication

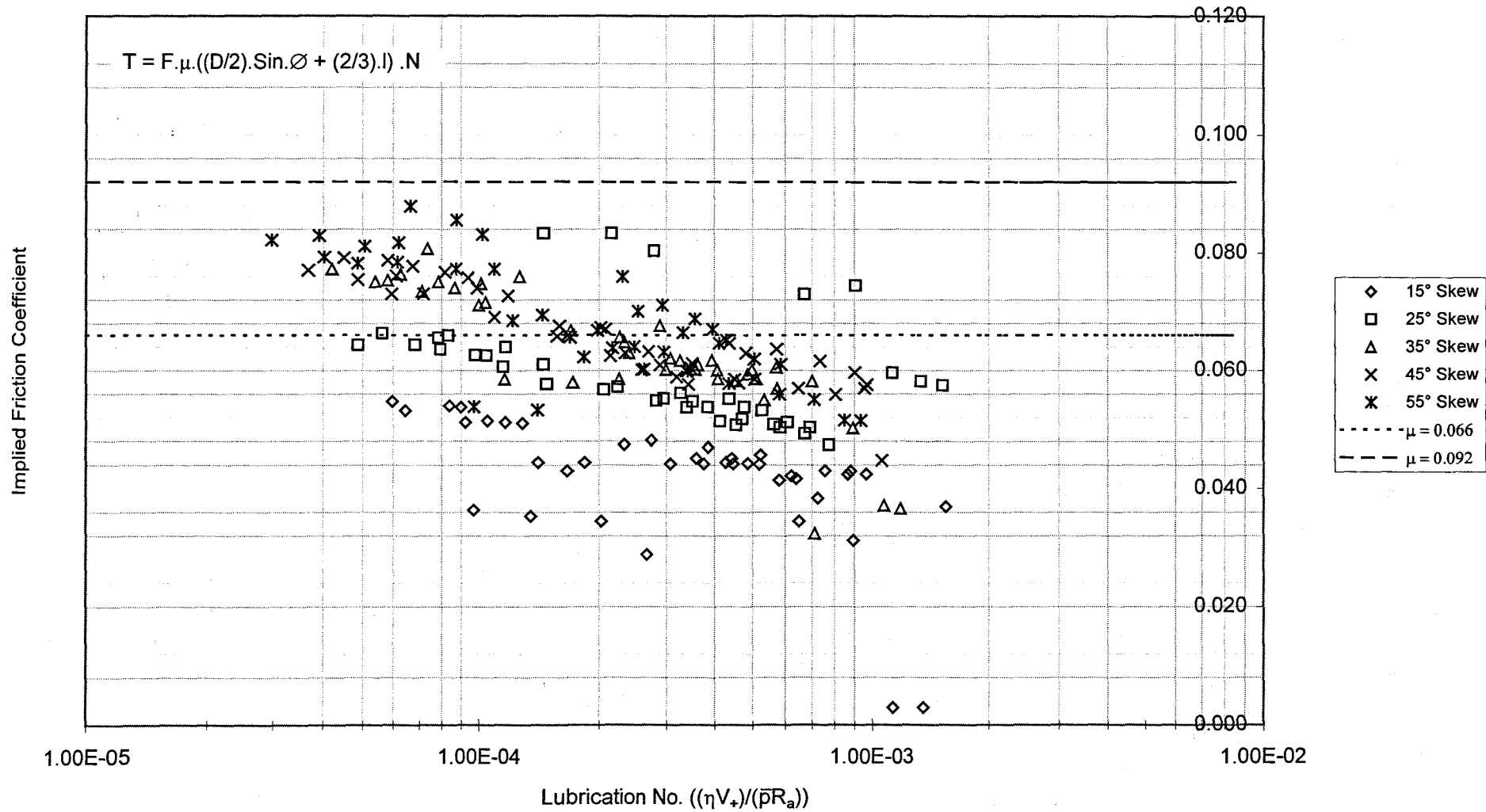


Figure 2.9-1. Friction Coefficient Values Grouped by Skew Angle, Brayco 795 Lubrication.

The error bands associated with the 1% variation in implied friction coefficient and 13% variation in lubrication number are shown on Figure 2.9-2 as example error bands. The 13% potential temperature error has a relatively weak effect on the result scatter. Hence, intuitively, the unquantified error associated with the difference between bulk and contact temperature is unlikely to explain the remaining scatter in the data. It is reasonable to conclude that other, as yet unexplained, parameters must influence the results, contributing to the scatter.

### 2.9.2 CATENEX 79

As in the case of the Brayco results, Figures 2.7-3 and 2.7-4 do not show the full Stribeck curve. The film thickness to roughness ratio calculations for Catenex gave  $\Lambda$  in the range 1.3 to 14.6, implying operation through the mixed and elastohydrodynamic lubrication mode. This would also imply decreasing friction coefficient with increasing lubrication number through the mixed regime, to a minimum value of approximately 0.03 to 0.04 in the ehl regime. Data provided by Evans and Johnson (1986b) and Schipper and de Gee (1995) underpin this assumption.

The test data presented on Figures 2.7-3 and 2.7-4 could be interpreted as confirming the film thickness to roughness ratio conclusions. The data is somewhat more scattered than the Brayco lubricant results, and again the 890N axial load values appear the least consistent. However, the general trend of the data is to decrease with increasing lubrication number, and then level off at a value between 0.02 and 0.04, consistent with elastohydrodynamic lubrication. As for Brayco, the alternative torque equation results, Figure 2.7-4, does not provide any significant practical improvement in the data collapse.

### 2.9.3 MAXIMUM AND MINIMUM FRICTION COEFFICIENTS

The deficiency of using simple maximum and minimum values for friction coefficient is clearly illustrated by the results shown on Figures 2.7-1 to 2.7-4. The approach is obviously unable to reflect the change in friction due to changes in the operational parameters.

For Brayco lubrication, some of the data points fall within the 0.066 - 0.092 band. Notably the 35° skew angle 4450N values which are nearest those of the unit currently in production at DAW and from which the values were originally derived. However, as lubrication number increases the measured friction coefficients fall below the minimum value.

The Catenex results, with lubrication number an order of magnitude higher than Brayco are almost entirely below the minimum of 0.066.

This data underlines the reason why prototype tests have always been considered necessary on new designs and reinforces the business case for the research.

### 2.9.4 COMBINING THE DATA POINTS

The Brayco and Catenex data can be combined on a single diagram and the results are shown on Figure 2.9-2.

Here a more complete version of the Stribeck diagram can be seen. This due to the wider range of lubrication number across which the data is spread caused by the difference in viscosity of the two lubricants.

### Brayco 795 and Catenex 79 Lubrication

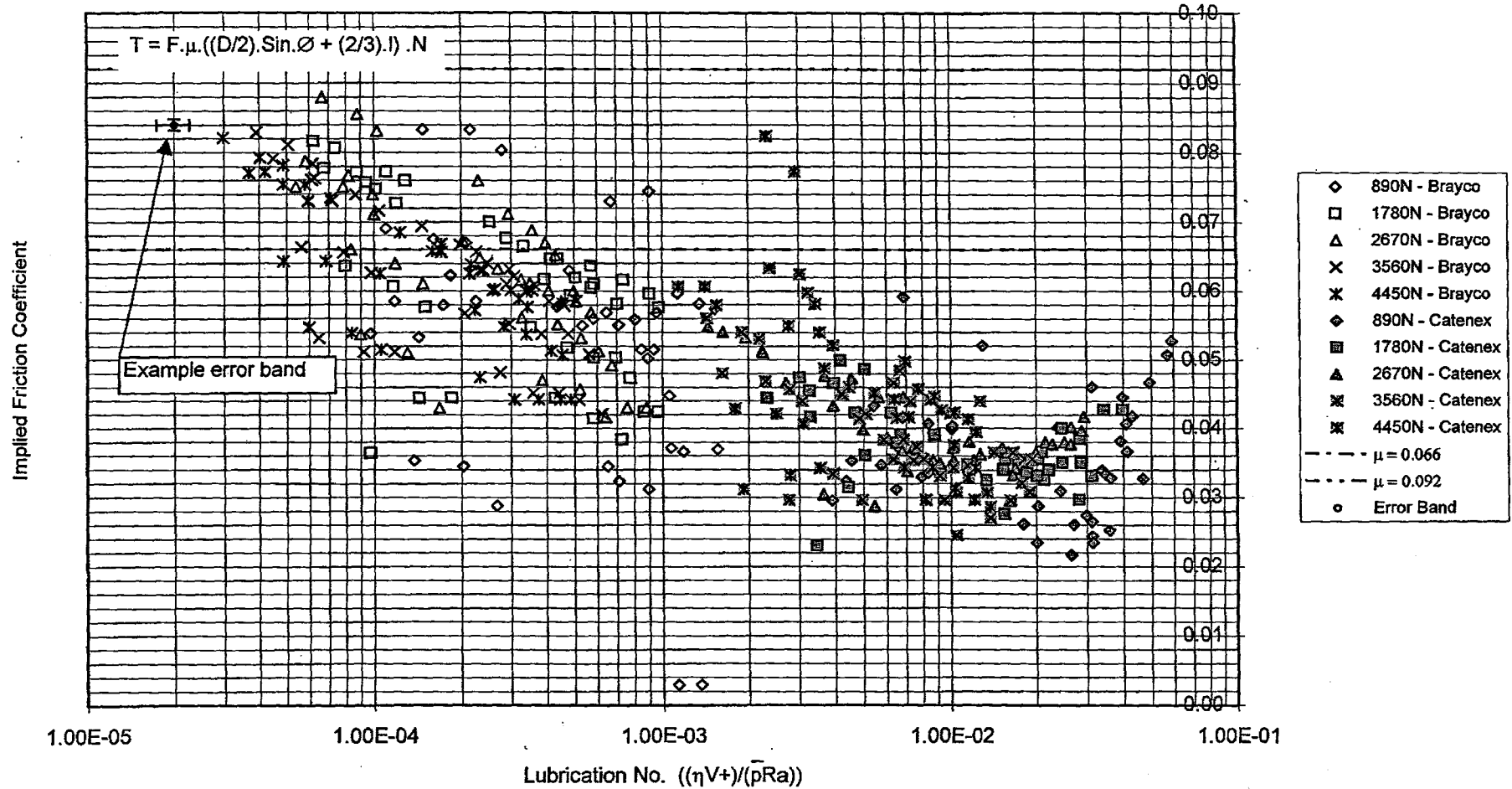


Figure 2.9-2. Friction Characteristics Combining the Brayco and Catenex Test Results

2-31



## 2.10 RESULTS CONCLUSION AND BUSINESS CASE IMPLICATIONS

The raw torque measurements taken from the rig torque transducer were adjusted to remove the effect of inherent drag within the test unit caused by seal friction, bearing and churning losses. The subsequent torque values, which relate only to the skewed roller elements, were used to calculate an implied friction coefficient. Presenting the friction coefficient data for each lubricant as a function of lubrication number appears to reproduce the mixed and ehl portions of the traditional Stribeck diagram.

The data is somewhat scattered, particularly for the results associated with the 890N axial load tests. This is probably due to the experimental errors being a more significant proportion of the measured parameter at these axial loads. However, the trends seem clear, and appear to follow the Stribeck diagram characteristic.

The traditional DAW method of selecting a maximum and minimum value for friction coefficient and applying those values irrespective of operational conditions does not map the characteristics of the device adequately.

Consequently, this means that the traditional DAW method is only applicable to a specific design configuration operating about a set criteria. It is clear from this why a prototype test has been necessary for each new design. On the other hand, the lubrication number analysis tool offers a method of predicting changes in friction coefficient as a function of changes in operational parameters.

The demonstration that lubrication number parameter can be used to predict quantitative changes in friction coefficient is, in itself, a significant step forward in the understanding of the performance of skewed roller devices. However, the business case for the research project was founded on the establishment of a design tool to allow the prediction of friction coefficient based on the operational parameters. The test results presented in this chapter

indicate that the development of such a tool is feasible if a link between friction coefficient and lubrication number is established. The work of Schipper and deGee is explained in the subsequent chapters, in order to satisfy the two objectives.

### **3. FRICTION COEFFICIENT MODELLING**

#### **Chapter Summary**

This chapter explores the theoretical friction coefficient models proposed by Schipper and de Gee (1995) and Hess and Soom (1990). The chapter is structured as follows:

- 3.1 Introduction
- 3.2 Lubricant - Liquid or Solid State
- 3.3 Friction Mode Diagram
- 3.4 Friction Coefficient
- 3.5 Hess and Soom Model
- 3.6 Conclusions and Implications for the Business Case

The model proposed by Hess and Soom was rejected from further study since it was found to predict values in the range 0.145 to 0.127. These values are significantly higher than experimental results of chapter 2 and do not show sufficient variation with changes in load and speed.

The Schipper and de Gee model appears more promising and the theoretical boundaries of the model are defined in this chapter. These boundaries were compared to the experimental data and the necessary developments to the design tool to ensure a good correlation are discussed in chapter 4.

### 3.1 INTRODUCTION

The literature review of chapter one indicated that the lubrication of line concentrated contacts in the full film condition has been studied extensively, for example Evans and Johnson (1986b) and (1987). However, prediction of friction behaviour in the mixed lubrication regime is still in its infancy.

Schipper and de Gee (1995) proposed a methodology for assessing the frictional characteristics based on the contacts operational parameters. In fact, a flow chart, Figure 1.2-3, was proposed which allows the lubrication mode and the frictional behaviour of the contact to be analytically predicted as a function of the operational parameters.

Use of the flow chart requires a knowledge and assessment of the following issues:

- i) Is the lubricant operating in the liquid or solid state?
- ii) If in the liquid state, a method of determining the lubrication mode is proposed, along with an equation to describe the friction coefficient in the mixed regime. Empirical values are provided for friction coefficient in the boundary regime and it is stated that the friction coefficient in the elastohydrodynamic region is available from established sources such as Evans and Johnson (1986b).
- iii) If in the solid state, an assessment criteria is proposed which allows the appropriate value of friction coefficient to be selected.

The flow chart and friction coefficient model proposed by Schipper and de Gee is reviewed in this chapter and applied to the skewed roller brake problem,

resulting in a theoretically based assessment of friction as a function of the operating parameters of the contact.

Also mentioned in chapter 1 was the work of Hess and Soom (1990) who conducted research into friction at a line contact operating under oscillating conditions. They proposed Equation 1.2-3 to describe the coefficient of friction. This model is also reviewed in this chapter.

### 3.2 LUBRICANT LIQUID OR SOLID STATE

Research work conducted by teams such as Alsaad et al (1978) has concluded that the lubricant within a concentrated contact can behave as a viscous liquid or as an elastic solid, under certain conditions of pressure and temperature. The transition from liquid to solid behaviour is known as the 'glass transition'.

In the solid state, the frictional behaviour of the contact is determined by the solid state characteristics of the lubricant, and not the usual rheological parameters such as viscosity, which are important in the liquid state. Indeed, many researchers including Alsaad et al (1978) and Evans and Johnson (1986b) show that in the solid state the maximum traction coefficient is associated with the plastic shearing of the lubricant.

The parameters dominant in determining liquid or solid state behaviour are pressure and temperature. At atmospheric pressure the glass transition temperatures are well below 0°C, but at the high pressures experienced in elastohydrodynamic contacts it has been shown that the transition temperatures rise to ambient levels and hence fall within the operating range of the devices.

Alsaad et al (1978) did not conduct any experiments using Catenex 79 or Brayco 795. Schipper and de Gee, who have tested with Catenex 79 (HVI 650), provide only schematic phase diagrams without numerical reference points to establish the lubricant state. Evans and Johnson (1986b) reproduced the Alsaad data, and stated that although no data for HVI 650 was available, it was thought to be similar to a fluid tested by Alsaad. Hence, the glass transition temperature as a function of pressure can be gleaned from this data for Catenex 79. To the authors knowledge no data is available for Brayco 795.

The experiments conducted to support this thesis were all completed with bulk lubricant temperatures between approximately 18°C and 40°C and mean pressures between 0.27 GPa and 0.61 GPa. The actual temperature in the contact will exceed the bulk temperature of the lubricant. Consideration of the glass transition temperature and pressures presented in Evans and Johnson (1986b) would indicate that the majority of the tested region should be in the liquid state. Solid state behaviour would only be expected for the 3560 N and 4450 N axial load tests for temperatures below 40°C. Considering that the shear heating in the contact would raise the contact temperature above the bulk lubricant temperature, it is likely that only a small proportion, if any, of the tests conducted with Catenex 79 were in the solid state.

Since glass transition data is not available for Brayco 795, it is not possible to be precise with regard to the lubricant state during the experiments. The design tool developed in this thesis assumes that the fluid is in the liquid state. The practical implications of this uncertainty are not too important in practice and this point is discussed further in section 3.4.2.

### 3.3 FRICTION MODE DIAGRAM

Schipper and de Gee proposed a mode transition diagram, which defines the lubrication mode of the contact as a function of the lubrication number and mean contact pressure.

The boundaries between the different modes are determined by the following equations:

$$L_{ml/bl} = \frac{1.25 \times 10^4}{\bar{p}}$$

$$L_{ehl/ml} = \frac{3.1 \times 10^4 \cdot R_a^{0.5}}{\bar{p}^{0.5}}$$

Figure 3.3-1 presents the mode transition diagram and indicates the range of lubrication number covered by the tests described in chapter 2, for Brayco 795 and Catenex 79.

Mean Hertzian Contact Pressure (Pa)

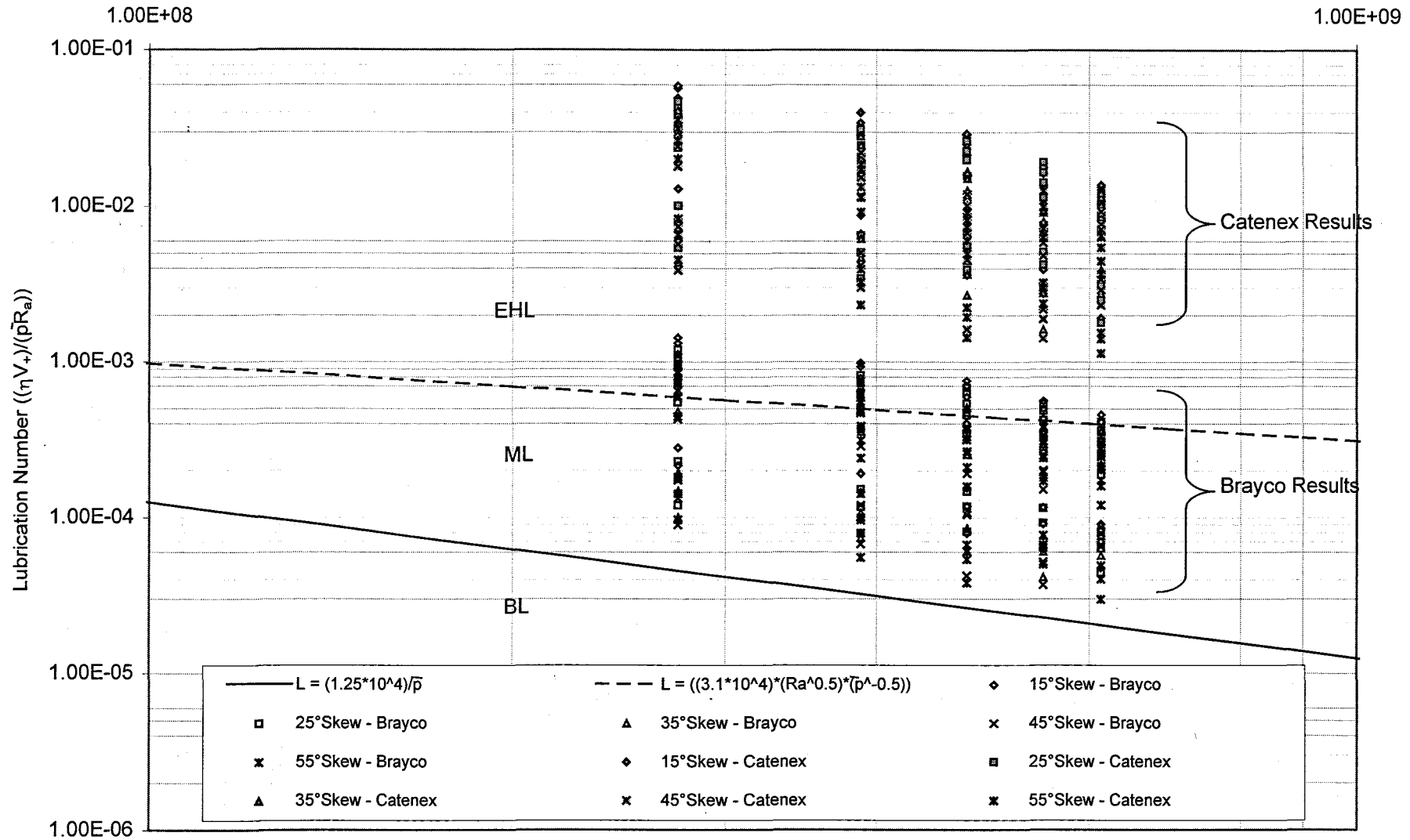


Figure 3.3-1 Mode Transition Diagram.



The mode transition diagram would predict that for Brayco 795 the tests cover both the elastohydrodynamic and the mixed lubrication regimes. For Catenex 79 the tests should be entirely in the elastohydrodynamic region due to the viscosity being an order higher than Brayco 795. These assertions are directly the result of the Schipper and de Gee work.

### 3.4 FRICTION COEFFICIENT

#### 3.4.1 MIXED LUBRICATION MODE

Schipper and de Gee provide Equation 1.2-3, reproduced below for calculating frictional behaviour in the mixed regime:

$$\mu_{ml} = \mu_{ehl} + \left[ \frac{\mu_{bl} - \mu_{ehl}}{\ln(2.5 \cdot \bar{P}^{0.5} \cdot R_a^{0.5})} \right] (\ln L_{ehl/ml} - \ln L)$$

The formula essentially provides a linear interpolation as a function of lubrication number, L, between the ‘constants’  $\mu_{ehl}$  and  $\mu_{bl}$ .

#### 3.4.2 BOUNDARY LUBRICATION MODE

The value of  $\mu_{bl}$  can take two principle values according to the operating conditions. The first value is equal to approximately 0.13 and is a typical value associated with boundary lubrication of metallic components.

The alternative to classical boundary lubrication is that micro-ehl takes place which yields a coefficient equal to the ratio of the lubricants limiting shear stress with pressure. This is the approximate value that could be achieved if the lubricant was operating in the solid state. Data presented by Schipper and de Gee indicates that this value is relatively independent of the lubricant type and equals  $0.09 \pm 0.02$ .

The flow chart and model proposed by Schipper and de Gee shows that for a contact operating with the lubricant in the solid state, the friction coefficient will take up one of three values. For certain conditions the contact operates as if it were in the ehl mode and hence a low coefficient would be observed with a value of approximately 0.03, as discussed in section 3.4.3. Alternatively the friction coefficient is governed by the limiting shear stress of the solid lubricant or the classical boundary lubrication value is achieved. In these cases the value will be approximately 0.13 or 0.09. The practical manifestation of this is that a detail knowledge of the phase of the lubricant is not necessary since the results of equation 1.2-3 reach the same values at high and low lubrication number.

### 3.4.3 ELASTOHYDRODYNAMIC REGIME

Schipper and de Gee refer to sources such as Evans and Johnson (1986b) and Johnson and Tevaarwerk (1977) for values describing  $\mu_{ehl}$ , stating that the value can be established from well known ehl theory.

Application of the theory requires detailed knowledge of the lubricant properties since friction in the ehl regime is determined by the bulk rheological properties of the lubricant. For example, detail knowledge of the pressure-viscosity index, temperature-viscosity index and the Eyring stress parameter is required in order to use the analytical tools.

For Catenex 79 this data is available and in fact maximum traction coefficients are presented in Evans and Johnson (1986b) for this fluid. From this data, the expected value for  $\mu_{ehl}$  would be approximately 0.04 to 0.05 for the temperature and pressure range tested to support this thesis.

Unfortunately for Brayco 795 very little data other than dynamic viscosity and a calculated value for pressure-viscosity index is available. Therefore it is

necessary to make some assumptions in order to move forward with the Brayco analysis.

Evans and Johnson (1986b) present traction maps in which four traction zones are defined, depending on the behaviour of the contact. A schematic diagram of the mineral oil map indicating the co-ordinates of the map is shown in Figure 3.4-1.

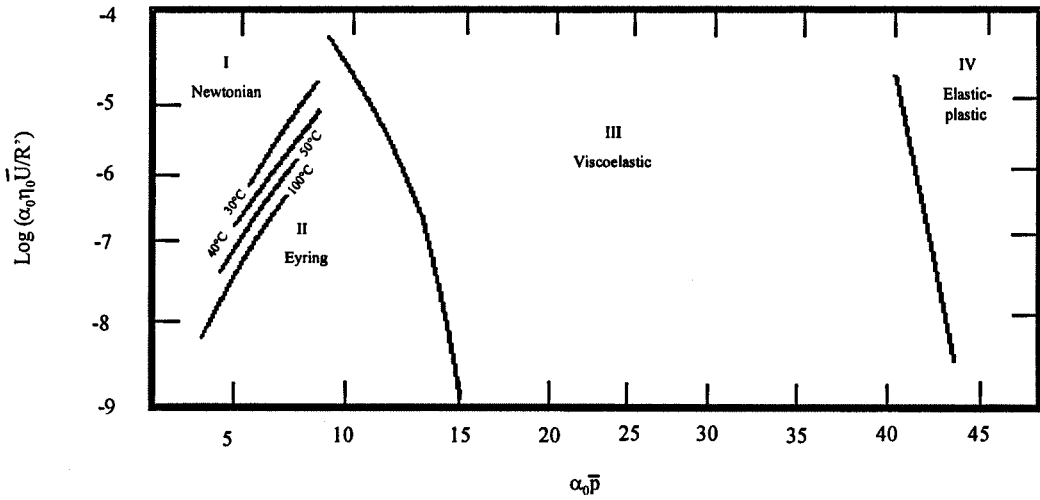


Figure 3.4-1 – Illustrative Elastohydrodynamic Friction Mode Map

Based on the rheological data presented in Appendix G, the tests conducted were predominantly the Eyring region for both Catenex 79 and Brayco 795. In this region the maximum traction coefficient is given by equation 3.4-1 (Evans and Johnson (1986b)), below.

$$\frac{T_m}{F} \approx 0.87\bar{\alpha}\tau_0 + 1.74 \frac{\tau_0}{\bar{p}} \cdot \ln \left[ \frac{1.2}{\tau_0 h} \left( \frac{2K\eta_0}{\beta(1+9.6\zeta)} \right)^{0.5} \right] \quad 3.4-1$$

where,  $T_m$  = maximum traction force,

$\bar{\alpha}$  = mean pressure-viscosity index,

$\tau_0$  = Eyring stress,

$K$  = thermal conductivity of the lubricant,

$\beta$  = temperature viscosity index,

$\zeta$  = non-dimensional parameter.

The assumption has been made that the map presented for Catenex 79 is applicable to other mineral oils such as Brayco 795. This is supported by Evans and Johnson since they refer to the map as a 'mineral oil map'.

The dominant influence of the  $\bar{\alpha}\tau_0$  term can be seen from equation 3.4-1 since the  $(\ln)$  term reduces the power of the terms in parenthesis and the  $\frac{\tau_0}{\bar{p}}$  term is generally a ratio in which the pressure term is two orders of magnitude larger than the Eyring stress term.

Unfortunately the  $\bar{\alpha}$  term is the mean value of the pressure-viscosity index over the pressure range concerned. Appendix G shows that at atmospheric pressure and 30°C, the  $\alpha_0$  values for Brayco and Catenex differ by a factor of 2, and hence would suggest that the maximum traction coefficients should differ by a similar amount. However, Johnson and Greenwood (1980) made the point that a low viscosity index oil can have an  $\bar{\alpha}$  value equal to that of a higher viscosity index oil, since the mean value over the pressure range is the critical characteristic.

Based on the experimental results reported in chapter 2, friction coefficients as low as 0.02 to 0.025 are not supported by the experimental evidence and such values would seem to be too low compared to typical 'book' values of 0.03 for  $\mu_{ehl}$ .

The incomplete rheological data for Brayco 795 is a specific example of a generic engineering problem where conclusions need to be drawn on incomplete data, otherwise progress cannot be made.

Clearly, in this instance progress can only be made in developing an engineering design tool if some assumptions are made with respect to  $\mu_{ehl}$  values. It is acknowledged that this approach leaves some holes in the academic theory, but the approach is acceptable in the development of an engineering tool.

In these circumstances the logical approach, is to assume that the Brayco and Catenex  $\mu_{ehl}$  values are equal at 0.04 to 0.05. These will later be tested by fitting experimental data to the theoretical predictions.

### 3.4.4 ANALYTICAL VALUES

Equation 1.2-3 can be applied using the following values for  $\mu_{bl}$  and  $\mu_{ehl}$ :

$$\mu_{bl} = 0.09 \pm 0.02$$

$$\mu_{ehl} = 0.045 \pm 0.005$$

These values, in conjunction with the mode transition points defined on Figure 3.3-1, at the maximum and minimum values of mean Hertzian stress of 0.27GPa and 0.61GPa, can be used to determine the boundaries of a friction coefficient model which is presented on Figure 3.4-2.

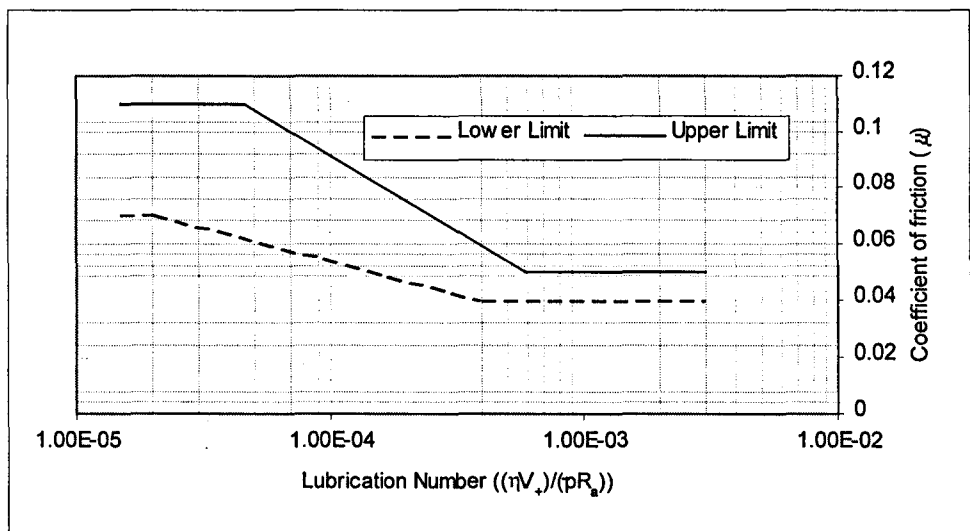


Figure 3.4-2 – Theoretical Friction Coefficient Value Boundaries

### 3.5 THE HESS AND SOOM MODEL

Although Hess and Soom were principally interested in friction in unsteady, oscillatory conditions, they proposed a model for friction coefficient, Equation 1.2-4, reproduced below. To generate their data a variety of lubricants were used covering the same viscosity range as Brayco 795 and Catenex 79. The test apparatus used a rotating disc against a steel button to create a line contact. For their apparatus and range of load and speed conditions the following formula was found to be a good model for friction coefficient.

$$\mu = \frac{\mu_{bl}}{1 + C_1 \left( \frac{\eta V}{\sqrt{FE}} \right)^2} + C_2 \cdot \frac{\eta V l}{F}$$

with  $\mu_{bl} = 0.145$ ,  $C_1 = 1.43 \times 10^{17}$  and  $C_2 = 8.19 \times 10^2$ .

Application of this equation to the skewed roller unit, predicts very high friction coefficients with an approximate value determined by the value of  $\mu_{bl}$  at 0.14. Also the effect of speed and load does not appear to be sufficiently strong. The calculated value varied from 0.145 to 0.127, whereas the measured values shown in chapter 2 vary from approximately 0.09 to 0.03.

The conclusion drawn from comparing the model predictions with experimental data was that the model did not predict the torque characteristics particularly well and hence was not pursued further.

### 3.6 CONCLUSIONS AND IMPLICATIONS FOR BUSINESS CASE

The work of Schipper and de Gee (1995) has been applied to create a theoretical model for the friction coefficient across the mean hertzian pressures tested. This model predicts the maximum and minimum values of friction coefficient as a function of lubrication number. The model uses a linear interpolation technique in the mixed lubrication regime. This regime is defined, as a function of lubrication number, by the theoretical transitions from boundary to mixed lubrication and mixed to elastohydrodynamic lubrication.

Due to the lack of rheological data for Brayco 795 the analytical tools of Evans and Johnson (1986b) cannot be applied to calculate maximum traction coefficients in the elastohydrodynamic regime. To overcome this, the engineering assumption has been made that the Catenex and Brayco  $\mu_{ehl}$  values are equal at 0.04 to 0.05. This assumption will be validated by comparing measured data with the theory in chapter 4.

If this comparison can be shown to have a good correlation between theory and experimental data, the technical research objective, which is central to the project business case will have been satisfied.

## 4. DESIGN TOOL DEVELOPMENT

### Chapter Summary

This chapter draws together the predictions of the theoretical friction coefficient model discussed in chapter three and the experimental evidence of chapter two.

The comparison has demonstrated that a very good correlation between the model and experimental results could be achieved. This has required adjustments to the tolerance range for  $\mu_{ehl}$  and the transition point between mixed and elastohydrodynamic lubrication regimes.

Consequently, the ability to predict friction coefficient and subsequently the torque produced by skewed roller devices as a function of operational parameters has been demonstrated. This chapter concludes that the technical research objective has been successfully achieved.

The chapter is structured as follows:

- 4.1 Introduction
- 4.2 Comparison of Predicted and Measured Friction Coefficients
- 4.3 Friction Coefficient Model Development
- 4.4 Achievement of the Technical Research Objective



## 4.1 INTRODUCTION

This chapter brings the theoretical predictions and experimental evidence from chapters 2 and 3 together and compares both. Hence, the viability of a design tool that predicts the torque characteristic of skewed roller brakes is assessed and proven.

The friction coefficient prediction model proposed by Schipper and de Gee (1996) is developed so as to provide an optimised correlation between the test evidence and the predicted values.

## 4.2 COMPARISON OF PREDICTED AND MEASURED FRICTION COEFFICIENTS

The experimental data and the friction coefficient model predictions are combined in Figure 4.2-1.

The following observations may be made:

- i) At low lubrication number the contact should be moving through the mixed lubrication regime, towards the boundary lubrication mode. Hence the friction coefficient should be increasing towards values typically in the range 0.07 to 0.11 indicated by the solid lines in the figure. The test result data does not support coefficients as high as 0.11, but provides a good fit to the bottom limit of 0.07.

# Brayco 795 and Catenex 79 Lubrication

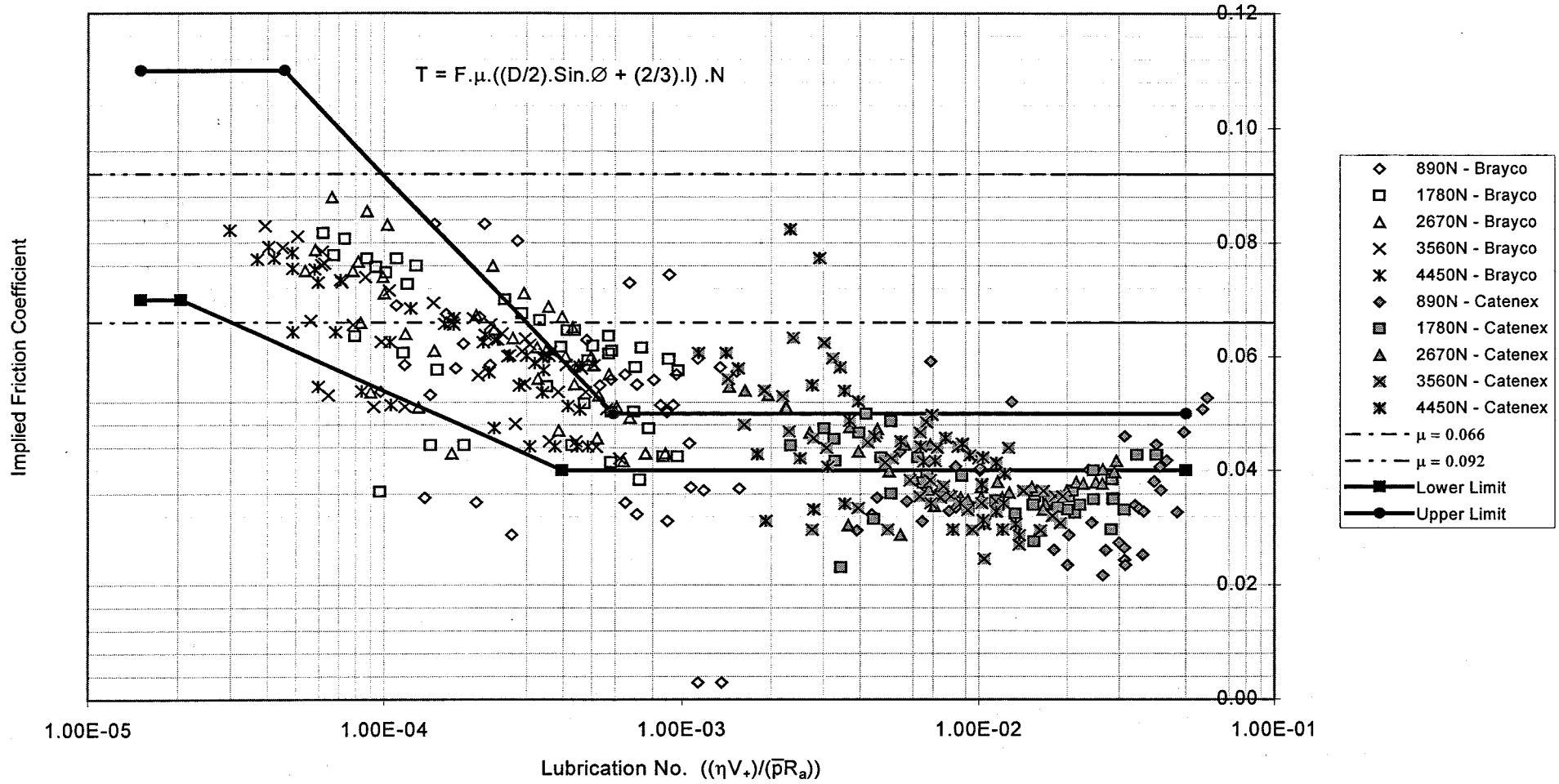


Figure 4.2-1 - Friction Coefficient Model and Experimental Test Results.

- ii) At high lubrication number, with the contact in the elastohydrodynamic regime the measured friction coefficient values are lower than the theoretically predicted minimum of 0.04. A better fit to the data would suggest a minimum value of approximately 0.024. The upper limit of 0.05 appears to give a good fit to the measured data.
- iii) As a consequence of ii) the theoretical friction coefficient range in the elastohydrodynamic regime of 0.04 to 0.05 is too narrow, the measured data does not collapse to such a tight band.
- iv) The test results at the upper limit of lubrication number for Brayco and those at the lower limit for Catenex, at approximately  $L=2 \times 10^{-3}$ , merge together and overlap slightly without signs of a significant discontinuity.
- v) The transition between mixed and elastohydrodynamic modes predicted by the Schipper and de Gee mode transition diagram appears to occur at too low a lubrication number, at approximately  $L=5 \times 10^{-4}$ , when compared to the test data. The experimental results would suggest that the transition point is perhaps an order of magnitude higher.
- vi) A consequence of v) is that the Brayco results would all lie within the mixed lubrication regime and the Catenex results would straddle the transition between mixed and elastohydrodynamic modes. For Catenex this would be consistent with the conclusions of film thickness to roughness ratio calculations discussed in section 2.8.

### 4.3 FRICTION COEFFICIENT MODEL DEVELOPMENT

Refinement of the model, based on the experimental data requires alterations in the following areas:

- i) Maximum friction coefficient in the boundary lubricated mode should be lower than 0.11, or alternatively the lubrication number at the transition point predicted by the Schipper and de Gee theory should be reduced. The lowest lubrication number test results are associated with the highest stress loading with Brayco lubricant. Here, the film thickness to roughness ratio is approximately 0.1. This is sufficiently thin to be traditionally considered as micro ehl and tending towards boundary mode, suggesting that the transition point should be approximately correct. The established maximum value for friction coefficient in use at DAW is 0.092, values higher than this have generally not been experienced. No evidence is available to justify moving the transition point, but evidence does suggest a maximum coefficient below 0.11, the alteration to the model should be to set the boundary lubrication friction coefficient range to 0.07 to 0.092.
- ii) The friction coefficient range in the elastohydrodynamic regime appears wider than 0.04 to 0.05. A more representative range based on the test evidence would be 0.024 to 0.05.
- iii) The transition point between mixed and elastohydrodynamic lubrication regimes should be at a higher value of lubrication number than predicted by the equation:

$$L_{ehl/ml} = \frac{3.1 \times 10^4 \cdot R_a^{0.5}}{\bar{P}^{0.5}}$$

Experimental error is possible for both the measurement of  $R_a$  values and the setting of the axial loads, which determine stress levels.

However, the square root term associated with both of these parameters means that gross errors would be needed to result in a change of lubrication number by an order of magnitude. The coefficient,  $3.1 \times 10^4$  is an empirical number selected by Schipper and de Gee (1995) to fit their own experimental data. Consideration of the data produced to support this thesis would imply a value an order higher.

Summarising these alterations to the friction coefficient model yields:

$$\mu_{bl} = 0.07 - 0.092$$

$$\mu_{ehl} = 0.024 - 0.05$$

$$L_{ehl/ml} = \frac{3.1 \times 10^5 \cdot R_a^{0.5}}{\bar{P}^{0.5}}$$

Recalculating the friction coefficient boundaries and overlaying the experimental data results can be seen to give a good correlation between theoretically predicted values and measured results, Figure 4.3-1.

### Brayco 795 and Catenex 79 Lubrication

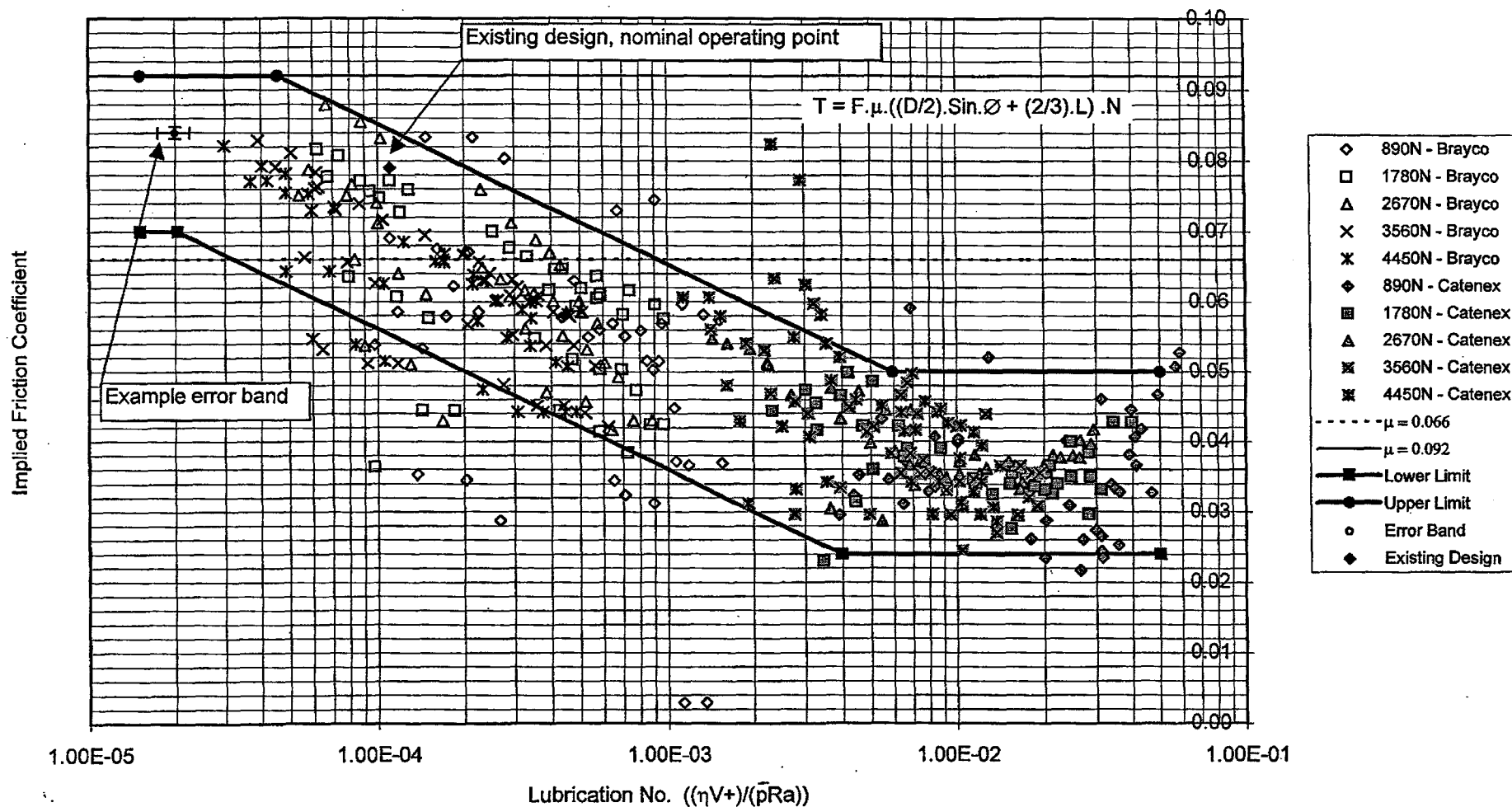


Figure 4.3-1 - Modified Friction Coefficient Model and Experimental Test Results

The test results nearly all fall within this boundary. Those results which are outside of the boundary are predominantly the 890N axial load results, which are probably more significantly affected by experimental error, as discussed in section 2.9.1.

The Brayco results which are close to the lower limit at approximately  $L = 10^{-4}$  cover various axial loads but are all  $15^\circ$  skew angle results. The lower limit was not reduced to include these values because they were deemed to be sufficiently close to the boundary. For an engineering design tool the number of points outside of the boundaries was deemed acceptable.

#### 4.4 ACHIEVEMENT OF THE TECHNICAL RESEARCH OBJECTIVES

##### 4.4.1 FRICTION COEFFICIENT MODEL

The comparison of experimental data with the theoretical predicted friction coefficient values presented in this chapter demonstrate that:

The friction coefficient can be predicted as a function of the operational parameters when the contact operates in the mixed or elastohydrodynamic lubrication modes. The value of the friction coefficient is given by the Schipper and de Gee theory expressed as Equation 1.2-2, reproduced below.

$$\mu_{ml} = \mu_{ehl} + \left[ \frac{\mu_{bl} - \mu_{ehl}}{\ln(2.5 \cdot \bar{p}^{0.5} \cdot R_a^{0.5})} \right] (\ln L_{ehl/ml} - \ln L) \quad \text{with,}$$

$$\mu_{ehl} = 0.024 - 0.05$$

$$\mu_{bl} = 0.07 - 0.092 \quad \text{and}$$

$$L_{ehl/ml} = \left[ \frac{3.1 \cdot 10^5 \cdot R_a^{0.5}}{\bar{p}^{0.5}} \right]$$

#### 4.4.2 TORQUE CHARACTERISTIC

For skewed roller analysis the established DAW equation for the torque generated, Equation 1.1-1 below, can be used.

$$T = F \cdot \mu \left[ \frac{D}{2} \sin \phi + \frac{2}{3} l \right] \cdot N$$

This equation is adequate. The modified version derived in this thesis replaces the  $\frac{2}{3}l$  term with  $\frac{1}{2}l$  and is analytically correct. In practice, however, the power of this term within the equation is low relative to the  $\frac{D}{2} \sin \phi$  term since the brake diameter is always significantly larger than the roller length and skew angles are unlikely to be less than approximately  $25^\circ$ . Hence, the roller length term will probably range from approximately 15% to 40% of the value of the skew angle term. Consequently, within the accuracy of the equation as a whole, the difference in the factor of  $2/3$  or  $1/2$  applied to the roller length is insignificant.



#### 4.4.3 TECHNICAL RESEARCH OBJECTIVE

The technical objective of this research was to establish a design tool which allows the torque characteristics of skewed roller devices to be predicted, based on a knowledge of the operational parameters of the device.

An equation for predicting torque was already in use at DAW and this research has confirmed that the equation is basically sound. However, the central weakness of the analysis tool has been the prediction of friction coefficient.

The comparison of experimental data with the friction coefficient model proposed by Schipper and de Gee has demonstrated a good correlation. By using the model, with constants as proposed in this thesis, friction coefficients can be predicted with a high degree of accuracy. Certainly, the accuracy is significantly higher than the all-encompassing maximum and minimum values currently in use at DAW. The data presented in this chapter demonstrates that the technical research objective has been met.

## **5. USE AND LIMITATIONS OF THE SKEWED ROLLER DESIGN TOOL**

### **Chapter Summary**

This chapter discusses the issues that must be considered in the design of aerospace actuation components and particularly those which are used in high lift actuation systems. Issues such as tolerance of the design to temperature variations and wear over large numbers of flight cycles are considered with direct reference to skewed roller devices. The conclusion is that the device should ideally operate in the mixed lubrication mode since this offers the best compromise between high friction coefficient and good wear characteristics.

The equations used in the design of skewed rollers are described, with particular emphasis on interpretation of the lubrication number parameter. Additionally, the author's recommendations for selecting stress levels, surface roughness values and skew angles are detailed. This discussion of the validated design tool forms the basis of an engineering design guide for use within DAW.

The principal limitation of the design tool at present is that it has not been validated for mean Hertzian stress values above 0.61 GPa.

The chapter is structured as follows:

- 5.1 Introduction
- 5.2 General Design Considerations
- 5.3 Design Equations
- 5.4 Limitations

## 5.1 INTRODUCTION

As with all formulae, the origin of the mathematical tools should be understood by the user, otherwise errors in application will occur. This chapter discusses the mathematical tools and provides a summarised background specifically for use by design engineers at DAW.

The context of design of aerospace actuation components is briefly discussed in this chapter and the general design considerations are related specifically to the design of skewed roller brake devices.

The equations for predicting torque, friction coefficient and probably, most crucially, lubrication numbers are described in this chapter. Advice is also given on quantitative values for parameters.

## 5.2 GENERAL DESIGN CONSIDERATIONS

When designing equipment for use on aircraft during a competitive tender process, many factors must be considered in the design. The following aspects are always critical:-

- cost
- meeting the performance specification
- reliability and maintainability
- weight
- space envelope

The company offering a solution with the best combination of engineering features, combined with a competitive commercial proposal should win the contract.

Aerospace actuation systems are required to function within performance specifications across a wide range of environmental temperatures and vibration conditions. Other environmental conditions such as humidity, resistance to chemical contaminants and electromagnetic effects may also be significant. The typical operating temperature range is  $-54^{\circ}\text{C}$  to  $+90^{\circ}\text{C}$ . High lift systems are generally not operational during cruise and therefore are exposed for long durations to temperatures of  $-54^{\circ}\text{C}$ . On other occasions, for example a take-off from a Middle Eastern location, the equipment may be exposed to very high temperatures. The performance of the equipment must be considered across the temperature range. Clearly, temperature variation will yield variation in viscosity of lubricants and a commensurate variation in lubrication number and friction coefficient.

With respect to skewed roller brake design this thesis has shown that the friction coefficient and hence brake torque can vary widely with changes in operating conditions.

Actuation equipment must also perform throughout the aircraft life, possibly up to 30 years and 60,000 flights. Consequently, the design must either be resistant to wear or the performance of the device must be tolerant of it.

With respect to speed, this will generally flow down from system level requirements and once selected, will remain constant. In certain instances, a system may have a primary, high speed, mode and a secondary, much lower, speed mode for emergency back up. These wide speed ranges have an impact on friction coefficient.

Stress levels and surface finish values are variables the designers may determine. High stress levels imply efficient use of materials and hence they should be maintained relatively high. Surface roughness values should also be maintained as small as possible. A lapping process should achieve surface roughness' of  $0.4\mu\text{m}$ . A running-in process is bound to occur during the first

few thousand cycles of operation. During this process the surface finish changes as the components rub together. This was demonstrated during development and qualification of the skewed roller brake unit in production at DAW. The majority of the running-in takes place over the first 2000 cycles of operation of the unit. The torque tends to have reduced to within approximately 15% of its asymptotic value over these cycles. The surface finish of the brake plates after a 50 000 flight cycle endurance test was found to be 0.1  $\mu\text{m}$ . The plates initially had lapped surfaces of 0.4  $\mu\text{m}$ .

As shown in Figure 4.3-1, the friction coefficient decreases with increasing lubrication number, through the mixed lubrication mode from values of approximately 0.09 to a low of 0.03 in the ehl regime.

Bearing these general design considerations in mind leads to the question, 'in which lubrication mode should skewed roller devices be designed to operate?'

In the pursuit of a stable and high friction coefficient one could conclude that it would be advantageous to operate in boundary lubrication. However, this is likely to lead to wear problems as asperity contact would lead to scuffing and excess wear over the life of the unit.

Considering the tolerance of the device to surface roughness variation and maximising the tolerance to wear suggests that elastohydrodynamic would be the best lubrication mode. The disadvantage of this is that the coefficient is, by definition low, and hence the design would possibly need extra stages to generate the required torque. This increases weight and space envelope requirements and is not preferable.

To achieve a design with an optimised compromise between good wear characteristics, low weight and high friction coefficient values, the device should be designed to operate in the mixed lubrication mode. The disadvantage of this is that changes in the operational parameters, such as, surface roughness, speed and viscosity imply significant changes in friction

coefficient and consequent torque values. The designer must take care to analyse the range of conditions over which the device will operate to ensure the design meets the specification.

## 5.3 DESIGN EQUATIONS

### 5.3.1 TORQUE EQUATION

The established torque equation at DAW is:

$$T = F \cdot \mu \left[ \frac{D}{2} \sin \phi + \frac{2}{3} l \right] \cdot N$$

In the test unit, the axial load was determined by the applied spring load. This type of design is typical of a brake device used in the transmission of a flap or slat system. The axial load is a variable entirely at the discretion of the designer. In other applications the axial load is provided directly by the aerodynamic force on the actuator and is not variable by the designer. In this case the Hertzian stresses must be controlled by sizing of the roller.

This research has conducted tests to mean Hertzian stress levels of 0.61 GPa. The unit which currently is in production at DAW has demonstrated its endurance life at approximately 0.57 GPa. Future designs will probably require higher stress values than 0.61 GPa. Since this thesis has not provided any evidence to support higher stress levels it is suggested that designs which require stresses above 0.61 GPa are supported by test evidence .

The 890 N axial load case results show more inconsistency than the more highly loaded tests. The corresponding mean Hertzian stress is 0.27 GPa. Low stress values imply inefficient use of material and are not recommended.

As a design starting point the author recommends that mean Hertzian stresses should be approximately 0.5 to 0.6 GPa.

The skew angle is an open variable which can be defined by the designer. Generally the skew angle should be in the range 30 to 50 degrees. Low skew angles imply a requirement for low torques which may be more efficiently achieved with fewer stages or a smaller PCD. Design constraints may lead to a situation where skew angle is in conflict with stress levels. In such a case the author suggests that stresses are maintained high and that smaller skew angles used.

Previous DAW experience indicated that skew angles above 55 degrees are not recommended. As the skew angle increases, the forces imparted on the roller by the cage increase and the rolling action is reduced. DAW are aware that a tendency to jam can occur at such high skew angles.

The brake pitch circle diameter is not normally an entirely free choice. The geometry of the components normally dictates the PCD to a large degree.

Roller lengths are again not entirely free. They should be kept in proportion to the PCD and maintain a suitable length to diameter ratio of up to 2. The roller length can be used to trim the contact stress levels.

The number of brake stages should be chosen to generate a required torque.

### 5.3.2 LUBRICATION NUMBER

The lubrication number is given by the equation:

$$L = \left[ \frac{\eta \cdot V_+}{\bar{p} \cdot R_a} \right] \quad 5.3-1$$

where,  $\eta$  = lubricant viscosity,

$V_+$  = the sum velocity,

$\bar{p}$  = mean Hertzian stress,

$R_a$  = surface roughness.

Dynamic viscosity is clearly a function of the lubricant selected. If data is not available in literature, then this parameter should be measured at a rheological test facility.

In practice, one of two lubricants are likely to be selected, depending on the end customer. These are Brayco 795, which is a hydraulic fluid, or semifluid. The author suggests that hydraulic fluids produce a lower dynamic viscosity, which is consistent with operation in the mixed regime. Higher dynamic viscosity lubricants tend to move the contact towards the elastohydrodynamic lubrication mode and hence generate lower coefficient of friction values. The brake torque must then be generated by higher skew angles and axial loads.

Brayco 795 is likely to have a lower dynamic viscosity than semifluid. The experimental work of this thesis has shown that the contact can be operated in the mixed lubrication regime when lubricated with Brayco 795.

Semifluid is likely to move the contact towards the elastohydrodynamic regime, and thus generate comparatively lower coefficient of friction values.



Consequently higher skew angles and perhaps higher stresses and PCD may be needed with a semifluid lubricated device. The limitations of the friction coefficient model with respect to semifluid are discussed in section 5.4.2.

The sum velocity term within the lubrication number parameter requires some interpretation. This is fully discussed in Appendix F. In terms of the PCD of the brake, the input shaft speed and skew angle, the sum velocity is given by equation 5.3-2.

$$V_s = \frac{D}{4} \cdot \left( \omega_{shaft} \cdot \frac{2 \cdot \pi}{60} \right) \cdot (2 - \sin \phi) \quad 5.3-2.$$

Standard text books such as Roark and Young can be used to find formulae for Hertzian contact stresses.

The surface roughness term,  $R_a$ , should be a measured or specified parameter.  $R_a$  is defined as the combined centre line surface roughness. The plates used in the tests were manufactured to  $0.4\mu\text{m}$ . They were also used on a 50 000 cycle endurance test which resulted in a  $0.1\mu\text{m}$  surface finish at the end of the test. These values were taken as a standard and used for comparing the surface finishes of the plates as the testing progressed.

### 5.3.3 FRICTION COEFFICIENT

The coefficient of friction is calculated by the Schipper and de Gee formula :

$$\mu_{ml} = \mu_{ehl} + \left[ \frac{\mu_{bl} - \mu_{ehl}}{\ln(2.5 \cdot \bar{p}^{0.5} \cdot R_a^{0.5})} \right] (\ln L_{ehl/ml} - \ln L) \quad \text{with,}$$

$$\mu_{ehl} = 0.024 - 0.05$$

$$\mu_{bl} = 0.07 - 0.092 \quad \text{and}$$

$$L_{ehl/ml} = \left[ \frac{3.1 \cdot 10^5 \cdot R_a^{0.5}}{\bar{p}^{0.5}} \right]$$

For design purposes it is probably more expedient to use the data from the values presented in Figure 4.3-1, based on the lubrication number calculated from Equation 5.3-1.

## 5.4 LIMITATIONS

### 5.4.1 CONTACT STRESS

Section 5.3.1 discussed the issue of contact stress, emphasising that the evidence for skewed roller device is limited to a maximum, mean Hertzian stress of 0.61Gpa.

This stress is low compared to the maximum allowable stress levels for the tool steel and S82 materials used for the roller and brake plates. It was also noted that in the situation where the axial loads are determined by

aerodynamic loads, it may be necessary to operate at higher stress levels than the test envelope available.

Two key questions arise when a stress increases, and consequently the lubrication number decreases. These are:

- i) Does the contact enter the boundary lubrication mode and is the maximum friction coefficient of 0.092 valid or are higher values obtained. As indicated earlier in this thesis, values up to 0.15 could be expected ?
- ii) What is the endurance performance of the device like when operated at high stress levels, possibly in the boundary lubrication mode ?

Ideally, the device should be tested at much higher stress levels, up to approximately 3Gpa in order to validate the model at these higher stresses. The designer should also be aware of a potential problem when operating skewed rollers, or any bearing, at very high stresses. The phenomenon of 'false brinelling' is characterised by damage to rollers and raceways, often in the form of flats and indentations. It is caused by high frequency static loads and is most likely to occur when loads are generated by aerodynamic forces rather than a spring. Expansion of the model to 3 GPa is necessary, but the designer should take care when the applied loads are expected to be oscillatory and the skewed roller device is not rotating.

## 5.4.2 SEMIFLUID LUBRICATION

Semifluid is a blend of grease and low viscosity base oil. In various forms it has been used as a lubricant in aerospace gearboxes for a number of years. If left to stand, this base oil tends to separate from the grease.

Semifluids are not widely available and very little rheological data is published. This lack of rheological data means that the lubrication numbers can not at present be calculated, inhibiting the use of this design tool. Also, the behaviour of semifluid under extreme pressures in skewed roller devices is not known.

Analytical work with semifluid is restricted at present by the lack of data. Basic research work is still required with this particular lubricant.

## **6. TECHNICAL REVIEW AND RECOMMENDATIONS FOR FURTHER WORK**

### **Chapter Summary**

This chapter summarises the main technical aspects of the research work and proposes what future work should be conducted to extend the envelope of the design tool and maximise its potential for marketing. The chapter structure is as follows:

- 6.1 Introduction
- 6.2 Technical Discussion
- 6.3 Direction of further work

A validated skewed roller design tool has been developed which meets the technical research objectives of this project.

The sponsoring organisation, as a direct result of this project, now has an analysis technique to predict friction coefficient, to a good degree of accuracy, depending on the operational parameters of the design. The theoretical calculation of friction coefficient allows the established torque equation to be used to calculate brake drag torque.

Further work should be directed at extending the validated envelope of the design tool to mean Hertzian stress levels in the range 1GPa to 3GPa. Also, the characteristics of semifluid as a skewed roller lubricant should be investigated by analysis and experiment. This will enhance the marketability of the skewed roller concept, particularly at Airbus.

## 6.1 INTRODUCTION

This research project has resulted in the creation of an extensive experimental database which details the friction characteristics of skewed roller devices as a function of skew angle, speed, stress and lubricant viscosity. This experimental data has enabled the validation and development of a theoretical friction coefficient model for use in the mixed lubrication regime. Hence, friction coefficient and subsequently the torque produced by a skewed roller device can be predicted based on knowledge of the operational parameters of the device. This chapter reviews and summaries the main technical aspects of the experimental work and the establishment of a validated skewed roller brake design tool.

The experimental work, has, by necessity covered a defined envelope in terms of speed, stress and lubricant viscosity parameters. Particularly with respect to mean Hertzian stresses above 1 GPa and to a lesser extent the choice of lubricant and roller length, the research work has not covered the whole of the possible envelope which may be experienced in practice.

This chapter proposes the direction which future research should take in order to extend the validated envelope of the design tool. The proposed future work would also allow DAW to maximise the potential of the research and the design tool as a marketing asset.

## 6.2 TECHNICAL DISCUSSION

The major technical achievement of this research project is the demonstration that friction coefficients for skewed roller devices can be predicted with a good degree of accuracy. In order to do this, knowledge of the operational parameters of the design is required. These operational parameters allow the lubrication number to be calculated, which in turn, either by calculation or by

reference to Figure 4.3-1 allows the maximum and minimum values for friction coefficient to be selected.

This friction coefficient value may then be inserted into the established DAW equation for predicting torque from skewed roller devices. This equation adequately predicts the correct torque characteristic as a function of skew angle and axial load. The key analysis techniques, including lubrication number analysis and the basic friction coefficient model in the mixed regime have been adopted from the works of Schipper and de Gee (1995).

This basic friction coefficient model was refined and developed using the experimental data gained from the tests conducted during the research. The resulting model provides a good match to the experimental data.

The good correlation of the friction coefficient model results and the experimental data gathered during this research satisfy the technical research objective of this project.

The project has generated an extensive experimental data set. This covers speed ranges from 50 to 650 rpm, mean Hertzian stress levels from 0.27 GPa to 0.61 GPa, and two lubricants with significantly different viscosities. These experiments confirmed that the torque produced by skewed roller brakes follows an approximate sine law for variations in skew angle and appears linear with axial load. The experimental work has also shown the apparent generation of the Stribeck curve showing performance in the mixed and elastohydrodynamically lubricated regimes.

Film thickness to roughness ratio analysis provided contradictory results. For Catenex 79 lubricant the analysis suggested that the contact was operating in both mixed and elastohydrodynamic regimes, depending on the speed and stress levels. This conclusion was largely confirmed by experimental friction coefficient values. These rose from a low of approximately 0.025, in the ehl

regime, to approximately 0.06 as lubrication number was decreased and the contact moved into the mixed lubrication mode. For Brayco 79,  $\Lambda$  was predominantly  $<1$  suggesting boundary lubrication. However, the experimental evidence of this project suggested a fairly linear decrease in friction coefficient with increasing lubrication number, this would indicate a mixed lubrication regime. This was not consistent with the expectations from analysis of the mode transition diagram of Schipper and de Gee, which indicated both mixed and elastohydrodynamic modes depending on speed and stress levels. The experimental evidence suggested that the transition from mixed to ehl lubrication modes should occur at higher lubrication numbers than indicated by Schipper and de Gee. This resulted in an adjustment to the transition point formula and a subsequently better correlation with the adjusted mode transition diagram.

With respect to general design principals, aerospace applications demand specifications to be met with minimum weight, space envelope and cost. The basic requirement of skewed roller devices, used as brakes and possibly clutches, is to produce drag torque. Therefore, they need a high friction coefficient value to minimise space and weight.

The highest friction coefficients are obtained in the boundary lubrication regime. However, boundary lubrication is not preferred because of uncertainty about wear stability of the components in a boundary lubrication mode contact. The device will be required to operate, without maintenance action for the full life of the aircraft. The conclusion is that the design should operate in the mixed regime. This probably implies thin lubricants such as Brayco 795 or other more common hydraulic fluids such as MIL-H-5606 or MIL-H-83282, rather than high viscosity fluids.



## 6.3 DIRECTION OF FURTHER WORK

### 6.3.1 HERTZIAN STRESS LEVELS

The mean Hertzian stress range across which tests were conducted for this research was 0.27 GPa to 0.61 GPa. Within the context of wider research on lubrication of concentrated contacts, 0.61 GPa is a fairly low stress level. Other researchers, Evans and Johnson (1986b), for example, have conducted tests up to approximately 3 GPa.

For an aerospace application, high stress levels imply an efficient use of metal and hence a weight optimised design.

The tests conducted for this thesis have not clearly established that the contact will enter the boundary lubrication mode, and hence confirmed the mixed mode to boundary mode transition point. Tests conducted at higher stress levels up to 3 GPa would populate the data set at the lower end of the lubrication number range and add usefully to the design tool.

In fact these tests, conducted by removing rollers from the existing test unit will be completed as part of an undergraduate final year project during 1998/99.

### 6.3.2 CHOICE OF LUBRICANT

The two lubricants chosen for this research were selected for specific reasons. Brayco 795 because it is used in the skewed roller device currently in production at DAW and some limited performance data was available at the start of the project. It is likely that it would be used again for the same customer and hence is clearly representative of an aerospace application. Catenex 79 was selected primarily because rheological data for it is widely

published and the friction model theories found in literature have been generally developed with this lubricant. Hence, a good linkage into published data was possible. The project benefited in an initially unforeseen way due to the viscosity of Catenex being approximately an order of magnitude higher than Brayco 795. This meant that the lubrication number ranges for each lubricant overlapped at their extremes, providing a wide range of lubrication number over which to validate the frictional behaviour of the device.

For aerospace applications it would seem reasonable to assume that the Brayco 795 data is applicable to other mineral oil based hydraulic fluids which may be used as lubricants. Examples would be the very common hydraulic fluids MIL-H-5606 and MIL-H-83282. Dynamic viscosity characteristics for these fluids would either have to be measured or obtained from published data.

The use of semifluid is increasing as a gearbox lubricant, particularly at Airbus. This lubricant consists of a mix of very low viscosity base oil and grease. The two principal constituents tend to separate out unless regularly mixed. This lubricant is becoming more widely used due to its claimed corrosion protection and good lubrication characteristics.

The detail rheological properties of semifluid are not published or known to DAW. Also the characteristic of semifluid when used as a skewed roller lubricant has not been established. The validity of the design tools in this thesis should be established for semifluid lubrication.

### 6.3.3 ENVIRONMENTAL TEMPERATURE VARIATIONS

The normal ambient temperature variation for civil aerospace products ranges from  $-54^{\circ}\text{C}$  to  $+90^{\circ}\text{C}$ , across which the devices are expected to perform within specification. Devices used within high lift systems are generally not

operative during cruise and hence soak to  $-54^{\circ}\text{C}$ . Clearly, low temperature operational characteristics are important. Friction characteristics should be predictable based on a knowledge of low temperature viscosity. This should increase dynamic viscosity and increase lubrication number, thus move the contact towards the ehl regime and decrease the friction coefficient.

An alternative possibility at low temperature is that the lubricant behaves as if in the solid rather than liquid state. Schipper and de Gee (1995) research shows that under solid state conditions the friction coefficient can approximate to two levels. Either a value consistent with ehl, as above, or a value associated with the lubricants ratio of limiting shear stress over pressure. For mineral oils this value is apparently approximately 0.09. The subsequent change in characteristics due to shear heating would probably restore operation in the liquid phase. It should be noted that such a dual level of friction coefficient at low temperature has not been seen during previous tests at DAW.

The uncertainty of the behaviour of the lubricant at very low temperature, coupled with the effect of shear heating on the performance of the device should be researched further.

Shear heating will also occur if the device has been subjected to high ambient temperatures. The heating effect is less likely to impact the frictional characteristics of the device since the viscosity characteristic is likely to be on the flat portion of the temperature-viscosity asymptote.

During engineering discussions with customers, the issue of performance at the extremes of temperature is always discussed. Although performance characteristics are analytically predictable, experimental test evidence is always more convincing. Thus, from a marketing perspective it would be worthwhile to conduct the extreme temperature tests. Again, this is planned as part of the undergraduate final year project mentioned above.

#### 6.3.4 ROLLER LENGTH

All the tests within this research project have been conducted with 10mm rollers. Some discussion about the effectiveness of the roller length term within the overall torque equation was detailed in section 4.4.2. Testing with longer rollers would allow clarification of this term.

#### 6.3.5 DESIGN CASE STUDY

Chapter 5 of this thesis has discussed the use of the design tool in general terms and provided guidance on the selection of critical parameters such as stress levels and skew angles. For use within the engineering department at DAW it would be useful to conduct a design case study, perhaps using an existing design as a reference example. The design case study, along with the general guidance of chapter 5, would then form a design guide for use within DAW. For reference, the operating point of the skewed roller brake unit currently supplied by DAW to Boeing is shown on Figure 4.3-1.

# 7. REVIEW OF THE BUSINESS CASE AND OVERALL CONCLUSIONS

## Chapter Summary

This chapter reviews the research business case and reports the conclusions that were drawn from the whole research program. The chapter structure is:

- 7.1 Introduction
- 7.2 The Business Case for the Research
- 7.3 Technical Conclusions
- 7.4 Business Case Conclusions
- 7.5 Directions For Future Work
- 7.6 Overall Conclusions

The project sponsors had identified a need to develop the existing skewed roller brake design tool. This tool was inadequate with respect to the prediction of friction coefficient. The technical objective was to develop a model to predict friction coefficient values as a function of operational parameters.

A cost benefit analysis indicated that a successful project could provide an opportunity for technically differentiating between DAW and their competitors. This could allow premium pricing, or enhance opportunities to enter new markets in the future. Additionally, requirements for design phase prototype tests would be redundant. Since these tests are both expensive and time consuming this yields operating benefits to the sponsors.

The technical research objective has been achieved. A validated friction coefficient model and design tool has been produced. The future opportunities for technical differentiation, new market penetration, premium pricing and time and cost savings are now realisable.

## 7.1 INTRODUCTION

Dowty Aerospace Wolverhampton, the project sponsors had identified a need to develop an improved analytical design tool to aid the design of skewed roller brake devices.

Skewed roller brakes are passive asymmetry protection devices, which find applications in flap, slat and trimmable horizontal stabiliser actuation systems. At the present time only Boeing Aircraft Company have widely accepted the use of these devices. Additionally, only a very small number of actuation systems suppliers have any service experience with these units. The device has yet to be introduced on any Airbus aircraft.

The design tool currently in use at DAW adequately predicts the torque produced by the device but requires a prior knowledge of the effective friction coefficient so that this term is a known value within the torque equation. Analytical methods of predicting the friction coefficient are not available at DAW and hence a prototype test has been required to determine this value for each new design. Conducting prototype tests is both time consuming and an expensive process. Without test evidence, a wide tolerance of friction coefficient is generally assumed, between 0.066 and 0.092. This is without any consideration of the variation in coefficient resulting from changes in operational parameters such as load and speed. Hence DAW have an inadequate analytical model for use in the design of skewed roller devices and an unconvincing understanding of the frictional behaviour of the devices. This hinders the marketing of the concept to potential customers, who may regard the concept as higher risk than traditional friction brakes.

The technical and business objectives of the project were defined as.

Technical Research Objective:

*To develop an analytical design tool such that skewed roller brake performance can be predicted from the operational and geometric design parameters of the device, without recourse to a design phase prototype test.*

Business Objectives

*To develop a cost benefit analysis based on the cost savings associated with removal of the need for conducting prototype testing in order to justify the project investment.*

*To develop a deeper technical understanding of the frictional characteristics of skewed roller devices so that DAW technical expertise may be used as a marketing tool when competing for new business. This technical differentiation relative to competitors may enable premium pricing of the DAW solution.*

## 7.2 THE BUSINESS CASE FOR THE RESEARCH

The project business case was founded on three principle issues; the development of technical expertise in the design of skewed roller devices allowing potential customer reservations concerning technical risk to be overcome and thus opening new markets; establishing a technical differentiation between DAW and competitors and thus providing an opportunity for premium pricing of the product; cost and time savings if prototype testing can be reduced or eliminated.

### 7.2.1 FINANCIAL JUSTIFICATION

The total project budget was defined as £38000. A cost benefit analysis using Net Present Value techniques was conducted with the principal benefit being that expensive prototype testing would not be required if the technical research objectives were achieved. Over the expected useful life of the project technical output, it was estimated that two prototype units and tests would not be required as a result of developing the design tool. These savings yielded an NPV of £10358 and hence the financial case for conducting the research was made.

### 7.2.2 TECHNICAL RISK

Skewed rollers are an accepted technology at Boeing and hence technical risk is not an issue with this customer. However, Airbus have never fitted such a device to their aircraft and hence the Airbus Engineering community consider that the technology is unproven and represents a technical risk. Part of the process of mitigating the risk, and hence opening new markets, is to have a detailed technical understanding of the characteristics of such units. The design philosophy, performance characteristics and benefits of the design solution over alternatives can then be clearly and confidently explained to the potential customer.

### 7.2.3 THE MARKETING TOOL

In conjunction with the reduction in technical risk described above, the development of the design tool and associated technical expertise should allow DAW to differentiate its engineering capabilities compared to competitors. The realisation of this will necessitate the presentation of the techniques to customers such as Boeing and Airbus.



Hence, the engineering capabilities of DAW are used as a marketing tool to enhance our probability of winning new business. This also enables the possibility for premium pricing the product if the technical differentiation is strong.

### 7.3 TECHNICAL CONCLUSIONS

- i) The existing equation for calculating the torque generated by the skewed roller brake was found to be adequate. The equation predicts the correct characteristic as a function of skew angle and axial load. The torque is approximately a sinusoidal function of skew angle and an apparently linear function of axial load.
- ii) Knowledge of the friction coefficient in the contact is fundamental to calculating the brake torque correctly. The existing DAW analysis method assumes a maximum and minimum value of friction coefficient of 0.092 and 0.066 respectively. This method does not accurately predict the friction coefficient with changes in operational parameters and is inadequate.
- iii) The Schipper and de Gee (1995) model predicts friction coefficient as a function of lubrication number. This model has been refined based on experimental data generated for this thesis. The result is a validated model for predicting friction coefficients based on the operational parameters, load, speed, lubricant viscosity and surface roughness.
- iv) Skewed roller brakes should be designed so that the line contact operates in the mixed lubrication regime. This provides the best compromise between achieving a high friction coefficient and a low wear rate contact.

- v) Selection of a relatively low viscosity lubricant is consistent with the conclusion in iv) above. Thus, hydraulic fluid lubricants such as Brayco 795 are probably preferable to higher viscosity lubricants such as semifluid.

#### 7.4 BUSINESS CASE CONCLUSIONS

- i) The technical research objective has been achieved.
- ii) The project was completed in the allocated time of four academic years. The project budget of £8600 was overspent by £427.
- iii) Achievement of the technical research objective has reduced the requirement for future prototype tests to support new business proposals and post contract design. Hence the financial benefits claimed within the NPV analysis should be realised.
- iv) The friction coefficient prediction tool represents a significant advance in the analysis techniques available at DAW. The research has probably put DAW ahead of their competitors and major customers in terms of skewed roller device technology. This should enable DAW to demonstrate a technical differentiation relative to their competitors and demonstrate an acceptable level of technical risk, in any future new business opportunities for skewed roller devices.
- v) If a clear technical differentiation can be demonstrated to the customer in a proposal situation, then the opportunity to premium price the product will have been established.

## 7.5 DIRECTIONS FOR FUTURE WORK

- i) The friction coefficient model has been validated to mean Hertzian stress values of 0.61 GPa. This is unlikely to be high enough to cover all applications of skewed roller brakes, particularly where aerodynamic forces generate the axial loads on the rollers. Research should continue to extend the envelope of the model to mean Hertzian stress values of 3 GPa.
- ii) The suitability of Brayco 795 as a lubricant for skewed roller devices has been established through in service experience. Additionally, DAW's knowledge of the rheological characteristics of Brayco 795 has been extended by the research of this project. Semifluid is becoming more prevalent as a lubricant for gearbox components, mainly due to its combined lubrication and corrosion protection characteristics. The rheological properties of semifluid are not well known to DAW. The characteristics of semifluid when used to lubricate skewed roller devices should be investigated and the validity of the design tools in this thesis established for this lubricant.
- iii) To enhance the use of the design tool as a marketing feature, the performance of the model should be assessed at the extremes of the operational temperature range,  $-54^{\circ}\text{C}$  to  $90^{\circ}\text{C}$ .
- iv) A specific research programme investigating the effect of roller length is not necessary. However, data will emerge as more designs are completed over the course of time. The model should be reviewed periodically as this data becomes available.
- v) Complete a design case study using an existing DAW design as an example. This specific design analysis, along with the general guidance described in chapter 5 of this thesis would then form a 'designers guide' for use within DAW.

## 7.6 OVERALL CONCLUSIONS

In conclusion, Dowty Aerospace Wolverhampton, as the project sponsor had identified a need to improve the existing design tool for predicting the torque characteristics of skewed roller brake devices. Fundamental to this design tool is the ability to predict friction coefficient values based on knowledge of the operational parameters of the design.

The above need defined the technical research objective for the project. A research methodology was devised to address the problem. This methodology was subjected to a thorough risk assessment and project management techniques were applied throughout the project to ensure that the technical objectives were achieved within the project budget and on time.

A cost benefit analysis identified that the project had a NPV of approximately £10K. This was based on the removal of need for future prototype tests if the technical research objective was achieved. The design tool should also enhance the marketing of DAW's skewed roller technical expertise and reduce the perceived technical risk of skewed roller devices, specifically at Airbus. This should enhance the probability of penetrating the Airbus market with this technology. The design tool should also potentially allow DAW to establish a technical differentiation relative to their competitors in future proposals to customers. This could allow premium pricing of the product.

A validated method of predicting the coefficient of friction based on operational parameters has been developed to meet the technical research objective. The method employs the lubrication number analysis technique of Schipper and de Gee. The analysis method has been incorporated into a design guide for use by DAW engineers. The business case has been satisfied for the stress range considered.

Future work should concentrate on extending the validated envelope of the design tool to mean Hertzian stress levels up to 3 GPa. The suitability and characteristics of semifluid as a skewed roller lubricant should also be researched.

## REFERENCES

- Alsaad, M. Bair, S. Samborn, D. M. Winer, W. O. 1978.** Glass Transitions in Lubricants. Its Relation to Elastohydrodynamic Lubrication (EHD). Trans. of ASME. Journal of Lubrication Technology. Vol 100, 404-417.
- Bair, S. Winer, W. O. 1982.** Regimes of Traction in Concentrated Contact Lubrication. Trans. of ASME. Vol 104, 382-391.
- Chang, L. Zhou, W. 1995.** Fundamental Differences Between Newtonian and Non-Newtonian Micro-EHL Results. Journal of Tribology. Vol 117, 29-35.
- DAW, (1998).** A340-500/600 Trimmable Horizontal Stabiliser Proposal. Proprietary Data.
- Dowson, D. Higginson, G. R. 1977.** Elasto-hydrodynamic Lubrication. Pergamon Press. 1977.
- Evans, C. R. Johnson, K. L. 1986a.** The Rheological Properties of Elastohydrodynamic Lubricants. Proc. Instn. Mech. Eng. Vol 200, C5, 303-312.
- Evans, C. R. Johnson, K. L. 1986b.** Regimes of Traction in Elastohydrodynamic Lubrication. Proc. Instn. Mech. Eng. Vol 200, C5, 313-324.
- Evans, C. R. Johnson, K. L. 1987.** The Influence of Surface Roughness on Elastohydrodynamic Traction. Proc. Instn. Mech. Eng. Vol 201, C2, 145-151.
- Flight International, 1998,** 15-21 July, 4.

**Glaeser, W. A. Erickson, R. C. Dufrane, K. F. Kannel, J. W. 1994.**

Tribology: The Science of Combatting Wear. Journal of the Society of Tribologists and Lubrication Engineers. Vol 50, 225-227.

**Hess, D. P. Soom, A. 1990.** Friction at a Lubricated Line Contact Operating at Sliding Velocities. Journal of Tribology. Vol 112, 147-152.

**Horng, J. H. Lin, J. F. Lee, K. Y. 1994.** The Effect of Surface Irregularities on the Tribological Behaviour of Steel Rollers Under Rolling-Sliding Contact. Journal of Tribology. Vol 116. 209-218.

**Houpert, L. G. Hamrock, B. J. 1986.** Fast Approach for Calculating Film Thickness and Pressures in EHL Contacts at High Loads. Journal of Tribology. Vol 108, 411-420.

**Jang, S. Tichy, J. 1995.** Rheological Models for Thin Film EHL Contacts. Journal of Tribology. Vol 117, 22-28.

**Jeng, J. R. 1990.** Experimental Study of the Effects of Surface Roughness on Friction. STLE Tribology Transactions. Vol 33, 3, 402-410.

**Johnson, K. L. Tevaarwerk, J. L. 1977.** Shear Behaviour of Elastohydrodynamic Oil Films. Proc. Royal Soc. of London. Vol A356, 215-236.

**Johnson, K. L. Greenwood, J. A. 1980.** Thermal Analysis of an Eyring Fluid in Elastohydrodynamic Traction. Wear 61, 353-374.

**Kempes Engineers Year Book. 1996.** Miller Freeman.

**Lin, J. F. Horng, J. H. Lee, K. Y. 1993.** Effect of an EP Additive on the Tribological Behaviour of Steel Rollers with Surface Irregularities. *Wear* 169, 107-118.

**MECH 5270.** Lubricants and Lubrication Module. Leeds University  
MSc(Eng) Tribology in Machine Design. 1996.

**Polycarpou, A. A. Soom, A. 1995.** Two Dimensional Models of Boundary and Mixed Friction at a Line Contact. *Journal of Tribology*. Vol 117, 178-184.

**Sanderson, M. L. Undated.** EngD Thesis, Non Technical Content Presentation.

**Sayles, R. S. Webster, M. N. 1985.** Characteristics of Surface Roughness Important to Gear and Rolling Element Bearing Problems. Tribology Section. Dept of Mech Eng. Imperial College. Gears and Transmission Systems for Helicopters and Turboprops. Propulsion and Energetics Panel Symposium (64). Jan 1985, 8-12 October 1984. Lisbon, Portugal.

**Sayles, R. S. Hammer, J. C. Ioannides, E. 1990.** The Effects of Particulate Contamination in Rolling Element Bearings - a State of the Art Review. *Proc. Instn Mech. Eng.* Vol. 204. 29-36.

**Schipper, D. J. Vroegop, P. H. de Gee, A. W. J. 1989.** Prediction of Lubrication Regimes of Concentrated Contacts. 5th International Congress of Tribology. Eurotrib 89, Helsinki, Finland. Vol 2, 171-177.

**Schipper, D. J. de Gee, A. W. J. 1995.** On the Transitions in the Lubrication of Concentrated Contacts. *Journal of Tribology*. Vol 117, 250-254.

**Schroeder, W. 1994.** Spherical Roller Bearing Basics. *Power Transmission Design*. Vol 36, 51-54.



**Shieh, J. Hamrock, B. J. 1991.** Film Collapse in EHL a Micro-EHL. Journal of Tribology. Vol 113, 372-377.

**Tichy, J. A. 1995.** A Porous Media Model for Thin Film Lubrication. Journal of Tribology. Vol 117, 16-20.

**Thomas, G. Harris, A. 1993.** Preliminary Design Review Data. Dowty Aerospace Wolverhampton Proprietary information. June 1993.

**Warren. C. Young.** Roark's formulas for Stress and Strain 6<sup>th</sup> edition. Mc Graw-Hill Book Company.

**Williams, J. A. 1996.** Engineering Tribology. Oxford Science Publications.

**Zhou, R. S. Hashimoto, F. 1995.** A New Rolling Contact Surface and 'No Run-In' Performance Bearings. Journal of Tribology. Vol 117, 166-170.

## **BIBLIOGRAPHY**

**Alliston-Greiner, A. F. 1991.** Testing Extreme Pressure and Anti-Wear Performance of Gear Lubricants. Proc. Instn. Mech. Eng. Vol 205, 89-101.

**Bayer, R. G. Sirico, J. L. 1975.** The Influence of Surface Roughness on Wear. Wear 35, 251-260.

**Bos, J. Moes, H. 1995.** Frictional Heating of Tribological Contacts. Journal of Tribology. Vol 117, 171-177.

**Hirst, W. Moore, A. J. 1980.** The Effect of Temperature on Traction in Elastohydrodynamic Lubrication. Proc. Royal Soc. Vol 298, 183-207.

**Horng, J. H. Lin, J. F. Kee, Y. L. 1995.** Effect of Surface Roughness on Steel Roller Scuffing. Wear 184, 203-212.

**Johnson, K. L. Greenwood, J. A. 1980.** Thermal Analysis of an Eyring Fluid in Elastohydrodynamic Traction. Wear 61, 353-374.

**Kimira, Y. Sugimura, J. 1984.** Microgeometry of Sliding Surfaces and Wear Particles in Lubricated Contact. Wear 100, 33-45.

**Kragelski, I. V. Kambalov, V. S. 1969.** Calculation of Value of Stable Roughness After Running-In (Elastic Contact). Wear 14, 137-140.

**Masouros, G. Dimanoganos, A. Lefas, K. 1977.** A Model for and Surface Roughness Transients During Running-In of Bearings. Wear 35, 375-382.

**Patir, N. Cheng, H. S. 1978.** An Average Flow Model for Determining the Effects of Three Dimensional Roughness on Partial Hydrodynamic Lubrication. Journal of Tribology. Vol 100, 12-17.

**Patir, N. Cheng, H. S. 1979.** Application of Average Flow Model to Lubrication Between Rough Sliding Surfaces. *Journal of Lubrication Technology*. Trans ASME. Vol 101, 221-231.

**Prasad, D. Singh, P. Sinha, P. 1993.** Thermal and Inertia Effects in Hydrodynamic Lubrication of Rollers by a Power Law Fluid Considering Cavitation. *Journal of Tribology*. Vol 115. 319-326.

**Rowe, G. W. Kaliszer, H. Trimal, G. Cotter, A. 1975.** Running-In of Plain Bearings. *Wear* 34, 1-14.

**Schipper, D. J. Vroegop, P. H. de Gee, A. W. J. 1990.** Micro EHL in Lubricated Concentrated Contacts. *Journal of Tribology*. Vol 112. 392-397.

**Schipper, D. J. Vroegop, P. H. de Gee, A. W. J. 1990.** On the Transitions Between Solid and Liquid State Behaviour of Lubricants in Concentrated Contacts. Proc. of Japan International Tribology Conf. Nagoya, Japan, April 1990. Vol 1, 379-384.

**Sui, P. C. Sadeghi, F. 1991.** Non-Newtonian Thermal Elastohydrodynamic Lubrication. *Journal of Tribology*. Vol 113, 390-396.

**Tripp, J. H. Ioannides, E. 1990.** Effects of Surface Roughness on Rolling Bearing Life. Proc. of the Japan International Tribology Conference. Nagoya, Japan, 1990. 797-803.

**Venner, C. H. Lubrecht, A. A. 1994.** Transient Analysis of Surface Features in an EHL Line Contact in the Case of Sliding. *Journal of Tribology*. Vol 116. 186-193.

**Zhu, D. Cheng, H. S. Hamrock, B. J. 1990.** Effects of Surface Roughness on Pressure Spike and Film Constriction in EHL Line Contacts. STLE Tribological Transactions. Vol 33, 2, 267-273.

# **APPENDIX A**

## **The Engineering Doctorate Programme**

### **Introduction**

The Engineering Doctorate was developed in response to the recommendations of the Science and Engineering Research Council's Parnaby working party report on the Engineering PhD. The working party concluded that industry required graduates who in addition to having good analytical skills, also understood the nature of business and industry and are capable of integrating into it easily. The working party recommended that a new degree should be established and christened it the Engineering Doctorate, EngD. The Engineering Doctorate has at least the intellectual effort of a traditional engineering PhD, but is enhanced by the addition of taught material, in both technical and management areas. These taught elements are designed to develop and increase those skills required by industry.

### **Core Skills**

The Parnaby working group required that the research engineer, in addition to undertaking a challenging technical problem, should develop competencies in management, written and oral communication, teamwork and leadership.

The core management material takes the form of selected modules from the Cranfield School of Management full time MBA course. The research engineer attends taught sessions and is assessed in exactly the same manner as an MBA student. The core material also includes a number of 1-3 day seminars covering those MBA modules considered less relevant to the research engineer, but still worthy of an overview.

The core technical material is covered by a number of bespoke courses provided by relevant departments at Cranfield University. The core specialist technical courses

must be directly relevant to the thesis and are generally selected Msc modules provided by any relevant University. The technical course elements are all assessed.

The core syllabus encompassed the following:

<b>Core Course</b>	<b>Assessment</b>	<b>Level</b>
<b>MBA Modules</b>		
Accountancy	Exam/WAC*	Masters
Financial Management	Exam	Masters
Marketing	Exam/WAC*	Masters
Strategic Management	Exam/Project	Masters
Project Management	Project	Masters
Personal Communication Skills	Attendance	n/a
*WAC - Written Assessment of Case		
<b>MBA Seminars</b>		
European Business Environment	Attendance	n/a
Economics	Attendance	n/a
Human Resource Management	Attendance	n/a
Information Systems	Attendance	n/a
Operations Management	Attendance	n/a
<b>Core Skills</b>		
Research Methodology	Attendance	n/a
Environmental and Social Assessment of Technology	Project	n/a
Engineering Design, Data Analysis and Modelling	Project	n/a
Advanced Computational Methods	Project	n/a
Learning Team Approach	Optional	n/a
<b>Specialist Engineering Courses</b>		
Instrumentation, AVE/16 Cranfield University	Exam	Masters
Lubricants and Lubrication, Mech 5270, Leeds University	Exam/Project	Masters
Surface Contact Phenomena, Mech 5125, Leeds Uni'ty	Exam	Masters

## Course Structure

The course began with 6 months full time attending the MBA modules. The second six months was spent on thesis preparatory work. The following three years concentrated on the engineering research and attendance of specialist engineering taught courses, and MBA and engineering skill development seminars.

### Year 1

Cranfield School of Management MBA modules	(6 months)	Assessed
Thesis related project	(6 months)	Assessed
Specialist engineering taught course	(3 months)	Assessed
Core skills	(3 months)	Assessed

### Year 2

Thesis work		
Cranfield School of Management MBA seminars	(2 weeks)	
Core skills seminars	(1 week)	Assessed

### Year 3

Thesis work		
Cranfield School of Management MBA seminars	(1 week)	
Core skills seminars	(1 week)	Assessed
Specialist Engineering taught course	(3 months)	Assessed

### Year 4

Thesis work		Assessed by viva
-------------	--	------------------

## **Supervisory Panel**

Academic Supervisor	Dr. Robert Jones (Cranfield University)
Industrial Supervisor	Mr. Paul Strothers (Dowty)
Management Supervisor	Dr Alan Harrison (Cranfield University)

## **Cranfield School of Management Results**

Accountancy	64%
Marketing	57%
Financial Management	61%
Project Management	52%
Strategic Management	65%

## **Engineering Core Subject Results**

Advanced Computational Methods	A
Engineering Design	C
Technological and Environmental Assessment	A

## **Engineering Specialist Courses**

Instrumentation	A
Lubricants and Lubrication	A
Surface Contact Phenomena	A



## **APPENDIX B**

### **COST BENEFIT ANALYSIS**

The financial analysis has considered the incremental costs associated with the project.

#### **Investments**

The investment elements cover the travel and subsistence cost of completing the full time MBA element of the Engineering Doctorate at Cranfield, from a home base in the Midlands. The travel costs also allow for the completion of two Msc modules at Leeds University. These modules required a return journey from Wolverhampton to Leeds 5 times per week, for an 11 week term.

The annual cost of the Undergraduate trainee was factored in proportion to the time estimated to be spent working on this project.

#### **Returns**

The costs associated with conducting a prototype test during a bid situation have been estimated at £16800 each. In this scenario, full time DAW engineers would complete the work, with test unit and rig manufacturing being sub-contracted. The engineering manhours have been costed at a nominal rate of £25 per hour.

#### **Discount Factor**

A discount factor of 15% has been chosen. This is consistent with the discount factor used by Dowty when assessing capital investment projects.

## Life of the Project

The life of the project was assumed to be 6 years after completion of the research. This time was expected to span two successful proposals, and the wider acceptance of skewed roller devices within the industry. Beyond this time the competitive advantage enhanced by the research specifically will have been eroded by competitors.

## APPENDIX B - Net Present Value of the Research

	Bought out cost, £	Engineering Manhour Cost, £
<b>Bid specific test unit</b>		
design/drawing		625
manufacture	3500	
assembly		250
sub-total	3500	875
<b>Bid specific test equipment</b>		
design/specification		750
manufacture	7500	
installation		375
calibration		300
commissioning		500
sub-total	7500	1925
<b>Prototype testing</b>		
test/analysis and report		3000
sub-total	0	3000
total	11000	5800
<b>grand total</b>		<b>16800</b>

## APPENDIX B - Net Present Value of the Research

	Year 0 1994	Year 1 1995	Year 2 1996	Year 3 1997	Year 4 1998	Year 5 1999	Year 6 2000	Year 7 2001	Year 8 2002	Year 9 2003	Year 10 2004	totals
<b>Investment</b>												
Accommodation at Cranfield, MBA	4400											4400
University Fees	3000	3000	3000	3000								12000
Travel costs	532	76	1424	174	76							2282
Test parts and consumables			1600	1100	500							3200
Undergraduate Trainee			6750	4500	4500							15750
<b>Total Investment</b>	<b>7932</b>	<b>3076</b>	<b>12773.5</b>	<b>8774</b>	<b>5076</b>	<b>0</b>	<b>0</b>	<b>0</b>	<b>0</b>	<b>0</b>	<b>0</b>	<b>37632</b>
<b>Returns</b>												
EPSERC Grant	8916	8916	8916	8916								35664
Cost of two bid support development tests						16800			16800			33600
<b>Total Returns</b>	<b>8916</b>	<b>8916</b>	<b>8916</b>	<b>8916</b>	<b>0</b>	<b>16800</b>	<b>0</b>	<b>0</b>	<b>16800</b>	<b>0</b>	<b>0</b>	<b>69264</b>
<b>Cash Flow</b>												
Tax Effect at 31%		305	1810	-1195.8	44	-1574	5208	0	0	5208	0	
<b>Net Cash Flow</b>	<b>984</b>	<b>5535</b>	<b>-5668</b>	<b>1338</b>	<b>-5120</b>	<b>18374</b>	<b>-5208</b>	<b>0</b>	<b>16800</b>	<b>-5208</b>	<b>0</b>	
Discount factor at 15%	1.000	0.870	0.756	0.658	0.572	0.497	0.432	0.376	0.327	0.284	0.247	
<b>Net Present Value</b>	<b>984</b>	<b>4813</b>	<b>-4286</b>	<b>880</b>	<b>-2927</b>	<b>9135</b>	<b>-2252</b>	<b>0</b>	<b>5492</b>	<b>-1480</b>	<b>0</b>	<b>10358</b>
<b>Total NPV</b>	<b>10358</b>											

# APPENDIX C1

## FOUR YEAR WORK PLAN

Included in this appendix is the four-year plan devised at the beginning of the project and a revised plan which illustrates the actual course of events as they occurred.

The primary problem which was encountered following the programme related to conflicts between the commitments associated with the authors full time employment and the requirements of the EngD project.

The most significant programme impact occurred as a result of business issues within the sponsoring organisation during the later half of 1994 and through 1995. These issues were associated with unacceptable business performance and were not connected in any way to this research project. As a consequence of these issues it was not possible to work on the project during this time. A resolution to this problem was the authors deregistration from the EngD programme for the year January to December 1996. This deregistered year was used to recover the time lost in the programme.

Since the author has been in full time employment all through the EngD programme, the conflicts between employment and research commitments have been recurrent. Relative to the major programme impact described above, a number of more minor conflicts resulted in the rescheduling of activities during 1997 and 1998. These were all successfully accommodated in the programme.

In general, resource conflicts between projects within an organisation are common place in industry. Maximising business profit margins necessitates that all elements within that business operate at maximum efficiency and productivity. Resources, particularly human resources, are generally controlled to minimise overcapacity. This by definition means that if the resource requirements of a number of projects exceeds the resource capacity, prioritisation decisions will be made which favours one project at the expense of another. Recover actions are almost always then needed to recover those projects which lost the resource argument.

The research was tribology based and because Cranfield do not run any specialist engineering courses in tribology, it was necessary to use the University of Leeds to cover these modules. These two modules were completed at the earliest opportunity, at the end of 1996.



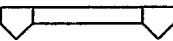




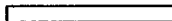




It is well known that the experimental work associated with research projects is time consuming, both to construct the test rig and to conduct the tests themselves. This research took advantage of an existing test rig at DAW so that the time needed to commission test equipment was minimised. Additionally, due to time constraints it was necessary to use undergraduate trainee's to conduct most of the actual experimental work under the authors supervision. In both cases the individuals used the data gathered as part of their final year projects. This approach provided approximately 1500 hours of resource.

APPENDIX C1  
Project Four Year Plan

ID	Task Name	1994				1995				1996				1997				
		Qtr 4	Qtr 1	Qtr 2	Qtr 3	Qtr 4	Qtr 1	Qtr 2	Qtr 3	Qtr 4	Qtr 1	Qtr 2	Qtr 3	Qtr 4	Qtr 1	Qtr 2	Qtr 3	Qtr 4
1	MBA Core Modules																	
2	Core Eng - Computational Methods																	
3	Specialist Eng - Instrumentation																	
4	Littrature Review																	
5	Summary of Friction Models																	
6	Test Data Set-Up																	
7	Core Eng - Engineering Design																	
8	Test Data Gathering																	
9	Specialist Engineering																	
10	Results Analysis																	
11	Reporting																	
12	Specialist Engineering																	
13	Comparison of Analysis and Test Results																	
14	Technology and Envrinmental Assessment																	
15	Development of Design Tool																	
16	Validation Testing																	
17	Thesis Preparation																	
18	Thesis Submission																	

↓ 30/09

Project: R.Hall - Eng D Programme  
Date:1/10/93

Task		Baseline Milestone		Baseline Summary	
Progress		Summary		Rolled Up Baseline	
Baseline		Rolled Up Task		Rolled Up Baseline Milestone	
Milestone		Rolled Up Milestone		Rolled Up Progress	

C1-3

**APPENDIX - C1**  
**Project Actual Events**

ID	Task Name	1994				1995				1996				1997				1998			
		Qtr 4	Qtr 1	Qtr 2	Qtr 3	Qtr 4	Qtr 1	Qtr 2	Qtr 3	Qtr 4	Qtr 1	Qtr 2	Qtr 3	Qtr 4	Qtr 1	Qtr 2	Qtr 3	Qtr 4	Qtr 1	Qtr 2	Qtr 3
1	MBA Core Modules	[Task bar]																			
2	Specialist Eng - Instrumentation	[Task bar]																			
3	Advanced Comptational Methods	[Task bar]																			
4	Literature Review - Part 1	[Task bar]																			
5	First Year Report	[Task bar]																			
6	DAW Employment Ful Time	[Task bar]																			
7	Engineering Design	[Task bar]																			
8	De-Registered Year	[Task bar]																			
9	Literature Review - Part 2	[Task bar]																			
10	Technology & Environmental Assessment	[Task bar]																			
11	Specialist Eng :-	[Task bar]																			
12	Lubricants + Lubrication	[Task bar]																			
13	Surface Contact Phenomena	[Task bar]																			
14	Test Data Set-Up	[Task bar]																			
15	Test Data Gathering	[Task bar]																			
16	Summary of Friction Models	[Task bar]																			
17	Comparison of Analysis and Test Resulte	[Task bar]																			
18	Development of Design Tool	[Task bar]																			
19	Validation Testing	[Task bar]																			
20	Thesis Preparation	[Task bar]																			
21	Thesis Submission	[Task bar]																			

30/09

Project: R.Hall - ENG D Programme  
Date: 15/04/98

Task		Baseline Milestone		Baseline Summary	
Progress		Summary		Rolled Up Baseline	
Baseline		Rolled Up Task		Rolled Up Baseline Milestone	
Milestone		Rolled Up Milestone		Rolled Up Progress	

CI-4

## APPENDIX C2 - PROJECT BUDGET

	1993 BUDGET	1993 ACTUAL	1994 BUDGET	1994 ACTUAL	1995 BUDGET	1995 ACTUAL	1996 BUDGET	1996 ACTUAL	1997 BUDGET	1997 ACTUAL	1998 BUDGET
MBA, Accomodation at Cranfield	2200	2200	2200	2200							
Travel for MBA studies (10p per mile)	228	228	228								
Travel, other courses and meeting at Cranfield	0	0	76		76		76		76		0
Travel, MSc modules at Leeds							0	1348	0	98	
Test components					2000			1100	250	1600	
Lubricants (Brayco 795, HVI 650)					250	0					
Viscosity measurements (Brayco 795)					150	0					0
Contingency	243		250		248		8		33		0
<b>totals</b>	<b>2671</b>	<b>2428</b>	<b>2754</b>	<b>2200</b>	<b>2724</b>	<b>0</b>	<b>84</b>	<b>2448</b>	<b>359</b>	<b>1698</b>	<b>0</b>
total budget	8591										
total expenditure	9019										
delta	-427										



# APPENDIX C3

## RISK ASSESSMENT

This risk assessment has been completed using the standard DAW method. Risks are assessed against the following matrix:

IMPACT	H/L	H/M	H/H
	M/L	M/M	H/M
	L/L	M/L	H/L
	PROBABILITY		

The y-axis of the matrix measures the impact on the project if the particular risk is realised. The x-axis measures the likelihood of the risk occurring. The key defines probability and impact as high, (H), medium, (M) and low, (L).

The objective is to define risk mitigation actions for those risks which occupy the top right hand corner of the matrix. It is also standard practice at DAW to define mitigation plans for those risks in the H/M and M/M regions.

For the purposes of this risk assessment the impact on the project has been assumed to be related to the technical objective of producing a design tool. This is the objective of the sponsoring organisation. It should be recognised that an equally important objective is that the EngD be successfully completed. This would form the subject of a separate risk assessment, not reproduced in this thesis.

RISK No	TYPE	RISK RATING	RISK DESCRIPTION	MITIGATION ACTION	POST ACTION RISK RATING
1	Technical	H/H	Insufficient data on Brayco 795 fluid. Lack of viscosity and pressure-viscosity index data	Have viscosity measured at a specialist lab. Compare data to literature values for pressure-viscosity index. Conduct some comparative tests with fluids which do have published data	
2	Technical	H/M	Test rig cannot measure contact temperatures, only bulk fluid temperature.	Monitor temperatures during test and assess temperature variation. A low variation should not distort the results excessively	
3	Technical	M/M	Literature research may not identify suitable friction models.	Assess after search	
4	Technical	M/M	Unable to establish link between analysis and experimental data. Thus design tool not provided.	Fallback position is to remain with existing design tool.	
5	Technical	M/M	Standard film thickness calculations may not be applicable to skewed roller devices.	Literature allows for sliding and rolling in the entrainment velocity calculation	
6	Technical	H/L	Test data limited to rollers of 5mm diameter and 10mm length at a PCD of 70.1mm. Applicability to other sizes will need to be established.	Speeds and stress levels can be varied and these terms are more dominant.	
7	Technical	H/L	Limited tribology expertise at Cranfield, even less at DAW.	Visit other institutions if required.	
8	Technical	H/L	No personal expertise in tribology field.	Training via specialist engineering courses at Leeds University.	
9	Technical	H/L	Tribology models may produce contradictory data.	Assess when results are available.	
10	Technical	M/L	Design tool may not be simple enough for use by designers.	Assess when tool has been developed.	

11	Resource	H/H	Involvement of more than one undergraduate trainee introduces possible inconsistencies in the test method and results.	Tests only to be conducted in accordance with a written test procedure to ensure consistency.	
12	Resource	H/M	Requirement to train at least two undergraduate trainees introduces delays in the project.	The benefit is greater than the cost. Manage the timescales.	
13	Resource	H/M	Supervision of undergraduates demands too much time whilst working full time.	The benefit is greater than the cost. Manage the timescales.	
14	Resource	M/H	Workload at DAW prevents the use of undergraduate trainee's to conduct the tests.	Trainee's are directly responsible to researcher, thus workload decisions can be made unilaterally.	
15	Resource	M/H	Changes in DAW management over the four year period, could lead to loss of commitment to the EngD training process.	No mitigation action possible.	
14	Budget	M/L	Test components may be significantly more expensive than budgeted.	Allowed for in contingency.	
15	Budget	M/L	Travel and accommodation costs may be significantly higher than budgeted.	Checked by quotes prior to project launch.	
16	Timescale	H/H	EngD has a fixed four year timescale. Whilst in full time employment, workload commitments at DAW may lead to insufficient time being available to complete the work.	Limited mitigation action possible. Use of undergraduate trainee to ease workload with testing.	
17	Timescale	M/H	Extra validation testing near the end of the project may use too much time.	Assess as the requirements become clearer.	
18	Timescale	M/L	Cranfield requirement for reporting and presentations consumes time.	No mitigation action.	

# APPENDIX D

## DETAILED TEST PROCEDURE

The testing of the skewed roller brake device was completed in accordance with the following test procedure.

### 1.0 INTRODUCTION

This document specifies testing to be conducted on the Skewed Roller Device to generate an analytical 'design tool' that will be used as a basis for future skewed roller projects. By changing critical test parameters such as load and speed, the variation of friction coefficient with these operational parameters may be examined. Analysis across all possible boundaries of operation may be obtained by varying the following four variables: -

- Speed (50, 75, 100, 250, 350, 450, 550, 600 and 650rpm)
- Axial Load (890, 1780, 2670, 3560 and 4450N)
- Hertzian Stresses (274, 388, 475, 549 and 613 N/mm<sup>2</sup>)
- Skew Angles (0, 15, 25, 35, 45 and 55°)
- Lubricant (Brayco 795 and Catenex 79)

The time of each test is determined by 320 revolutions, which is dictated by the speed.

### 2.0 THE UNIT

#### 2.1 Description of Unit, Figure D-1.

The function of the Skewed Roller Brake is to ensure that the flaps are not back - driven by the air loads acting on the flap surfaces. To accomplish this the brake is configured to provide a holding torque in the retract sense only, whilst providing minimal resistance to flap movement when extending against the air loads.

In the extend direction the stator carrier is allowed to rotate freely with the through shaft. In the retract direction either of the two pawls engage to prevent the stator carrier rotating and the brake torque is applied, via the pre loaded skewed rollers, to the through shaft.

## 2.2 Pre-Test Requirements

Prior to starting the test, identify that the unit conforms to the respective general assembly and installation drawing requirements.

Within the test procedures, reference is made to the Skewed Roller Brake extend and retract directions. These are defined as follows; extend is the direction in which the ratchet mechanism allows the unit to ' free wheel ', retract is the direction in which the brake provides a resistive torque. During the retract mode the brake absorbs energy which is dissipated as heat.

## 2.3 Build of Unit

The unit is built identically to the production build standard with a few variations: -

- There are only two brake stages used with the four spacers to accommodate the space generated by the loss of the other three brake stages.
- With 890N pre-load seven springs are positioned alternately in the spring housing and with all other pre-loads the standard 14 springs are used.
- The high viscosity of the Catenex lubricant requires the unit to be filled with the top casing removed as opposed to via the fill plug.

## 3.0 TEST PROCEDURE

### 3.1 Test Data

#### 3.1.1 General Test Data

Standard laboratory conditions apply

Skewed Roller Brake: Qualification unit (DAW-02-94)

Test Rig: GAC 16245

Lubricants: Brayco 795 and Catenex 79

Thermocouple: Type 'K'

Stopwatch: GAC 6124

### 3.1.2 Environmental Conditions

Unless otherwise specified, the following conditions will apply:

Ambient Temperature +15°C to +35°C

Relative humidity lab ambient

Barometric pressure lab ambient

### 3.1.3 Test Equipment and Tolerances

Unless otherwise specified the maximum tolerances on test conditions and measured test parameters are as follows :

Temperature  $\pm 1^\circ\text{C}$  of full scale

Torque  $\pm 2\%$  of full scale

rpm  $\pm 3\%$  except transient conditions

Test arrangements are detailed in each part, the test instrumentation will carry a valid calibration conforming to the following table :

PARAMETER	MEASURED METHOD	RANGE $\pm$	ACCURACY
Drive Torque	Torque Transducer	0-500 lbinch	$\pm 2\%$ of full scale
Drive speed	DC Tacho	0-500 rpm	$\pm 1\%$ of full scale

## 3.2 General Set-up

### 3.2.1 Build

With the can removed from the casing, cleaned and stripped perform the following instructions using Table D-3 as a guide to the order of build/test :-

- i. Place the base brake plate (stator) into the can with the locating ring (castlled) in place and position the first cage on this plate with the ten rollers inserted into there respective slots.
- ii. Slide the can over the main shaft ensuring that all the rollers in the first cage remain in place.

D-4

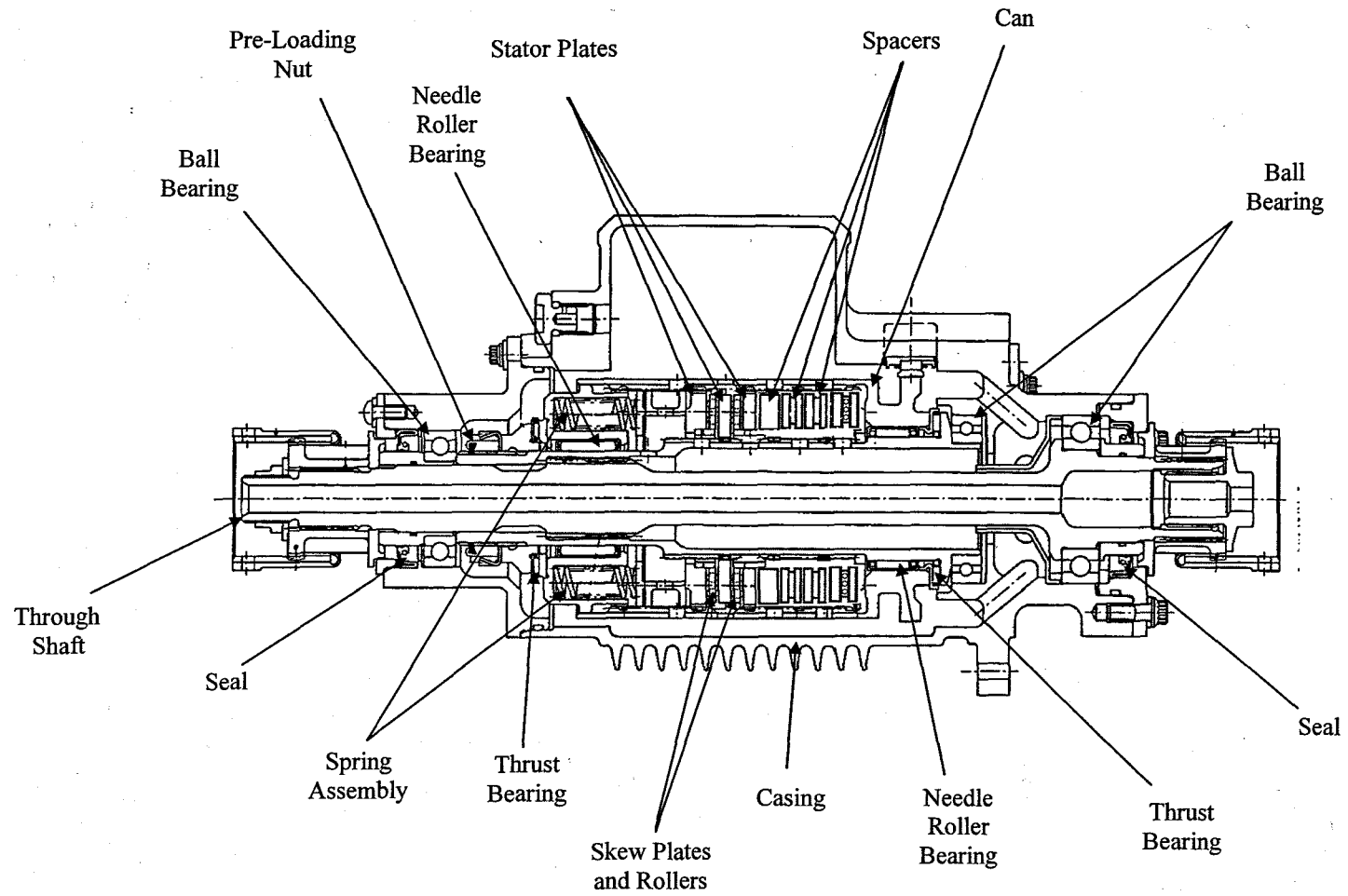


Figure D-1- Sectional View of the Skewed Roller Test Unit

- iii. Position the central brake plate (rotor) over the central shaft and slide it down the splines until it rests on the rollers in the first cage.
- iv. Locate the second stage onto the rotor and using a pair of long nosed pliers insert the rollers into the cage (holding the rollers on the ends).
- v. Position the end brake plate on top of the second cage of rollers ensuring no disturbance.
- vi. Put the four spacers onto the assembled stages.
- vii. After the last spacer position the spring plate (flat side up)
- viii. Turn the can and its contents onto its side ensuring that all the components stay in their positions (by applying a hand load to the spring plate).
- ix. With the appropriate number of springs in the housing, (890N=7 springs, 1780/2670/3560 and 4450N = 14 springs) offer it to the can and ensure the splines have mated.
- x. With hand pressure applied to the base of the can and the top of the spring housing upright the can and put the thrust bearing, keyed collar, locking collar and pre-loading nut into position.

### 3.2.2 Pre-Loading

Using the production standard equipment (including plotter) continue as follows: -

- i. Slide the can onto the loading ram and swing the locking plate into position.
- ii. Position a piece of graph paper into the plotter with all the relevant information on it.
- iii. Pump the hydraulic pump until the desired pre-load – 100lb (Table D-1) is reached.
- iv. Mark a line on the graph paper using the plotter and label this load.
- v. Apply the extra 100lb required to gain the required pre-load value and mark this on the graph paper.
- vi. Tighten the pre-loading nut until the plotter pen starts to move down, indicating that the pre-load value has been reached.
- vii. Release the pressure in the jack and then with the plotter pen on the paper re-apply the pre-load until the pen plot on the graph passes the required pre-load value.
- viii. At the passing point a knee point should appear. If the knee point is above (pre-load too high) or below (pre-load too low) then the pre-loading nut should be adjusted accordingly.
- ix. A further plot should be taken and repeated until the knee point coincides the required pre-load value.



Pre-Load (N)	Pre-Load (lb)	Pre-Load – 100lb (lb)
890	200	100
1780	400	300
2670	600	500
3560	800	700
4450	1000	900

Table D-1 – Pre-Loading Conditions

### 3.2.3 Final Assembly

With the casing located on the splined holding fixture conduct the following: -

- i Take the ratchet suppresser and hold them back. Lower the assembled/pre-loaded can down the main shaft and into the casing (then remove the suppresser).
- ii Ensure that the unit 'freewheels' in the extend direction (clicking sound produced by ratchets) and gives an opposing torque in the retract direction.
- iii Position the sleeved roller bearing over the shaft and pour 1250ml of the applicable fluid around the can and into the casing.
- iv Torque tighten (550-650lbinch) the top casing with the washer and splined bush below the nut.

### 3.2.4 Test

After assembly, the unit outer casing should be clean from any lubricant and taken to the test rig.

- i. Remove the base drain plug and insert the modified drain plug (so the thermocouple is in direct contact with the lubricant).
- ii. Position the unit onto the mounting plate with the splined interface allowing direct drive via a coupling to the motor.
- iii. Turn on the test rig and increase the speed to 50rpm for 10 revolutions (12seconds) in the retract direction to allow the unit to bed-in.
- iv. Start testing at 50rpm for 320 revolutions (6mins 24 sec's), take a trace of the running torque and measure the temperature of the unit at 1 second intervals (N.B. start the temperature measurement before the start of testing and continue recording after test until the temperature has stabilised).

v. The second test should start at 75rpm and be carried out in the same manor as the 50rpm test with the time of test as shown in Table D-2. The testing then continues in the order shown in Table D-2 until the 650rpm test has been completed.

vi. The torque and temperature traces should be suitably labelled and retained for future reference.

Order Number	Speed (RPM)	Time (Minutes-Seconds) based on 320 revolutions
1	50	06-24
2	75	04-16
3	100	03-12
4	250	01-17
5	350	00-55
6	450	00-43
7	550	00-35
8	600	00-32
9	650	00-30

Table D-2 – Test Measurement Times

### 3.2.5 Re-Build

After test the unit should be removed from the rig, the lubricant drained and retained for further testing. Repeat sections 3.2.1 and 3.2.2 for pre loads given in Table D-1 suggested test sequence is given in Table D-3 (N.B. between changing lubricants the unit has to be thoroughly stripped and cleaned).

Test Sequence Number	Skew Angle (°)	Fluid Type	Pre-Load (N)	Number of Springs	Extent of assembly needed (Sections)
1	0	Brayco 795	890	7	3.2.1 – 3.2.3
2			1780	14	3.2.1 (ix) – 3.2.3
3			2670	14	3.2.2 – 3.2.3
4			3560		
5			4450		
6	15	Brayco 795	890	7	3.2.1 – 3.2.3
7			1780	14	3.2.1 (ix) – 3.2.3
8			2670	14	3.2.2 – 3.2.3
9			3560		
10			4450		
11	25	Brayco 795	890	7	3.2.1 – 3.2.3
12			1780	14	3.2.1 (ix) – 3.2.3
13			2670	14	3.2.2 – 3.2.3
14			3560		
15			4450		
16	35	Brayco 795	890	7	3.2.1 – 3.2.3
17			1780	14	3.2.1 (ix) – 3.2.3
18			2670	14	3.2.2 – 3.2.3
19			3560		
20			4450		
21	45	Brayco 795	890	7	3.2.1 – 3.2.3
22			1780	14	3.2.1 (ix) – 3.2.3
23			2670	14	3.2.2 – 3.2.3
24			3560		
25			4450		
26	55	Brayco 795	890	7	3.2.1 – 3.2.3
27			1780	14	3.2.1 (ix) – 3.2.3
28			2670	14	3.2.2 – 3.2.3
29			3560		
30			4450		

Table D-3(Part 1) – The Suggested Test Sequence

Test Sequence Number	Skew Angle (°)	Fluid Type	Pre-Load (N)	Number of Springs	Extent of assembly needed (Sections)
31	0	Catenex 79	890	7	3.2.1 – 3.2.3
32			1780	14	3.2.1 (ix) – 3.2.3
33			2670	14	3.2.2 – 3.2.3
34			3560		
35			4450		
36	15	Catenex 79	890	7	3.2.1 – 3.2.3
37			1780	14	3.2.1 (ix) – 3.2.3
38			2670	14	3.2.2 – 3.2.3
39			3560		
40			4450		
41	25	Catenex 79	890	7	3.2.1 – 3.2.3
42			1780	14	3.2.1 (ix) – 3.2.3
43			2670	14	3.2.2 – 3.2.3
44			3560		
45			4450		
46	35	Catenex 79	890	7	3.2.1 – 3.2.3
47			1780	14	3.2.1 (ix) – 3.2.3
48			2670	14	3.2.2 – 3.2.3
49			3560		
50			4450		
51	45	Catenex 79	890	7	3.2.1 – 3.2.3
52			1780	14	3.2.1 (ix) – 3.2.3
53			2670	14	3.2.2 – 3.2.3
54			3560		
55			4450		
56	55	Catenex 79	890	7	3.2.1 – 3.2.3
57			1780	14	3.2.1 (ix) – 3.2.3
58			2670	14	3.2.2 – 3.2.3
59			3560		
60			4450		

Table D-3 (Part 2) – The Suggested Test Sequence





## **APPENDIX E**

### **SKEWED ROLLER TORQUE CHARACTERISTICS**

The test results illustrating the torque characteristics of the skewed roller device are presented in this Appendix as functions of the operational parameters, speed, skew angle and axial load. The data presented are the measured torque values with the inherent drag of the bearings and seals removed. Hence, the characteristics shown are those of the skewed roller friction elements only.

Figures E-1 through E-16 present the test results with the unit lubricated by Brayco 795 fluid. Figures E-17 through E-32 are the equivalent results with the unit lubricated with Catenex.

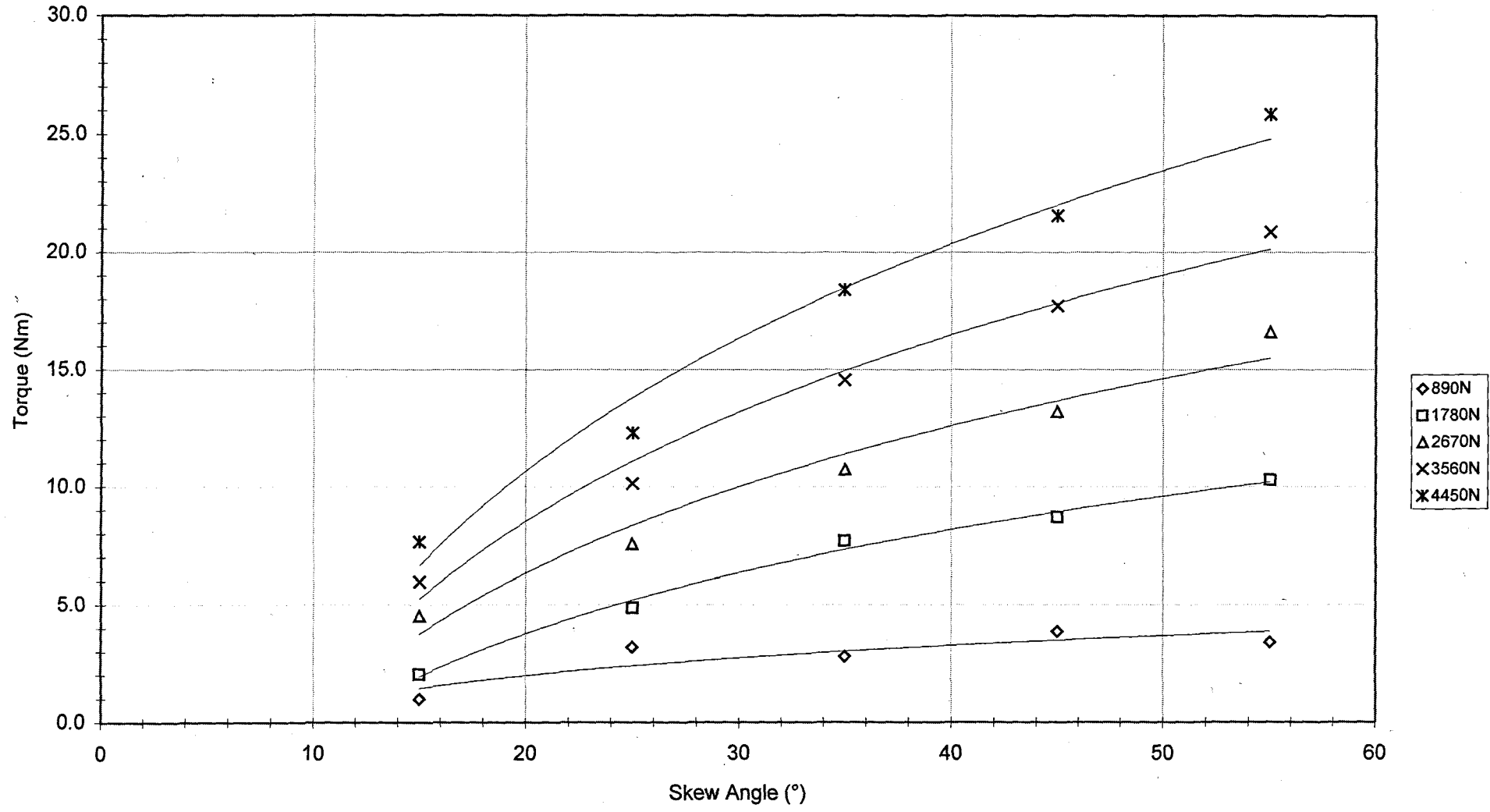


Figure E-1  
Torque Characteristics with Skew Angle at 50RPM with Brayco 795 Lubrication



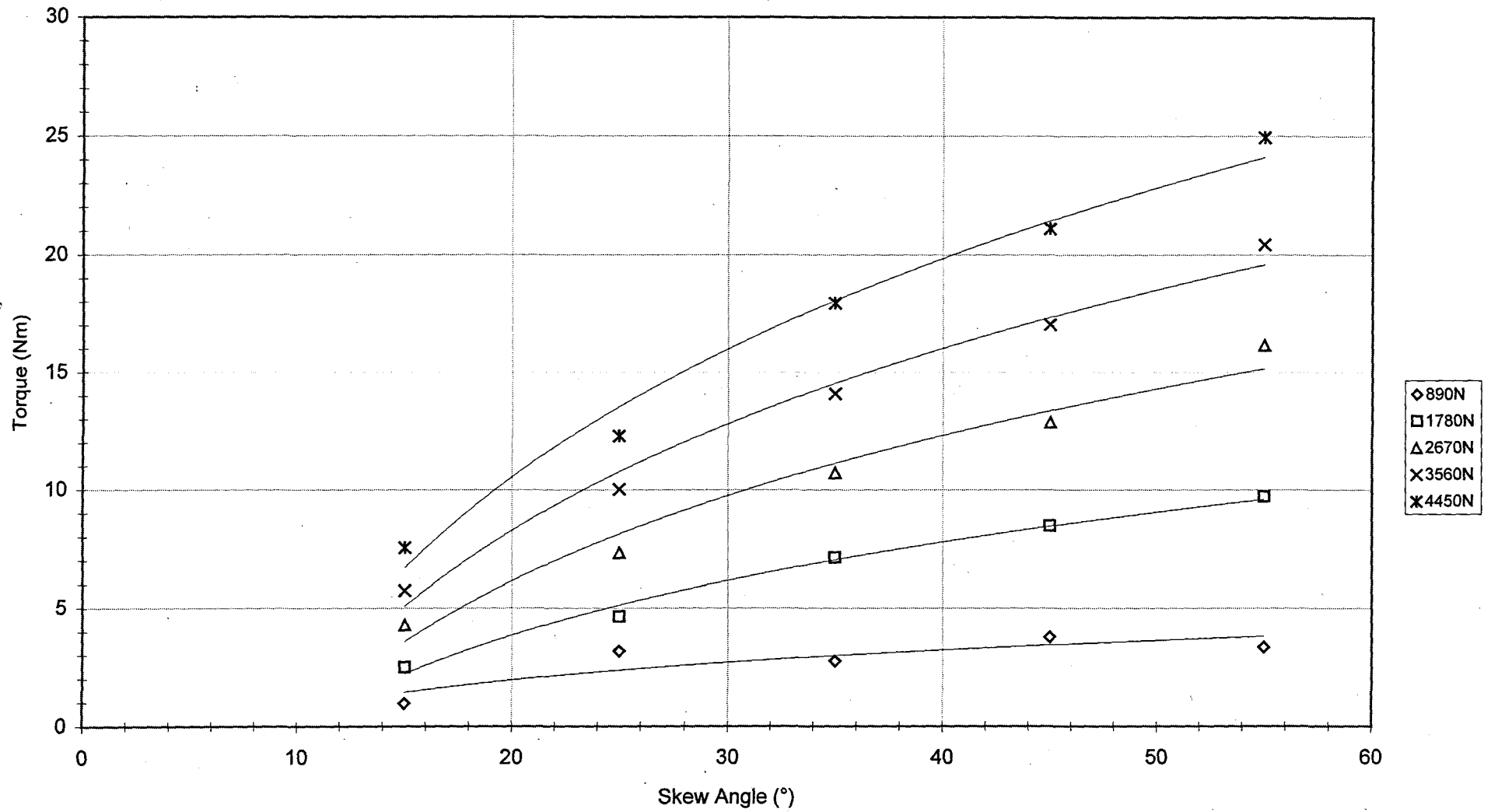


Figure E-2  
Torque Characteristics with Skew Angle at 75RPM with Brayco 795 Lubrication

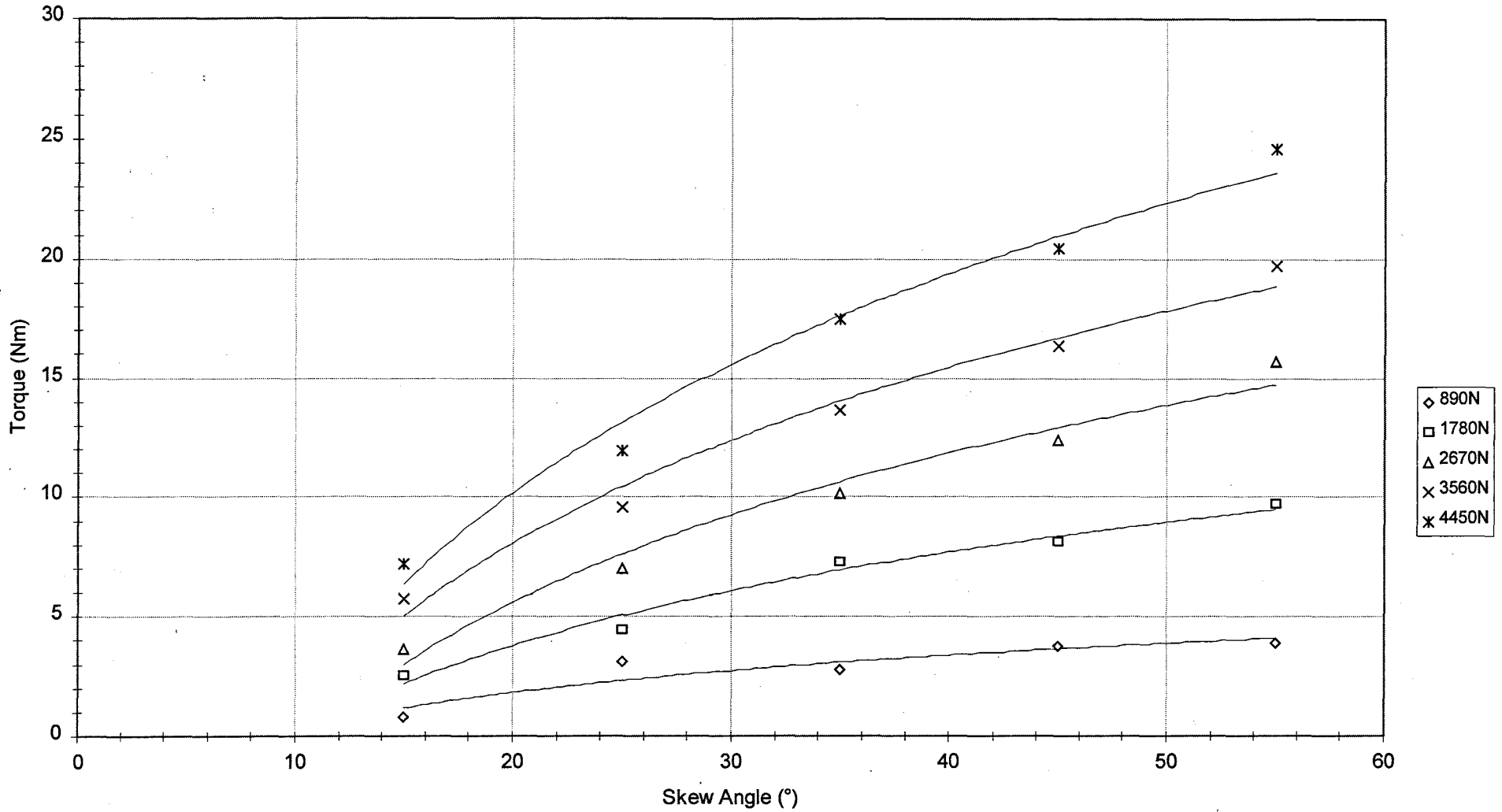


Figure E-3  
Torque Characteristics with Skew Angle at 100RPM with Brayco 795 Lubrication

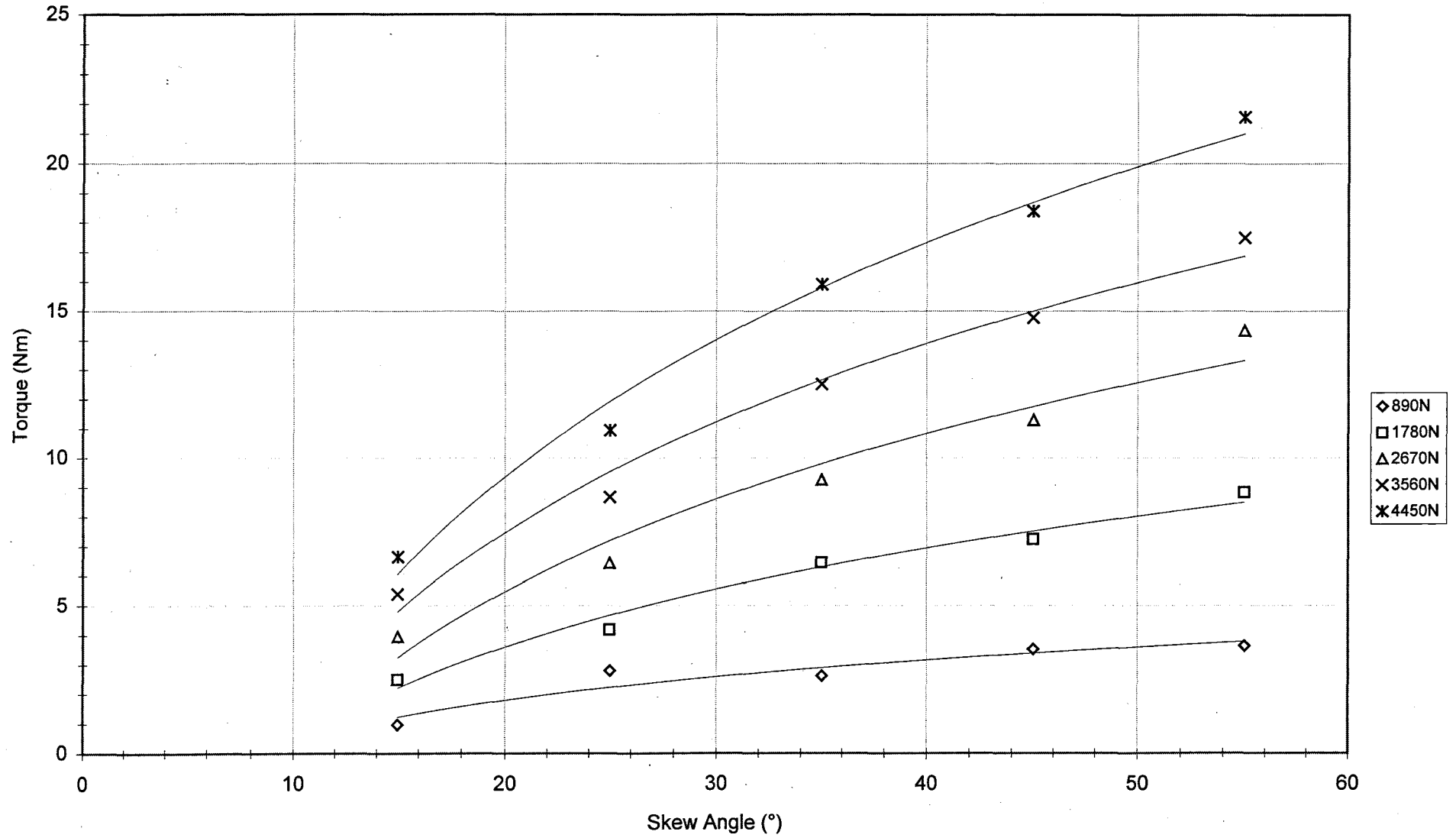


Figure E-4  
Torque Characteristics with Skew Angle at 250RPM with Brayco 795 Lubrication

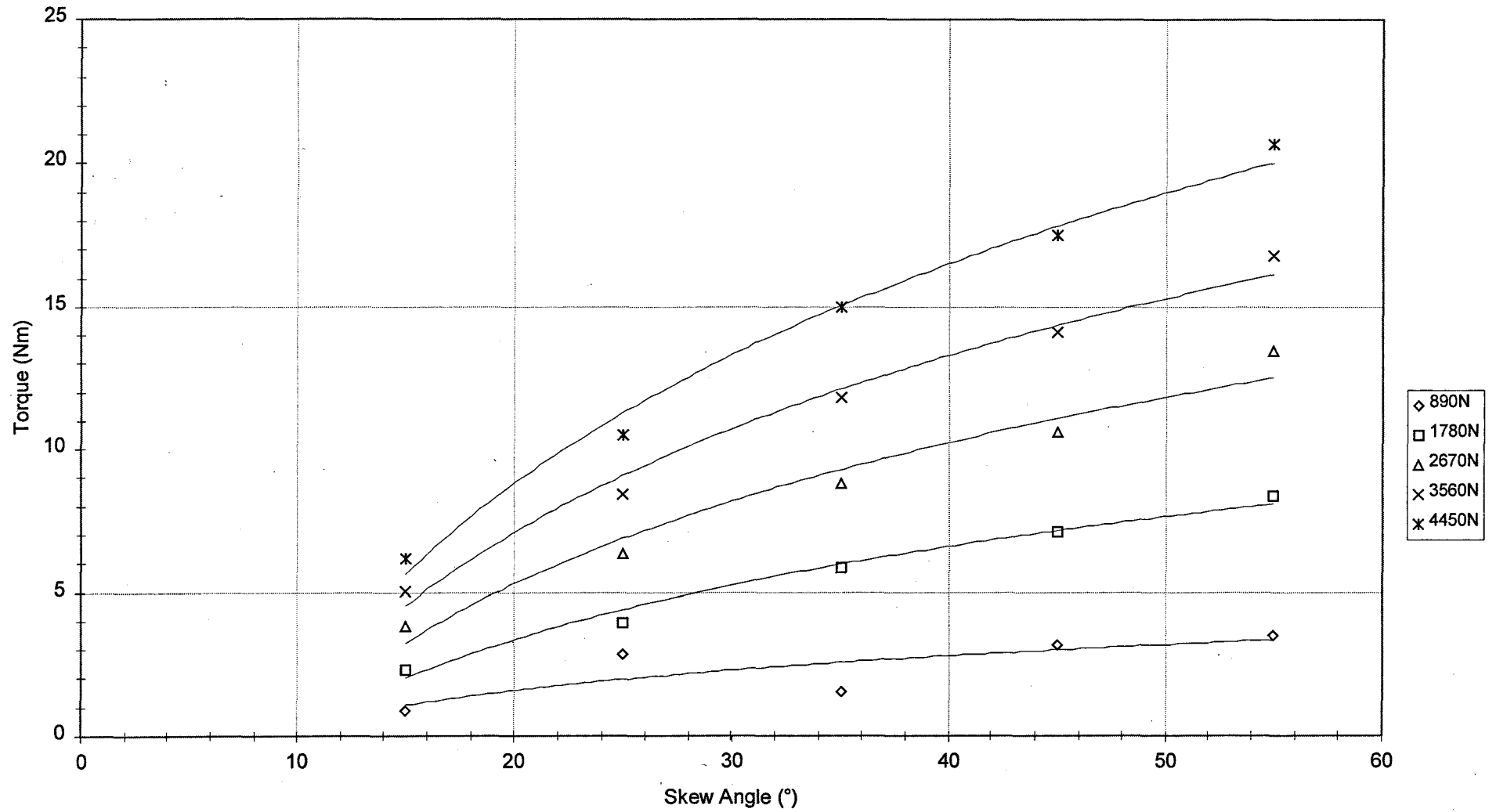


Figure E-5  
Torque Characteristics with Skew Angle at 350RPM with Brayco 795 Lubrication

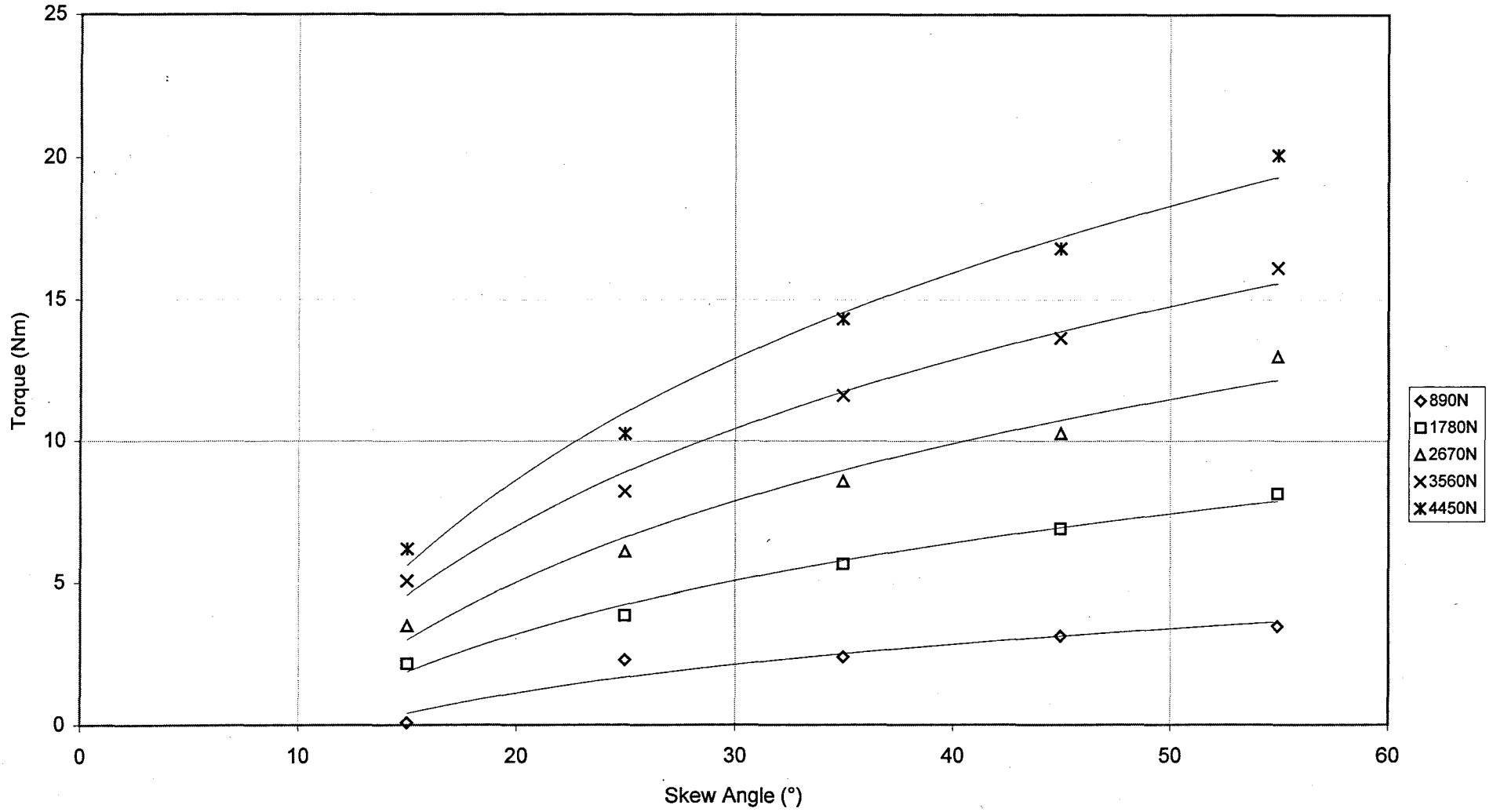


Figure E-6  
Torque Characteristics with Skew Angle at 450RPM with Brayco 795 Lubrication

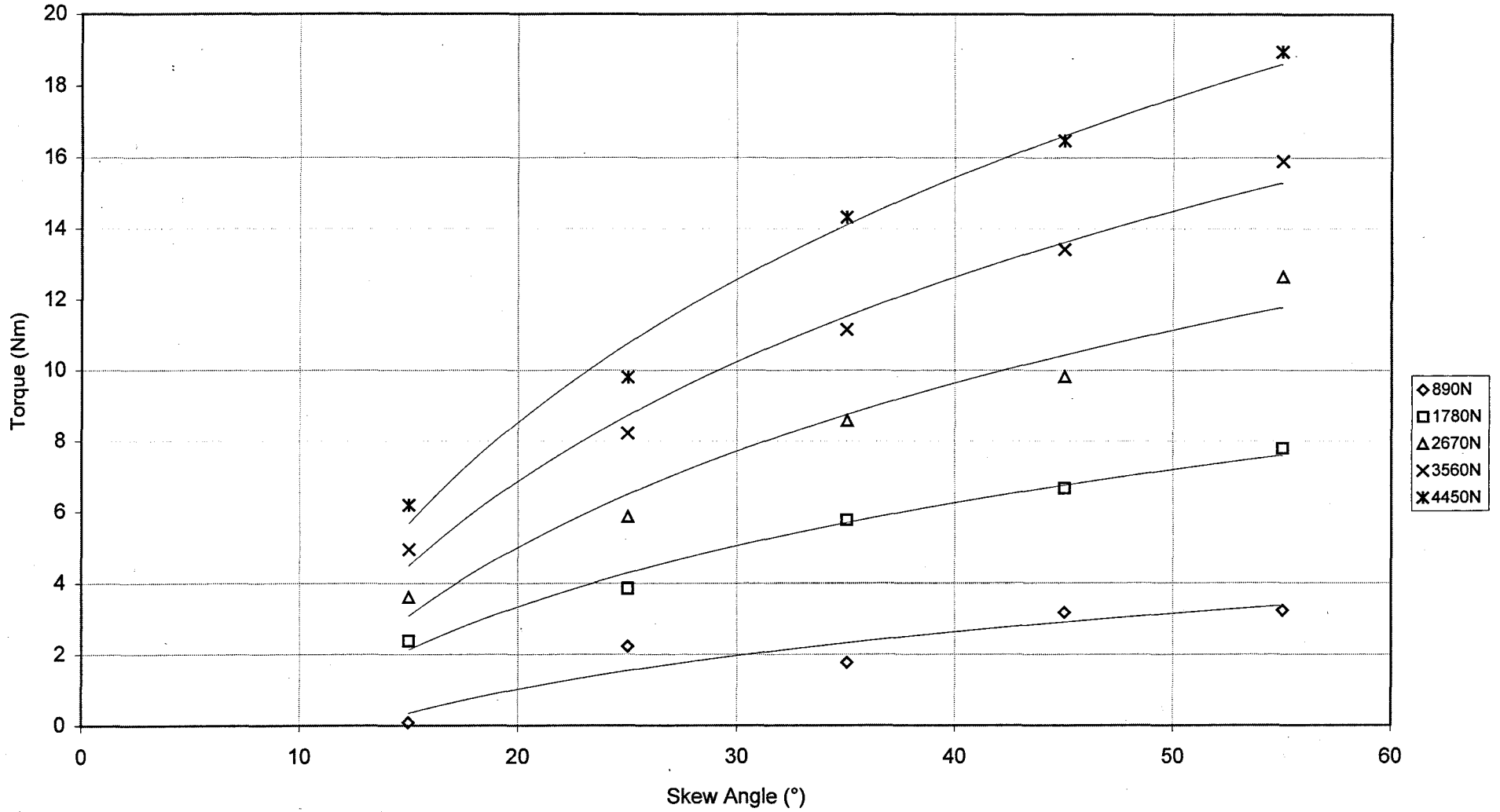


Figure E-7  
Torque Characteristics with Skew Angle at 550RPM with Brayco 795 Lubrication

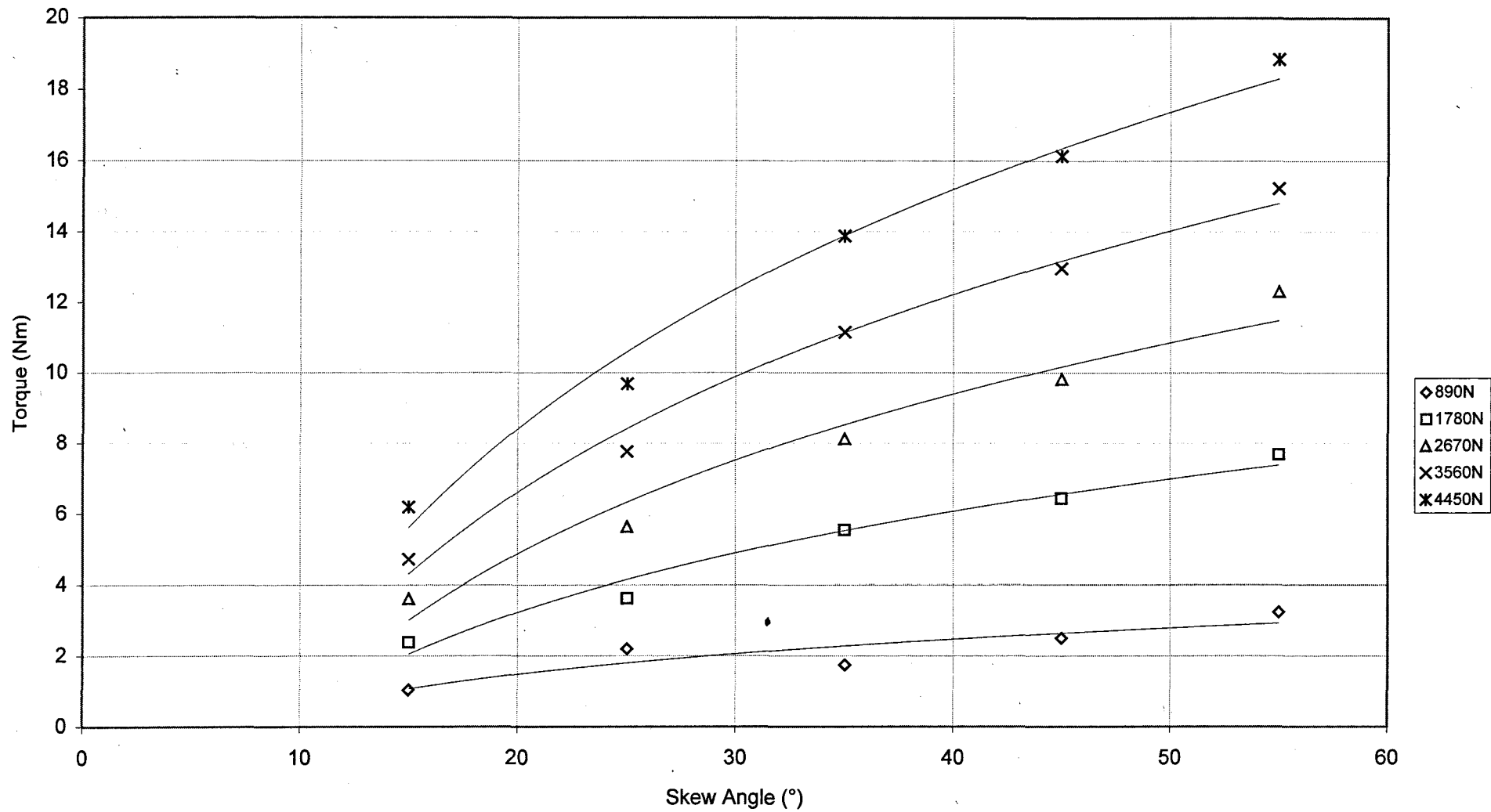


Figure E-8  
Torque Characteristics with Skew Angle at 650RPM with Brayco 795 Lubrication

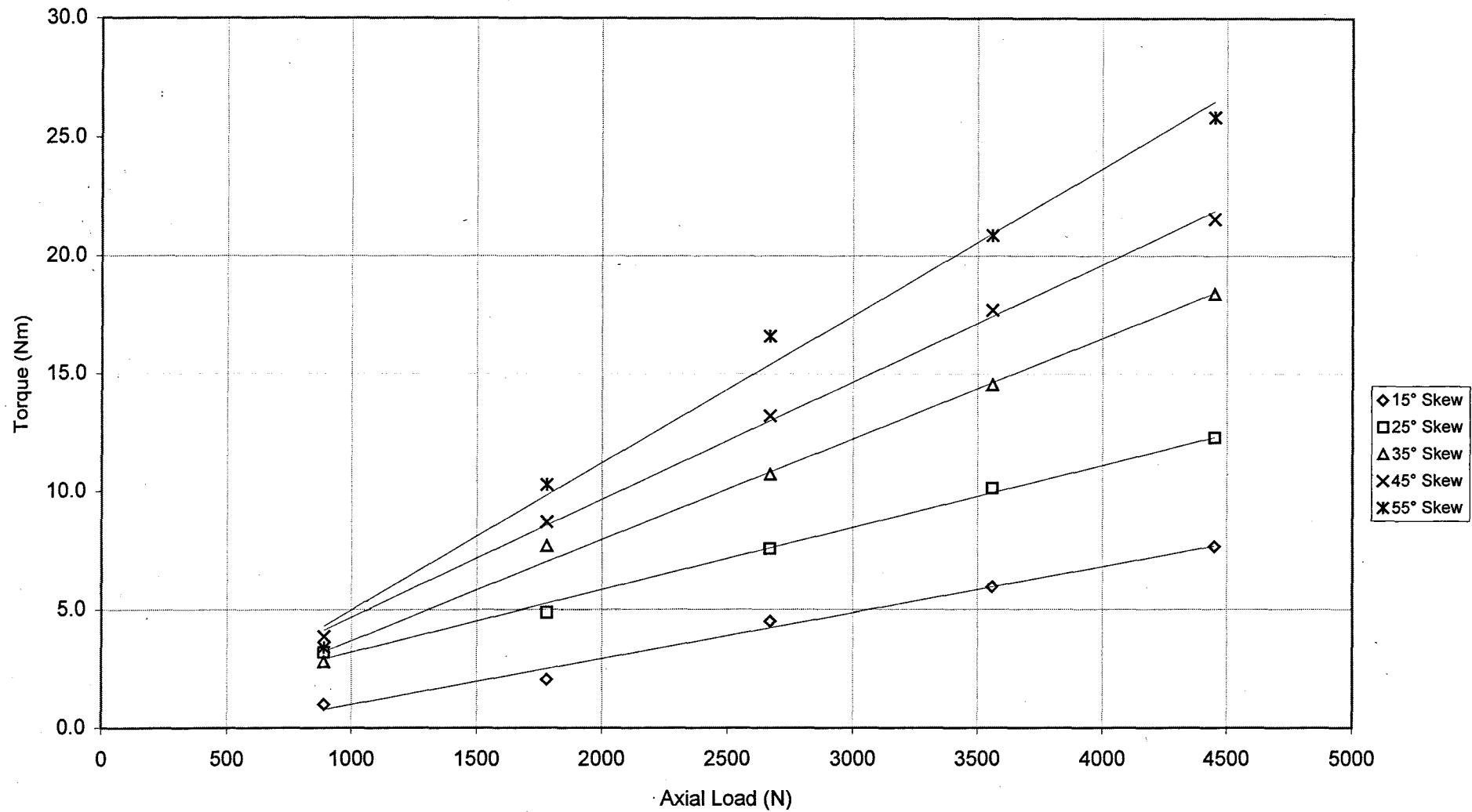


Figure E-9  
Torque Characteristics with Axial Load at 50RPM with Brayco 795 Lubrication



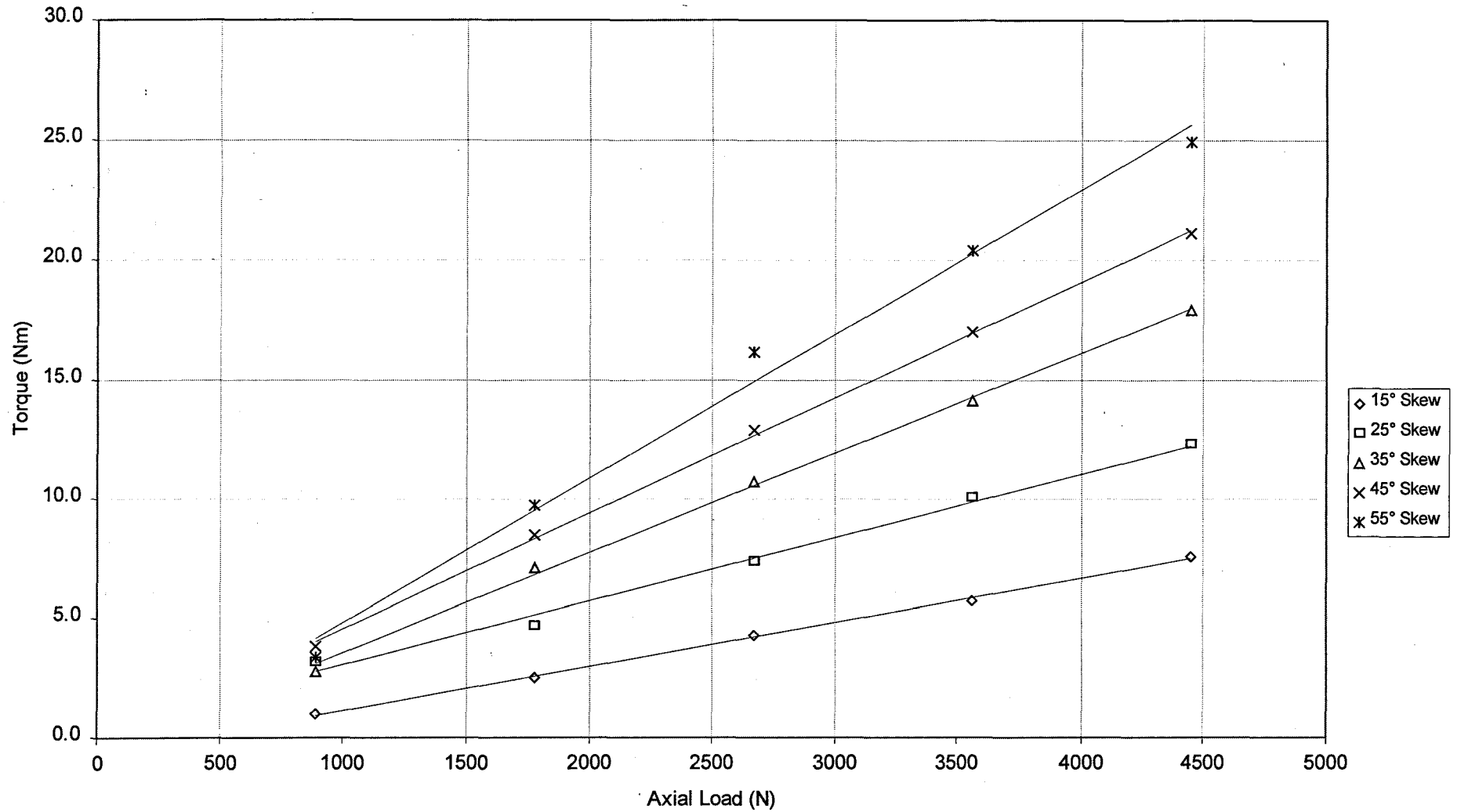


Figure E-10  
Torque Characteristics with Axial Load at 75RPM with Brayco 795 Lubrication

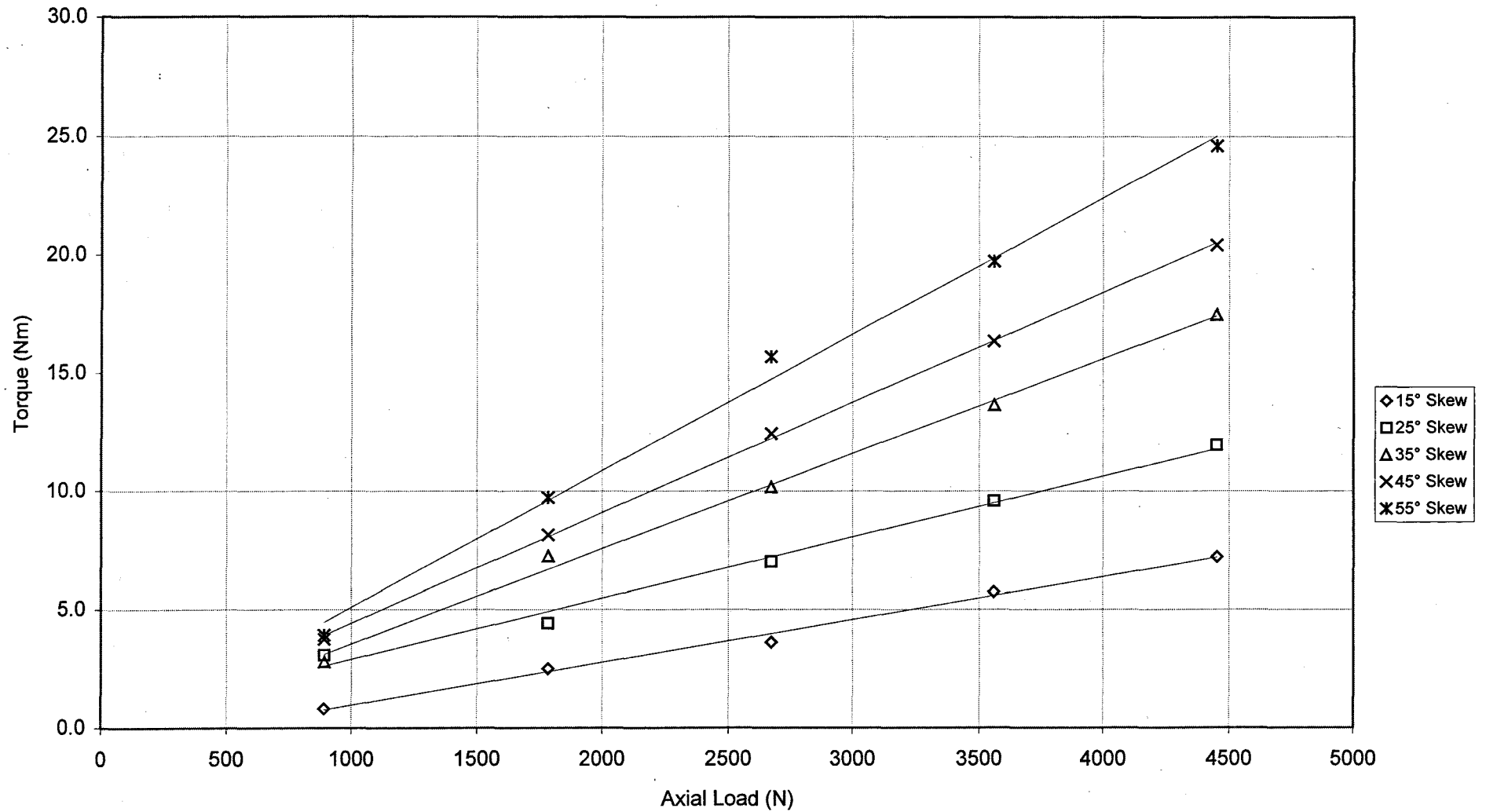


Figure E-11  
Torque Characteristics with Axial Load at 100RPM with Brayco 795 Lubrication

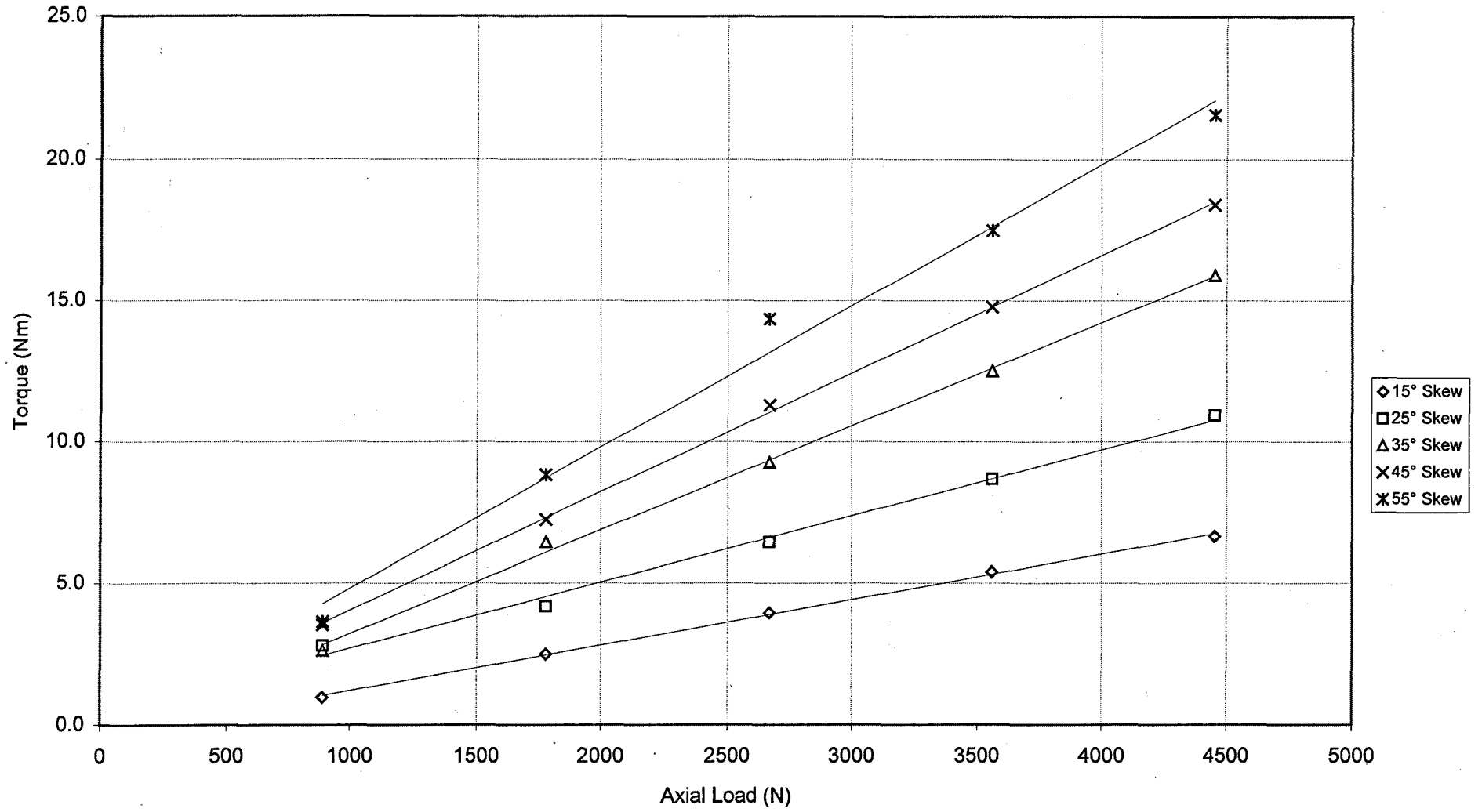


Figure E-12  
Torque Characteristics with Axial Load at 250RPM with Brayco 795 Lubrication

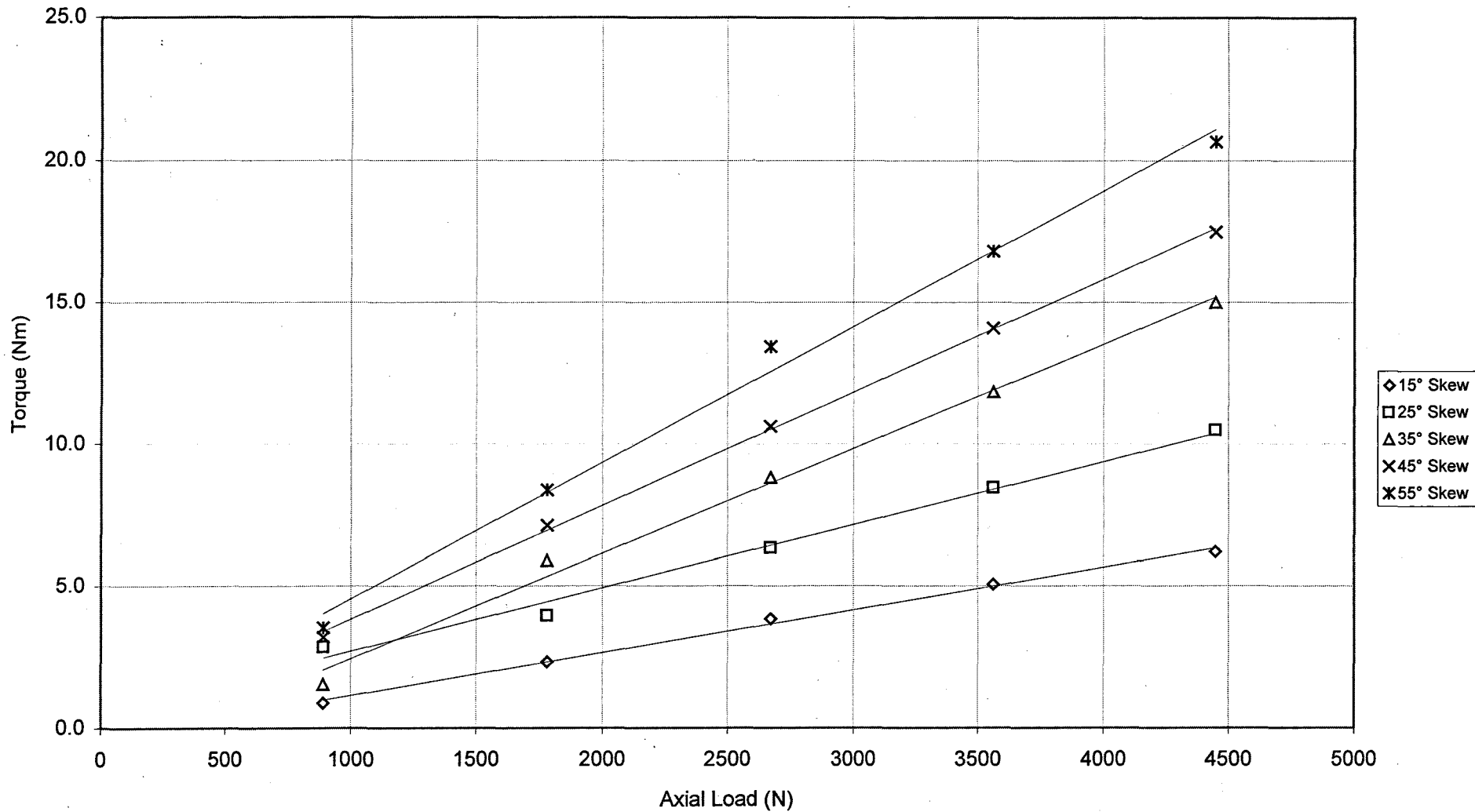


Figure E-13  
Torque Characteristics with Axial Load at 350RPM with Brayco 795 Lubrication

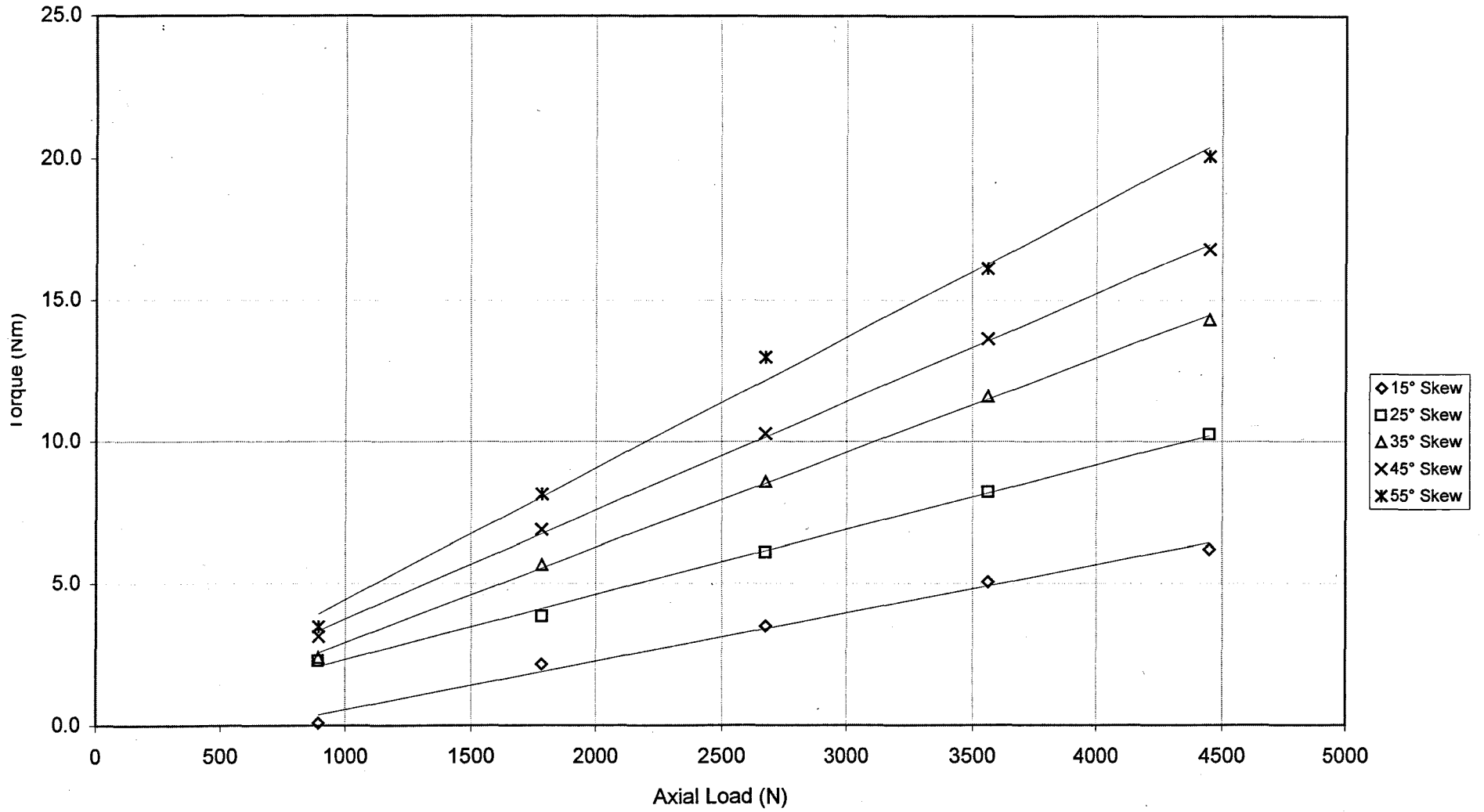


Figure E-14  
Torque Characteristics with Axial Load at 450RPM with Brayco 795 Lubrication

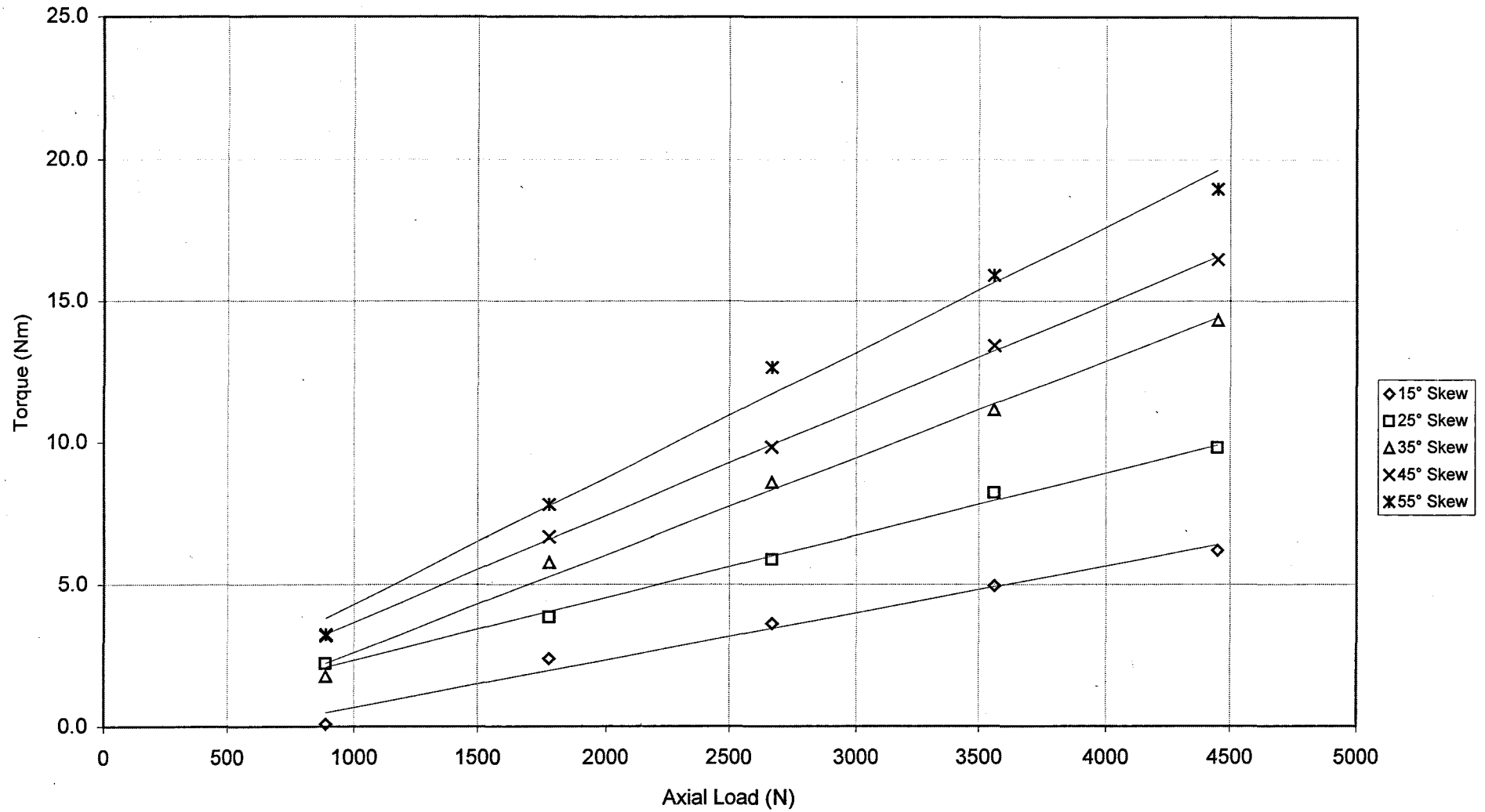


Figure E-15  
Torque Characteristics with Axial Load at 550RPM with Brayco 795 Lubrication

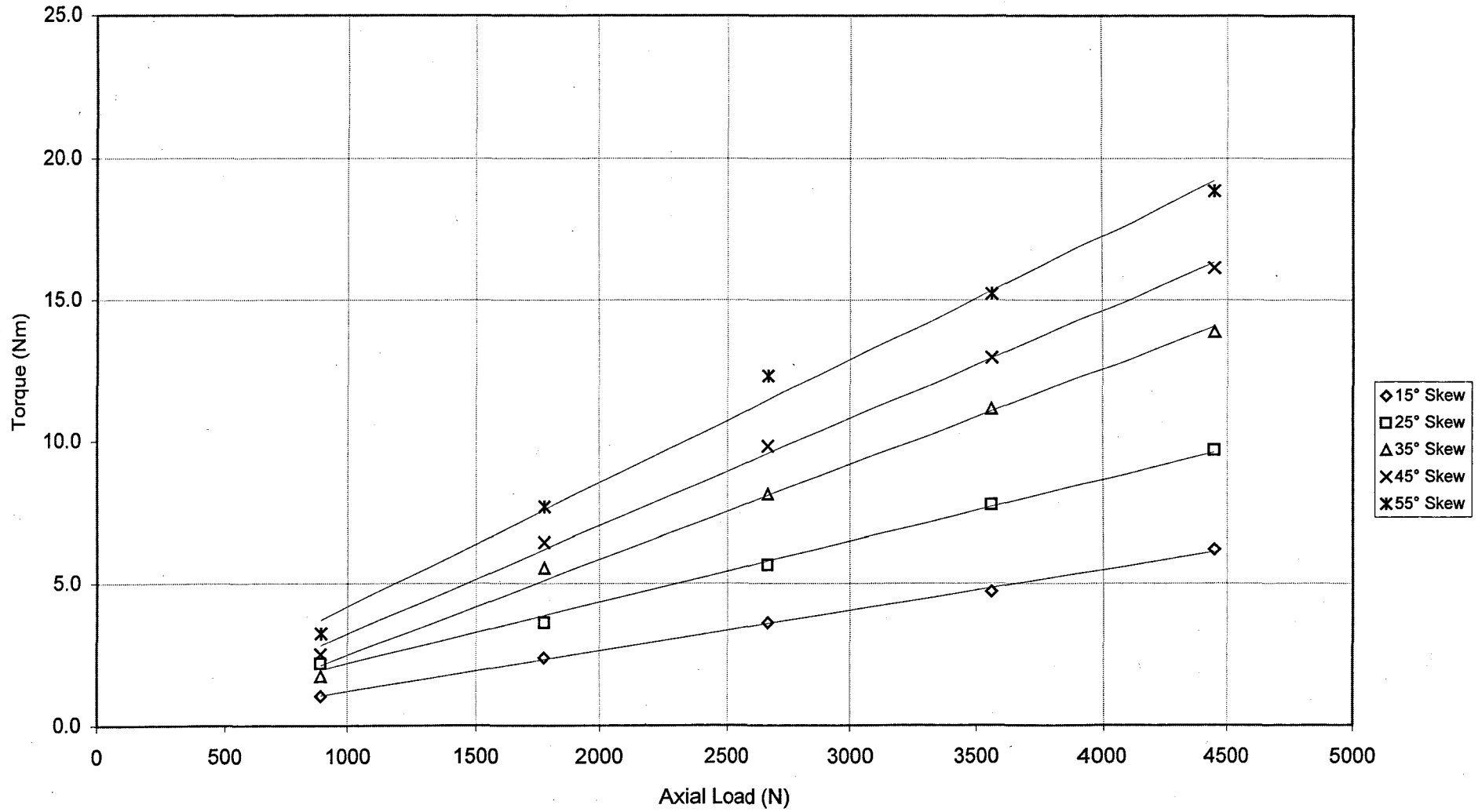


Figure E-16  
Torque Characteristics with Axial Load at 650RPM with Brayco 795 Lubrication

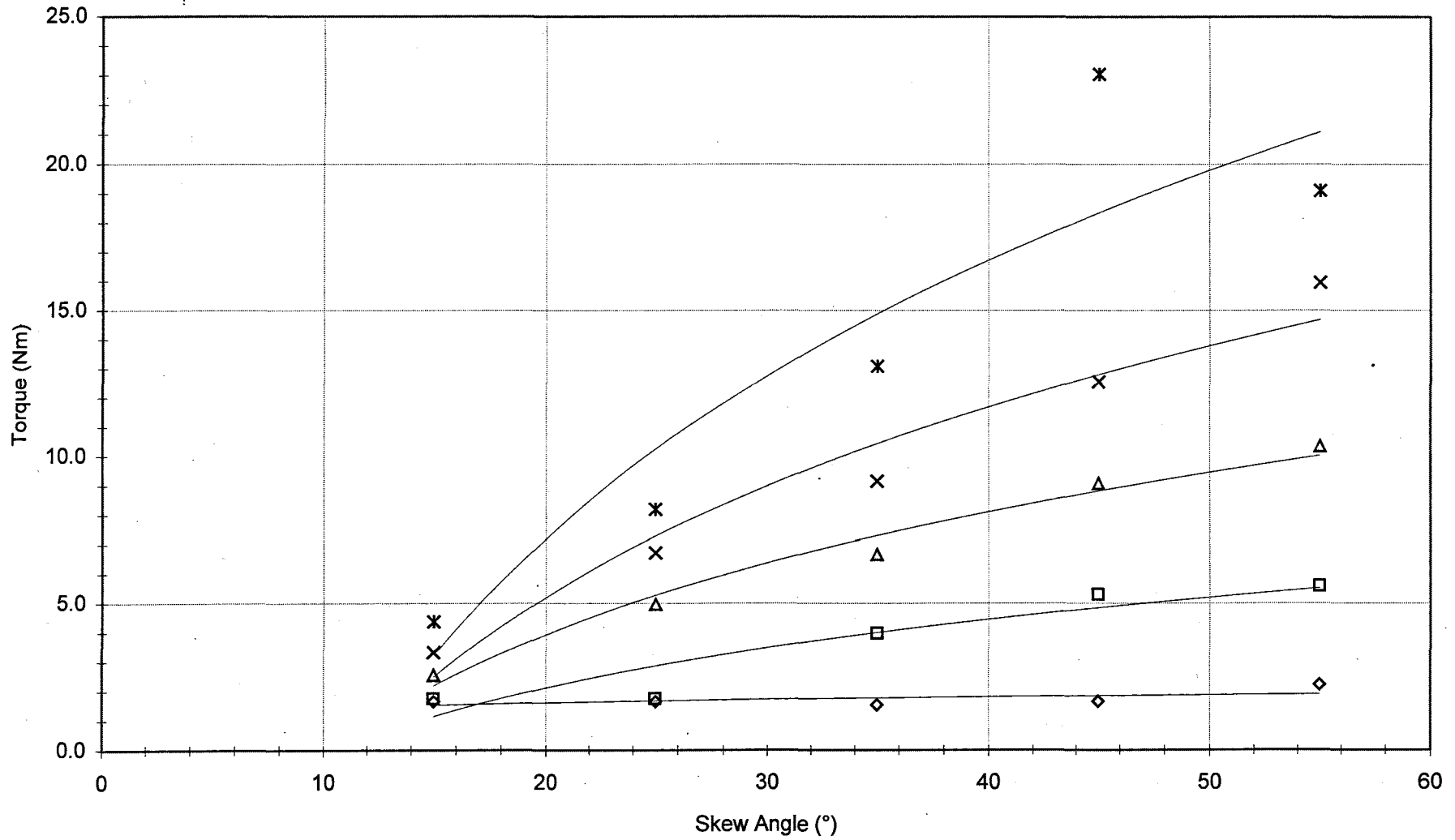


Figure E-17  
Torque Characteristics with Skew Angle at 50RPM with Catenex 79 Lubrication



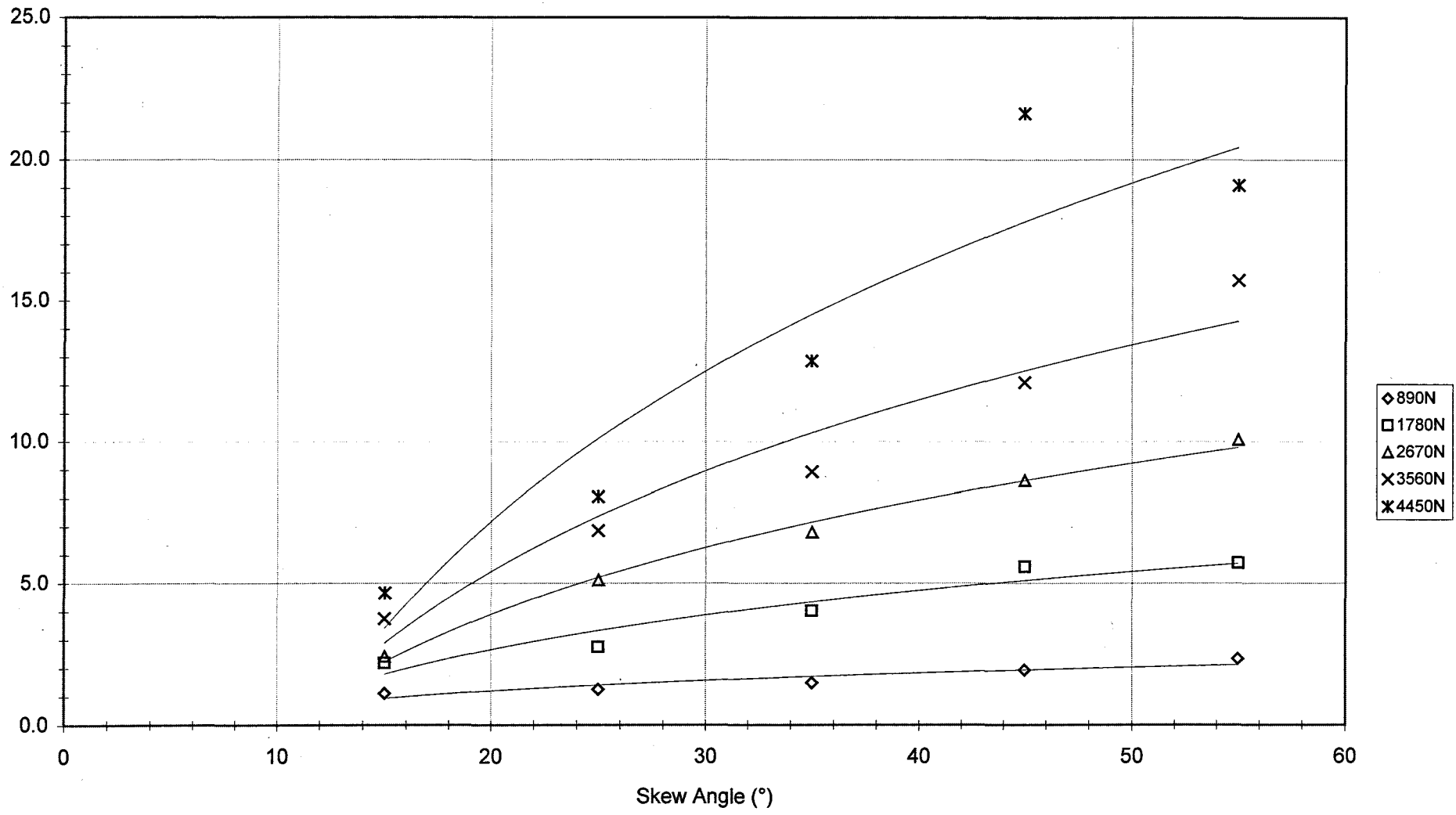


Figure E-18  
Torque Characteristics with Skew Angle at 75RPM with Catenex 79 Lubrication

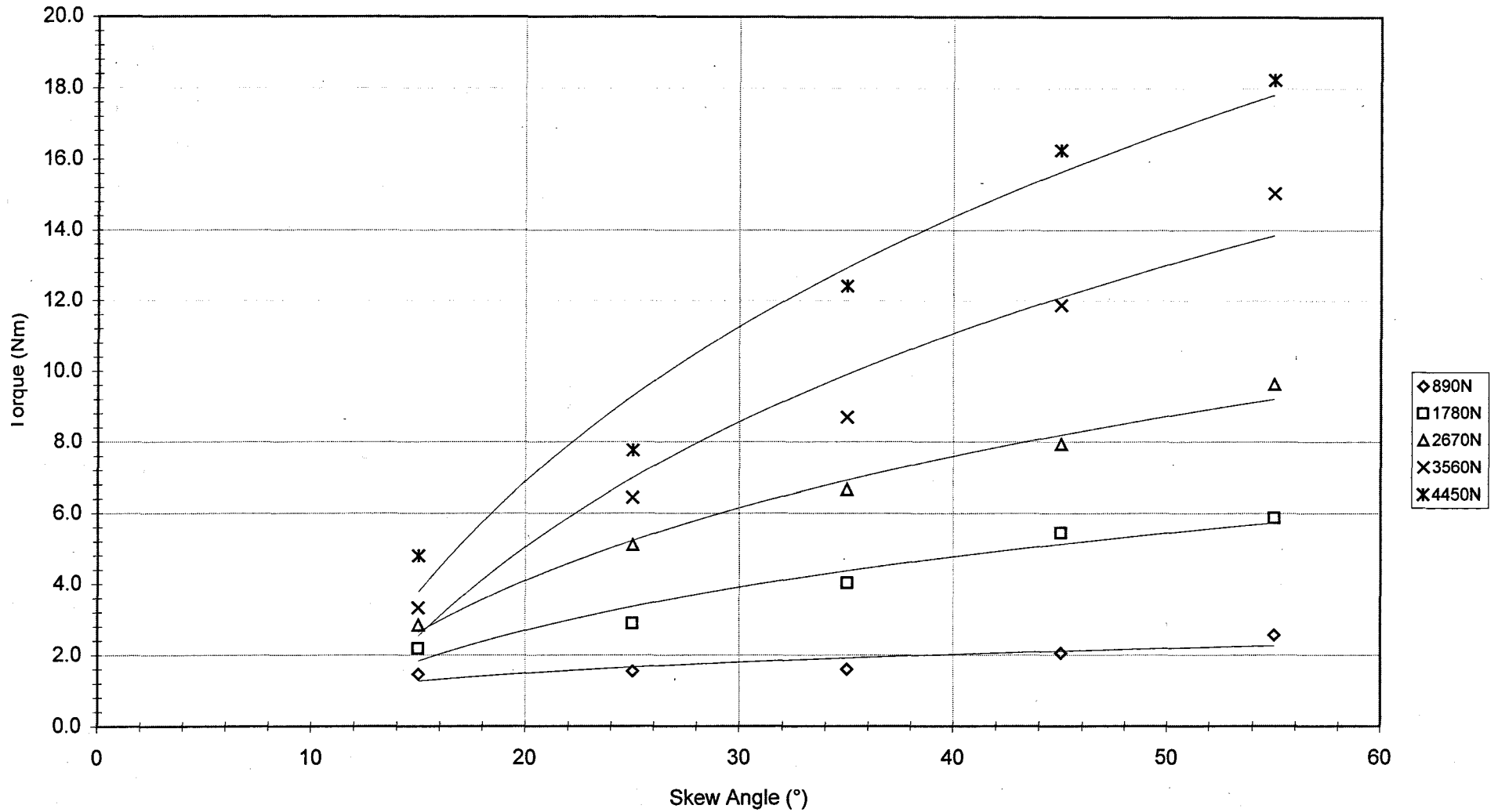


Figure E-19  
Torque Characteristics with Skew Angle at 100RPM with Catenex 79 Lubrication

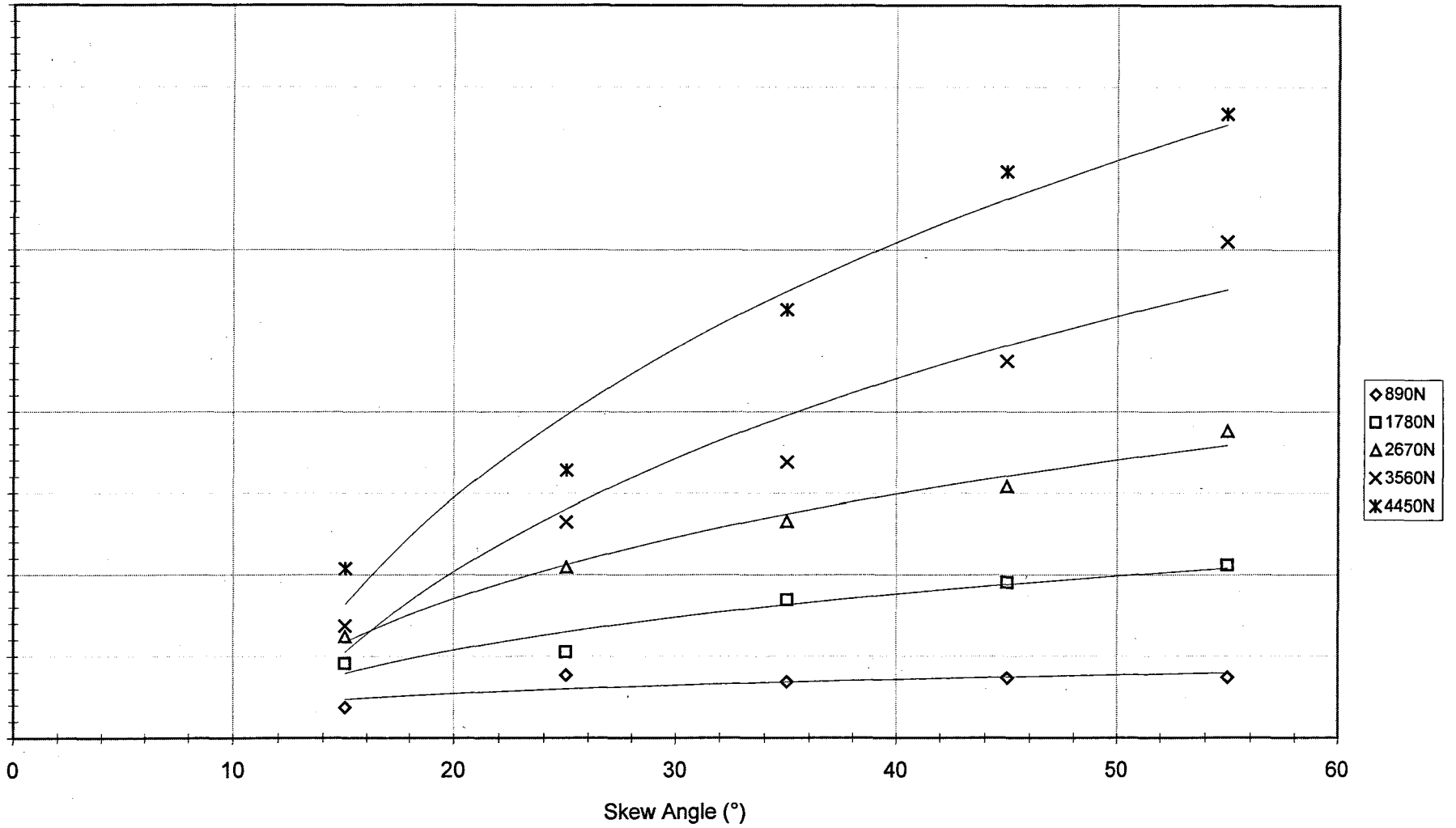


Figure E-20  
Torque Characteristics with Skew Angle at 250RPM with Catenex 79 Lubrication

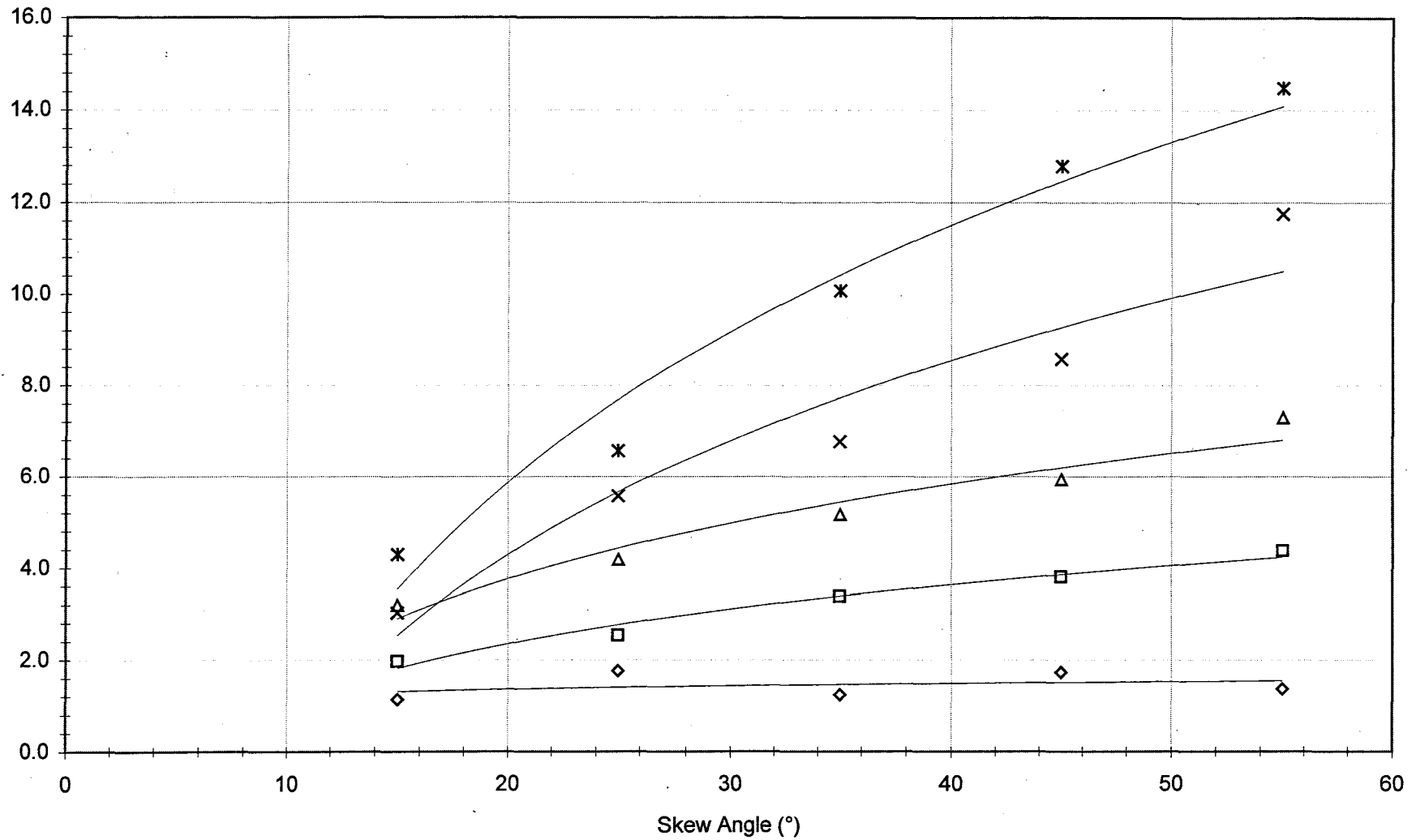


Figure E-21  
Torque Characteristics with Skew Angle at 350RPM with Catenex 79 Lubrication

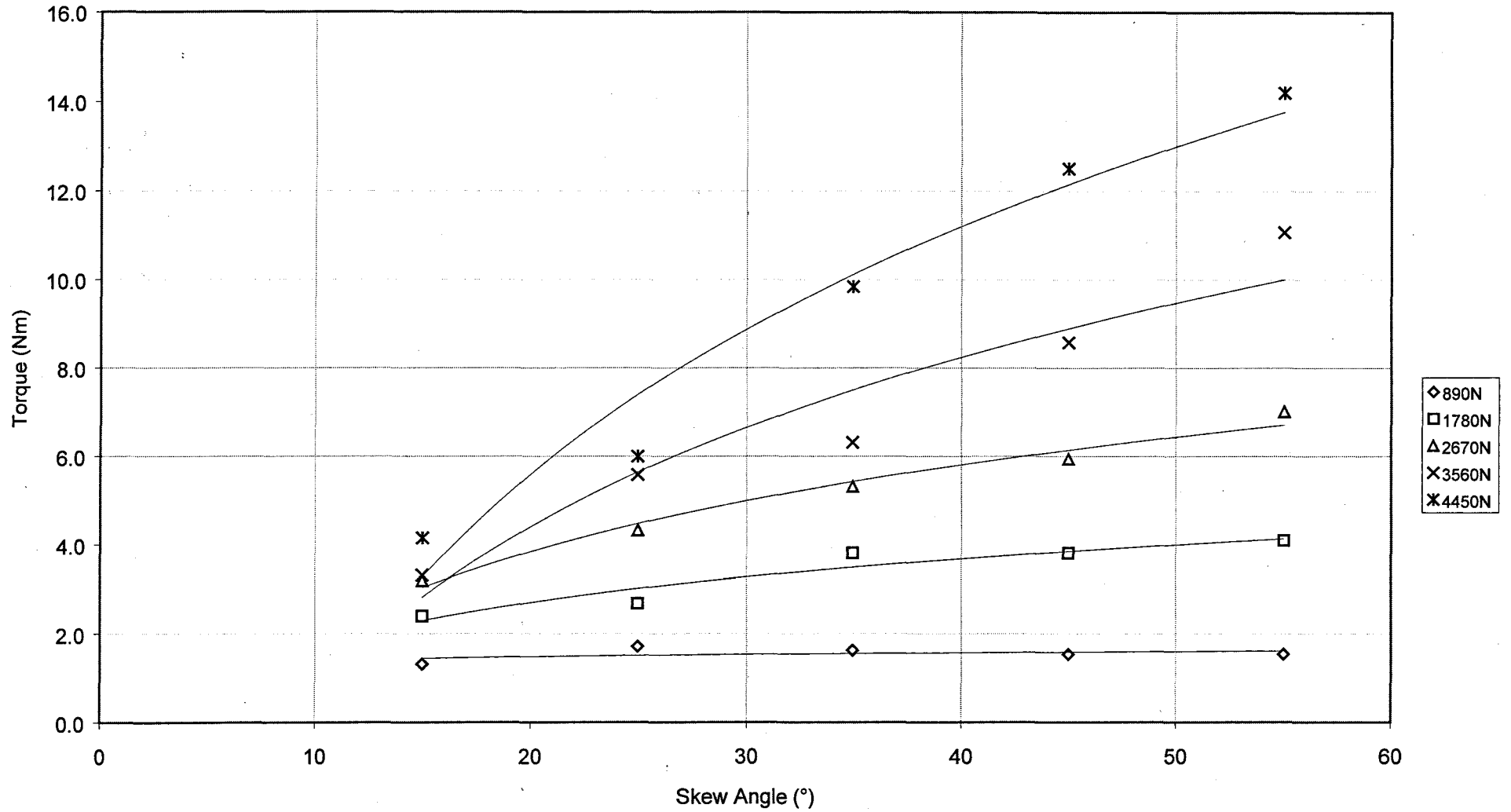


Figure E-22  
Torque Characteristics with Skew Angle at 450RPM with Catenex 79 Lubrication

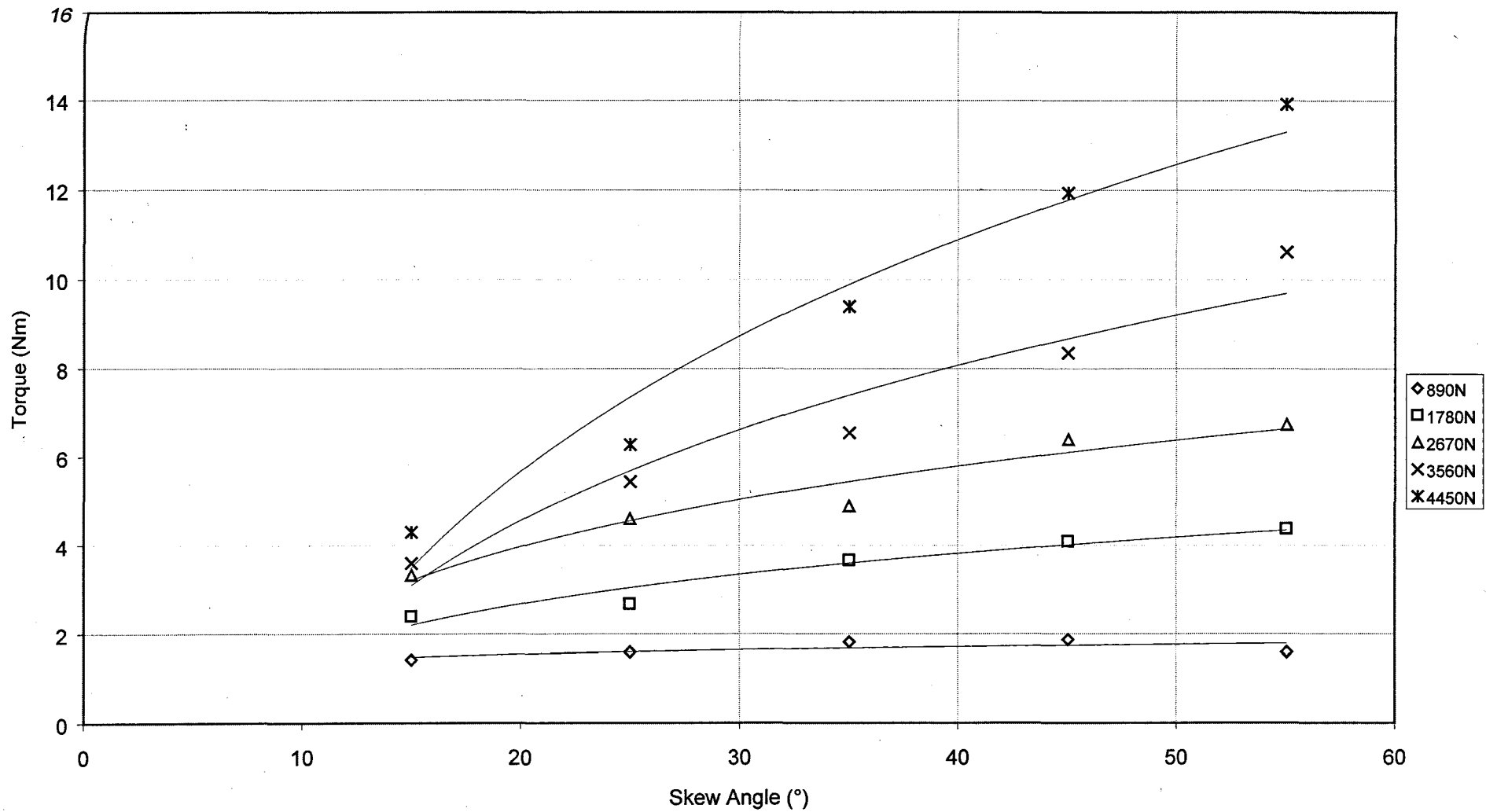


Figure E-23  
Torque Characteristics with Skew Angle at 550RPM with Catenex 79 Lubrication

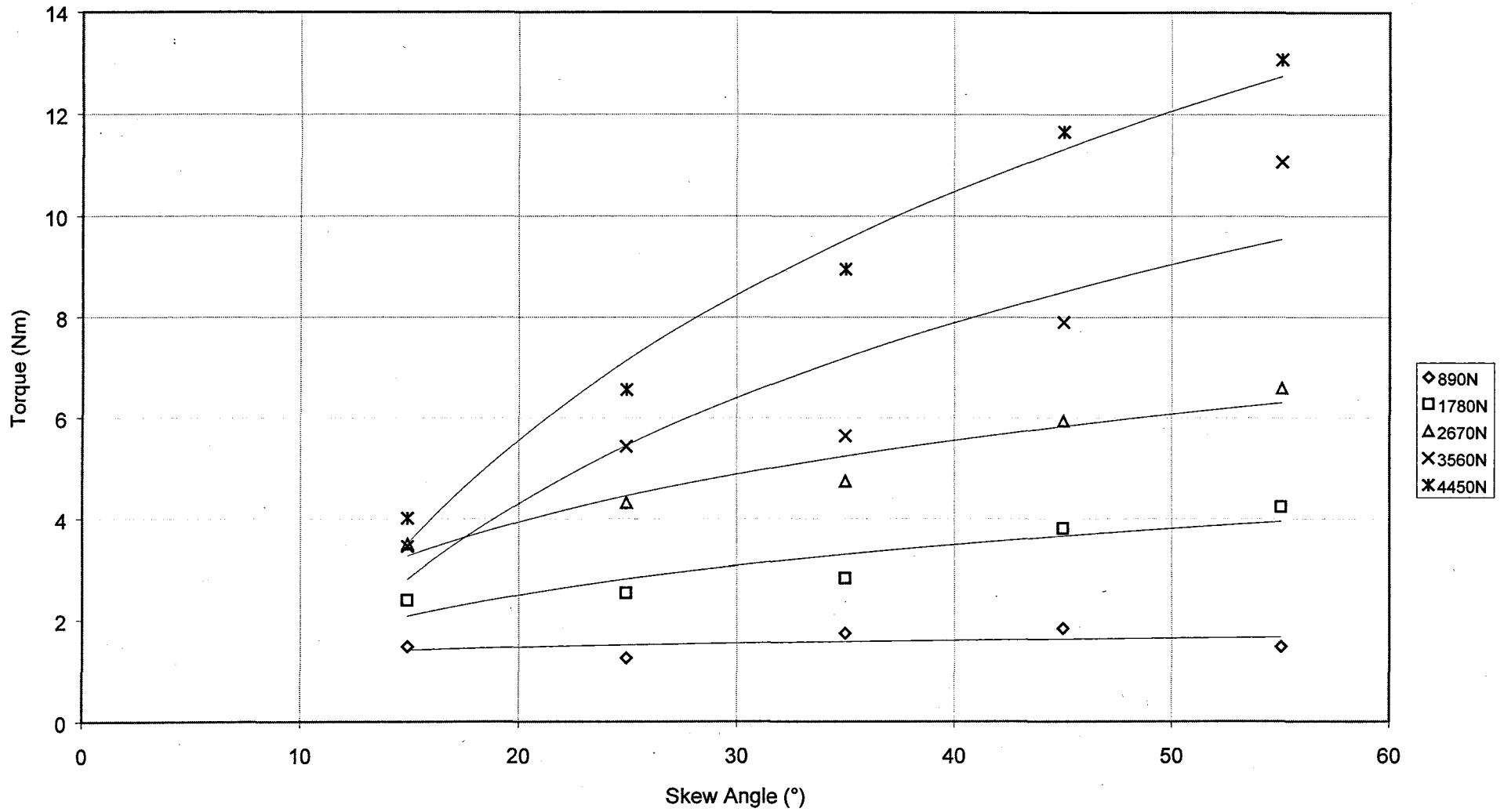


Figure E-24  
Torque Characteristics with Skew Angle at 650RPM with Catenex 79 Lubrication

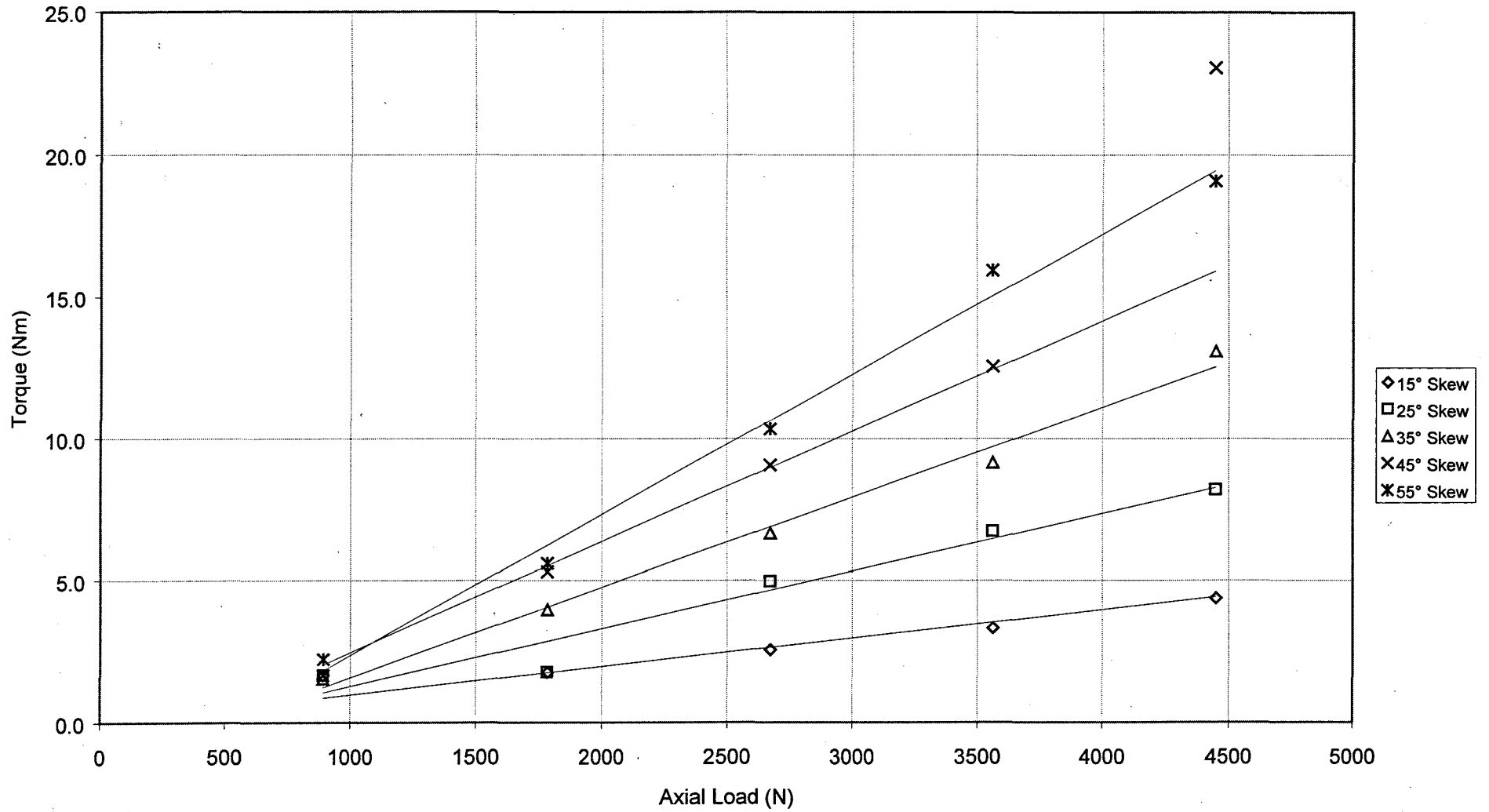


Figure E-25  
Torque Characteristics with Axial Loading at 50RPM with Catenex 79 Lubrication



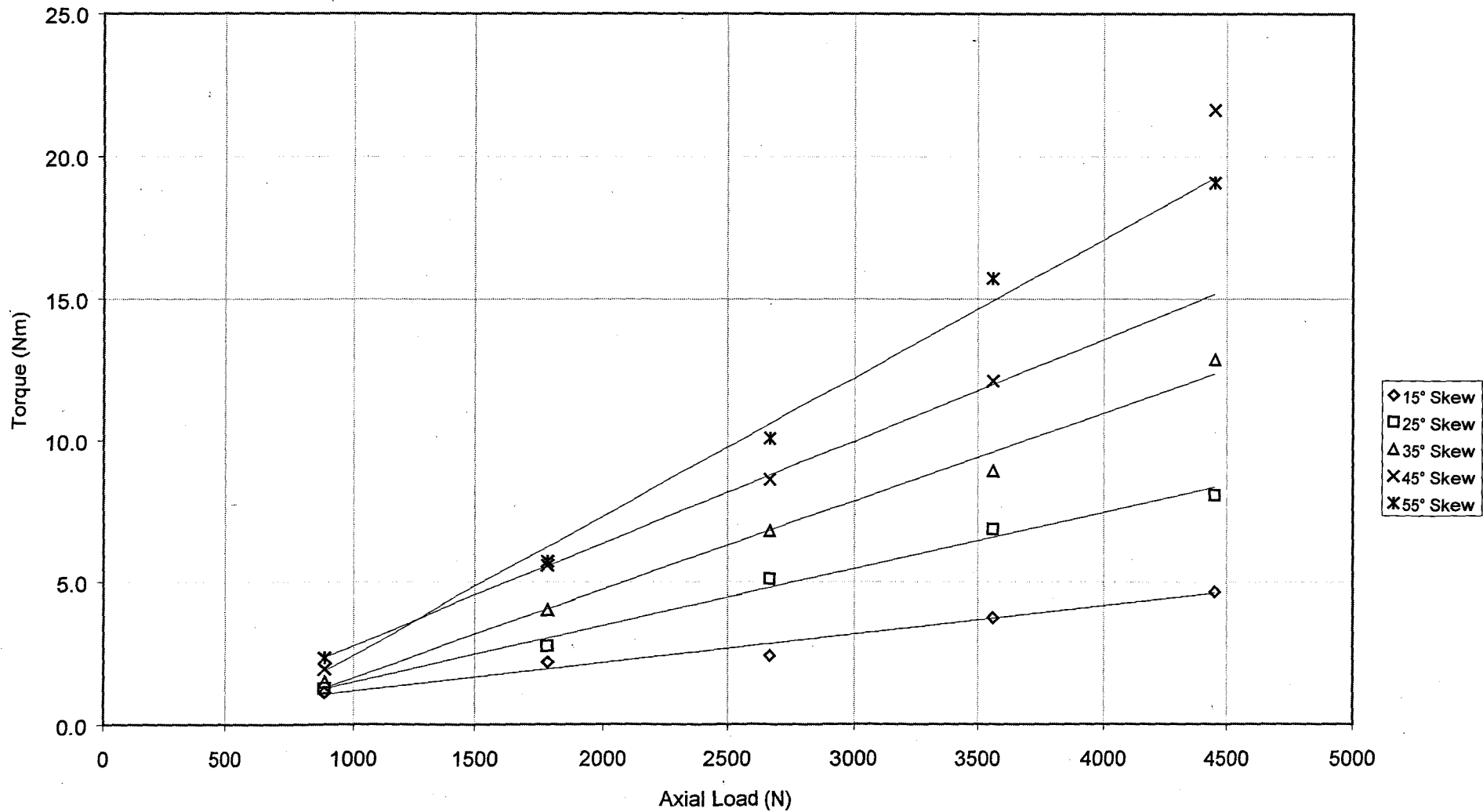


Figure E-26  
Torque Characteristics with Axial Loading at 75RPM with Catenex 79 Lubrication

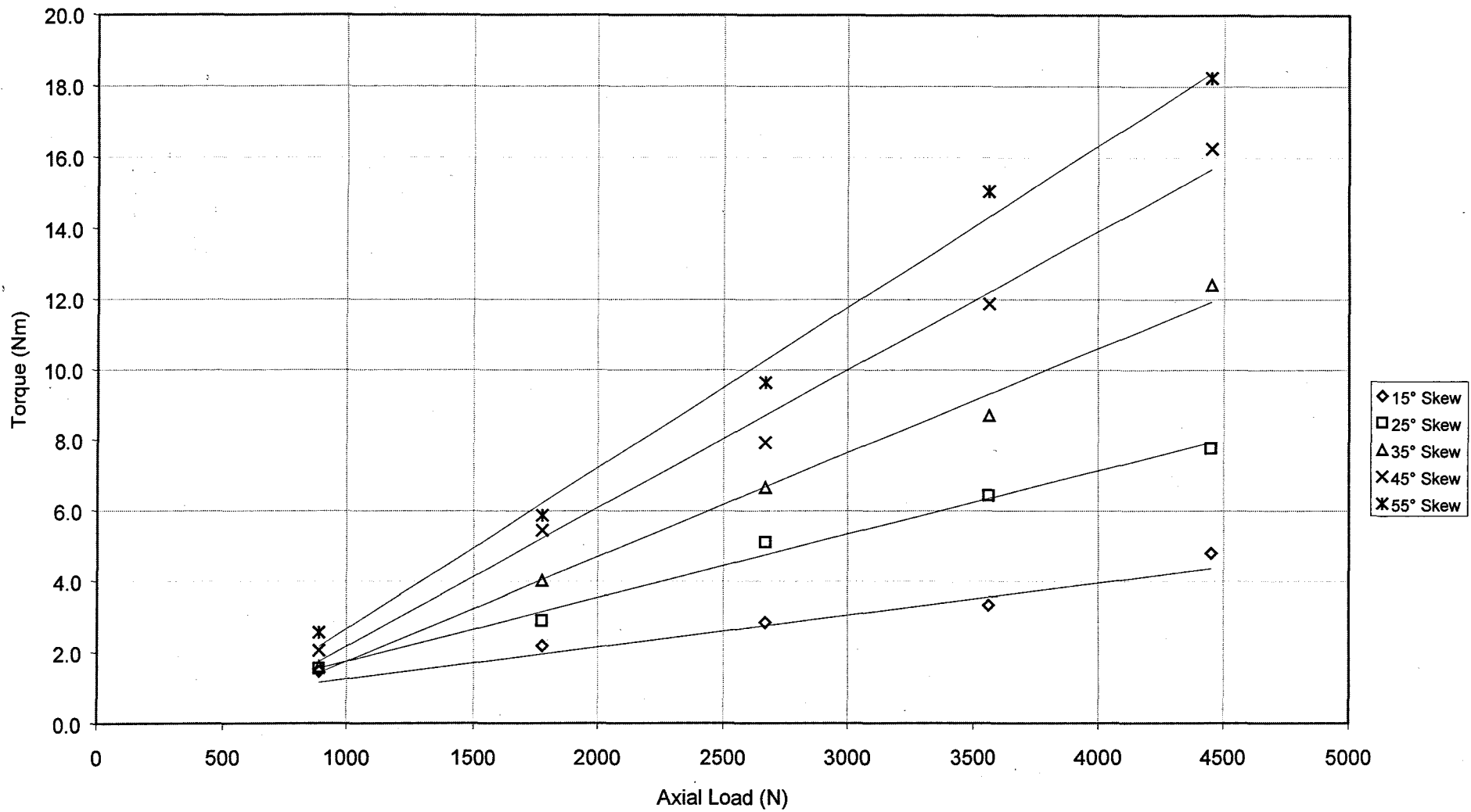


Figure E-27  
Torque Characteristics with Axial Loading at 100RPM with Catenex 79 Lubrication

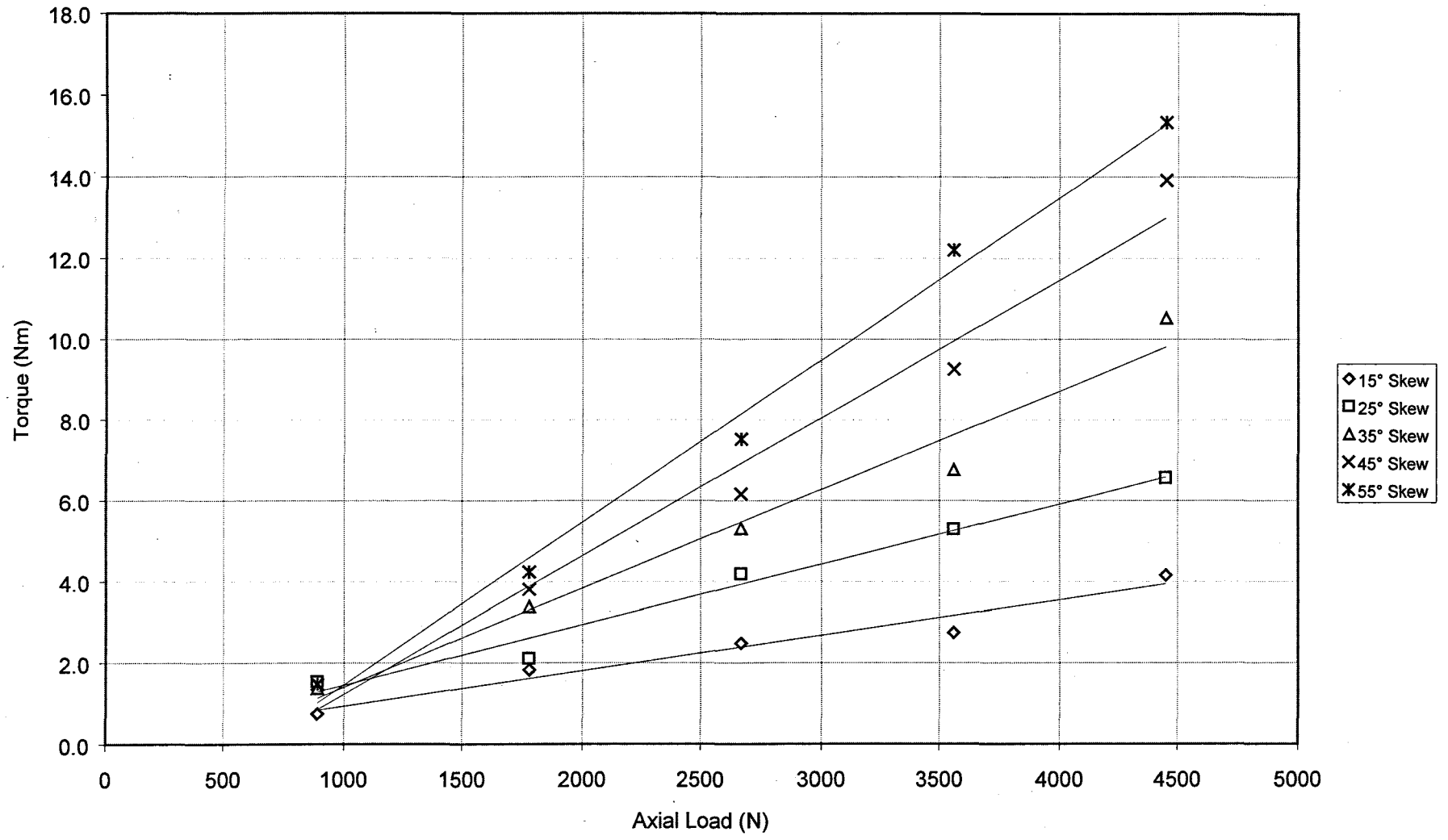


Figure E-28  
Torque Characteristics with Axial Loading at 250RPM with Catenex 79 Lubrication

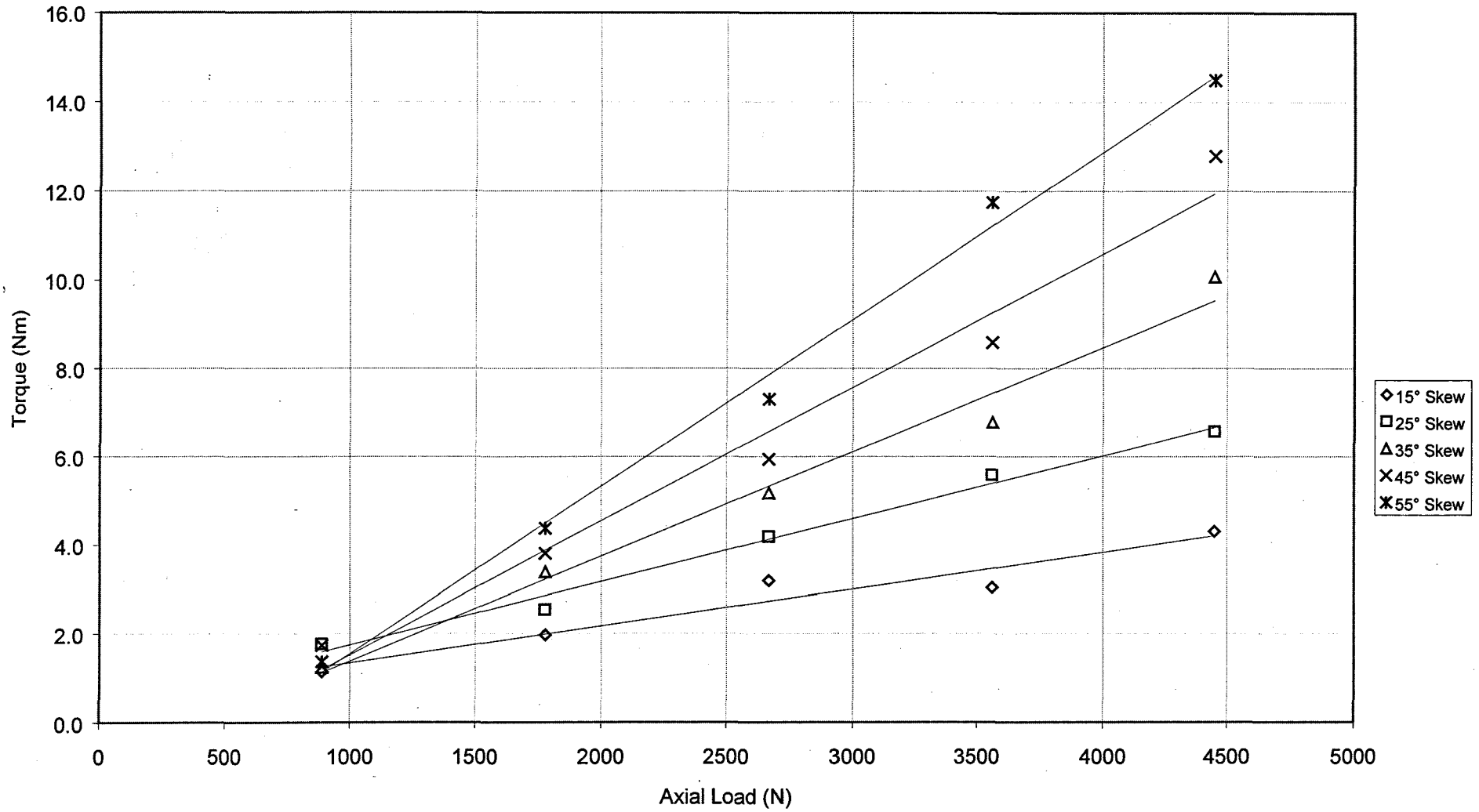


Figure E-29  
Torque Characteristics with Axial Loading at 350RPM with Catenex 79 Lubrication

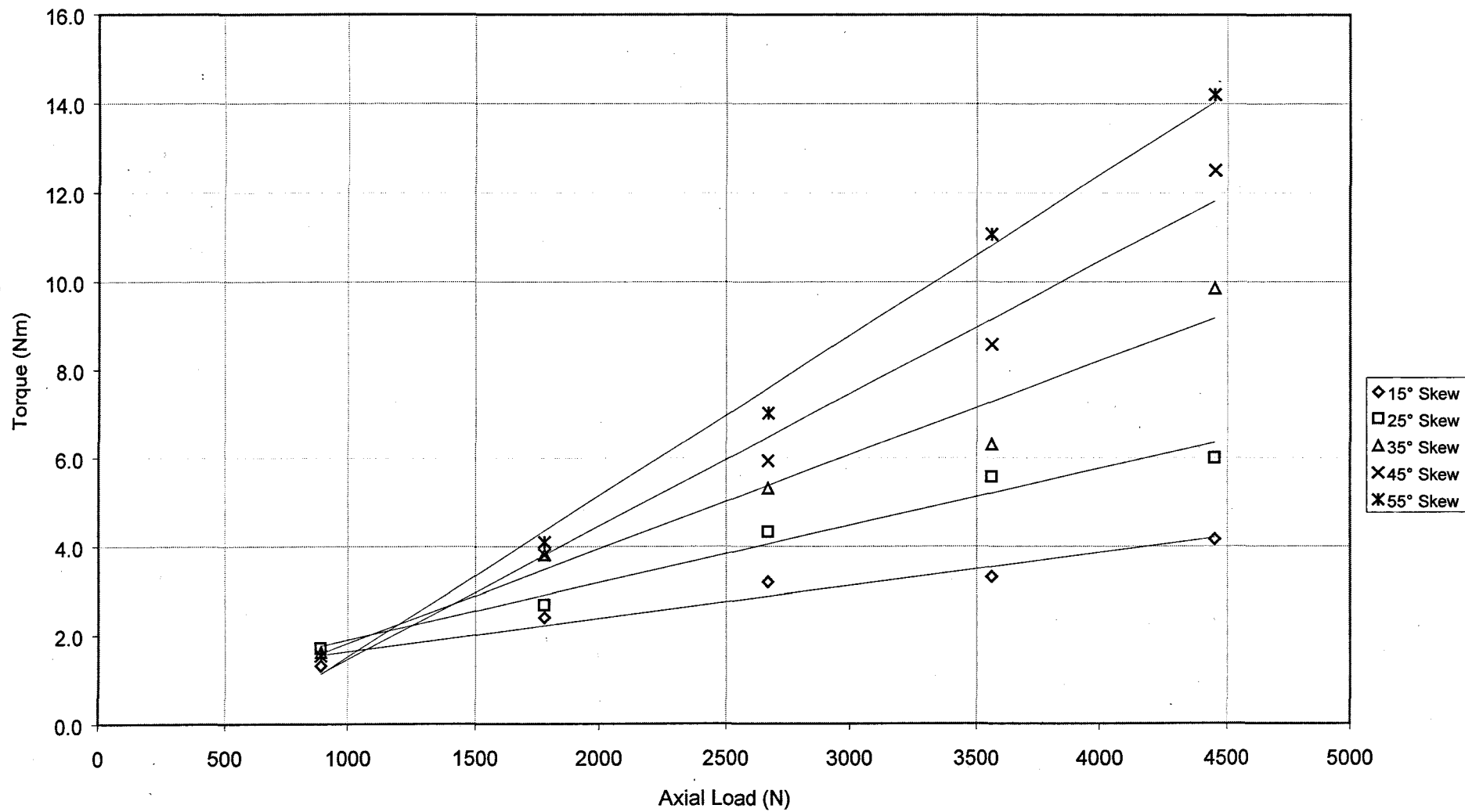


Figure E-30  
Torque Characteristics with Axial Loading at 450RPM with Catenex 79 Lubrication

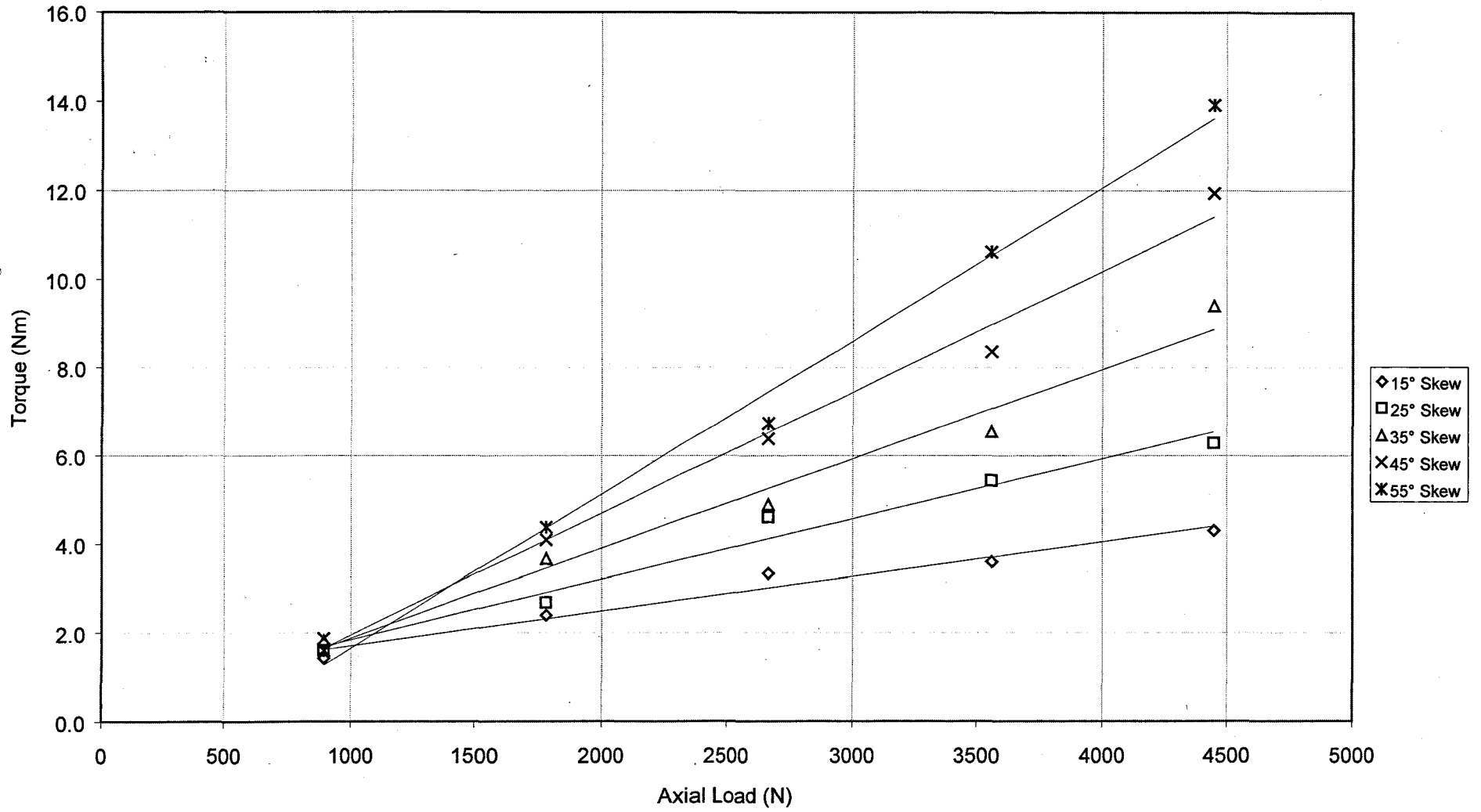


Figure E-31  
Torque Characteristics with Axial Loading at 450RPM with Catenex 79 Lubrication

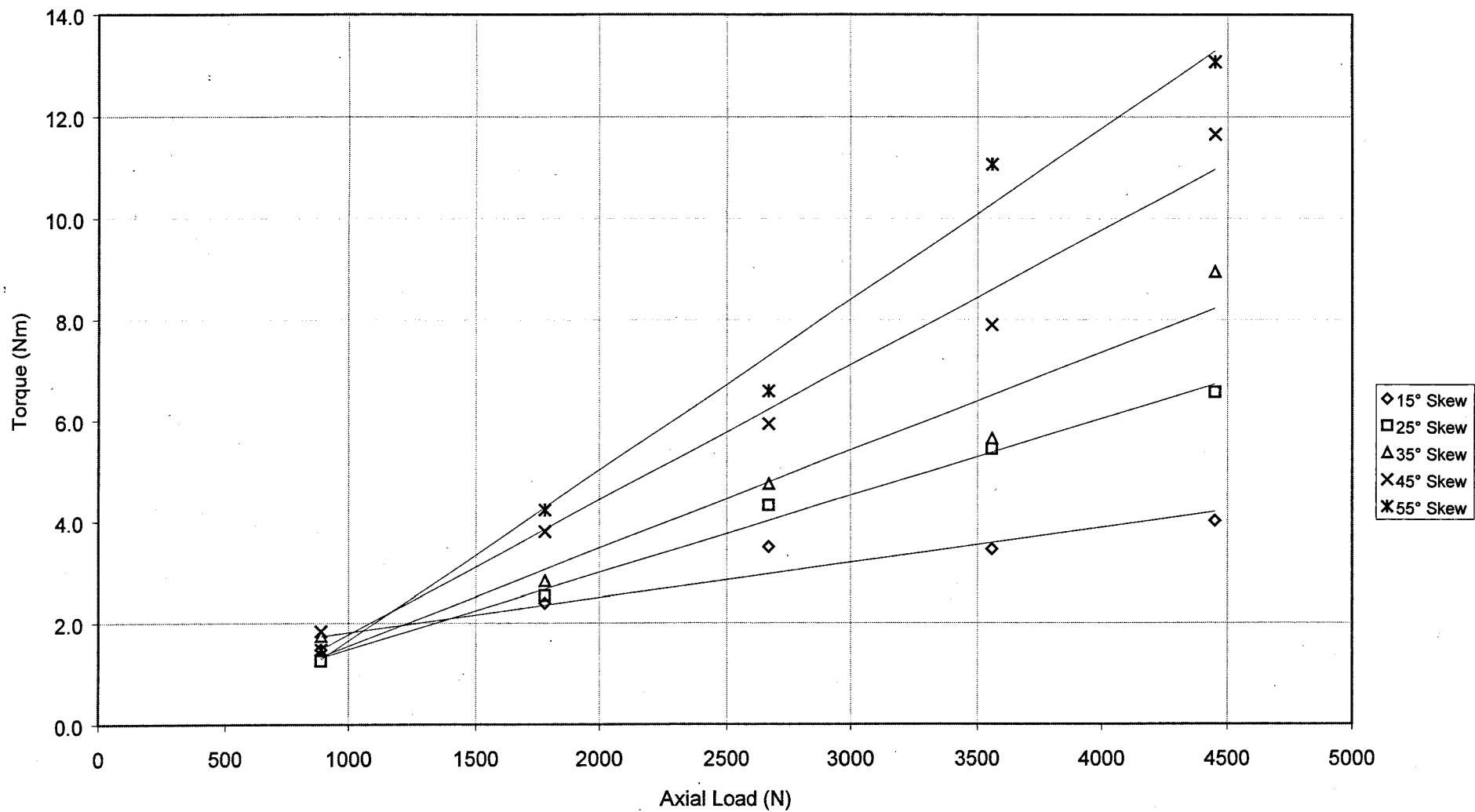


Figure E-32  
Torque Characteristics with Axial Loading at 650RPM with Catenex 79 Lubrication

# APPENDIX F

## LUBRICATION NUMBER ANALYSIS

Construction of Stribeck diagrams requires the abscissa parameter to represent the fluid viscosity, entrainment velocity and the load or stress. The lubrication number proposed by Shipper and de Gee (1995) introduces the average surface roughness of the roller and plate also, such that

$$L = \left( \frac{\eta \cdot V_+}{\bar{p} \cdot R_a} \right)$$

Each term is discussed below.

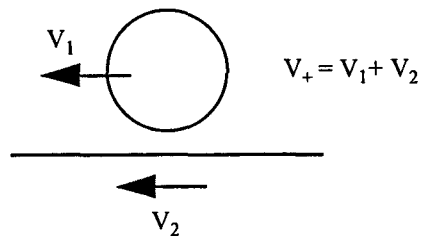
### **Dynamic viscosity term, $\eta$ .**

Appendix G presents the rheological data associated with the two fluids used in this project. Dynamic viscosity is temperature and pressure dependent. The temperature which is of most interest is that in the thin film layer between roller and plate. However, measurement of this value is extremely difficult and not possible within this project. The bulk temperature of the fluid contained within the test unit was however measured during each test. During the course of a particular test, the temperature of the fluid would rise from the ambient to a peak value and then cool back to ambient before the next test. The maximum temperature rise during any test was approximately 10° C. The average temperature was used in this analysis.

### **Velocity Term, $V_+$**

Considering the motion of a point or line contact and a plate, Figure F-1, Schipper and de Gee define the sum velocity term and slide velocity term as





$$V_+ = V_1 + V_2 \quad \text{and} \quad V_- = V_1 - V_2$$

Figure F-1. Velocity Definitions

The sum and sliding velocity can be related to the entrainment velocity calculations used in elastohydrodynamic film thickness calculations. Consider the conventional thrust bearing case, zero skew angle, shown in Figure F-2.

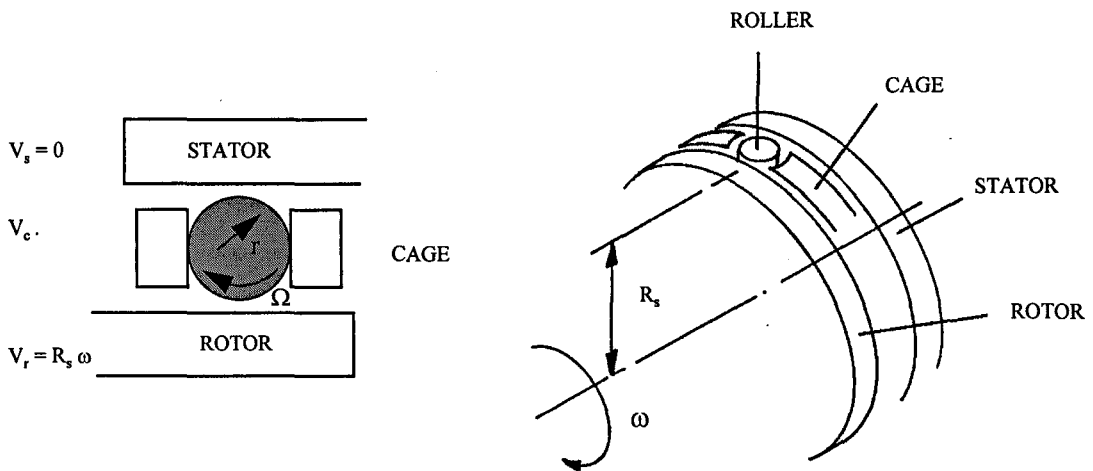


Figure F-2. Entrainment Velocity

The situation is similar to that of a rolling element bearing and the entrainment velocity for this case is presented in textbooks such as Dowson and Higginson (1977). In the situation sketched in Figure F-2, we have

$$\text{relative velocity at stator/roller interface} = Vc$$

$$\text{relative velocity at roller/rotor interface} = Vr - Vc$$

$$\text{and the roller surface velocity} = r\Omega.$$

Hence at the stator/roller interface and the roller/rotor interface:

$$r\Omega = Vc$$

and

$$r\Omega = Vr - Vc$$

hence

$$Vr = 2Vc = R_{shaft} \times \omega$$

Entrainment velocity at the stator/roller interface and roller/rotor interface are equal, hence the entrainment velocity from Figure F-3 is given by:

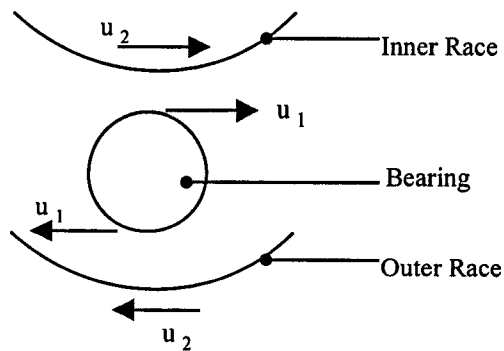


Figure F-3. Surface Velocities and Entrainment Velocity

$$\bar{u} = \frac{1}{2}(u_1 + u_2) = \frac{1}{2} \cdot R_{shaft} \cdot \omega$$

Considering the sum and sliding velocities,  $V_+$  and  $V_-$  it can be seen that,

$$V_+ \equiv 2\bar{u}$$

and

$$V_- = |u_1 - u_2|$$

Intuitively the entrainment velocity will change with increasing skew angle. As the skew angle increases the roller generates more sliding action and less rolling action, until in the limit with the skew angle of  $90^\circ$ , no roll takes place, only sliding. By following a similar analysis to that described above it can be shown that the entrainment velocity is given by

$$\bar{u} = \frac{1}{4} \cdot R_{shaft} \cdot \omega$$

Hence from the zero degree thrust bearing case to the ninety-degree pure sliding case the entrainment velocity has reduced by 50%. The rolling effect is likely to reduce at a higher rate at small angles than as the skew angle approaches ninety-degrees. Therefore, it seems reasonable to assume a sine variation with skew angle to describe the change in entrainment velocity, hence

$$\bar{u} = \frac{1}{4} \cdot R_{shaft} \cdot \omega \cdot (2 - \sin \phi)$$

This expression has been used to calculate the entrainment velocities presented in this thesis.

Further, the sum velocity,  $V_+$ , is given by

$$V_+ = 2\bar{u}$$

hence

$$V_+ = \frac{R_{shaft}}{2} \cdot \omega \cdot (2 - \sin \phi)$$

### **Hertzian Stress Term, $\bar{p}$**

The mean stress has been used in all calculations. This has been calculated using conventional Hertzian stress formula which can be found in standard texts.

### **Surface Roughness Term, R.**

The centre-line average surface roughness of the rotor and stator plates has been used. This was found to be constant through the test at 0.1  $\mu\text{m}$ .

### **Lubrication Number Analysis**

Tables F1 to F10 present the lubrication number analysis results and tables F11 to F20 show the film thickness calculations.

LUBRICATION NUMBER ANALYSIS

		SI units			SI units
roller length	0.01	m	poissons ratio	0.267	
roller diameter	0.005	m	Youngs Modulus	2.00E+11	N/m <sup>2</sup>
skew angle	15	°	Equivalent Radius	0.0025	m
PCD	0.0701	m	Equivalent E	2.15E+11	N/m <sup>2</sup>
number of rollers	10		Average surface roughness (R <sub>a</sub> )	1.00E-07	m

$$\mu = \frac{\text{Running Torque}}{\text{Pre load} \cdot \left(\frac{PCD}{2}\right) \cdot \text{No Brake Stages}}$$

$$\mu_1 = \frac{\text{Running Torque}}{\text{Pre load} \cdot \left[\left(\frac{PCD}{2} \cdot \sin \phi\right) + \left(\frac{2}{3} \cdot \text{Roller Length}\right)\right] \cdot \text{No Brake Stages}}$$

$$\mu_2 = \frac{\text{Running Torque}}{\text{Pre load} \cdot \left[\left(\frac{PCD}{2} \cdot \sin \phi\right) + \left(\frac{1}{2} \cdot \text{Roller Length}\right)\right] \cdot \text{No Brake Stages}}$$

preload (lb)	preload (N)	Rotational speed (rpm)	Running Torque (lbin)	$\mu$	$\mu_1$	$\mu_2$	contact width b (mm)	Pmax (N/mm2)	Pmean (N/mm2)	entraining velocity (m/s)	sum velocity (m/s)	sliding velocity (m/s)	average lubricant temp	dynamic viscosity (kg/ms)	lubrication number
200	890	50	8.7	0.016	0.035	0.039	0.0162	349.31	274.35	0.08	0.16	0.16	22.3	2.35E-02	1.37E-04
200	890	75	8.5	0.015	0.034	0.039	0.0162	349.31	274.35	0.12	0.24	0.24	22.6	2.32E-02	2.03E-04
200	890	100	7.1	0.013	0.029	0.032	0.0162	349.31	274.35	0.16	0.32	0.32	23.1	2.29E-02	2.66E-04
200	890	250	8.5	0.015	0.034	0.039	0.0162	349.31	274.35	0.40	0.80	0.80	23.8	2.23E-02	6.50E-04
200	890	350	7.7	0.014	0.031	0.035	0.0162	349.31	274.35	0.56	1.12	1.12	24.4	2.19E-02	8.94E-04
200	890	450	0.7	0.001	0.003	0.003	0.0162	349.31	274.35	0.72	1.44	1.44	24.9	2.16E-02	1.13E-03
200	890	550	0.7	0.001	0.003	0.003	0.0162	349.31	274.35	0.88	1.76	1.76	25.4	2.12E-02	1.36E-03
200	890	650	9.1	0.017	0.037	0.041	0.0162	349.31	274.35	1.04	2.08	2.08	26.4	2.05E-02	1.55E-03
400	1780	50	18.0	0.016	0.036	0.041	0.0229	494.00	387.98	0.08	0.16	0.16	22.2	2.35E-02	9.69E-05
400	1780	75	22.0	0.020	0.044	0.050	0.0229	494.00	387.98	0.12	0.24	0.24	22.8	2.31E-02	1.43E-04
400	1780	100	22.0	0.020	0.044	0.050	0.0229	494.00	387.98	0.16	0.32	0.32	23.7	2.24E-02	1.84E-04
400	1780	250	22.0	0.020	0.044	0.050	0.0229	494.00	387.98	0.40	0.80	0.80	26.0	2.08E-02	4.28E-04
400	1780	350	20.5	0.019	0.041	0.046	0.0229	494.00	387.98	0.56	1.12	1.12	27.0	2.01E-02	5.81E-04
400	1780	450	19.0	0.017	0.038	0.043	0.0229	494.00	387.98	0.72	1.44	1.44	28.0	1.95E-02	7.24E-04
400	1780	550	21.0	0.019	0.042	0.047	0.0229	494.00	387.98	0.88	1.76	1.76	28.7	1.91E-02	8.66E-04
400	1780	650	21.0	0.019	0.042	0.047	0.0229	494.00	387.98	1.04	2.08	2.08	30.7	1.80E-02	9.64E-04
600	2670	50	40.0	0.024	0.054	0.050	0.0281	605.02	475.18	0.08	0.16	0.16	18.4	2.68E-02	9.00E-05
600	2670	75	38.0	0.023	0.051	0.057	0.0281	605.02	475.18	0.12	0.24	0.24	19.5	2.58E-02	1.30E-04
600	2670	100	32.0	0.019	0.043	0.048	0.0281	605.02	475.18	0.16	0.32	0.32	20.5	2.49E-02	1.68E-04
600	2670	250	35.0	0.021	0.047	0.053	0.0281	605.02	475.18	0.40	0.80	0.80	23.0	2.29E-02	3.85E-04
600	2670	350	34.0	0.021	0.046	0.051	0.0281	605.02	475.18	0.56	1.12	1.12	24.0	2.22E-02	5.22E-04
600	2670	450	31.0	0.019	0.042	0.047	0.0281	605.02	475.18	0.72	1.44	1.44	25.5	2.11E-02	6.39E-04
600	2670	550	32.0	0.019	0.043	0.048	0.0281	605.02	475.18	0.88	1.76	1.76	26.5	2.05E-02	7.57E-04
600	2670	650	32.0	0.019	0.043	0.048	0.0281	605.02	475.18	1.04	2.08	2.08	27.0	2.01E-02	8.80E-04
800	3560	50	52.7	0.024	0.053	0.050	0.0324	698.62	548.69	0.08	0.16	0.16	24.0	2.22E-02	6.46E-05
800	3560	75	50.7	0.023	0.051	0.057	0.0324	698.62	548.69	0.12	0.24	0.24	25.5	2.11E-02	9.23E-05
800	3560	100	50.7	0.023	0.051	0.057	0.0324	698.62	548.69	0.16	0.32	0.32	27.0	2.01E-02	1.17E-04
800	3560	250	47.7	0.022	0.048	0.054	0.0324	698.62	548.69	0.40	0.80	0.80	29.2	1.88E-02	2.74E-04
800	3560	350	44.7	0.020	0.045	0.050	0.0324	698.62	548.69	0.56	1.12	1.12	31.5	1.76E-02	3.59E-04
800	3560	450	44.7	0.020	0.045	0.050	0.0324	698.62	548.69	0.72	1.44	1.44	33.0	1.69E-02	4.42E-04
800	3560	550	43.7	0.020	0.044	0.049	0.0324	698.62	548.69	0.88	1.76	1.76	34.5	1.62E-02	5.19E-04
800	3560	650	41.7	0.019	0.042	0.047	0.0324	698.62	548.69	1.04	2.08	2.08	34.0	1.64E-02	6.21E-04
1000	4450	50	67.8	0.025	0.055	0.051	0.0363	781.08	613.46	0.08	0.16	0.16	23.0	2.29E-02	5.97E-05
1000	4450	75	66.8	0.024	0.054	0.050	0.0363	781.08	613.46	0.12	0.24	0.24	25.0	2.15E-02	8.39E-05
1000	4450	100	63.8	0.023	0.051	0.058	0.0363	781.08	613.46	0.16	0.32	0.32	26.8	2.03E-02	1.06E-04
1000	4450	250	58.8	0.021	0.047	0.053	0.0363	781.08	613.46	0.40	0.80	0.80	31.0	1.78E-02	2.32E-04
1000	4450	350	54.8	0.020	0.044	0.049	0.0363	781.08	613.46	0.56	1.12	1.12	33.0	1.69E-02	3.07E-04
1000	4450	450	54.8	0.020	0.044	0.049	0.0363	781.08	613.46	0.72	1.44	1.44	35.0	1.60E-02	3.75E-04
1000	4450	550	54.8	0.020	0.044	0.049	0.0363	781.08	613.46	0.88	1.76	1.76	36.0	1.56E-02	4.46E-04
1000	4450	650	54.8	0.020	0.044	0.049	0.0363	781.08	613.46	1.04	2.08	2.08	39.5	1.43E-02	4.86E-04

Table F-1, Lubrication Analysis Results, Brayco 795, 15° Skew.

# LUBRICATION NUMBER ANALYSIS

		SI units			SI units
roller length	0.01	m	poissons ratio	0.267	
roller diameter	0.005	m	Youngs Modulus	2.00E+11	N/m <sup>2</sup>
skew angle	25	°	Equivalent Radius	0.0025	m
PCD	0.0701	m	Equivalent E	2.15E+11	N/m <sup>2</sup>
number of rollers	10		Average surface roughness (R <sub>a</sub> )	1.00E-07	m

$$\mu = \frac{\text{Running Torque}}{\text{Preload} \cdot \left( \frac{PCD}{2} \right) \cdot \text{No Brake Stages}}$$

$$\mu_1 = \frac{\text{Running Torque}}{\text{Preload} \cdot \left[ \left( \frac{PCD}{2} \cdot \sin \phi \right) + \left( \frac{2}{3} \cdot \text{Roller Length} \right) \right] \cdot \text{No Brake Stages}}$$

$$\mu_2 = \frac{\text{Running Torque}}{\text{Preload} \cdot \left[ \left( \frac{PCD}{2} \cdot \sin \phi \right) + \left( \frac{1}{2} \cdot \text{Roller Length} \right) \right] \cdot \text{No Brake Stages}}$$

preload (lb)	preload (N)	Rotational speed (rpm)	Running Torque (lbin)	$\mu$	$\mu_1$	$\mu_2$	contact width b (mm)	Pmax (N/mm <sup>2</sup> )	Pmean (N/mm <sup>2</sup> )	entraining velocity (m/s)	sum velocity (m/s)	sliding velocity (m/s)	average lubricant temp (kg/ms)	dynamic viscosity (kg/ms)	Lubrication number
200	890	50	28.2	0.051	0.083	0.090	0.0162	349.31	274.35	0.07	0.14	0.14	17.2	2.79E-02	1.47E-04
200	890	75	28.2	0.051	0.083	0.090	0.0162	349.31	274.35	0.11	0.22	0.22	17.9	2.72E-02	2.16E-04
200	890	100	27.2	0.049	0.080	0.087	0.0162	349.31	274.35	0.14	0.29	0.29	18.8	2.64E-02	2.78E-04
200	890	250	24.7	0.045	0.073	0.079	0.0162	349.31	274.35	0.36	0.72	0.72	19.9	2.54E-02	6.70E-04
200	890	350	25.2	0.046	0.074	0.081	0.0162	349.31	274.35	0.51	1.01	1.01	21.0	2.45E-02	9.05E-04
200	890	450	20.2	0.037	0.060	0.065	0.0162	349.31	274.35	0.65	1.30	1.30	21.9	2.38E-02	1.13E-03
200	890	550	19.7	0.036	0.058	0.063	0.0162	349.31	274.35	0.80	1.59	1.59	22.8	2.31E-02	1.34E-03
200	890	650	19.4	0.035	0.057	0.062	0.0162	349.31	274.35	0.94	1.88	1.88	23.9	2.22E-02	1.52E-03
400	1780	50	43.0	0.039	0.064	0.069	0.0229	494.00	387.98	0.07	0.14	0.14	25.2	2.13E-02	7.96E-05
400	1780	75	41.0	0.037	0.061	0.066	0.0229	494.00	387.98	0.11	0.22	0.22	26.1	2.07E-02	1.16E-04
400	1780	100	39.0	0.035	0.058	0.063	0.0229	494.00	387.98	0.14	0.29	0.29	27.1	2.01E-02	1.50E-04
400	1780	250	37.0	0.034	0.055	0.059	0.0229	494.00	387.98	0.36	0.72	0.72	29.2	1.88E-02	3.51E-04
400	1780	350	35.0	0.032	0.052	0.056	0.0229	494.00	387.98	0.51	1.01	1.01	30.6	1.81E-02	4.72E-04
400	1780	450	34.0	0.031	0.050	0.055	0.0229	494.00	387.98	0.65	1.30	1.30	32.0	1.73E-02	5.82E-04
400	1780	550	34.0	0.031	0.050	0.055	0.0229	494.00	387.98	0.80	1.59	1.59	33.0	1.69E-02	6.92E-04
400	1780	650	32.0	0.029	0.047	0.051	0.0229	494.00	387.98	0.94	1.88	1.88	35.0	1.60E-02	7.75E-04
600	2670	50	67.0	0.040	0.066	0.072	0.0281	605.02	475.18	0.07	0.14	0.14	17.8	2.73E-02	8.33E-05
600	2670	75	65.0	0.039	0.064	0.069	0.0281	605.02	475.18	0.11	0.22	0.22	19.5	2.58E-02	1.18E-04
600	2670	100	62.0	0.037	0.061	0.066	0.0281	605.02	475.18	0.14	0.29	0.29	21.5	2.41E-02	1.47E-04
600	2670	250	57.0	0.034	0.056	0.061	0.0281	605.02	475.18	0.36	0.72	0.72	25.0	2.15E-02	3.27E-04
600	2670	350	56.0	0.034	0.055	0.060	0.0281	605.02	475.18	0.51	1.01	1.01	26.5	2.05E-02	4.36E-04
600	2670	450	54.0	0.033	0.053	0.058	0.0281	605.02	475.18	0.65	1.30	1.30	28.5	1.92E-02	5.27E-04
600	2670	550	52.0	0.031	0.051	0.056	0.0281	605.02	475.18	0.80	1.59	1.59	30.5	1.81E-02	6.07E-04
600	2670	650	50.0	0.030	0.049	0.053	0.0281	605.02	475.18	0.94	1.88	1.88	32.8	1.70E-02	6.72E-04
800	3560	50	89.7	0.041	0.066	0.072	0.0324	698.62	548.69	0.07	0.14	0.14	25.2	2.13E-02	5.63E-05
800	3560	75	88.7	0.040	0.066	0.071	0.0324	698.62	548.69	0.11	0.22	0.22	27.5	1.98E-02	7.85E-05
800	3560	100	84.7	0.038	0.063	0.068	0.0324	698.62	548.69	0.14	0.29	0.29	29.7	1.85E-02	9.78E-05
800	3560	250	76.7	0.035	0.057	0.061	0.0324	698.62	548.69	0.36	0.72	0.72	36.0	1.56E-02	2.05E-04
800	3560	350	74.7	0.034	0.055	0.060	0.0324	698.62	548.69	0.51	1.01	1.01	35.0	1.60E-02	2.95E-04
800	3560	450	72.7	0.033	0.054	0.058	0.0324	698.62	548.69	0.65	1.30	1.30	34.5	1.62E-02	3.84E-04
800	3560	550	72.7	0.033	0.054	0.058	0.0324	698.62	548.69	0.80	1.59	1.59	34.0	1.64E-02	4.76E-04
800	3560	650	68.7	0.031	0.051	0.055	0.0324	698.62	548.69	0.94	1.88	1.88	34.0	1.64E-02	5.63E-04
1000	4450	50	108.8	0.039	0.064	0.070	0.0363	781.08	613.46	0.07	0.14	0.14	26.2	2.07E-02	4.87E-05
1000	4450	75	108.8	0.039	0.064	0.070	0.0363	781.08	613.46	0.11	0.22	0.22	28.4	1.93E-02	6.83E-05
1000	4450	100	105.8	0.038	0.063	0.068	0.0363	781.08	613.46	0.14	0.29	0.29	24.0	2.22E-02	1.05E-04
1000	4450	250	96.8	0.035	0.057	0.062	0.0363	781.08	613.46	0.36	0.72	0.72	29.0	1.89E-02	2.23E-04
1000	4450	350	92.8	0.034	0.055	0.059	0.0363	781.08	613.46	0.51	1.01	1.01	32.5	1.71E-02	2.82E-04
1000	4450	450	90.8	0.033	0.054	0.058	0.0363	781.08	613.46	0.65	1.30	1.30	35.0	1.60E-02	3.39E-04
1000	4450	550	86.8	0.031	0.051	0.056	0.0363	781.08	613.46	0.80	1.59	1.59	35.0	1.60E-02	4.15E-04
1000	4450	650	85.8	0.031	0.051	0.055	0.0363	781.08	613.46	0.94	1.88	1.88	38.0	1.48E-02	4.55E-04

Table F-2, Lubrication Analysis Results, Brayco 795, 25° Skew.

**LUBRICATION NUMBER ANALYSIS**

		SI units		SI units
roller length	0.01	m	poissons ratio	0.267
roller diameter	0.005	m	Youngs Modulus	2.00E+11 N/m <sup>2</sup>
skew angle	35	°	Equivalent Radius	0.0025 m
PCD	0.0701	m	Equivalent E	2.15E+11 N/m <sup>2</sup>
number of rollers	10		Average surface roughness (R <sub>a</sub> )	1.00E-07 m

$$\mu = \frac{\text{Running Torque}}{\text{Preload} \cdot \left( \frac{PCD}{2} \right) \cdot \text{No Brake Stages}}$$

$$\mu_1 = \frac{\text{Running Torque}}{\text{Preload} \cdot \left[ \left( \frac{PCD}{2} \cdot \sin \phi \right) + \left( \frac{2}{3} \cdot \text{Roller Length} \right) \right] \cdot \text{No Brake Stages}}$$

$$\mu_2 = \frac{\text{Running Torque}}{\text{Preload} \cdot \left[ \left( \frac{PCD}{2} \cdot \sin \phi \right) + \left( \frac{1}{2} \cdot \text{Roller Length} \right) \right] \cdot \text{No Brake Stages}}$$

preload (lb)	preload (N)	Rotational speed (rpm)	Running Torque (lbin)	$\mu$	$\mu_1$	$\mu_2$	contact width b (mm)	Pmax (N/mm <sup>2</sup> )	Pmean (N/mm <sup>2</sup> )	entraining velocity (m/s)	sum velocity (m/s)	sliding velocity (m/s)	average lubricant temp	dynamic viscosity (kg/ms)	lubrication number
200	890	50	24.7	0.045	0.059	0.062	0.0162	349.31	274.35	0.07	0.13	0.13	21.0	2.45E-02	1.17E-04
200	890	75	24.4	0.044	0.058	0.062	0.0162	349.31	274.35	0.10	0.20	0.20	21.4	2.42E-02	1.73E-04
200	890	100	24.7	0.045	0.059	0.062	0.0162	349.31	274.35	0.13	0.26	0.26	22.1	2.36E-02	2.25E-04
200	890	250	23.2	0.042	0.055	0.059	0.0162	349.31	274.35	0.33	0.65	0.65	23.8	2.23E-02	5.33E-04
200	890	350	13.7	0.025	0.032	0.035	0.0162	349.31	274.35	0.46	0.92	0.92	25.3	2.12E-02	7.09E-04
200	890	450	21.2	0.038	0.050	0.054	0.0162	349.31	274.35	0.59	1.18	1.18	26.1	2.07E-02	8.91E-04
200	890	550	15.7	0.028	0.037	0.040	0.0162	349.31	274.35	0.72	1.44	1.44	26.6	2.04E-02	1.07E-03
200	890	650	15.4	0.028	0.037	0.039	0.0162	349.31	274.35	0.85	1.70	1.70	28.8	1.90E-02	1.18E-03
400	1780	50	68.0	0.062	0.081	0.086	0.0229	494.00	387.98	0.07	0.13	0.13	24.6	2.17E-02	7.34E-05
400	1780	75	63.0	0.057	0.075	0.080	0.0229	494.00	387.98	0.10	0.20	0.20	27.2	2.00E-02	1.01E-04
400	1780	100	64.0	0.058	0.076	0.081	0.0229	494.00	387.98	0.13	0.26	0.26	29.0	1.89E-02	1.28E-04
400	1780	250	57.0	0.052	0.068	0.072	0.0229	494.00	387.98	0.33	0.65	0.65	32.5	1.71E-02	2.88E-04
400	1780	350	52.0	0.047	0.062	0.066	0.0229	494.00	387.98	0.46	0.92	0.92	33.5	1.66E-02	3.93E-04
400	1780	450	50.0	0.045	0.059	0.063	0.0229	494.00	387.98	0.59	1.18	1.18	35.0	1.60E-02	4.85E-04
400	1780	550	51.0	0.046	0.061	0.065	0.0229	494.00	387.98	0.72	1.44	1.44	36.5	1.54E-02	5.71E-04
400	1780	650	49.0	0.044	0.058	0.062	0.0229	494.00	387.98	0.85	1.70	1.70	35.0	1.60E-02	7.01E-04
600	2670	50	95.0	0.057	0.075	0.080	0.0281	605.02	475.18	0.07	0.13	0.13	28.0	1.95E-02	5.38E-05
600	2670	75	95.0	0.057	0.075	0.080	0.0281	605.02	475.18	0.10	0.20	0.20	29.0	1.89E-02	7.82E-05
600	2670	100	90.0	0.054	0.071	0.076	0.0281	605.02	475.18	0.13	0.26	0.26	30.4	1.82E-02	1.00E-04
600	2670	250	82.0	0.049	0.065	0.069	0.0281	605.02	475.18	0.33	0.65	0.65	33.0	1.69E-02	2.32E-04
600	2670	350	78.0	0.047	0.062	0.066	0.0281	605.02	475.18	0.46	0.92	0.92	33.0	1.69E-02	3.25E-04
600	2670	450	76.0	0.046	0.060	0.064	0.0281	605.02	475.18	0.59	1.18	1.18	34.0	1.64E-02	4.07E-04
600	2670	550	76.0	0.046	0.060	0.064	0.0281	605.02	475.18	0.72	1.44	1.44	34.0	1.64E-02	4.97E-04
600	2670	650	72.0	0.043	0.057	0.061	0.0281	605.02	475.18	0.85	1.70	1.70	35.0	1.60E-02	5.72E-04
800	3560	50	128.7	0.058	0.076	0.081	0.0324	698.62	548.69	0.07	0.13	0.13	19.0	2.62E-02	6.26E-05
800	3560	75	124.7	0.056	0.074	0.079	0.0324	698.62	548.69	0.10	0.20	0.20	21.4	2.42E-02	8.65E-05
800	3560	100	120.7	0.055	0.072	0.076	0.0324	698.62	548.69	0.13	0.26	0.26	24.5	2.18E-02	1.04E-04
800	3560	250	110.7	0.050	0.066	0.070	0.0324	698.62	548.69	0.33	0.65	0.65	29.0	1.89E-02	2.26E-04
800	3560	350	104.7	0.047	0.062	0.066	0.0324	698.62	548.69	0.46	0.92	0.92	30.0	1.84E-02	3.07E-04
800	3560	450	102.7	0.047	0.061	0.065	0.0324	698.62	548.69	0.59	1.18	1.18	33.0	1.69E-02	3.62E-04
800	3560	550	98.7	0.045	0.059	0.062	0.0324	698.62	548.69	0.72	1.44	1.44	36.0	1.56E-02	4.09E-04
800	3560	650	98.7	0.045	0.059	0.062	0.0324	698.62	548.69	0.85	1.70	1.70	34.0	1.64E-02	5.09E-04
1000	4450	50	162.8	0.059	0.077	0.082	0.0363	781.08	613.46	0.07	0.13	0.13	27.7	1.97E-02	4.20E-05
1000	4450	75	158.8	0.058	0.075	0.080	0.0363	781.08	613.46	0.10	0.20	0.20	30.5	1.81E-02	5.80E-05
1000	4450	100	154.8	0.056	0.073	0.078	0.0363	781.08	613.46	0.13	0.26	0.26	33.5	1.66E-02	7.10E-05
1000	4450	250	140.8	0.051	0.067	0.071	0.0363	781.08	613.46	0.33	0.65	0.65	35.0	1.60E-02	1.71E-04
1000	4450	350	132.8	0.048	0.063	0.067	0.0363	781.08	613.46	0.46	0.92	0.92	35.0	1.60E-02	2.39E-04
1000	4450	450	126.8	0.046	0.060	0.064	0.0363	781.08	613.46	0.59	1.18	1.18	36.0	1.56E-02	2.99E-04
1000	4450	550	126.8	0.046	0.060	0.064	0.0363	781.08	613.46	0.72	1.44	1.44	37.0	1.52E-02	3.57E-04
1000	4450	650	122.8	0.044	0.058	0.062	0.0363	781.08	613.46	0.85	1.70	1.70	34.0	1.64E-02	4.55E-04

Table F-3, Lubrication Analysis Results, Brayco 795, 35° Skew.

# LUBRICATION NUMBER ANALYSIS

			SI units				SI units
roller length	0.01	m	poissons ratio	0.267			
roller diameter	0.005	m	Youngs Modulus	2.00E+11	N/m <sup>2</sup>		
skew angle	45	°	Equivalent Radius	0.0025	m		
PCD	0.0701	m	Equivalent E	2.15E+11	N/m <sup>2</sup>		
number of rollers	10		Average surface roughness (R <sub>a</sub> )	1.00E-07	m		

$$\mu = \frac{\text{Running Torque}}{\text{Preload} \cdot \left(\frac{\text{PCD}}{2}\right) \cdot \text{No Brake Stages}}$$

$$\mu_1 = \frac{\text{Running Torque}}{\text{Preload} \cdot \left[\left(\frac{\text{PCD}}{2} \cdot \sin \phi\right) + \left(\frac{2}{3} \cdot \text{Roller Length}\right)\right] \cdot \text{No Brake Stages}}$$

$$\mu_2 = \frac{\text{Running Torque}}{\text{Preload} \cdot \left[\left(\frac{\text{PCD}}{2} \cdot \sin \phi\right) + \left(\frac{1}{2} \cdot \text{Roller Length}\right)\right] \cdot \text{No Brake Stages}}$$

preload (lb)	preload (N)	Rotational speed (rpm)	Running Torque (lbin)	$\mu$	$\mu_1$	$\mu_2$	contact width b (mm)	Pmax (N/mm2)	Pmean (N/mm2)	entraining velocity (m/s)	sum velocity (m/s)	sliding velocity (m/s)	average lubricant temp (K/gms)	dynamic viscosity	lubrication number
200	890	50	34.2	0.062	0.069	0.073	0.0162	349.31	274.35	0.06	0.12	0.12	19.9	2.54E-02	1.10E-04
200	890	75	33.4	0.061	0.068	0.071	0.0162	349.31	274.35	0.09	0.18	0.18	20.7	2.46E-02	1.61E-04
200	890	100	33.2	0.060	0.067	0.071	0.0162	349.31	274.35	0.12	0.24	0.24	21.6	2.40E-02	2.08E-04
200	890	250	31.2	0.057	0.063	0.066	0.0162	349.31	274.35	0.30	0.59	0.59	23.9	2.22E-02	4.80E-04
200	890	350	28.2	0.051	0.057	0.060	0.0162	349.31	274.35	0.42	0.83	0.83	25.1	2.14E-02	6.47E-04
200	890	450	27.7	0.050	0.056	0.059	0.0162	349.31	274.35	0.53	1.07	1.07	26.1	2.07E-02	8.06E-04
200	890	550	28.2	0.051	0.057	0.060	0.0162	349.31	274.35	0.65	1.31	1.31	27.0	2.01E-02	9.57E-04
200	890	650	22.2	0.040	0.045	0.047	0.0162	349.31	274.35	0.77	1.54	1.54	29.3	1.88E-02	1.06E-03
400	1780	50	77.0	0.070	0.078	0.082	0.0229	494.00	387.98	0.06	0.12	0.12	24.2	2.20E-02	6.74E-05
400	1780	75	75.0	0.068	0.076	0.080	0.0229	494.00	387.98	0.09	0.18	0.18	26.5	2.05E-02	9.39E-05
400	1780	100	72.0	0.065	0.073	0.077	0.0229	494.00	387.98	0.12	0.24	0.24	28.0	1.95E-02	1.19E-04
400	1780	250	64.0	0.058	0.065	0.068	0.0229	494.00	387.98	0.30	0.59	0.59	16.5	2.85E-02	4.37E-04
400	1780	350	63.0	0.057	0.064	0.067	0.0229	494.00	387.98	0.42	0.83	0.83	18.5	2.67E-02	5.71E-04
400	1780	450	61.0	0.055	0.062	0.065	0.0229	494.00	387.98	0.53	1.07	1.07	18.5	2.67E-02	7.34E-04
400	1780	550	59.0	0.053	0.060	0.063	0.0229	494.00	387.98	0.65	1.31	1.31	18.3	2.69E-02	9.04E-04
400	1780	650	57.0	0.052	0.058	0.061	0.0229	494.00	387.98	0.77	1.54	1.54	21.1	2.44E-02	9.71E-04
600	2670	50	117.0	0.071	0.079	0.083	0.0281	605.02	475.18	0.06	0.12	0.12	22.5	2.33E-02	5.82E-05
600	2670	75	114.0	0.069	0.077	0.081	0.0281	605.02	475.18	0.09	0.18	0.18	24.5	2.18E-02	8.17E-05
600	2670	100	110.0	0.066	0.074	0.078	0.0281	605.02	475.18	0.12	0.24	0.24	27.5	1.98E-02	9.90E-05
600	2670	250	100.0	0.060	0.067	0.071	0.0281	605.02	475.18	0.30	0.59	0.59	34.5	1.62E-02	2.02E-04
600	2670	350	94.0	0.057	0.063	0.067	0.0281	605.02	475.18	0.42	0.83	0.83	36.5	1.54E-02	2.69E-04
600	2670	450	91.0	0.055	0.061	0.065	0.0281	605.02	475.18	0.53	1.07	1.07	36.0	1.56E-02	3.50E-04
600	2670	550	87.0	0.053	0.059	0.062	0.0281	605.02	475.18	0.65	1.31	1.31	34.0	1.64E-02	4.51E-04
600	2670	650	87.0	0.053	0.059	0.062	0.0281	605.02	475.18	0.77	1.54	1.54	36.0	1.56E-02	5.06E-04
800	3560	50	156.7	0.071	0.079	0.084	0.0324	698.62	548.69	0.06	0.12	0.12	26.0	2.08E-02	4.50E-05
800	3560	75	150.7	0.068	0.076	0.080	0.0324	698.62	548.69	0.09	0.18	0.18	29.2	1.88E-02	6.11E-05
800	3560	100	144.7	0.066	0.073	0.077	0.0324	698.62	548.69	0.12	0.24	0.24	33.6	1.66E-02	7.17E-05
800	3560	250	130.7	0.059	0.066	0.070	0.0324	698.62	548.69	0.30	0.59	0.59	36.0	1.56E-02	1.68E-04
800	3560	350	124.7	0.056	0.063	0.066	0.0324	698.62	548.69	0.42	0.83	0.83	36.5	1.54E-02	2.33E-04
800	3560	450	120.7	0.055	0.061	0.064	0.0324	698.62	548.69	0.53	1.07	1.07	38.0	1.48E-02	2.89E-04
800	3560	550	118.7	0.054	0.060	0.063	0.0324	698.62	548.69	0.65	1.31	1.31	40.0	1.42E-02	3.37E-04
800	3560	650	114.7	0.052	0.058	0.061	0.0324	698.62	548.69	0.77	1.54	1.54	34.0	1.64E-02	4.61E-04
1000	4450	50	190.8	0.069	0.077	0.081	0.0363	781.08	613.46	0.06	0.12	0.12	28.8	1.91E-02	3.68E-05
1000	4450	75	186.8	0.068	0.075	0.080	0.0363	781.08	613.46	0.09	0.18	0.18	33.2	1.68E-02	4.87E-05
1000	4450	100	180.8	0.066	0.073	0.077	0.0363	781.08	613.46	0.12	0.24	0.24	36.5	1.54E-02	5.95E-05
1000	4450	250	162.8	0.059	0.066	0.069	0.0363	781.08	613.46	0.30	0.59	0.59	34.0	1.64E-02	1.59E-04
1000	4450	350	154.8	0.056	0.063	0.066	0.0363	781.08	613.46	0.42	0.83	0.83	35.5	1.58E-02	2.14E-04
1000	4450	450	148.8	0.054	0.060	0.063	0.0363	781.08	613.46	0.53	1.07	1.07	38.0	1.48E-02	2.58E-04
1000	4450	550	145.8	0.053	0.059	0.062	0.0363	781.08	613.46	0.65	1.31	1.31	37.5	1.50E-02	3.19E-04
1000	4450	650	142.8	0.052	0.058	0.061	0.0363	781.08	613.46	0.77	1.54	1.54	42.0	1.36E-02	3.42E-04

Table F-4, Lubrication Analysis Results, Brayco 795, 45° Skew.



# LUBRICATION NUMBER ANALYSIS

	SI units		SI units
roller length (m)	0.01	m	poissons ratio
roller diameter (m)	0.005	m	Youngs Modulus (N/m <sup>2</sup> )
skew angle	55	°	Equivalent Radius (m)
roller PCD (m)	0.0701	m	Equivalent E (N/m <sup>2</sup> )
number of rollers	10		Average surface roughness (R <sub>a</sub> )
			1.00E-07

$$\mu = \frac{\text{Running Torque}}{\text{Preload} \cdot \left(\frac{PCD}{2}\right) \cdot \text{No Brake Stages}}$$

$$\mu_1 = \frac{\text{Running Torque}}{\text{Preload} \cdot \left\{ \left(\frac{PCD}{2} \cdot \sin \theta\right) \cdot \left(\frac{2}{3} \cdot \text{Roller Length}\right) \right\} \cdot \text{No Brake Stages}}$$

$$\mu_2 = \frac{\text{Running Torque}}{\text{Preload} \cdot \left\{ \left(\frac{PCD}{2} \cdot \sin \theta\right) \cdot \left(\frac{1}{2} \cdot \text{Roller Length}\right) \right\} \cdot \text{No Brake Stages}}$$

preload (lb)	preload (N)	Rotational speed (rpm)	Running Torque (lbin)	$\mu$	$\mu_1$	$\mu_2$	contact width b (mm)	Pmax (N/mm <sup>2</sup> )	Pmean (N/mm <sup>2</sup> )	entraining velocity (m/s)	sum velocity (m/s)	sliding velocity (m/s)	average lubricant temp	dynamic viscosity (kg/ms)	lubrication number
200	890	50	30.0	0.054	0.054	0.056	0.0162	349.31	274.35	0.05	0.11	0.11	20.9	2.46E-02	9.73E-05
200	890	75	29.7	0.054	0.053	0.056	0.0162	349.31	274.35	0.08	0.16	0.16	21.6	2.40E-02	1.42E-04
200	890	100	34.7	0.063	0.062	0.065	0.0162	349.31	274.35	0.11	0.22	0.22	22.6	2.32E-02	1.83E-04
200	890	250	32.2	0.058	0.058	0.061	0.0162	349.31	274.35	0.27	0.54	0.54	24.2	2.21E-02	4.38E-04
200	890	350	31.2	0.057	0.056	0.059	0.0162	349.31	274.35	0.38	0.76	0.76	25.7	2.10E-02	5.81E-04
200	890	450	30.7	0.056	0.055	0.058	0.0162	349.31	274.35	0.49	0.98	0.98	27.3	2.00E-02	7.10E-04
200	890	550	28.7	0.052	0.051	0.054	0.0162	349.31	274.35	0.60	1.19	1.19	28.0	1.95E-02	8.49E-04
200	890	650	28.7	0.052	0.051	0.054	0.0162	349.31	274.35	0.70	1.41	1.41	30.4	1.82E-02	9.33E-04
400	1780	50	91.0	0.082	0.082	0.086	0.0229	494.00	387.98	0.05	0.11	0.11	24.0	2.22E-02	6.19E-05
400	1780	75	86.0	0.078	0.077	0.081	0.0229	494.00	387.98	0.08	0.16	0.16	25.9	2.09E-02	8.74E-05
400	1780	100	86.0	0.078	0.077	0.081	0.0229	494.00	387.98	0.11	0.22	0.22	27.7	1.97E-02	1.10E-04
400	1780	250	78.0	0.071	0.070	0.073	0.0229	494.00	387.98	0.27	0.54	0.54	30.6	1.81E-02	2.52E-04
400	1780	350	74.0	0.067	0.066	0.070	0.0229	494.00	387.98	0.38	0.76	0.76	32.8	1.70E-02	3.32E-04
400	1780	450	72.0	0.065	0.065	0.068	0.0229	494.00	387.98	0.49	0.98	0.98	34.0	1.64E-02	4.13E-04
400	1780	550	69.0	0.063	0.062	0.065	0.0229	494.00	387.98	0.60	1.19	1.19	34.0	1.64E-02	5.04E-04
400	1780	650	68.0	0.062	0.061	0.064	0.0229	494.00	387.98	0.70	1.41	1.41	34.7	1.61E-02	5.85E-04
600	2670	50	147.0	0.089	0.088	0.092	0.0281	605.02	475.18	0.05	0.11	0.11	16.0	2.91E-02	6.84E-05
600	2670	75	143.0	0.086	0.086	0.090	0.0281	605.02	475.18	0.08	0.16	0.16	19.7	2.56E-02	8.76E-05
600	2670	100	139.0	0.084	0.083	0.087	0.0281	605.02	475.18	0.11	0.22	0.22	23.6	2.25E-02	1.02E-04
600	2670	250	127.0	0.077	0.076	0.080	0.0281	605.02	475.18	0.27	0.54	0.54	27.0	2.01E-02	2.30E-04
600	2670	350	119.0	0.072	0.071	0.075	0.0281	605.02	475.18	0.38	0.76	0.76	30.0	1.84E-02	2.93E-04
600	2670	450	115.0	0.069	0.069	0.072	0.0281	605.02	475.18	0.49	0.98	0.98	32.0	1.73E-02	3.56E-04
600	2670	550	112.0	0.068	0.067	0.070	0.0281	605.02	475.18	0.60	1.19	1.19	35.5	1.58E-02	3.96E-04
600	2670	650	109.0	0.066	0.065	0.068	0.0281	605.02	475.18	0.70	1.41	1.41	39.0	1.45E-02	4.30E-04
800	3560	50	184.7	0.084	0.083	0.087	0.0324	698.62	548.89	0.05	0.11	0.11	27.5	1.98E-02	3.92E-05
800	3560	75	180.7	0.082	0.081	0.085	0.0324	698.62	548.89	0.08	0.16	0.16	32.5	1.71E-02	5.07E-05
800	3560	100	174.7	0.079	0.078	0.082	0.0324	698.62	548.89	0.11	0.22	0.22	36.0	1.56E-02	6.15E-05
800	3560	250	154.7	0.070	0.069	0.073	0.0324	698.62	548.89	0.27	0.54	0.54	38.2	1.48E-02	1.46E-04
800	3560	350	148.7	0.067	0.067	0.070	0.0324	698.62	548.89	0.38	0.76	0.76	39.5	1.43E-02	1.98E-04
800	3560	450	142.7	0.065	0.064	0.067	0.0324	698.62	548.89	0.49	0.98	0.98	41.0	1.39E-02	2.47E-04
800	3560	550	140.7	0.064	0.063	0.066	0.0324	698.62	548.89	0.60	1.19	1.19	42.0	1.36E-02	2.96E-04
800	3560	650	134.7	0.061	0.060	0.063	0.0324	698.62	548.89	0.70	1.41	1.41	42.5	1.35E-02	3.46E-04
1000	4450	50	226.8	0.083	0.082	0.086	0.0363	781.08	613.46	0.05	0.11	0.11	33.0	1.69E-02	2.98E-05
1000	4450	75	220.8	0.080	0.079	0.083	0.0363	781.08	613.46	0.08	0.16	0.16	37.0	1.52E-02	4.03E-05
1000	4450	100	217.8	0.079	0.078	0.082	0.0363	781.08	613.46	0.11	0.22	0.22	41.5	1.38E-02	4.86E-05
1000	4450	250	190.8	0.069	0.068	0.072	0.0363	781.08	613.46	0.27	0.54	0.54	41.0	1.39E-02	1.23E-04
1000	4450	350	182.8	0.066	0.066	0.069	0.0363	781.08	613.46	0.38	0.76	0.76	41.5	1.38E-02	1.70E-04
1000	4450	450	177.8	0.064	0.064	0.067	0.0363	781.08	613.46	0.49	0.98	0.98	42.0	1.36E-02	2.17E-04
1000	4450	550	167.8	0.061	0.060	0.063	0.0363	781.08	613.46	0.60	1.19	1.19	42.5	1.35E-02	2.62E-04
1000	4450	650	166.8	0.060	0.060	0.063	0.0363	781.08	613.46	0.70	1.41	1.41	38.0	1.48E-02	3.41E-04

Table F-5, Lubrication Analysis Results, Brayco 795, 55° Skew.

LUBRICATION NUMBER ANALYSIS

			SI units			SI units
roller length	0.01	m	poissons ratio	0.267		
roller diameter	0.005	m	Youngs Modulus	2.00E+11	N/m <sup>2</sup>	
skew angle	15	°	Equivalent Radius	0.0025	m	
PCD	0.0701	m	Equivalent E	2.15E+11	N/m <sup>2</sup>	
number of rollers	10		Average surface roughness (R <sub>a</sub> )	1.00E-07	m	

$$\mu = \frac{\text{Running Torque}}{\text{Preload} \cdot \left(\frac{PCD}{2}\right) \cdot \text{No Brake Stages}}$$

$$\mu_1 = \frac{\text{Running Torque}}{\text{Preload} \cdot \left[\left(\frac{PCD}{2} \cdot \sin \phi\right) + \left(\frac{2}{3} \cdot \text{Roller Length}\right)\right] \cdot \text{No Brake Stages}}$$

$$\mu_2 = \frac{\text{Running Torque}}{\text{Preload} \cdot \left[\left(\frac{PCD}{2} \cdot \sin \phi\right) + \left(\frac{1}{2} \cdot \text{Roller Length}\right)\right] \cdot \text{No Brake Stages}}$$

preload (lb)	preload (N)	Rotational speed (rpm)	Running Torque (lbin)	$\mu$	$\mu_1$	$\mu_2$	contact width b (mm)	Pmax (N/mm2)	Pmean (N/mm2)	entraining velocity (m/s)	sum velocity (m/s)	sliding velocity (m/s)	average lubricant temp	dynamic viscosity (kg/ms)	lubrication number
200	890	50	14.7	0.027	0.059	0.066	0.0162	349.31	274.35	0.08	0.16	0.16	20.4	1.18E+00	6.87E-03
200	890	75	9.9	0.018	0.040	0.045	0.0162	349.31	274.35	0.12	0.24	0.24	20.9	1.15E+00	1.01E-02
200	890	100	12.9	0.023	0.052	0.058	0.0162	349.31	274.35	0.16	0.32	0.32	21.6	1.11E+00	1.30E-02
200	890	250	6.6	0.012	0.027	0.030	0.0162	349.31	274.35	0.40	0.80	0.80	22.4	1.07E+00	3.12E-02
200	890	350	10.1	0.018	0.041	0.045	0.0162	349.31	274.35	0.56	1.12	1.12	23.8	1.00E+00	4.09E-02
200	890	450	11.6	0.021	0.047	0.052	0.0162	349.31	274.35	0.72	1.44	1.44	25.1	9.40E-01	4.93E-02
200	890	550	12.6	0.023	0.051	0.057	0.0162	349.31	274.35	0.88	1.76	1.76	26.3	8.90E-01	5.70E-02
200	890	650	13.1	0.024	0.053	0.059	0.0162	349.31	274.35	1.04	2.08	2.08	29.0	7.79E-01	5.90E-02
400	1780	50	15.6	0.014	0.031	0.035	0.0229	494.00	387.98	0.08	0.16	0.16	22.3	1.08E+00	4.43E-03
400	1780	75	19.4	0.018	0.039	0.044	0.0229	494.00	387.98	0.12	0.24	0.24	22.2	1.08E+00	6.68E-03
400	1780	100	19.4	0.018	0.039	0.044	0.0229	494.00	387.98	0.16	0.32	0.32	22.6	1.06E+00	8.76E-03
400	1780	250	16.2	0.015	0.033	0.036	0.0229	494.00	387.98	0.40	0.80	0.80	23.2	1.03E+00	2.12E-02
400	1780	350	17.4	0.016	0.035	0.039	0.0229	494.00	387.98	0.56	1.12	1.12	24.0	9.92E-01	2.86E-02
400	1780	450	21.2	0.019	0.043	0.048	0.0229	494.00	387.98	0.72	1.44	1.44	25.4	9.27E-01	3.44E-02
400	1780	550	21.2	0.019	0.043	0.048	0.0229	494.00	387.98	0.88	1.76	1.76	26.4	8.83E-01	4.00E-02
400	1780	650	21.2	0.019	0.043	0.048	0.0229	494.00	387.98	1.04	2.08	2.08	30.0	7.43E-01	3.98E-02
600	2670	50	22.7	0.014	0.030	0.034	0.0281	605.02	475.18	0.08	0.16	0.16	22.2	1.08E+00	3.64E-03
600	2670	75	21.4	0.013	0.029	0.032	0.0281	605.02	475.18	0.12	0.24	0.24	22.3	1.08E+00	5.44E-03
600	2670	100	25.2	0.015	0.034	0.038	0.0281	605.02	475.18	0.16	0.32	0.32	22.8	1.05E+00	7.07E-03
600	2670	250	22.0	0.013	0.030	0.033	0.0281	605.02	475.18	0.40	0.80	0.80	24.8	9.56E-01	1.61E-02
600	2670	350	28.2	0.017	0.038	0.042	0.0281	605.02	475.18	0.56	1.12	1.12	25.8	9.11E-01	2.15E-02
600	2670	450	28.2	0.017	0.038	0.042	0.0281	605.02	475.18	0.72	1.44	1.44	27.8	8.28E-01	2.50E-02
600	2670	550	29.5	0.018	0.040	0.044	0.0281	605.02	475.18	0.88	1.76	1.76	29.0	7.79E-01	2.88E-02
600	2670	650	31.0	0.019	0.042	0.047	0.0281	605.02	475.18	1.04	2.08	2.08	32.1	6.71E-01	2.93E-02
800	3560	50	29.4	0.013	0.030	0.033	0.0324	698.62	548.69	0.08	0.16	0.16	25.0	9.47E-01	2.76E-03
800	3560	75	33.2	0.015	0.033	0.037	0.0324	698.62	548.69	0.12	0.24	0.24	26.0	9.01E-01	3.93E-03
800	3560	100	29.4	0.013	0.030	0.033	0.0324	698.62	548.69	0.16	0.32	0.32	27.3	8.48E-01	4.94E-03
800	3560	250	24.3	0.011	0.025	0.027	0.0324	698.62	548.69	0.40	0.80	0.80	30.8	7.16E-01	1.04E-02
800	3560	350	26.8	0.012	0.027	0.030	0.0324	698.62	548.69	0.56	1.12	1.12	32.0	6.74E-01	1.37E-02
800	3560	450	29.3	0.013	0.030	0.033	0.0324	698.62	548.69	0.72	1.44	1.44	33.8	6.20E-01	1.62E-02
800	3560	550	31.8	0.014	0.032	0.036	0.0324	698.62	548.69	0.88	1.76	1.76	36.0	5.56E-01	1.78E-02
800	3560	650	30.6	0.014	0.031	0.034	0.0324	698.62	548.69	1.04	2.08	2.08	38.2	5.00E-01	1.89E-02
1000	4450	50	38.7	0.014	0.031	0.035	0.0363	781.08	613.46	0.08	0.16	0.16	30.2	7.35E-01	1.92E-03
1000	4450	75	41.2	0.015	0.033	0.037	0.0363	781.08	613.46	0.12	0.24	0.24	30.8	7.15E-01	2.79E-03
1000	4450	100	42.4	0.015	0.034	0.038	0.0363	781.08	613.46	0.16	0.32	0.32	31.8	6.81E-01	3.55E-03
1000	4450	250	36.8	0.013	0.030	0.033	0.0363	781.08	613.46	0.40	0.80	0.80	33.5	6.27E-01	8.17E-03
1000	4450	350	38.0	0.014	0.031	0.034	0.0363	781.08	613.46	0.56	1.12	1.12	35.4	5.72E-01	1.04E-02
1000	4450	450	36.8	0.013	0.030	0.033	0.0363	781.08	613.46	0.72	1.44	1.44	37.6	5.15E-01	1.21E-02
1000	4450	550	38.0	0.014	0.031	0.034	0.0363	781.08	613.46	0.88	1.76	1.76	39.6	4.68E-01	1.34E-02
1000	4450	650	35.5	0.013	0.029	0.032	0.0363	781.08	613.46	1.04	2.08	2.08	42.5	4.07E-01	1.38E-02

Table F-6, Lubrication Analysis Results, Catenex 79, 15° Skew.

LUBRICATION NUMBER ANALYSIS

			SI units			SI units
roller length	0.01	m	poissons ratio	0.267		
roller diameter	0.005	m	Youngs Modulus	2.00E+11	N/m <sup>2</sup>	
skew angle	25	°	Equivalent Radius	0.0025	m	
PCD	0.0701	m	Equivalent E	2.15E+11	N/m <sup>2</sup>	
number of rollers	10		Average surface roughness (R <sub>a</sub> )	1.00E-07	m	

$$\mu = \left[ \frac{\text{Running Torque}}{\text{Preload} \cdot \left( \frac{PCD}{2} \right) \cdot \text{No Brake Stages}} \right]$$

$$\mu_1 = \left[ \frac{\text{Running Torque}}{\text{Preload} \cdot \left[ \left( \frac{PCD}{2} \cdot \sin \phi \right) + \left( \frac{2}{3} \cdot \text{Roller Length} \right) \right] \cdot \text{No Brake Stages}} \right]$$

$$\mu_2 = \left[ \frac{\text{Running Torque}}{\text{Preload} \cdot \left[ \left( \frac{PCD}{2} \cdot \sin \phi \right) + \left( \frac{1}{2} \cdot \text{Roller Length} \right) \right] \cdot \text{No Brake Stages}} \right]$$

preload (lb)	preload (N)	Rotational speed (rpm)	Running Torque (lbin)	$\mu$	$\mu_1$	$\mu_2$	contact width b (mm)	Pmax (N/mm <sup>2</sup> )	Pmean (N/mm <sup>2</sup> )	entraining velocity (m/s)	sum velocity (m/s)	sliding velocity (m/s)	average lubricant temp	dynamic viscosity (kg/ms)	lubrication number
200	890	50	14.6	0.027	0.043	0.047	0.0162	349.31	274.35	0.07	0.14	0.14	23.3	1.03E+00	5.42E-03
200	890	75	11.2	0.020	0.033	0.036	0.0162	349.31	274.35	0.11	0.22	0.22	23.8	1.00E+00	7.92E-03
200	890	100	13.7	0.025	0.040	0.044	0.0162	349.31	274.35	0.14	0.29	0.29	24.8	9.56E-01	1.01E-02
200	890	250	13.6	0.025	0.040	0.043	0.0162	349.31	274.35	0.36	0.72	0.72	26.0	9.01E-01	2.38E-02
200	890	350	15.6	0.028	0.046	0.050	0.0162	349.31	274.35	0.51	1.01	1.01	27.3	8.48E-01	3.13E-02
200	890	450	15.1	0.027	0.045	0.048	0.0162	349.31	274.35	0.65	1.30	1.30	27.5	8.38E-01	3.98E-02
200	890	550	14.1	0.026	0.042	0.045	0.0162	349.31	274.35	0.80	1.59	1.59	30.0	7.43E-01	4.31E-02
200	890	650	11.1	0.020	0.033	0.036	0.0162	349.31	274.35	0.94	1.88	1.88	31.8	6.83E-01	4.68E-02
400	1780	50	15.6	0.014	0.023	0.025	0.0229	494.00	387.98	0.07	0.14	0.14	25.5	9.22E-01	3.44E-03
400	1780	75	24.4	0.022	0.036	0.039	0.0229	494.00	387.98	0.11	0.22	0.22	25.9	9.05E-01	5.06E-03
400	1780	100	25.6	0.023	0.038	0.041	0.0229	494.00	387.98	0.14	0.29	0.29	26.7	8.71E-01	6.50E-03
400	1780	250	18.7	0.017	0.028	0.030	0.0229	494.00	387.98	0.36	0.72	0.72	27.8	8.28E-01	1.54E-02
400	1780	350	22.4	0.020	0.033	0.036	0.0229	494.00	387.98	0.51	1.01	1.01	29.3	7.68E-01	2.01E-02
400	1780	450	23.7	0.021	0.035	0.038	0.0229	494.00	387.98	0.65	1.30	1.30	30.3	7.34E-01	2.46E-02
400	1780	550	23.7	0.021	0.035	0.038	0.0229	494.00	387.98	0.80	1.59	1.59	31.3	6.99E-01	2.87E-02
400	1780	650	22.4	0.020	0.033	0.036	0.0229	494.00	387.98	0.94	1.88	1.88	33.0	6.43E-01	3.12E-02
600	2670	50	44.0	0.027	0.043	0.047	0.0281	605.02	475.18	0.07	0.14	0.14	18.5	1.29E+00	3.94E-03
600	2670	75	45.2	0.027	0.045	0.048	0.0281	605.02	475.18	0.11	0.22	0.22	19.5	1.23E+00	5.63E-03
600	2670	100	45.2	0.027	0.045	0.048	0.0281	605.02	475.18	0.14	0.29	0.29	21.4	1.12E+00	6.85E-03
600	2670	250	37.0	0.022	0.036	0.040	0.0281	605.02	475.18	0.36	0.72	0.72	23.2	1.03E+00	1.57E-02
600	2670	350	37.0	0.022	0.036	0.040	0.0281	605.02	475.18	0.51	1.01	1.01	25.3	9.34E-01	1.99E-02
600	2670	450	38.3	0.023	0.038	0.041	0.0281	605.02	475.18	0.65	1.30	1.30	27.8	8.28E-01	2.27E-02
600	2670	550	40.8	0.025	0.040	0.044	0.0281	605.02	475.18	0.80	1.59	1.59	28.8	7.89E-01	2.64E-02
600	2670	650	38.3	0.023	0.038	0.041	0.0281	605.02	475.18	0.94	1.88	1.88	32.3	6.65E-01	2.63E-02
800	3560	50	59.5	0.027	0.044	0.048	0.0324	698.62	548.69	0.07	0.14	0.14	20.7	1.17E+00	3.07E-03
800	3560	75	60.7	0.028	0.045	0.049	0.0324	698.62	548.69	0.11	0.22	0.22	22.4	1.07E+00	4.24E-03
800	3560	100	57.0	0.026	0.042	0.046	0.0324	698.62	548.69	0.14	0.29	0.29	24.5	9.68E-01	5.11E-03
800	3560	250	46.9	0.021	0.036	0.038	0.0324	698.62	548.69	0.36	0.72	0.72	26.8	8.69E-01	1.15E-02
800	3560	350	49.4	0.022	0.036	0.040	0.0324	698.62	548.69	0.51	1.01	1.01	29.3	7.70E-01	1.42E-02
800	3560	450	49.4	0.022	0.036	0.040	0.0324	698.62	548.69	0.65	1.30	1.30	31.3	6.99E-01	1.66E-02
800	3560	550	48.1	0.022	0.036	0.039	0.0324	698.62	548.69	0.80	1.59	1.59	33.5	6.27E-01	1.82E-02
800	3560	650	48.1	0.022	0.036	0.039	0.0324	698.62	548.69	0.94	1.88	1.88	35.8	5.63E-01	1.93E-02
1000	4450	50	72.5	0.026	0.043	0.046	0.0363	781.08	613.46	0.07	0.14	0.14	29.6	7.59E-01	1.79E-03
1000	4450	75	71.3	0.026	0.042	0.046	0.0363	781.08	613.46	0.11	0.22	0.22	31.0	7.08E-01	2.50E-03
1000	4450	100	68.7	0.025	0.041	0.044	0.0363	781.08	613.46	0.14	0.29	0.29	32.5	6.58E-01	3.11E-03
1000	4450	250	58.1	0.021	0.034	0.037	0.0363	781.08	613.46	0.36	0.72	0.72	35.0	5.84E-01	6.88E-03
1000	4450	350	58.1	0.021	0.034	0.037	0.0363	781.08	613.46	0.51	1.01	1.01	37.3	5.24E-01	8.65E-03
1000	4450	450	53.1	0.019	0.031	0.034	0.0363	781.08	613.46	0.65	1.30	1.30	38.8	4.87E-01	1.03E-02
1000	4450	550	55.6	0.020	0.033	0.036	0.0363	781.08	613.46	0.80	1.59	1.59	40.8	4.42E-01	1.15E-02
1000	4450	650	58.1	0.021	0.034	0.037	0.0363	781.08	613.46	0.94	1.88	1.88	43.0	3.97E-01	1.22E-02

Table F-7, Lubrication Analysis Results, Catenex 79, 25° Skew.

LUBRICATION NUMBER ANALYSIS

			SI units							
roller length	0.01	m	poissons ratio	0.267						
roller diameter	0.005	m	Youngs Modulus	2.00E+11	N/m <sup>2</sup>					
skew angle	35	°	Equivalent Radius	0.0025	m					
PCD	0.0701	m	Equivalent E	2.15E+11	N/m <sup>2</sup>					
number of rollers	10		Average surface roughness (R <sub>a</sub> )	1.00E-07	m					

SI units

$$\mu = \frac{\text{Running Torque}}{\text{Preload} \cdot \left(\frac{PCD}{2}\right) \cdot \text{No Brake Stages}}$$

$$\mu_1 = \frac{\text{Running Torque}}{\text{Preload} \cdot \left[ \left(\frac{PCD}{2} \cdot \sin \phi\right) + \left(\frac{2}{3} \cdot \text{Roller Length}\right) \right] \cdot \text{No Brake Stages}}$$

$$\mu_2 = \frac{\text{Running Torque}}{\text{Preload} \cdot \left[ \left(\frac{PCD}{2} \cdot \sin \phi\right) + \left(\frac{1}{2} \cdot \text{Roller Length}\right) \right] \cdot \text{No Brake Stages}}$$

preload (lb)	preload (N)	Rotational speed (rpm)	Running Torque (lbin)	$\mu$	$\mu_1$	$\mu_2$	contact width b (mm)	Pmax (N/mm2)	Pmean (N/mm2)	entraining velocity (m/s)	sum velocity (m/s)	siding velocity (m/s)	average lubricant temp	dynamic viscosity (kg/ms)	lubrication number
200	890	50	13.7	0.025	0.032	0.035	0.0162	349.31	274.35	0.07	0.13	0.13	25.7	9.14E-01	4.36E-03
200	890	75	13.2	0.024	0.031	0.033	0.0162	349.31	274.35	0.10	0.20	0.20	26.0	9.01E-01	6.44E-03
200	890	100	14.2	0.026	0.034	0.036	0.0162	349.31	274.35	0.13	0.26	0.26	26.6	8.75E-01	8.35E-03
200	890	250	12.1	0.022	0.029	0.031	0.0162	349.31	274.35	0.33	0.65	0.65	27.2	8.50E-01	2.03E-02
200	890	350	11.0	0.020	0.026	0.028	0.0162	349.31	274.35	0.46	0.92	0.92	28.2	8.10E-01	2.70E-02
200	890	450	14.3	0.026	0.034	0.036	0.0162	349.31	274.35	0.59	1.18	1.18	28.8	7.87E-01	3.38E-02
200	890	550	16.1	0.029	0.038	0.041	0.0162	349.31	274.35	0.72	1.44	1.44	29.9	7.46E-01	3.92E-02
200	890	650	15.4	0.028	0.037	0.039	0.0162	349.31	274.35	0.85	1.70	1.70	32.3	6.65E-01	4.12E-02
400	1780	50	35.1	0.032	0.042	0.044	0.0229	494.00	387.98	0.07	0.13	0.13	24.4	9.75E-01	3.29E-03
400	1780	75	35.7	0.032	0.042	0.045	0.0229	494.00	387.98	0.10	0.20	0.20	25.4	9.27E-01	4.69E-03
400	1780	100	35.7	0.032	0.042	0.045	0.0229	494.00	387.98	0.13	0.26	0.26	25.5	9.22E-01	6.22E-03
400	1780	250	30.0	0.027	0.036	0.038	0.0229	494.00	387.98	0.33	0.65	0.65	25.6	9.20E-01	1.55E-02
400	1780	350	30.0	0.027	0.036	0.038	0.0229	494.00	387.98	0.46	0.92	0.92	27.0	8.58E-01	2.03E-02
400	1780	450	33.7	0.031	0.040	0.043	0.0229	494.00	387.98	0.59	1.18	1.18	28.2	8.10E-01	2.46E-02
400	1780	550	32.5	0.029	0.038	0.041	0.0229	494.00	387.98	0.72	1.44	1.44	29.4	7.64E-01	2.84E-02
400	1780	650	25.0	0.023	0.030	0.032	0.0229	494.00	387.98	0.85	1.70	1.70	33.0	6.43E-01	2.82E-02
600	2670	50	59.0	0.036	0.047	0.050	0.0281	605.02	475.18	0.07	0.13	0.13	24.3	9.80E-01	2.70E-03
600	2670	75	60.2	0.036	0.048	0.051	0.0281	605.02	475.18	0.10	0.20	0.20	26.3	8.90E-01	3.68E-03
600	2670	100	59.0	0.036	0.047	0.050	0.0281	605.02	475.18	0.13	0.26	0.26	28.0	8.18E-01	4.51E-03
600	2670	250	47.0	0.028	0.037	0.040	0.0281	605.02	475.18	0.33	0.65	0.65	30.1	7.39E-01	1.02E-02
600	2670	350	45.8	0.028	0.036	0.039	0.0281	605.02	475.18	0.46	0.92	0.92	32.5	6.58E-01	1.27E-02
600	2670	450	47.0	0.028	0.037	0.040	0.0281	605.02	475.18	0.59	1.18	1.18	34.0	6.12E-01	1.52E-02
600	2670	550	43.3	0.026	0.034	0.036	0.0281	605.02	475.18	0.72	1.44	1.44	36.0	5.56E-01	1.69E-02
600	2670	650	42.0	0.025	0.033	0.035	0.0281	605.02	475.18	0.85	1.70	1.70	39.8	4.63E-01	1.66E-02
800	3560	50	81.0	0.037	0.048	0.051	0.0324	698.62	548.69	0.07	0.13	0.13	31.9	6.78E-01	1.62E-03
800	3560	75	79.0	0.036	0.047	0.050	0.0324	698.62	548.69	0.10	0.20	0.20	33.0	6.43E-01	2.30E-03
800	3560	100	77.0	0.035	0.046	0.049	0.0324	698.62	548.69	0.13	0.26	0.26	35.0	5.84E-01	2.78E-03
800	3560	250	59.9	0.027	0.036	0.038	0.0324	698.62	548.69	0.33	0.65	0.65	37.0	5.30E-01	6.32E-03
800	3560	350	59.9	0.027	0.036	0.038	0.0324	698.62	548.69	0.46	0.92	0.92	39.0	4.81E-01	8.04E-03
800	3560	450	55.9	0.025	0.033	0.035	0.0324	698.62	548.69	0.59	1.18	1.18	41.5	4.27E-01	9.16E-03
800	3560	550	57.9	0.026	0.034	0.037	0.0324	698.62	548.69	0.72	1.44	1.44	43.4	3.89E-01	1.02E-02
800	3560	650	50.0	0.023	0.030	0.032	0.0324	698.62	548.69	0.85	1.70	1.70	48.4	3.06E-01	9.49E-03
1000	4450	50	115.8	0.042	0.055	0.059	0.0363	781.08	613.46	0.07	0.13	0.13	18.5	1.29E+00	2.76E-03
1000	4450	75	113.8	0.041	0.054	0.058	0.0363	781.08	613.46	0.10	0.20	0.20	21.8	1.11E+00	3.54E-03
1000	4450	100	109.8	0.040	0.052	0.056	0.0363	781.08	613.46	0.13	0.26	0.26	25.5	9.22E-01	3.94E-03
1000	4450	250	93.1	0.034	0.044	0.047	0.0363	781.08	613.46	0.33	0.65	0.65	28.5	7.98E-01	8.52E-03
1000	4450	350	89.1	0.032	0.042	0.045	0.0363	781.08	613.46	0.46	0.92	0.92	31.5	6.91E-01	1.03E-02
1000	4450	450	87.1	0.032	0.041	0.044	0.0363	781.08	613.46	0.59	1.18	1.18	34.5	5.98E-01	1.15E-02
1000	4450	550	83.1	0.030	0.039	0.042	0.0363	781.08	613.46	0.72	1.44	1.44	37.3	5.22E-01	1.23E-02
1000	4450	650	79.2	0.029	0.038	0.040	0.0363	781.08	613.46	0.85	1.70	1.70	44.5	3.69E-01	1.02E-02

Table F-8, Lubrication Analysis Results, Catenex 79, 35° Skew.

LUBRICATION NUMBER ANALYSIS

		SI units		SI units
roller length	0.01	m	poissons ratio	0.287
roller diameter	0.005	m	Youngs Modulus	2.00E+11 N/m <sup>2</sup>
skew angle	45	°	Equivalent Radius	0.0025 m
PCD	0.0701	m	Equivalent E	2.15E+11 N/m <sup>2</sup>
number of rollers	10		Average surface roughness (R <sub>a</sub> )	1.00E-07 m

$$\mu = \frac{\text{Running Torque}}{\text{Preload} \cdot \left(\frac{PCD}{2}\right) \cdot \text{No Brake Stages}}$$

$$\mu_1 = \frac{\text{Running Torque}}{\text{Preload} \cdot \left[\left(\frac{PCD}{2} \cdot \sin \phi\right) + \left(\frac{2}{3} \cdot \text{Roller Length}\right)\right] \cdot \text{No Brake Stages}}$$

$$\mu_2 = \frac{\text{Running Torque}}{\text{Preload} \cdot \left[\left(\frac{PCD}{2} \cdot \sin \phi\right) + \left(\frac{1}{2} \cdot \text{Roller Length}\right)\right] \cdot \text{No Brake Stages}}$$

preload (lb)	preload (N)	Rotational speed (rpm)	Running Torque (lbin)	μ	μ <sub>1</sub>	μ <sub>2</sub>	contact width b (mm)	Pmax (N/mm2)	Pmean (N/mm2)	entraining velocity (m/s)	sum velocity (m/s)	sliding velocity (m/s)	average lubricant temp	dynamic viscosity (kg/ms)	lubrication number
200	890	50	14.7	0.027	0.030	0.031	0.0162	349.31	274.35	0.06	0.12	0.12	26.0	9.01E-01	3.89E-03
200	890	75	17.2	0.031	0.035	0.037	0.0162	349.31	274.35	0.09	0.18	0.18	26.4	8.83E-01	5.73E-03
200	890	100	18.2	0.033	0.037	0.039	0.0162	349.31	274.35	0.12	0.24	0.24	27.0	8.58E-01	7.42E-03
200	890	250	13.0	0.023	0.026	0.028	0.0162	349.31	274.35	0.30	0.59	0.59	27.6	8.34E-01	1.80E-02
200	890	350	15.3	0.028	0.031	0.033	0.0162	349.31	274.35	0.42	0.83	0.83	28.4	8.02E-01	2.43E-02
200	890	450	13.6	0.025	0.027	0.029	0.0162	349.31	274.35	0.53	1.07	1.07	29.3	7.68E-01	2.99E-02
200	890	550	16.5	0.030	0.033	0.035	0.0162	349.31	274.35	0.65	1.31	1.31	30.3	7.32E-01	3.48E-02
200	890	650	16.3	0.029	0.033	0.035	0.0162	349.31	274.35	0.77	1.54	1.54	33.0	6.43E-01	3.61E-02
400	1780	50	46.9	0.043	0.047	0.050	0.0229	494.00	387.98	0.06	0.12	0.12	24.1	9.87E-01	3.02E-03
400	1780	75	49.4	0.045	0.050	0.053	0.0229	494.00	387.98	0.09	0.18	0.18	25.8	9.11E-01	4.18E-03
400	1780	100	48.2	0.044	0.049	0.051	0.0229	494.00	387.98	0.12	0.24	0.24	27.8	8.28E-01	5.06E-03
400	1780	250	33.7	0.031	0.034	0.036	0.0229	494.00	387.98	0.30	0.59	0.59	29.5	7.61E-01	1.16E-02
400	1780	350	33.7	0.031	0.034	0.036	0.0229	494.00	387.98	0.42	0.83	0.83	30.8	7.16E-01	1.53E-02
400	1780	450	33.7	0.031	0.034	0.036	0.0229	494.00	387.98	0.53	1.07	1.07	32.8	6.50E-01	1.79E-02
400	1780	550	36.2	0.033	0.037	0.039	0.0229	494.00	387.98	0.65	1.31	1.31	33.8	6.20E-01	2.08E-02
400	1780	650	33.7	0.031	0.034	0.036	0.0229	494.00	387.98	0.77	1.54	1.54	36.0	5.56E-01	2.21E-02
600	2670	50	80.3	0.048	0.054	0.057	0.0281	605.02	475.18	0.06	0.12	0.12	32.8	6.50E-01	1.62E-03
600	2670	75	76.3	0.046	0.051	0.054	0.0281	605.02	475.18	0.09	0.18	0.18	34.5	5.98E-01	2.24E-03
600	2670	100	70.3	0.042	0.047	0.050	0.0281	605.02	475.18	0.12	0.24	0.24	25.8	9.11E-01	4.55E-03
600	2670	250	54.5	0.033	0.037	0.039	0.0281	605.02	475.18	0.30	0.59	0.59	36.5	5.43E-01	6.78E-03
600	2670	350	52.5	0.032	0.035	0.037	0.0281	605.02	475.18	0.42	0.83	0.83	38.4	4.95E-01	8.66E-03
600	2670	450	52.5	0.032	0.035	0.037	0.0281	605.02	475.18	0.53	1.07	1.07	40.3	4.53E-01	1.02E-02
600	2670	550	56.5	0.034	0.038	0.040	0.0281	605.02	475.18	0.65	1.31	1.31	41.8	4.22E-01	1.16E-02
600	2670	650	52.5	0.032	0.035	0.037	0.0281	605.02	475.18	0.77	1.54	1.54	44.5	3.70E-01	1.20E-02
800	3560	50	111.1	0.050	0.056	0.059	0.0324	698.62	548.69	0.06	0.12	0.12	32.5	6.58E-01	1.42E-03
800	3560	75	107.1	0.048	0.054	0.057	0.0324	698.62	548.69	0.09	0.18	0.18	35.0	5.84E-01	1.89E-03
800	3560	100	105.1	0.048	0.053	0.056	0.0324	698.62	548.69	0.12	0.24	0.24	38.0	5.05E-01	2.18E-03
800	3560	250	81.9	0.037	0.041	0.044	0.0324	698.62	548.69	0.30	0.59	0.59	40.5	4.48E-01	4.84E-03
800	3560	350	75.9	0.034	0.038	0.040	0.0324	698.62	548.69	0.42	0.83	0.83	43.5	3.87E-01	5.86E-03
800	3560	450	75.9	0.034	0.038	0.040	0.0324	698.62	548.69	0.53	1.07	1.07	45.5	3.52E-01	6.85E-03
800	3560	550	73.9	0.033	0.037	0.039	0.0324	698.62	548.69	0.65	1.31	1.31	47.5	3.19E-01	7.60E-03
800	3560	650	69.9	0.032	0.035	0.037	0.0324	698.62	548.69	0.77	1.54	1.54	51.5	2.63E-01	7.41E-03
1000	4450	50	204.0	0.074	0.082	0.087	0.0363	781.08	613.46	0.06	0.12	0.12	20.0	1.20E+00	2.33E-03
1000	4450	75	191.4	0.069	0.077	0.082	0.0363	781.08	613.46	0.09	0.18	0.18	23.7	1.01E+00	2.92E-03
1000	4450	100	143.9	0.052	0.058	0.061	0.0363	781.08	613.46	0.12	0.24	0.24	26.4	8.83E-01	3.42E-03
1000	4450	250	123.2	0.045	0.050	0.053	0.0363	781.08	613.46	0.30	0.59	0.59	30.7	7.18E-01	6.94E-03
1000	4450	350	113.2	0.041	0.046	0.048	0.0363	781.08	613.46	0.42	0.83	0.83	35.5	5.70E-01	7.71E-03
1000	4450	450	110.7	0.040	0.045	0.047	0.0363	781.08	613.46	0.53	1.07	1.07	38.0	5.05E-01	8.79E-03
1000	4450	550	105.7	0.038	0.043	0.045	0.0363	781.08	613.46	0.65	1.31	1.31	41.0	4.37E-01	9.30E-03
1000	4450	650	103.2	0.037	0.042	0.044	0.0363	781.08	613.46	0.77	1.54	1.54	50.0	2.83E-01	7.12E-03

Table F-9, Lubrication Analysis Results, Catenex 79, 45° Skew.

LUBRICATION NUMBER ANALYSIS

		SI units		SI units
roller length (m)	0.01	m	poissons ratio	0.267
roller diameter (m)	0.005	m	Youngs Modulus (N/mm <sup>2</sup> )	2.00E+11
skew angle	55	°	Equivalent Radius (m)	0.0025
roller PCD (m)	0.0701	m	Equivalent E (N/mm <sup>2</sup> )	2.15E+11
number of rollers	10		Average surface roughness (R <sub>a</sub> )	1.00E-07

$$\mu = \frac{\text{Running Torque}}{\text{Preload} \cdot \left( \frac{PCD}{2} \right) \cdot \text{No Brake Stages}}$$

$$\mu_1 = \frac{\text{Running Torque}}{\text{Preload} \cdot \left[ \left( \frac{PCD}{2} \cdot \sin \phi \right) + \left( \frac{2}{3} \cdot \text{Roller Length} \right) \right] \cdot \text{No Brake Stages}}$$

$$\mu_2 = \frac{\text{Running Torque}}{\text{Preload} \cdot \left[ \left( \frac{PCD}{2} \cdot \sin \phi \right) + \left( \frac{1}{2} \cdot \text{Roller Length} \right) \right] \cdot \text{No Brake Stages}}$$

preload (lb)	preload (N)	Rotational speed (rpm)	Running Torque (lbin)	μ	μ <sub>1</sub>	μ <sub>2</sub>	contact width b (mm)	Pmax (N/mm2)	Pmean (N/mm2)	entraining velocity (m/s)	sum velocity (m/s)	sliding velocity (m/s)	average lubricant temp	dynamic viscosity (kg/ms)	lubrication number
200	890	50	19.7	0.036	0.035	0.037	0.0162	349.31	274.35	0.05	0.11	0.11	20.9	1.15E+00	4.55E-03
200	890	75	20.7	0.037	0.037	0.039	0.0162	349.31	274.35	0.08	0.16	0.16	21.6	1.11E+00	6.60E-03
200	890	100	22.7	0.041	0.041	0.043	0.0162	349.31	274.35	0.11	0.22	0.22	22.7	1.06E+00	8.34E-03
200	890	250	13.1	0.024	0.023	0.025	0.0162	349.31	274.35	0.27	0.54	0.54	23.5	1.02E+00	2.01E-02
200	890	350	12.1	0.022	0.022	0.023	0.0162	349.31	274.35	0.38	0.76	0.76	24.8	9.56E-01	2.64E-02
200	890	450	13.6	0.025	0.024	0.026	0.0162	349.31	274.35	0.49	0.98	0.98	26.5	8.79E-01	3.12E-02
200	890	550	14.1	0.026	0.025	0.027	0.0162	349.31	274.35	0.60	1.19	1.19	27.8	8.26E-01	3.59E-02
200	890	650	13.1	0.024	0.023	0.025	0.0162	349.31	274.35	0.70	1.41	1.41	34.0	6.12E-01	3.14E-02
400	1780	50	49.5	0.045	0.044	0.047	0.0229	494.00	387.98	0.05	0.11	0.11	27.6	8.34E-01	2.33E-03
400	1780	75	50.7	0.046	0.045	0.048	0.0229	494.00	387.98	0.08	0.16	0.16	29.0	7.79E-01	3.26E-03
400	1780	100	51.9	0.047	0.047	0.049	0.0229	494.00	387.98	0.11	0.22	0.22	31.0	7.08E-01	3.95E-03
400	1780	250	37.5	0.034	0.034	0.035	0.0229	494.00	387.98	0.27	0.54	0.54	32.5	6.58E-01	9.19E-03
400	1780	350	38.7	0.035	0.035	0.036	0.0229	494.00	387.98	0.38	0.76	0.76	35.0	5.84E-01	1.14E-02
400	1780	450	38.2	0.033	0.033	0.034	0.0229	494.00	387.98	0.49	0.98	0.98	37.0	5.30E-01	1.33E-02
400	1780	550	38.7	0.035	0.035	0.036	0.0229	494.00	387.98	0.60	1.19	1.19	35.8	5.63E-01	1.73E-02
400	1780	650	37.5	0.034	0.034	0.035	0.0229	494.00	387.98	0.70	1.41	1.41	37.8	5.11E-01	1.86E-02
600	2670	50	91.5	0.055	0.055	0.057	0.0281	605.02	475.18	0.05	0.11	0.11	33.4	6.30E-01	1.44E-03
600	2670	75	89.0	0.054	0.053	0.056	0.0281	605.02	475.18	0.08	0.16	0.16	35.5	5.70E-01	1.95E-03
600	2670	100	85.3	0.052	0.051	0.054	0.0281	605.02	475.18	0.11	0.22	0.22	38.5	4.93E-01	2.25E-03
600	2670	250	66.6	0.040	0.040	0.042	0.0281	605.02	475.18	0.27	0.54	0.54	41.0	4.37E-01	4.98E-03
600	2670	350	64.8	0.039	0.039	0.041	0.0281	605.02	475.18	0.38	0.76	0.76	44.0	3.78E-01	6.04E-03
600	2670	450	62.1	0.037	0.037	0.039	0.0281	605.02	475.18	0.49	0.98	0.98	45.0	3.60E-01	7.40E-03
600	2670	550	59.6	0.036	0.036	0.037	0.0281	605.02	475.18	0.60	1.19	1.19	47.0	3.27E-01	8.21E-03
600	2670	650	58.3	0.035	0.035	0.037	0.0281	605.02	475.18	0.70	1.41	1.41	48.2	3.09E-01	9.16E-03
800	3560	50	141.1	0.064	0.063	0.066	0.0324	698.62	548.69	0.05	0.11	0.11	20.0	1.20E+00	2.37E-03
800	3560	75	139.1	0.063	0.062	0.066	0.0324	698.62	548.69	0.08	0.16	0.16	23.4	1.02E+00	3.02E-03
800	3560	100	133.1	0.060	0.060	0.063	0.0324	698.62	548.69	0.11	0.22	0.22	28.0	8.18E-01	3.23E-03
800	3560	250	108.0	0.049	0.048	0.051	0.0324	698.62	548.69	0.27	0.54	0.54	32.0	6.74E-01	6.66E-03
800	3560	350	104.0	0.047	0.047	0.049	0.0324	698.62	548.69	0.38	0.76	0.76	40.0	4.59E-01	6.34E-03
800	3560	450	98.0	0.044	0.044	0.046	0.0324	698.62	548.69	0.49	0.98	0.98	42.5	4.07E-01	7.23E-03
800	3560	550	94.0	0.043	0.042	0.044	0.0324	698.62	548.69	0.60	1.19	1.19	40.0	4.59E-01	9.96E-03
800	3560	650	98.0	0.044	0.044	0.046	0.0324	698.62	548.69	0.70	1.41	1.41	38.5	4.93E-01	1.27E-02
1000	4450	50	168.9	0.061	0.061	0.064	0.0363	781.08	613.46	0.05	0.11	0.11	33.0	6.43E-01	1.14E-03
1000	4450	75	168.9	0.061	0.061	0.064	0.0363	781.08	613.46	0.08	0.16	0.16	37.0	5.30E-01	1.40E-03
1000	4450	100	161.4	0.058	0.058	0.061	0.0363	781.08	613.46	0.11	0.22	0.22	41.1	4.36E-01	1.54E-03
1000	4450	250	135.7	0.049	0.049	0.051	0.0363	781.08	613.46	0.27	0.54	0.54	42.0	4.16E-01	3.68E-03
1000	4450	350	128.2	0.046	0.046	0.048	0.0363	781.08	613.46	0.38	0.76	0.76	45.0	3.60E-01	4.46E-03
1000	4450	450	125.7	0.046	0.045	0.047	0.0363	781.08	613.46	0.49	0.98	0.98	46.0	3.43E-01	5.46E-03
1000	4450	550	123.2	0.045	0.044	0.046	0.0363	781.08	613.46	0.60	1.19	1.19	47.0	3.27E-01	6.36E-03
1000	4450	650	115.7	0.042	0.042	0.044	0.0363	781.08	613.46	0.70	1.41	1.41	50.0	2.83E-01	6.50E-03

Table F-10, Lubrication Analysis Results, Catenex 79, 55° Skew.

## ELASTO HYDRODYNAMIC FILM THICKNESS CALCULATIONS

equivalent radius =	0.0025	m	number rollers =	10	
Youngs modulus =	2.00E+11	N/m <sup>2</sup>	roller length =	10	mm
Poisson ratio =	0.267		Surface Roughness (R <sub>a</sub> ) =	0.1	μm
			skew angle =	15	°
viscosity index =	1.52E-08	m <sup>2</sup> /N			
Equivalent Modulus =	2.15E+11	N/m <sup>2</sup>			

preload (lbs)	preload (N)	load/length (N/m)	speed rpm	roller speed (rad/s)	b (mm)	Pmax (N/mm <sup>2</sup> )	Pmean (N/mm <sup>2</sup> )	ent vel (m/s)	dynamic viscosity (kg/ms)	h min (μm)	h/Ra
200	890	8900	50	74.4	0.016	349.31	274.35	0.080	2.35E-02	0.021	0.2
200	890	8900	75	111.5	0.016	349.31	274.35	0.120	2.32E-02	0.028	0.3
200	890	8900	100	148.7	0.016	349.31	274.35	0.160	2.29E-02	0.033	0.3
200	890	8900	250	371.8	0.016	349.31	274.35	0.399	2.23E-02	0.062	0.6
200	890	8900	350	520.5	0.016	349.31	274.35	0.559	2.19E-02	0.078	0.8
200	890	8900	450	669.2	0.016	349.31	274.35	0.719	2.16E-02	0.092	0.9
200	890	8900	550	817.9	0.016	349.31	274.35	0.879	2.12E-02	0.104	1.0
200	890	8900	650	966.6	0.016	349.31	274.35	1.039	2.05E-02	0.115	1.1
400	1780	17800	50	74.4	0.023	494.00	387.98	0.080	2.35E-02	0.019	0.2
400	1780	17800	75	111.5	0.023	494.00	387.98	0.120	2.31E-02	0.025	0.3
400	1780	17800	100	148.7	0.023	494.00	387.98	0.160	2.24E-02	0.030	0.3
400	1780	17800	250	371.8	0.023	494.00	387.98	0.399	2.08E-02	0.054	0.5
400	1780	17800	350	520.5	0.023	494.00	387.98	0.559	2.01E-02	0.067	0.7
400	1780	17800	450	669.2	0.023	494.00	387.98	0.719	1.95E-02	0.078	0.8
400	1780	17800	550	817.9	0.023	494.00	387.98	0.879	1.91E-02	0.089	0.9
400	1780	17800	650	966.6	0.023	494.00	387.98	1.039	1.80E-02	0.096	1.0
600	2670	26700	50	74.4	0.028	605.02	475.18	0.080	2.68E-02	0.020	0.2
600	2670	26700	75	111.5	0.028	605.02	475.18	0.120	2.58E-02	0.026	0.3
600	2670	26700	100	148.7	0.028	605.02	475.18	0.160	2.49E-02	0.031	0.3
600	2670	26700	250	371.8	0.028	605.02	475.18	0.399	2.29E-02	0.055	0.5
600	2670	26700	350	520.5	0.028	605.02	475.18	0.559	2.22E-02	0.068	0.7
600	2670	26700	450	669.2	0.028	605.02	475.18	0.719	2.11E-02	0.078	0.8
600	2670	26700	550	817.9	0.028	605.02	475.18	0.879	2.05E-02	0.088	0.9
600	2670	26700	650	966.6	0.028	605.02	475.18	1.039	2.01E-02	0.098	1.0
800	3560	35600	50	74.4	0.032	698.62	548.69	0.080	2.22E-02	0.017	0.2
800	3560	35600	75	111.5	0.032	698.62	548.69	0.120	2.11E-02	0.022	0.2
800	3560	35600	100	148.7	0.032	698.62	548.69	0.160	2.01E-02	0.025	0.3
800	3560	35600	250	371.8	0.032	698.62	548.69	0.399	1.88E-02	0.046	0.5
800	3560	35600	350	520.5	0.032	698.62	548.69	0.559	1.76E-02	0.056	0.6
800	3560	35600	450	669.2	0.032	698.62	548.69	0.719	1.69E-02	0.064	0.6
800	3560	35600	550	817.9	0.032	698.62	548.69	0.879	1.62E-02	0.072	0.7
800	3560	35600	650	966.6	0.032	698.62	548.69	1.039	1.64E-02	0.082	0.8
1000	4450	44500	50	74.4	0.036	781.08	613.46	0.080	2.29E-02	0.017	0.2
1000	4450	44500	75	111.5	0.036	781.08	613.46	0.120	2.15E-02	0.021	0.2
1000	4450	44500	100	148.7	0.036	781.08	613.46	0.160	2.03E-02	0.025	0.2
1000	4450	44500	250	371.8	0.036	781.08	613.46	0.399	1.78E-02	0.043	0.4
1000	4450	44500	350	520.5	0.036	781.08	613.46	0.559	1.69E-02	0.053	0.5
1000	4450	44500	450	669.2	0.036	781.08	613.46	0.719	1.60E-02	0.060	0.6
1000	4450	44500	550	817.9	0.036	781.08	613.46	0.879	1.56E-02	0.068	0.7
1000	4450	44500	650	966.6	0.036	781.08	613.46	1.039	1.43E-02	0.072	0.7

Table F-11, Elastohydrodynamic Film Thickness Calculations, Brayco 795, 15° Skew.

## ELASTO HYDRODYNAMIC FILM THICKNESS CALCULATIONS

equivalent radius =	0.0025	m	number rollers =	10	
Youngs modulus =	2.00E+11	N/m <sup>2</sup>	roller length =	10	mm
Poisson ratio =	0.267		Surface Roughness (R <sub>a</sub> ) =	0.1	μm
			skew angle =	25	°
viscosity index =	1.52E-08	m <sup>2</sup> /N			
Equivalent Modulus =	2.1535E+11	N/m <sup>2</sup>			

preload (lbs)	preload (N)	load/length (N/m)	speed rpm	roller speed (rad/s)	b (mm)	Pmax (N/mm <sup>2</sup> )	Pmean (N/mm <sup>2</sup> )	ent vel (m/s)	dynamic viscosity (kg/ms)	h min (μm)	h/Ra
200	890	8900	50	74.35	0.0162	349.31	274.35	0.072	2.79E-02	0.0220	0.2
200	890	8900	75	111.53	0.0162	349.31	274.35	0.109	2.72E-02	0.0288	0.3
200	890	8900	100	148.70	0.0162	349.31	274.35	0.145	2.64E-02	0.0344	0.3
200	890	8900	250	371.76	0.0162	349.31	274.35	0.362	2.54E-02	0.0636	0.6
200	890	8900	350	520.46	0.0162	349.31	274.35	0.507	2.45E-02	0.0786	0.8
200	890	8900	450	669.16	0.0162	349.31	274.35	0.651	2.38E-02	0.0916	0.9
200	890	8900	550	817.86	0.0162	349.31	274.35	0.796	2.31E-02	0.1034	1.0
200	890	8900	650	966.56	0.0162	349.31	274.35	0.941	2.22E-02	0.1131	1.1
400	1780	17800	50	74.35	0.0229	494.00	387.98	0.072	2.13E-02	0.0167	0.2
400	1780	17800	75	111.53	0.0229	494.00	387.98	0.109	2.07E-02	0.0217	0.2
400	1780	17800	100	148.70	0.0229	494.00	387.98	0.145	2.01E-02	0.0260	0.3
400	1780	17800	250	371.76	0.0229	494.00	387.98	0.362	1.88E-02	0.0471	0.5
400	1780	17800	350	520.46	0.0229	494.00	387.98	0.507	1.81E-02	0.0579	0.6
400	1780	17800	450	669.16	0.0229	494.00	387.98	0.651	1.73E-02	0.0672	0.7
400	1780	17800	550	817.86	0.0229	494.00	387.98	0.796	1.69E-02	0.0758	0.8
400	1780	17800	650	966.56	0.0229	494.00	387.98	0.941	1.60E-02	0.0820	0.8
600	2670	26700	50	74.35	0.0281	605.02	475.18	0.072	2.73E-02	0.0188	0.2
600	2670	26700	75	111.53	0.0281	605.02	475.18	0.109	2.58E-02	0.0240	0.2
600	2670	26700	100	148.70	0.0281	605.02	475.18	0.145	2.41E-02	0.0280	0.3
600	2670	26700	250	371.76	0.0281	605.02	475.18	0.362	2.15E-02	0.0490	0.5
600	2670	26700	350	520.46	0.0281	605.02	475.18	0.507	2.05E-02	0.0600	0.6
600	2670	26700	450	669.16	0.0281	605.02	475.18	0.651	1.92E-02	0.0685	0.7
600	2670	26700	550	817.86	0.0281	605.02	475.18	0.796	1.81E-02	0.0756	0.8
600	2670	26700	650	966.56	0.0281	605.02	475.18	0.941	1.70E-02	0.0811	0.8
800	3560	35600	50	74.35	0.0324	698.62	548.69	0.072	2.13E-02	0.0152	0.2
800	3560	35600	75	111.53	0.0324	698.62	548.69	0.109	1.98E-02	0.0192	0.2
800	3560	35600	100	148.70	0.0324	698.62	548.69	0.145	1.85E-02	0.0224	0.2
800	3560	35600	250	371.76	0.0324	698.62	548.69	0.362	1.56E-02	0.0377	0.4
800	3560	35600	350	520.46	0.0324	698.62	548.69	0.507	1.60E-02	0.0486	0.5
800	3560	35600	450	669.16	0.0324	698.62	548.69	0.651	1.62E-02	0.0585	0.6
800	3560	35600	550	817.86	0.0324	698.62	548.69	0.796	1.64E-02	0.0679	0.7
800	3560	35600	650	966.56	0.0324	698.62	548.69	0.941	1.64E-02	0.0764	0.8
1000	4450	44500	50	74.35	0.0363	781.08	613.46	0.072	2.07E-02	0.0145	0.1
1000	4450	44500	75	111.53	0.0363	781.08	613.46	0.109	1.93E-02	0.0183	0.2
1000	4450	44500	100	148.70	0.0363	781.08	613.46	0.145	2.22E-02	0.0247	0.2
1000	4450	44500	250	371.76	0.0363	781.08	613.46	0.362	1.89E-02	0.0420	0.4
1000	4450	44500	350	520.46	0.0363	781.08	613.46	0.507	1.71E-02	0.0495	0.5
1000	4450	44500	450	669.16	0.0363	781.08	613.46	0.651	1.60E-02	0.0563	0.6
1000	4450	44500	550	817.86	0.0363	781.08	613.46	0.796	1.60E-02	0.0648	0.6
1000	4450	44500	650	966.56	0.0363	781.08	613.46	0.941	1.48E-02	0.0691	0.7

Table F-12, Elastohydrodynamic Film Thickness Calculations, Brayco 795, 25° Skew.



## ELASTO HYDRODYNAMIC FILM THICKNESS CALCULATIONS

equivalent radius =	0.0025	m	number rollers =	10	
Youngs modulus =	2.00E+11	N/m <sup>2</sup>	roller length =	10mm	mm
Poisson ratio =	0.267		Surface Roughness (R <sub>a</sub> ) =	0.1	μm
viscosity index =	1.52E-08	m <sup>2</sup> /N	skew angle =	35	°
Equivalent Modulus =	2.154E+11	N/m <sup>2</sup>			

preload (lbs)	preload (N)	load/length (N/m)	speed rpm	roller speed (rad/s)	b (mm)	Pmax (N/mm <sup>2</sup> )	Pmean (N/mm <sup>2</sup> )	ent vel (m/s)	dynamic viscosity (kg/ms)	h min (μm)	h/Ra
200	890	8900	50	74.35	0.0162	349.31	274.35	0.065	2.45E-02	0.0188	0.2
200	890	8900	75	111.53	0.0162	349.31	274.35	0.098	2.42E-02	0.0247	0.2
200	890	8900	100	148.70	0.0162	349.31	274.35	0.131	2.36E-02	0.0296	0.3
200	890	8900	250	371.76	0.0162	349.31	274.35	0.327	2.23E-02	0.0542	0.5
200	890	8900	350	520.46	0.0162	349.31	274.35	0.458	2.12E-02	0.0662	0.7
200	890	8900	450	669.16	0.0162	349.31	274.35	0.589	2.07E-02	0.0776	0.8
200	890	8900	550	817.86	0.0162	349.31	274.35	0.720	2.04E-02	0.0882	0.9
200	890	8900	650	966.56	0.0162	349.31	274.35	0.851	1.90E-02	0.0946	0.9
400	1780	17800	50	74.35	0.0229	494.00	387.98	0.065	2.17E-02	0.0158	0.2
400	1780	17800	75	111.53	0.0229	494.00	387.98	0.098	2.00E-02	0.0197	0.2
400	1780	17800	100	148.70	0.0229	494.00	387.98	0.131	1.89E-02	0.0232	0.2
400	1780	17800	250	371.76	0.0229	494.00	387.98	0.327	1.71E-02	0.0411	0.4
400	1780	17800	350	520.46	0.0229	494.00	387.98	0.458	1.66E-02	0.0510	0.5
400	1780	17800	450	669.16	0.0229	494.00	387.98	0.589	1.60E-02	0.0591	0.6
400	1780	17800	550	817.86	0.0229	494.00	387.98	0.720	1.54E-02	0.0662	0.7
400	1780	17800	650	966.56	0.0229	494.00	387.98	0.851	1.60E-02	0.0765	0.8
600	2670	26700	50	74.35	0.0281	605.02	475.18	0.065	1.95E-02	0.0139	0.1
600	2670	26700	75	111.53	0.0281	605.02	475.18	0.098	1.89E-02	0.0180	0.2
600	2670	26700	100	148.70	0.0281	605.02	475.18	0.131	1.82E-02	0.0214	0.2
600	2670	26700	250	371.76	0.0281	605.02	475.18	0.327	1.69E-02	0.0386	0.4
600	2670	26700	350	520.46	0.0281	605.02	475.18	0.458	1.69E-02	0.0488	0.5
600	2670	26700	450	669.16	0.0281	605.02	475.18	0.589	1.64E-02	0.0571	0.6
600	2670	26700	550	817.86	0.0281	605.02	475.18	0.720	1.64E-02	0.0657	0.7
600	2670	26700	650	966.56	0.0281	605.02	475.18	0.851	1.60E-02	0.0725	0.7
800	3560	35600	50	74.35	0.0324	698.62	548.69	0.065	2.62E-02	0.0164	0.2
800	3560	35600	75	111.53	0.0324	698.62	548.69	0.098	2.42E-02	0.0206	0.2
800	3560	35600	100	148.70	0.0324	698.62	548.69	0.131	2.18E-02	0.0234	0.2
800	3560	35600	250	371.76	0.0324	698.62	548.69	0.327	1.89E-02	0.0403	0.4
800	3560	35600	350	520.46	0.0324	698.62	548.69	0.458	1.84E-02	0.0500	0.5
800	3560	35600	450	669.16	0.0324	698.62	548.69	0.589	1.69E-02	0.0561	0.6
800	3560	35600	550	817.86	0.0324	698.62	548.69	0.720	1.56E-02	0.0611	0.6
800	3560	35600	650	966.56	0.0324	698.62	548.69	0.851	1.64E-02	0.0712	0.7
1000	4450	44500	50	74.35	0.0363	781.08	613.46	0.065	1.97E-02	0.0131	0.1
1000	4450	44500	75	111.53	0.0363	781.08	613.46	0.098	1.81E-02	0.0163	0.2
1000	4450	44500	100	148.70	0.0363	781.08	613.46	0.131	1.66E-02	0.0188	0.2
1000	4450	44500	250	371.76	0.0363	781.08	613.46	0.327	1.60E-02	0.0348	0.3
1000	4450	44500	350	520.46	0.0363	781.08	613.46	0.458	1.60E-02	0.0440	0.4
1000	4450	44500	450	669.16	0.0363	781.08	613.46	0.589	1.56E-02	0.0515	0.5
1000	4450	44500	550	817.86	0.0363	781.08	613.46	0.720	1.52E-02	0.0583	0.6
1000	4450	44500	650	966.56	0.0363	781.08	613.46	0.851	1.64E-02	0.0691	0.7

Table F-13, Elastohydrodynamic Film Thickness Calculations, Brayco 795, 35° Skew.

## ELASTO HYDRODYNAMIC FILM THICKNESS CALCULATIONS

equivalent radius =	0.0025	m	number rollers =	10
Youngs modulus =	2.00E+11	N/m <sup>2</sup>	roller length =	10mm
Poisson ratio =	0.267		Surface Roughness (R <sub>a</sub> ) =	0.1
viscosity index =	1.52E-08	m <sup>2</sup> /N	skew angle =	45
Equivalent Modulus =	2.1535E+11	N/m <sup>2</sup>		

preload (lbs)	preload (N)	load/length (N/m)	speed rpm	roller speed (rad/s)	b (mm)	Pmax (N/mm <sup>2</sup> )	Pmean (N/mm <sup>2</sup> )	ent vel (m/s)	dynamic viscosity (kg/ms)	h min (μm)	h/Ra
200	890	8900	50	74.35	0.0162	349.31	274.35	0.059	2.54E-02	0.0179	0.2
200	890	8900	75	111.53	0.0162	349.31	274.35	0.089	2.48E-02	0.0234	0.2
200	890	8900	100	148.70	0.0162	349.31	274.35	0.119	2.40E-02	0.0280	0.3
200	890	8900	250	371.76	0.0162	349.31	274.35	0.297	2.22E-02	0.0504	0.5
200	890	8900	350	520.46	0.0162	349.31	274.35	0.415	2.14E-02	0.0621	0.6
200	890	8900	450	669.16	0.0162	349.31	274.35	0.534	2.07E-02	0.0724	0.7
200	890	8900	550	817.86	0.0162	349.31	274.35	0.653	2.01E-02	0.0816	0.8
200	890	8900	650	966.56	0.0162	349.31	274.35	0.771	1.88E-02	0.0875	0.9
400	1780	17800	50	74.35	0.0229	494.00	387.98	0.059	2.20E-02	0.0148	0.1
400	1780	17800	75	111.53	0.0229	494.00	387.98	0.089	2.05E-02	0.0187	0.2
400	1780	17800	100	148.70	0.0229	494.00	387.98	0.119	1.95E-02	0.0222	0.2
400	1780	17800	250	371.76	0.0229	494.00	387.98	0.297	2.86E-02	0.0549	0.5
400	1780	17800	350	520.46	0.0229	494.00	387.98	0.415	2.67E-02	0.0663	0.7
400	1780	17800	450	669.16	0.0229	494.00	387.98	0.534	2.67E-02	0.0790	0.8
400	1780	17800	550	817.86	0.0229	494.00	387.98	0.653	2.69E-02	0.0913	0.9
400	1780	17800	650	966.56	0.0229	494.00	387.98	0.771	2.44E-02	0.0960	1.0
600	2670	26700	50	74.35	0.0281	605.02	475.18	0.059	2.33E-02	0.0146	0.1
600	2670	26700	75	111.53	0.0281	605.02	475.18	0.089	2.18E-02	0.0186	0.2
600	2670	26700	100	148.70	0.0281	605.02	475.18	0.119	1.98E-02	0.0212	0.2
600	2670	26700	250	371.76	0.0281	605.02	475.18	0.297	1.62E-02	0.0350	0.4
600	2670	26700	350	520.46	0.0281	605.02	475.18	0.415	1.54E-02	0.0427	0.4
600	2670	26700	450	669.16	0.0281	605.02	475.18	0.534	1.56E-02	0.0514	0.5
600	2670	26700	550	817.86	0.0281	605.02	475.18	0.653	1.64E-02	0.0614	0.6
600	2670	26700	650	966.56	0.0281	605.02	475.18	0.771	1.56E-02	0.0665	0.7
800	3560	35600	50	74.35	0.0324	698.62	548.69	0.059	2.08E-02	0.0130	0.1
800	3560	35600	75	111.53	0.0324	698.62	548.69	0.089	1.88E-02	0.0161	0.2
800	3560	35600	100	148.70	0.0324	698.62	548.69	0.119	1.86E-02	0.0181	0.2
800	3560	35600	250	371.76	0.0324	698.62	548.69	0.297	1.56E-02	0.0328	0.3
800	3560	35600	350	520.46	0.0324	698.62	548.69	0.415	1.54E-02	0.0412	0.4
800	3560	35600	450	669.16	0.0324	698.62	548.69	0.534	1.48E-02	0.0479	0.5
800	3560	35600	550	817.86	0.0324	698.62	548.69	0.653	1.42E-02	0.0534	0.5
800	3560	35600	650	966.56	0.0324	698.62	548.69	0.771	1.64E-02	0.0664	0.7
1000	4450	44500	50	74.35	0.0363	781.08	613.46	0.059	1.91E-02	0.0119	0.1
1000	4450	44500	75	111.53	0.0363	781.08	613.46	0.089	1.68E-02	0.0145	0.1
1000	4450	44500	100	148.70	0.0363	781.08	613.46	0.119	1.54E-02	0.0166	0.2
1000	4450	44500	250	371.76	0.0363	781.08	613.46	0.297	1.64E-02	0.0331	0.3
1000	4450	44500	350	520.46	0.0363	781.08	613.46	0.415	1.58E-02	0.0407	0.4
1000	4450	44500	450	669.16	0.0363	781.08	613.46	0.534	1.48E-02	0.0465	0.5
1000	4450	44500	550	817.86	0.0363	781.08	613.46	0.653	1.50E-02	0.0540	0.5
1000	4450	44500	650	966.56	0.0363	781.08	613.46	0.771	1.36E-02	0.0567	0.6

Table F-14, Elastohydrodynamic Film Thickness Calculations, Brayco 795, 45° Skew.

### ELASTO HYDRODYNAMIC FILM THICKNESS CALCULATIONS

equivalent radius =	0.0025	m	number rollers =	10	
Youngs modulus =	2.00E+11	N/m <sup>2</sup>	roller length =	10	mm
Poisson ratio =	0.267		Surface Roughness (R <sub>a</sub> ) =	0.1	μm
			skew angle =	55	°
viscosity index =	1.52E-08	m <sup>2</sup> /N			
Equivalent Modulus =	2.1535E+11	N/m <sup>2</sup>			

preload (lbs)	preload (N)	load/length (N/m)	speed rpm	roller speed (rad/s)	b (mm)	Pmax (N/mm <sup>2</sup> )	Pmean (N/mm <sup>2</sup> )	ent vel (m/s)	dynamic viscosity (kg/ms)	h min (μm)	h/Ra
200	890	8900	50	74.35	0.0162	349.31	274.35	0.054	2.46E-02	0.0165	0.2
200	890	8900	75	111.53	0.0162	349.31	274.35	0.081	2.40E-02	0.0215	0.2
200	890	8900	100	148.70	0.0162	349.31	274.35	0.108	2.32E-02	0.0257	0.3
200	890	8900	250	371.76	0.0162	349.31	274.35	0.271	2.21E-02	0.0471	0.5
200	890	8900	350	520.46	0.0162	349.31	274.35	0.379	2.10E-02	0.0576	0.6
200	890	8900	450	669.16	0.0162	349.31	274.35	0.488	2.00E-02	0.0662	0.7
200	890	8900	550	817.86	0.0162	349.31	274.35	0.596	1.95E-02	0.0750	0.8
200	890	8900	650	966.56	0.0162	349.31	274.35	0.704	1.82E-02	0.0802	0.8
400	1780	17800	50	74.35	0.0229	494.00	387.98	0.054	2.22E-02	0.0140	0.1
400	1780	17800	75	111.53	0.0229	494.00	387.98	0.081	2.09E-02	0.0178	0.2
400	1780	17800	100	148.70	0.0229	494.00	387.98	0.108	1.97E-02	0.0209	0.2
400	1780	17800	250	371.76	0.0229	494.00	387.98	0.271	1.81E-02	0.0374	0.4
400	1780	17800	350	520.46	0.0229	494.00	387.98	0.379	1.70E-02	0.0453	0.5
400	1780	17800	450	669.16	0.0229	494.00	387.98	0.488	1.64E-02	0.0528	0.5
400	1780	17800	550	817.86	0.0229	494.00	387.98	0.596	1.64E-02	0.0607	0.6
400	1780	17800	650	966.56	0.0229	494.00	387.98	0.704	1.61E-02	0.0674	0.7
600	2670	26700	50	74.35	0.0281	605.02	475.18	0.054	2.91E-02	0.0161	0.2
600	2670	26700	75	111.53	0.0281	605.02	475.18	0.081	2.56E-02	0.0195	0.2
600	2670	26700	100	148.70	0.0281	605.02	475.18	0.108	2.25E-02	0.0218	0.2
600	2670	26700	250	371.76	0.0281	605.02	475.18	0.271	2.01E-02	0.0383	0.4
600	2670	26700	350	520.46	0.0281	605.02	475.18	0.379	1.84E-02	0.0454	0.5
600	2670	26700	450	669.16	0.0281	605.02	475.18	0.488	1.73E-02	0.0520	0.5
600	2670	26700	550	817.86	0.0281	605.02	475.18	0.596	1.58E-02	0.0560	0.6
600	2670	26700	650	966.56	0.0281	605.02	475.18	0.704	1.45E-02	0.0594	0.6
800	3560	35600	50	74.35	0.0324	698.62	548.69	0.054	1.98E-02	0.0118	0.1
800	3560	35600	75	111.53	0.0324	698.62	548.69	0.081	1.71E-02	0.0142	0.1
800	3560	35600	100	148.70	0.0324	698.62	548.69	0.108	1.56E-02	0.0162	0.2
800	3560	35600	250	371.76	0.0324	698.62	548.69	0.271	1.48E-02	0.0297	0.3
800	3560	35600	350	520.46	0.0324	698.62	548.69	0.379	1.43E-02	0.0368	0.4
800	3560	35600	450	669.16	0.0324	698.62	548.69	0.488	1.39E-02	0.0429	0.4
800	3560	35600	550	817.86	0.0324	698.62	548.69	0.596	1.36E-02	0.0487	0.5
800	3560	35600	650	966.56	0.0324	698.62	548.69	0.704	1.35E-02	0.0544	0.5
1000	4450	44500	50	74.35	0.0363	781.08	613.46	0.054	1.69E-02	0.0103	0.1
1000	4450	44500	75	111.53	0.0363	781.08	613.46	0.081	1.52E-02	0.0127	0.1
1000	4450	44500	100	148.70	0.0363	781.08	613.46	0.108	1.38E-02	0.0144	0.1
1000	4450	44500	250	371.76	0.0363	781.08	613.46	0.271	1.39E-02	0.0276	0.3
1000	4450	44500	350	520.46	0.0363	781.08	613.46	0.379	1.38E-02	0.0347	0.3
1000	4450	44500	450	669.16	0.0363	781.08	613.46	0.488	1.36E-02	0.0411	0.4
1000	4450	44500	550	817.86	0.0363	781.08	613.46	0.596	1.35E-02	0.0470	0.5
1000	4450	44500	650	966.56	0.0363	781.08	613.46	0.704	1.48E-02	0.0565	0.6

Table F-15, Elastohydrodynamic Film Thickness Calculations, Brayco 795, 55° Skew.

## ELASTO HYDRODYNAMIC FILM THICKNESS CALCULATIONS

equivalent radius =	0.0025	m		number rollers =	10
Youngs modulus =	2.00E+11	N/m <sup>2</sup>		roller length =	10
Poisson ratio =	0.267			Surface Roughness (R <sub>a</sub> ) =	0.1
				skew angle =	15
viscosity index =	1.52E-08	m <sup>2</sup> /N			
Equivalent Modulus =	2.1535E+11	N/m <sup>2</sup>			

preload (lbs)	preload (N)	load/length (N/m)	speed rpm	roller speed (rad/s)	b (mm)	Pmax (N/mm <sup>2</sup> )	Pmean (N/mm <sup>2</sup> )	ent vel (m/s)	dynamic viscosity (kg/ms)	h min (μm)	h/Ra
200	890	8900	50	74.35	0.0162	349.31	274.35	0.080	1.31E+00	0.3482	3.5
200	890	8900	75	111.53	0.0162	349.31	274.35	0.120	1.30E+00	0.4609	4.6
200	890	8900	100	148.70	0.0162	349.31	274.35	0.160	1.27E+00	0.5543	5.5
200	890	8900	250	371.76	0.0162	349.31	274.35	0.399	1.22E+00	1.0247	10.2
200	890	8900	350	520.46	0.0162	349.31	274.35	0.559	1.16E+00	1.2517	12.5
200	890	8900	450	669.16	0.0162	349.31	274.35	0.719	1.08E+00	1.4212	14.2
200	890	8900	550	817.86	0.0162	349.31	274.35	0.879	1.04E+00	1.5893	15.9
200	890	8900	650	966.56	0.0162	349.31	274.35	1.039	9.40E-01	1.6671	16.7
400	1780	17800	50	74.35	0.0229	494.00	387.98	0.080	1.08E+00	0.2780	2.8
400	1780	17800	75	111.53	0.0229	494.00	387.98	0.120	1.08E+00	0.3705	3.7
400	1780	17800	100	148.70	0.0229	494.00	387.98	0.160	1.06E+00	0.4479	4.5
400	1780	17800	250	371.76	0.0229	494.00	387.98	0.399	1.03E+00	0.8321	8.3
400	1780	17800	350	520.46	0.0229	494.00	387.98	0.559	9.92E-01	1.0251	10.3
400	1780	17800	450	669.16	0.0229	494.00	387.98	0.719	9.27E-01	1.1659	11.7
400	1780	17800	550	817.86	0.0229	494.00	387.98	0.879	8.83E-01	1.2972	13.0
400	1780	17800	650	966.56	0.0229	494.00	387.98	1.039	7.43E-01	1.2913	12.9
600	2670	26700	50	74.35	0.0281	605.02	475.18	0.080	1.08E+00	0.2646	2.6
600	2670	26700	75	111.53	0.0281	605.02	475.18	0.120	1.08E+00	0.3509	3.5
600	2670	26700	100	148.70	0.0281	605.02	475.18	0.160	1.05E+00	0.4213	4.2
600	2670	26700	250	371.76	0.0281	605.02	475.18	0.399	9.56E-01	0.7492	7.5
600	2670	26700	350	520.46	0.0281	605.02	475.18	0.559	9.11E-01	0.9167	9.2
600	2670	26700	450	669.16	0.0281	605.02	475.18	0.719	8.28E-01	1.0217	10.2
600	2670	26700	550	817.86	0.0281	605.02	475.18	0.879	7.79E-01	1.1272	11.3
600	2670	26700	650	966.56	0.0281	605.02	475.18	1.039	6.71E-01	1.1412	11.4
800	3560	35600	50	74.35	0.0324	698.62	548.69	0.080	9.47E-01	0.2323	2.3
800	3560	35600	75	111.53	0.0324	698.62	548.69	0.120	9.01E-01	0.2979	3.0
800	3560	35600	100	148.70	0.0324	698.62	548.69	0.160	8.48E-01	0.3493	3.5
800	3560	35600	250	371.76	0.0324	698.62	548.69	0.399	7.16E-01	0.5894	5.9
800	3560	35600	350	520.46	0.0324	698.62	548.69	0.559	6.74E-01	0.7152	7.2
800	3560	35600	450	669.16	0.0324	698.62	548.69	0.719	6.20E-01	0.8038	8.0
800	3560	35600	550	817.86	0.0324	698.62	548.69	0.879	5.56E-01	0.8574	8.6
800	3560	35600	650	966.56	0.0324	698.62	548.69	1.039	5.00E-01	0.8948	8.9
1000	4450	44500	50	74.35	0.0363	781.08	613.46	0.080	7.35E-01	0.1891	1.9
1000	4450	44500	75	111.53	0.0363	781.08	613.46	0.120	7.15E-01	0.2461	2.5
1000	4450	44500	100	148.70	0.0363	781.08	613.46	0.160	6.81E-01	0.2910	2.9
1000	4450	44500	250	371.76	0.0363	781.08	613.46	0.399	6.27E-01	0.5218	5.2
1000	4450	44500	350	520.46	0.0363	781.08	613.46	0.559	5.72E-01	0.6194	6.2
1000	4450	44500	450	669.16	0.0363	781.08	613.46	0.719	5.15E-01	0.6857	6.9
1000	4450	44500	550	817.86	0.0363	781.08	613.46	0.879	4.68E-01	0.7376	7.4
1000	4450	44500	650	966.56	0.0363	781.08	613.46	1.039	4.07E-01	0.7519	7.5

Table F-16, Elastohydrodynamic Film Thickness Calculations, Catenex 79, 15° Skew.

## ELASTO HYDRODYNAMIC FILM THICKNESS CALCULATIONS

equivalent radius =	0.0025	m	number rollers =	10	
Youngs modulus =	2.00E+11	N/m <sup>2</sup>	roller length =	10	mm
Poisson ratio =	0.287		Surface Roughness (R <sub>a</sub> ) =	0.1	μm
viscosity index =	1.52E-08	m <sup>2</sup> /N	skew angle =	25	°
Equivalent Modulus =	2.1535E+11	N/m <sup>2</sup>			

preload (lbs)	preload (N)	load/length (N/m)	speed rpm	roller speed (rad/s)	b (mm)	Pmax (N/mm <sup>2</sup> )	Pmean (N/mm <sup>2</sup> )	ent vel (m/s)	dynamic viscosity (kg/ms)	h min (μm)	h/Ra
200	890	8900	50	74.35	0.0162	349.31	274.35	0.072	1.45E+00	0.3494	3.5
200	890	8900	75	111.53	0.0162	349.31	274.35	0.109	1.40E+00	0.4540	4.5
200	890	8900	100	148.70	0.0162	349.31	274.35	0.145	1.34E+00	0.5378	5.4
200	890	8900	250	371.76	0.0162	349.31	274.35	0.362	1.26E+00	0.9791	9.8
200	890	8900	350	520.46	0.0162	349.31	274.35	0.507	1.20E+00	1.1980	12.0
200	890	8900	450	669.16	0.0162	349.31	274.35	0.651	1.15E+00	1.3811	13.8
200	890	8900	550	817.86	0.0162	349.31	274.35	0.796	1.08E+00	1.5263	15.3
200	890	8900	650	966.56	0.0162	349.31	274.35	0.941	9.45E-01	1.5610	15.6
400	1780	17800	50	74.35	0.0229	494.00	387.98	0.072	9.22E-01	0.2329	2.3
400	1780	17800	75	111.53	0.0229	494.00	387.98	0.109	9.05E-01	0.3052	3.1
400	1780	17800	100	148.70	0.0229	494.00	387.98	0.145	8.71E-01	0.3633	3.6
400	1780	17800	250	371.76	0.0229	494.00	387.98	0.362	8.28E-01	0.6660	6.7
400	1780	17800	350	520.46	0.0229	494.00	387.98	0.507	7.68E-01	0.7999	8.0
400	1780	17800	450	669.16	0.0229	494.00	387.98	0.651	7.34E-01	0.9237	9.2
400	1780	17800	550	817.86	0.0229	494.00	387.98	0.796	6.99E-01	1.0278	10.3
400	1780	17800	650	966.56	0.0229	494.00	387.98	0.941	6.43E-01	1.0890	10.9
600	2670	26700	50	74.35	0.0281	605.02	475.18	0.072	1.29E+00	0.2798	2.8
600	2670	26700	75	111.53	0.0281	605.02	475.18	0.109	1.23E+00	0.3593	3.6
600	2670	26700	100	148.70	0.0281	605.02	475.18	0.145	1.12E+00	0.4122	4.1
600	2670	26700	250	371.76	0.0281	605.02	475.18	0.362	1.03E+00	0.7379	7.4
600	2670	26700	350	520.46	0.0281	605.02	475.18	0.507	9.34E-01	0.8700	8.7
600	2670	26700	450	669.16	0.0281	605.02	475.18	0.651	8.28E-01	0.9534	9.5
600	2670	26700	550	817.86	0.0281	605.02	475.18	0.796	7.89E-01	1.0608	10.6
600	2670	26700	650	966.56	0.0281	605.02	475.18	0.941	6.65E-01	1.0578	10.6
800	3560	35600	50	74.35	0.0324	698.62	548.69	0.072	1.17E+00	0.2507	2.5
800	3560	35600	75	111.53	0.0324	698.62	548.69	0.109	1.07E+00	0.3139	3.1
800	3560	35600	100	148.70	0.0324	698.62	548.69	0.145	9.68E-01	0.3576	3.6
800	3560	35600	250	371.76	0.0324	698.62	548.69	0.362	8.69E-01	0.6295	6.3
800	3560	35600	350	520.46	0.0324	698.62	548.69	0.507	7.70E-01	0.7322	7.3
800	3560	35600	450	669.16	0.0324	698.62	548.69	0.651	6.99E-01	0.8161	8.2
800	3560	35600	550	817.86	0.0324	698.62	548.69	0.796	6.27E-01	0.8705	8.7
800	3560	35600	650	966.56	0.0324	698.62	548.69	0.941	5.63E-01	0.9070	9.1
1000	4450	44500	50	74.35	0.0363	781.08	613.46	0.072	7.59E-01	0.1803	1.8
1000	4450	44500	75	111.53	0.0363	781.08	613.46	0.109	7.08E-01	0.2281	2.3
1000	4450	44500	100	148.70	0.0363	781.08	613.46	0.145	6.58E-01	0.2652	2.7
1000	4450	44500	250	371.76	0.0363	781.08	613.46	0.362	5.84E-01	0.4629	4.6
1000	4450	44500	350	520.46	0.0363	781.08	613.46	0.507	5.24E-01	0.5430	5.4
1000	4450	44500	450	669.16	0.0363	781.08	613.46	0.651	4.87E-01	0.6155	6.2
1000	4450	44500	550	817.86	0.0363	781.08	613.46	0.796	4.42E-01	0.6621	6.6
1000	4450	44500	650	966.56	0.0363	781.08	613.46	0.941	3.97E-01	0.6899	6.9

Table F-17, Elastohydrodynamic Film Thickness Calculations, Catenex 79, 25° Skew.

## ELASTO HYDRODYNAMIC FILM THICKNESS CALCULATIONS

equivalent radius =	0.0025	m	number rollers =	10
Youngs modulus =	2.00E+11	N/m <sup>2</sup>	roller length =	10 mm
Poisson ratio =	0.267		Surface Roughness (R <sub>a</sub> ) =	0.1 μm
			skew angle =	35 °
viscosity index =	1.52E-08	m <sup>2</sup> /N		
Equivalent Modulus =	2.154E+11	N/m <sup>2</sup>		

preload (lbs)	preload (N)	load/length (N/m)	speed rpm	roller speed (rad/s)	b (mm)	Pmax (N/mm <sup>2</sup> )	Pmean (N/mm <sup>2</sup> )	ent vel (m/s)	dynamic viscosity (kg/ms)	h min (μm)	h/Ra
200	890	8900	50	74.35	0.0162	349.31	274.35	0.065	1.18E+00	0.2817	2.8
200	890	8900	75	111.53	0.0162	349.31	274.35	0.098	1.13E+00	0.3635	3.6
200	890	8900	100	148.70	0.0162	349.31	274.35	0.131	1.10E+00	0.4357	4.4
200	890	8900	250	371.76	0.0162	349.31	274.35	0.327	1.06E+00	0.8082	8.1
200	890	8900	350	520.46	0.0162	349.31	274.35	0.458	9.92E-01	0.9756	9.8
200	890	8900	450	669.16	0.0162	349.31	274.35	0.589	9.34E-01	1.1152	11.2
200	890	8900	550	817.86	0.0162	349.31	274.35	0.720	8.69E-01	1.2201	12.2
200	890	8900	650	966.56	0.0162	349.31	274.35	0.851	7.64E-01	1.2541	12.5
400	1780	17800	50	74.35	0.0229	494.00	387.98	0.065	9.75E-01	0.2257	2.3
400	1780	17800	75	111.53	0.0229	494.00	387.98	0.098	9.27E-01	0.2893	2.9
400	1780	17800	100	148.70	0.0229	494.00	387.98	0.131	9.22E-01	0.3526	3.5
400	1780	17800	250	371.76	0.0229	494.00	387.98	0.327	9.20E-01	0.6686	6.7
400	1780	17800	350	520.46	0.0229	494.00	387.98	0.458	8.58E-01	0.8057	8.1
400	1780	17800	450	669.16	0.0229	494.00	387.98	0.589	8.10E-01	0.9226	9.2
400	1780	17800	550	817.86	0.0229	494.00	387.98	0.720	7.64E-01	1.0196	10.2
400	1780	17800	650	966.56	0.0229	494.00	387.98	0.851	6.43E-01	1.0150	10.1
600	2670	26700	50	74.35	0.0281	605.02	475.18	0.065	9.80E-01	0.2148	2.1
600	2670	26700	75	111.53	0.0281	605.02	475.18	0.098	8.90E-01	0.2667	2.7
600	2670	26700	100	148.70	0.0281	605.02	475.18	0.131	8.18E-01	0.3075	3.1
600	2670	26700	250	371.76	0.0281	605.02	475.18	0.327	7.39E-01	0.5440	5.4
600	2670	26700	350	520.46	0.0281	605.02	475.18	0.458	6.58E-01	0.6349	6.3
600	2670	26700	450	669.16	0.0281	605.02	475.18	0.589	6.12E-01	0.7196	7.2
600	2670	26700	550	817.86	0.0281	605.02	475.18	0.720	5.56E-01	0.7741	7.7
600	2670	26700	650	966.56	0.0281	605.02	475.18	0.851	4.63E-01	0.7655	7.7
800	3560	35600	50	74.35	0.0324	698.62	548.69	0.065	6.78E-01	0.1598	1.6
800	3560	35600	75	111.53	0.0324	698.62	548.69	0.098	6.43E-01	0.2046	2.0
800	3560	35600	100	148.70	0.0324	698.62	548.69	0.131	5.84E-01	0.2339	2.3
800	3560	35600	250	371.76	0.0324	698.62	548.69	0.327	5.30E-01	0.4152	4.2
800	3560	35600	350	520.46	0.0324	698.62	548.69	0.458	4.81E-01	0.4911	4.9
800	3560	35600	450	669.16	0.0324	698.62	548.69	0.589	4.27E-01	0.5382	5.4
800	3560	35600	550	817.86	0.0324	698.62	548.69	0.720	3.89E-01	0.5810	5.8
800	3560	35600	650	966.56	0.0324	698.62	548.69	0.851	3.06E-01	0.5516	5.5
1000	4450	44500	50	74.35	0.0363	781.08	613.46	0.065	1.29E+00	0.2440	2.4
1000	4450	44500	75	111.53	0.0363	781.08	613.46	0.098	1.11E+00	0.2905	2.9
1000	4450	44500	100	148.70	0.0363	781.08	613.46	0.131	9.22E-01	0.3130	3.1
1000	4450	44500	250	371.76	0.0363	781.08	613.46	0.327	7.98E-01	0.5373	5.4
1000	4450	44500	350	520.46	0.0363	781.08	613.46	0.458	6.91E-01	0.6145	6.1
1000	4450	44500	450	669.16	0.0363	781.08	613.46	0.589	5.98E-01	0.6621	6.6
1000	4450	44500	550	817.86	0.0363	781.08	613.46	0.720	5.22E-01	0.6933	6.9
1000	4450	44500	650	966.56	0.0363	781.08	613.46	0.851	3.69E-01	0.6112	6.1

Table F-18, Elastohydrodynamic Film Thickness Calculations, Catenex 79, 35° Skew.

## ELASTO HYDRODYNAMIC FILM THICKNESS CALCULATIONS

equivalent radius =	0.0025	m	number rollers =	10	
Youngs modulus =	2.00E+11	N/m <sup>2</sup>	roller length =	10	mm
Poisson ratio =	0.267		Surface Roughness (R <sub>a</sub> ) =	0.1	μm
viscosity index =	1.52E-08	m <sup>2</sup> /N	skew angle =	45	°
Equivalent Modulus =	2.1535E+11	N/m <sup>2</sup>			

preload (lbs)	preload (N)	load/length (N/m)	speed rpm	roller speed (rad/s)	b (mm)	Pmax (N/mm <sup>2</sup> )	Pmean (N/mm <sup>2</sup> )	ent vel (m/s)	dynamic viscosity (kg/ms)	h min (μm)	h/Ra
200	890	8900	50	74.35	0.0162	349.31	274.35	0.059	8.81E-01	0.2147	2.1
200	890	8900	75	111.53	0.0162	349.31	274.35	0.089	8.62E-01	0.2809	2.8
200	890	8900	100	148.70	0.0162	349.31	274.35	0.119	8.30E-01	0.3344	3.3
200	890	8900	250	371.76	0.0162	349.31	274.35	0.297	7.98E-01	0.6183	6.2
200	890	8900	350	520.46	0.0162	349.31	274.35	0.415	7.68E-01	0.7616	7.6
200	890	8900	450	669.16	0.0162	349.31	274.35	0.534	7.43E-01	0.8869	8.9
200	890	8900	550	817.86	0.0162	349.31	274.35	0.653	6.74E-01	0.9541	9.5
200	890	8900	650	966.56	0.0162	349.31	274.35	0.771	6.12E-01	1.0024	10.0
400	1780	17800	50	74.35	0.0229	494.00	387.98	0.059	9.87E-01	0.2124	2.1
400	1780	17800	75	111.53	0.0229	494.00	387.98	0.089	9.11E-01	0.2669	2.7
400	1780	17800	100	148.70	0.0229	494.00	387.98	0.119	8.28E-01	0.3051	3.1
400	1780	17800	250	371.76	0.0229	494.00	387.98	0.297	7.61E-01	0.5462	5.5
400	1780	17800	350	520.46	0.0229	494.00	387.98	0.415	7.16E-01	0.6628	6.6
400	1780	17800	450	669.16	0.0229	494.00	387.98	0.534	6.50E-01	0.7387	7.4
400	1780	17800	550	817.86	0.0229	494.00	387.98	0.653	6.20E-01	0.8219	8.2
400	1780	17800	650	966.56	0.0229	494.00	387.98	0.771	5.56E-01	0.8563	8.6
600	2670	26700	50	74.35	0.0281	605.02	475.18	0.059	6.50E-01	0.1505	1.5
600	2670	26700	75	111.53	0.0281	605.02	475.18	0.089	5.98E-01	0.1885	1.9
600	2670	26700	100	148.70	0.0281	605.02	475.18	0.119	9.11E-01	0.3097	3.1
600	2670	26700	250	371.76	0.0281	605.02	475.18	0.297	5.43E-01	0.4092	4.1
600	2670	26700	350	520.46	0.0281	605.02	475.18	0.415	4.95E-01	0.4857	4.9
600	2670	26700	450	669.16	0.0281	605.02	475.18	0.534	4.53E-01	0.5441	5.4
600	2670	26700	550	817.86	0.0281	605.02	475.18	0.653	4.22E-01	0.5952	6.0
600	2670	26700	650	966.56	0.0281	605.02	475.18	0.771	3.70E-01	0.6108	6.1
800	3560	35600	50	74.35	0.0324	698.62	548.69	0.059	6.58E-01	0.1462	1.5
800	3560	35600	75	111.53	0.0324	698.62	548.69	0.089	5.84E-01	0.1785	1.8
800	3560	35600	100	148.70	0.0324	698.62	548.69	0.119	5.05E-01	0.1973	2.0
800	3560	35600	250	371.76	0.0324	698.62	548.69	0.297	4.48E-01	0.3444	3.4
800	3560	35600	350	520.46	0.0324	698.62	548.69	0.415	3.87E-01	0.3939	3.9
800	3560	35600	450	669.16	0.0324	698.62	548.69	0.534	3.52E-01	0.4390	4.4
800	3560	35600	550	817.86	0.0324	698.62	548.69	0.653	3.19E-01	0.4723	4.7
800	3560	35600	650	966.56	0.0324	698.62	548.69	0.771	2.63E-01	0.4638	4.6
1000	4450	44500	50	74.35	0.0363	781.08	613.46	0.059	1.20E+00	0.2166	2.2
1000	4450	44500	75	111.53	0.0363	781.08	613.46	0.089	1.01E+00	0.2539	2.5
1000	4450	44500	100	148.70	0.0363	781.08	613.46	0.119	8.83E-01	0.2835	2.8
1000	4450	44500	250	371.76	0.0363	781.08	613.46	0.297	7.18E-01	0.4657	4.7
1000	4450	44500	350	520.46	0.0363	781.08	613.46	0.415	5.70E-01	0.5012	5.0
1000	4450	44500	450	669.16	0.0363	781.08	613.46	0.534	5.05E-01	0.5493	5.5
1000	4450	44500	550	817.86	0.0363	781.08	613.46	0.653	4.37E-01	0.5713	5.7
1000	4450	44500	650	966.56	0.0363	781.08	613.46	0.771	2.83E-01	0.4740	4.7

Table F-19, Elastohydrodynamic Film Thickness Calculations, Catenex 79, 45° Skew.

## ELASTO HYDRODYNAMIC FILM THICKNESS CALCULATIONS

equivalent radius =	0.0025	m	number rollers =	10	
Youngs modulus =	2.00E+11	N/m <sup>2</sup>	roller length =	10	mm
Poisson ratio =	0.267		Surface Roughness (R <sub>a</sub> ) =	0.1	μm
			skew angle =	55	°
viscosity index =	1.52E-08	m <sup>2</sup> /N			
Equivalent Modulus =	2.1535E+11	N/m <sup>2</sup>			

preload (lbs)	preload (N)	load/length (N/m)	speed rpm	roller speed (rad/s)	b (mm)	Pmax (N/mm <sup>2</sup> )	Pmean (N/mm <sup>2</sup> )	ent vel (m/s)	dynamic viscosity (kg/ms)	h min (μm)	h/Ra
200	890	8900	50	74.35	0.0162	349.31	274.35	0.054	8.54E-01	0.1972	2.0
200	890	8900	75	111.53	0.0162	349.31	274.35	0.081	8.58E-01	0.2628	2.6
200	890	8900	100	148.70	0.0162	349.31	274.35	0.108	8.26E-01	0.3128	3.1
200	890	8900	250	371.76	0.0162	349.31	274.35	0.271	1.00E+00	0.6811	6.8
200	890	8900	350	520.46	0.0162	349.31	274.35	0.379	8.83E-01	0.7883	7.9
200	890	8900	450	669.16	0.0162	349.31	274.35	0.488	8.02E-01	0.8785	8.8
200	890	8900	550	817.86	0.0162	349.31	274.35	0.596	7.50E-01	0.9644	9.6
200	890	8900	650	966.56	0.0162	349.31	274.35	0.704	6.55E-01	0.9863	9.9
400	1780	17800	50	74.35	0.0229	494.00	387.98	0.054	8.34E-01	0.1772	1.8
400	1780	17800	75	111.53	0.0229	494.00	387.98	0.081	7.79E-01	0.2245	2.2
400	1780	17800	100	148.70	0.0229	494.00	387.98	0.108	7.08E-01	0.2568	2.6
400	1780	17800	250	371.76	0.0229	494.00	387.98	0.271	6.58E-01	0.4633	4.6
400	1780	17800	350	520.46	0.0229	494.00	387.98	0.379	5.84E-01	0.5389	5.4
400	1780	17800	450	669.16	0.0229	494.00	387.98	0.488	5.30E-01	0.6006	6.0
400	1780	17800	550	817.86	0.0229	494.00	387.98	0.596	5.63E-01	0.7210	7.2
400	1780	17800	650	966.56	0.0229	494.00	387.98	0.704	5.11E-01	0.7576	7.6
600	2670	26700	50	74.35	0.0281	605.02	475.18	0.054	6.30E-01	0.1382	1.4
600	2670	26700	75	111.53	0.0281	605.02	475.18	0.081	5.70E-01	0.1710	1.7
600	2670	26700	100	148.70	0.0281	605.02	475.18	0.108	4.93E-01	0.1890	1.9
600	2670	26700	250	371.76	0.0281	605.02	475.18	0.271	4.37E-01	0.3299	3.3
600	2670	26700	350	520.46	0.0281	605.02	475.18	0.379	3.78E-01	0.3774	3.8
600	2670	26700	450	669.16	0.0281	605.02	475.18	0.488	3.60E-01	0.4350	4.4
600	2670	26700	550	817.86	0.0281	605.02	475.18	0.596	3.27E-01	0.4679	4.7
600	2670	26700	650	966.56	0.0281	605.02	475.18	0.704	3.09E-01	0.5051	5.1
800	3560	35600	50	74.35	0.0324	698.62	548.69	0.054	1.20E+00	0.2092	2.1
800	3560	35600	75	111.53	0.0324	698.62	548.69	0.081	1.02E+00	0.2478	2.5
800	3560	35600	100	148.70	0.0324	698.62	548.69	0.108	8.18E-01	0.2595	2.6
800	3560	35600	250	371.76	0.0324	698.62	548.69	0.271	6.74E-01	0.4306	4.3
800	3560	35600	350	520.46	0.0324	698.62	548.69	0.379	4.59E-01	0.4160	4.2
800	3560	35600	450	669.16	0.0324	698.62	548.69	0.488	4.07E-01	0.4559	4.6
800	3560	35600	550	817.86	0.0324	698.62	548.69	0.596	4.59E-01	0.5709	5.7
800	3560	35600	650	966.56	0.0324	698.62	548.69	0.704	4.93E-01	0.6750	6.7
1000	4450	44500	50	74.35	0.0363	781.08	613.46	0.054	6.43E-01	0.1311	1.3
1000	4450	44500	75	111.53	0.0363	781.08	613.46	0.081	5.30E-01	0.1521	1.5
1000	4450	44500	100	148.70	0.0363	781.08	613.46	0.108	4.36E-01	0.1623	1.6
1000	4450	44500	250	371.76	0.0363	781.08	613.46	0.271	4.16E-01	0.2985	3.0
1000	4450	44500	350	520.46	0.0363	781.08	613.46	0.379	3.60E-01	0.3414	3.4
1000	4450	44500	450	669.16	0.0363	781.08	613.46	0.488	3.43E-01	0.3936	3.9
1000	4450	44500	550	817.86	0.0363	781.08	613.46	0.596	3.27E-01	0.4379	4.4
1000	4450	44500	650	966.56	0.0363	781.08	613.46	0.704	2.83E-01	0.4448	4.4

Table F-20, Elastohydrodynamic Film Thickness Calculations, Catenex 79, 55° Skew.



## **APPENDIX G**

### **FLUID RHEOLOGICAL DATA**

Brayco 795 is a petroleum based, low viscosity, ISO grade 10 hydraulic fluid for aircraft and industrial use. DAW obtain the fluid from Castrol Speciality Lubricants Division. Data presented in this Appendix was obtained from Castrol unless stated specifically otherwise.

Catenex 79, or HVI 650 as it is also known, is a mineral oil typical of gear lubricants. It has been used widely in experimental research work and consequently the rheological data on this lubricant is widely published. Literature sources are indicated as appropriate.

#### **Dynamic Viscosity**

Dynamic viscosity is plotted in Figure G-1 for both fluids. For Brayco 795, the measurements were conducted by RAPRA Technology Ltd using a Rheologica StressTech HR rotational rheometer, Edwards (1998).

The HVI 650 data was taken from Evans and Johnson (1986) and Schipper et al (1990).

G-2

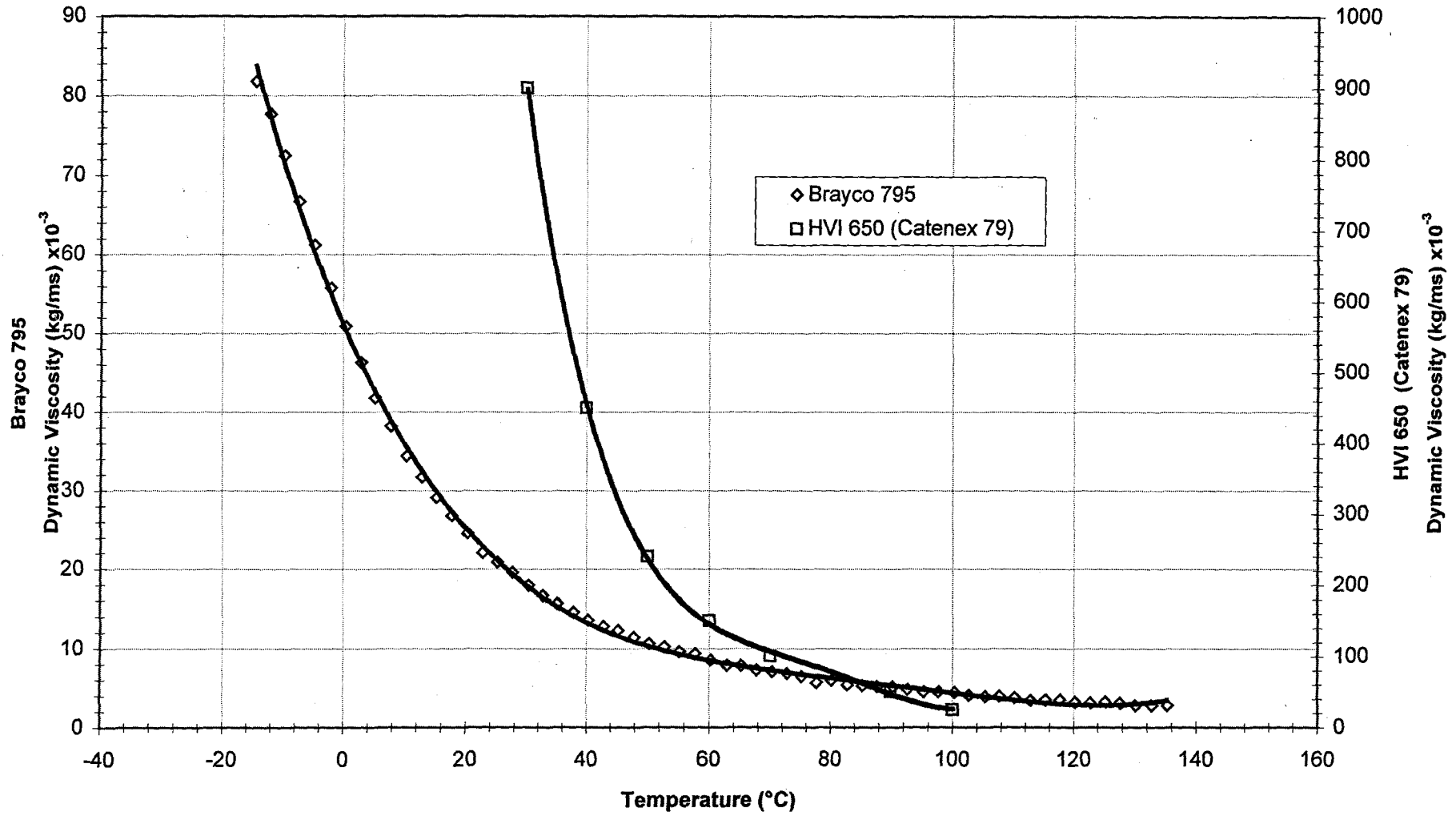


Figure G-1. Dynamic Viscosity with Temperature, Brayco 795 and HVI 650 (Catenex 79)

## Pressure-Viscosity

The Brayco 795 pressure-viscosity index values are not available from the manufacturer. Tests in commercial laboratories can be conducted but were beyond the scope of the project budget. The maximum pressure to which tests can be conducted commercially also is restricted to approximately 100 Mpa. Extrapolation is required beyond this pressure. RHP Aerospace Ltd have a proprietary software package which calculates pressure-viscosity coefficients across temperature. This formula states:

$$\alpha = 7.74 \times 10^{-4} \left( \frac{\nu_0}{10^4} \right)^{0.163}$$

where  $\nu_0$  is the kinematic viscosity of the fluid in stokes and the  $\alpha$  value is in imperial units.

The Brayco 795 values were calculated by the RHP Aerospace software on behalf of DAW. The HVI 650 data was taken from Evans and Johnson (1986). The data is presented below.

Temperature	Brayco 795	HVI 650
°C	$\alpha$ (m <sup>2</sup> /N)×10 <sup>-8</sup>	$\alpha$ (m <sup>2</sup> /N)×10 <sup>-8</sup>
20	1.59	
30	1.52	3.02
60	1.38	2.29
90	1.32	1.84
120	1.28	1.64

Table G-1 – Rheological Data

### Specific Gravity

Brayco 795 at 16°C = 0.874

HVI 650 at 40°C = 0.888

## APPENDIX H

### DERIVATION OF SKEWED ROLLER TORQUE

The equation for prediction of torque generated by skewed roller brakes was developed at DAW by Harris and Thomas during 1993 to support the design of the Boeing 777 No-Back brake.

The equation was derived by considering the work done by a rollers as it moves from point A to B, Figure H-1.

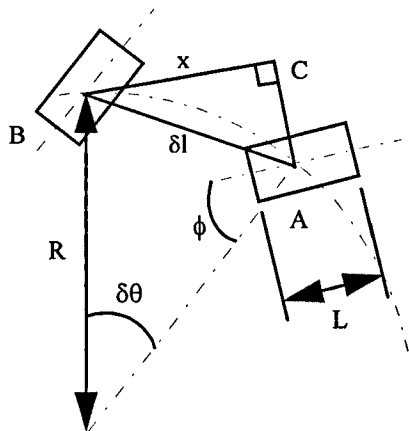


Figure H-1 Skewed Roller Geometry

By the principal of super-position, the roller motion from A to B can be considered as:

- a) pure roll from A to C
- b) pure sliding from C to B

c) rotation about an axis through the centre of the roller at point B

Work done during the pure roll phase was assumed to be negligible. Work done during the slide phase is given by

$$WD = \mu \cdot F \cdot x$$

for  $\delta\theta$  as a small angle,  $\delta l = R\delta\theta$

$$x = \delta l \cdot \sin \phi$$

$$\text{and } x = R \cdot \delta\theta \cdot \sin \phi$$

$$\text{for 1 revolution, } \int_{\theta=0}^{\theta=2\pi} R \cdot \delta\theta = 2\pi R$$

hence in 1 revolution  $x = 2\pi \cdot R \cdot \sin \phi$

$$\text{and hence work done, } WD = \mu \cdot F \cdot (2\pi \cdot R \cdot \sin \phi) \quad \text{H1.}$$

Work done during the spinning of the roller about its own axis can be interpreted from Figure H-2.

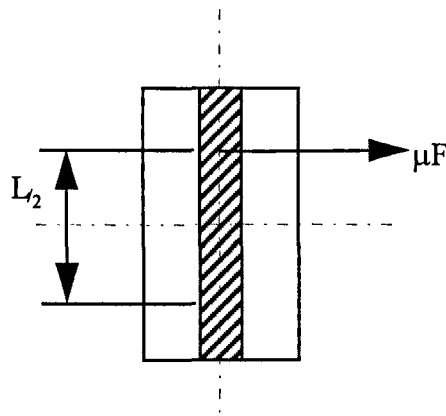


Figure H-2 Work Done During Rotation of the Roller.

torque on the roller,  $= \mu \cdot F \cdot \frac{l}{2}$ , and work done during 1 revolution

$$WD = \mu \cdot F \cdot \frac{l}{2} \cdot 2\pi$$

H2

$$WD = \mu \cdot F \cdot l \cdot \pi$$

In this analysis the assumption has been made that the load is distributed evenly along the length of the roller and that any end effects will be small and hence can be ignored. This is supported by the fact that the ends of the roller usually have a small chamfer whose length is small in comparison to the length of the roller.

Harris and Thomas assumed that as the roller rotates about its own axis, the resultant torque acts at a point  $\frac{2}{3}$  of the way along the roller, hence the torque on the roller  $= \mu \cdot F \cdot \frac{2}{3} \cdot l$ .

Hence total work done per revolution is given by addition of H1 and H2 and this is equal to the work done by the externally applied torque, hence

$$T \cdot 2\pi = \mu \cdot F \cdot \pi \cdot (2R \cdot \sin \phi + l)$$

and torque is given by,

$$T = \mu \cdot F \cdot \left( R \cdot \sin \phi + \frac{l}{2} \right)$$

H3